Structural and Functional Analysis of the Molecular Chaperone Calnexin

Inaugural-Dissertation

to obtain the degree of
Doctor rerum naturalium (Dr. rer. nat.)
of the Faculty of Mathematics and Natural Sciences
of the Heinrich-Heine-University Düsseldorf

submitted by

Achim Brockmeier

from Emsdetten

Düsseldorf, May 2010

Strukturelle und funktionelle Analyse des molekularen Chaperons Calnexin

Inaugural-Dissertation

zur Erlangung des Doktorgrades
der Mathematisch-Naturwissenschaftlichen Fakultät
der Heinrich-Heine-Universität Düsseldorf

vorgelegt von

Achim Brockmeier

aus Emsdetten

Düsseldorf, Mai 2010

Aus dem Institut für Biochemie
der Heinrich-Heine Universität Düsseldorf

Gedruckt mit der Genehmigung der
Mathematisch-Naturwissenschaftlichen Fakultät der
Heinrich-Heine-Universität Düsseldorf

Referent: Prof. Dr. Lutz Schmitt
Korreferent: PD Dr. Ulrich Schulte

Tag der mündlichen Prüfung: 04.05.2010

Für Ulla

In, through, and beyond…

Acknowledgements

First of all, I would like to express my deepest gratitude to my supervisor Prof. Dr. David B. Williams from the Department of Biochemistry at the University of Toronto for offering me the opportunity to conduct my doctoral research in his laboratory. He introduced me into the exciting and challenging field of protein folding and I would like to thank him for numerous stimulating discussions, his encouragement, support, and the freedom bestowed upon me during the course of this thesis.

I am also very grateful to Prof. Dr. Lutz Schmitt. My doctoral thesis would not have been possible without his helpfulness and agreement to externally supervise and referee my work.

I would like to thank PD Dr. Ulrich Schulte for agreeing to co-referee this thesis.

My sincere thanks are due to Prof. Dr. David E. Isenman for his expert advice and helpful suggestions which have been of great value for this study.

I greatly acknowledge Dr. Arianna Rath for providing peptides, her constructive recommendations around my thesis and friendly help during my CD experiments.

Much appreciation goes to Elisa Leung for her guidance with Biacore experiments and sharing much of her experimental expertise with me.

I wish to thank Myrna Cohen-Doyle for expert technical assistance in the Williams laboratory over the years.

I am grateful to Lori Rutkevich for critical reading of the manuscript and helpful comments.

I would like to express my thanks to all members of the Williams laboratory for a wonderful time that I was allowed to experience in a pleasant and friendly working atmosphere.

Finally, I wish to thank my family and friends for their continuous and unconditional support, specially my brother Ulf whose assistance, companionship, and sense of humor have been invaluable in all facets of my life in Toronto.

Publications

Brockmeier, A., Skopnik, M., Koch, B., Herrmann, C., Hengstenberg, W., Welti, S., and K. Scheffzek. 2009. Activity of the *Enterococcus faecalis* $EIIA^{gnt}$ PTS component and its strong interaction with $EIIB^{gnt}$. Biochem Biophys Res Commun **388**:630-6.

Brockmeier, A., Brockmeier U., and D. B. Williams. 2009. Distinct contributions of the lectin and arm domains of calnexin to its molecular chaperone function. J Biol Chem **284**:3433-44.

Brockmeier, A., and D. B. Williams. 2006. Potent lectin-independent chaperone function of calnexin under conditions prevalent within the lumen of the endoplasmic reticulum. Biochemistry **45**:12906-16.

Poster presentations

Brockmeier, A., and D. B. Williams. 2008. The aggregation suppression function of calnexin resides in its globular domain at a location distinct from its lectin site. International Symposium Celebrating the 100th Anniversary of the Department of Biochemistry at the University of Toronto, 28.-30.05.2008, Toronto, Canada.

Brockmeier, A., and D. B. Williams. 2008. The aggregation suppression function of calnexin resides in its globular domain at a location distinct from its lectin site. 2008 CSHL Meeting on Molecular Chaperones and Stress Responses, 30.04.-04.05.2008, Cold Spring Harbor, USA.

Brockmeier, A., and D. B. Williams. 2007. Molecular chaperone characteristics of calnexin under physiological calcium/ATP concentrations of the endoplasmic reticulum. Annual Research Day of the Department of Biochemistry at the University of Toronto, 29.05.2007, Toronto, Canada.

Brockmeier, A., and D. B. Williams. 2006. Molecular chaperone characteristics of calnexin under physiological calcium/ATP concentrations of the endoplasmic reticulum. The second International Symposium on Protein Folding: Principles and Diseases, 25.-26.05.2006, Toronto, Canada.

Brockmeier, A., and D. B. Williams. 2006. Molecular chaperone characteristics of calnexin under physiological calcium/ATP concentrations of the endoplasmic reticulum. Seventh International Workshop on Calreticulin, 22.-24.04.2006, Niagara Falls, Canada.

Contents

List of Figures

List of Tables

Abbreviations

Δarm1	S-Cnx with truncated arm domain1
Δarm2	S-Cnx with truncated arm domain2
°C	degree Celsius
Å	angstrom
aa	amino acid
ADP	adenosine 5`-diphosphate
AMP	adenosine 5`-monophosphate
Amp	ampicillin
arm	arm domain
ATP	adenosine 5`-triphosphate
ATPase	adenosine 5`-triphosphatase
BAP	BiP-associated protein
BiP	binding protein
bis-ANS	1,1'-bis(4-anilino)naphthalene-5,5'-disulfonic acid
bp	base pair
Ca	calcium
CD	circular dichroism
cDNA	complementary DNA
CFTR	cystic fibrosis transmembrane conductance regulator
Ci	curie
Cl	chloride
Cnx	calnexin
Crt	calreticulin
CS	citrate synthase
CST	castanospermine
C-terminal	carboxy-terminal
Cyp	cyclophilin
Da	dalton
deg	degree
DMSO	dimethyl sulfoxide
DNA	deoxyribonucleic acid
DNase	deoxyribonuclease
dNTP	deoxyribonucleoside triphosphate
DTT	dithiothreitol
E. coli	*Escherichia coli*
EDEM	ER degradation enhancing α-mannosidase-like protein
EDTA	ethylenediaminetetraacetic acid
ELISA	enzyme-linked immunosorbent assay
Endo H	endoglycosidase H
ER	endoplasmic reticulum
ERAD	ER-associated degradation
Erdj	ER DnaJ-like protein
Ero	ER oxidoreductin
ERp	ER protein
Fig.	figure
FKBP	FK506-binding protein
FL	firefly luciferase
FPLC	fast performance liquid chromatography
FRET	Förster resonance energy transfer
g	gram
Glc	glucose
GlcNAc	N-acetylglucosamine
glob	globular domain
Golgi	Golgi apparatus
gp	glycoprotein
GRP	glucose-regulated protein
GST	glutathione S-transferase

GTP	guanosine 5`-triphosphate
h	hour
HA	hemagglutinin
HEPES	4-(2-hydroxyethyl)-1-piperazineethanesulfonic acid
HIV	human immunodeficiency virus
HLA	human leukocyte antigen
Hsp	heat shock protein
Ig	immunoglobulin
IPTG	isopropyl-ß-D-thiogalactoside
k	kilo
K_d	dissociation constant
L	liter
LB	Luria-Bertani
LD-S-Cnx	lectin-deficient S-Cnx
m	meter
M	molar
Man	mannose
MDH	malate dehydrogenase
Mg	magnesium
MHC	major histocompatibility complex
min	minute
mRNA	messenger RNA
Na	sodium
NEF	nucleotide exchange factor
Ni	nickel
NLS	nuclear localization signal
NMR	nuclear magnetic resonance
N-terminal	amino-terminal
OD	optical density
OST	oligosaccharyltransferase
Pa	pascal
PAGE	polyacrylamide gel electrophoresis
PCR	polymerase chain reaction
PDI	protein disulfide isomerase
pH	negative logarithm of the hydronium ion concentration
pI	isoelectric point of protein
PLC	peptide loading complex
PPI	peptidyl prolyl *cis-trans* isomerases
R-CMLA	reduced carboxymethylated α-lactalbumin
redox	reduction-oxidation
RNA	ribonucleic acid
RNase	ribonuclease
RT	room temperature
RU	resonance units
s	second
S	Svedberg unit
SBA	soybean agglutinin
S-Cnx	soluble ER-luminal domain of calnexin
SDS	Sodium dodecyl sulfate
Sec	secretion
SERCA	sarcoplasmic/endoplasmic reticulum Ca^{2+}-ATPase
sHsp	small Hsp
SPR	surface plasmon resonance
SR	SRP-receptor
SRP	signal recognition particle
Tab.	table
TAP	transporter associated with antigen processing
TCR	T cell receptor
tER	transitional ER
TFA	trifluoroacetic acid
TLD	thioredoxin-like domains
T_m	transition midpoint temperature of thermal unfolding

TM	transmembrane
Tris	tris(hydroxylmethyl)aminomethane
tRNA	transfer RNA
U	enzyme unit
Ub	ubiquitin
UGGT	UDP-glucose: glycoprotein glucosyltransferase
UPR	unfolded protein response
UV	ultraviolet
V	Volt
v/v	volume per volume
VSV	vesicular stomatitis virus
w/v	weight per volume
w/w	weight per weight
Zn	zinc
β_2m	β_2-microglobulin

Bases

A	adenine
C	cytosine
G	guanine
T	thymine

Amino acids

Amino acids are designated by the single or three letter codes according to the IUPAC nomenclature.

1 Introduction

The two related proteins calnexin (Cnx) and calreticulin (Crt) are oligosaccharide-binding chaperones of the endoplasmic reticulum (ER) that ensure proper folding of newly synthesized glycoproteins as components of an elaborate quality control system. The goal of this thesis is to elucidate the molecular chaperone function of Cnx under physiological conditions of the ER. This introductory chapter is intended to give first a general overview of protein folding in this organelle before introducing the principal folding enzymes and classical chaperones in more detail. Following this, the introduction focuses specifically on Cnx and Crt and examines their controversial mechanisms of chaperone action which is either solely lectin- or additionally polypeptide-based.

1.1 Overview of protein folding in the endoplasmic reticulum

The ER is one of the largest intracellular compartments found in all eukaryotes and it serves a variety of specialized functions including the synthesis of cholesterol and steroids (1), lipid transfer to other organelles (2), biogenesis of organelles (3), and Ca^{2+} homeostasis (4). In addition, and most importantly, the ER represents the site of synthesis for proteins that are destined either for secretion or for the plasma membrane, as well as for the lysosomes, the Golgi, and the ER (5-8).

As soon as the N-terminal signal sequence of a growing polypeptide chain emerges from the ribosome it is recognized by the signal recognition particle (SRP), an RNA-protein complex (9, 10), that transiently delays the elongation process and targets the ribosome-nascent chain-complex to the SRP-receptor (SR) of the translocation apparatus in the ER membrane (11). Following dissociation of the SRP, nascent proteins are transported wholly or partially (if exhibiting internal signal-anchor and/or stop transfer sequences (12-15)) during the translation process into the lumen of the ER. This occurs through the translocon, a pore of 40-60 Å diameter, which in mammals consists of Sec61 α, β, γ, and the translocation associated membrane protein (TRAM) (16-18).

The ER environment

A nascent polypeptide chain typically begins to fold cotranslationally (19-21) and, once inside the ER, faces an apparently inhospitable environment for further posttranslational folding.

The particularly crowed lumen with a protein concentration of ~100 mg/ml probably resembles a gel-like protein matrix (22), where a presumably restricted protein mobility in combination with a high percentage of unfolded or partially unfolded proteins would be expected to potentiate the risk for inappropriate protein interactions and aggregation. However, the ER also provides certain advantages for conformational maturation of nascent proteins compared to the cytosol. The ER lumen possesses a significantly higher oxidizing potential due to an approximately 30 times lower ratio of reduced to oxidized forms of the redox buffer glutathione (23). This promotes the formation of inter- and intramolecular disulfide bonds, whereas a low redox state in the cytosol results in less disulfide formation (24, 25).

The ER also functions as the cell's main repository of Ca^{2+}, which is involved in diverse cellular signaling pathways as a secondary messenger (26), and consequently efficient protein folding has evolved in a Ca^{2+} rich environment. The proper arrangement and interactions of side chains can be promoted by Ca^{2+} binding to acidic residues on proteins that are required to achieve the native conformation (27, 28). Indeed, Ca^{2+} reduction in this organelle results in impaired protein folding (29). A steep Ca^{2+} gradient across the ER membrane is generated by the sarcoplasmic/endoplasmic reticulum Ca^{2+}-ATPase (SERCA), maintaining Ca^{2+} in the ER and in the cytosol at millimolar and nanomolar concentrations, respectively (30). Although the majority of the total ER-luminal Ca^{2+} (1-3 mM) is stored in a protein-bound form (31-33), a significant portion of Ca^{2+} is free, fluctuating in a range from 60-400 μM, representative of the full ER, to 1-50 μM, when the ER is empty (34).

Oligosaccharide processing and quality control

Most proteins of the secretory pathway are modified co- and post-translationally by components of the ER glycosylation system. The translocon associated oligosaccharyltransferase (OST) initially mediates transfer of an N-glycan complex of the form $Glc_3Man_9GlcNAc_2$ (Fig. 1) from a lipid pyrophosphate donor in the ER membrane, dolichol-PP, to asparagine side chains within Asn-X-Ser/Thr consensus sites of the emerging polypeptide chain (35-37). The presence of highly hydrophilic sugar moieties can influence general properties of a nascent protein, as those attachments lead to an enhanced solubility of the folding polypeptides, altering the exposure of otherwise buried protein regions and limiting folding pathways (38). Following glycosylation, the newly N-linked oligosaccharide is rapidly subjected to further processing by a set of enzymes continuously removing and

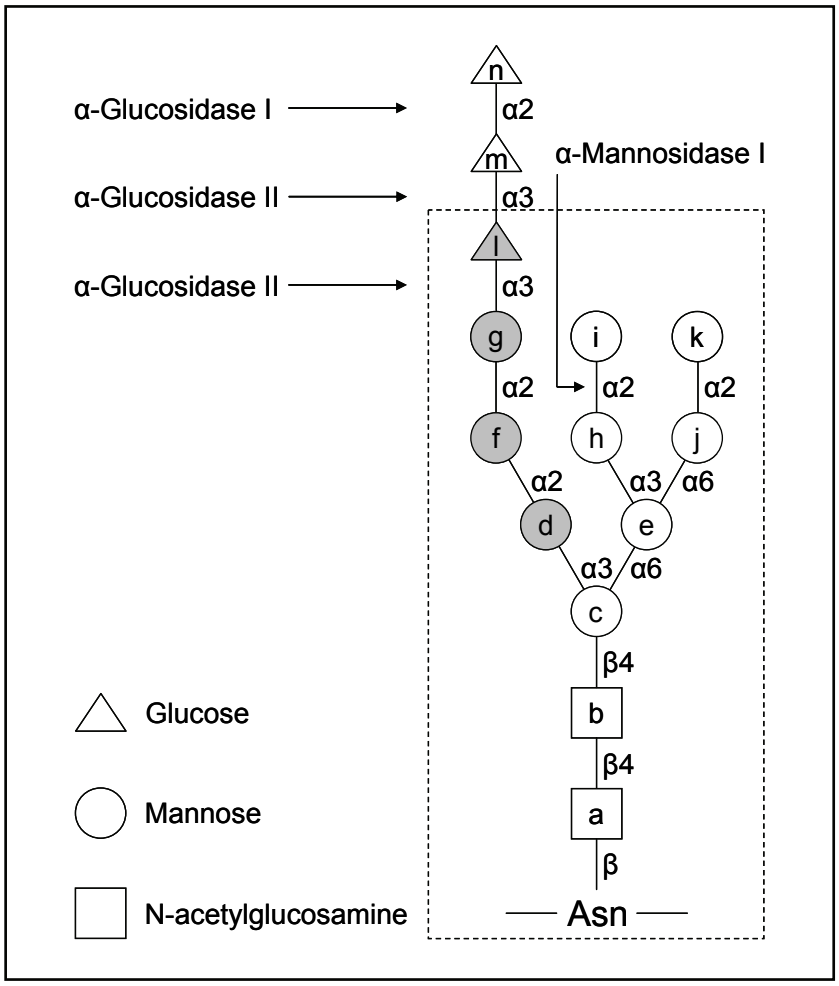

Fig. 1: Structure of the N-linked $Glc_3Man_9GlcNAc_2$ oligosaccharide transferred to nascent polypeptides. The labeling (a-n) of monosaccharides represents their order of addition during synthesis of the dolichol-PP-glycan. Initial cleavage of the terminal glucose residue n by α-glucosidase I and further trimming of glucose residue m by α-glucosidase II generates the monoglucosylated species (dashed box), which is recognized by the two ER chapeones Cnx and Crt. The lectin sites of both proteins interact with the remaining glucose residue as well as with the three underlying mannose residues (grey symbols). Removal of mannose residue i by α-mannosidase I and further mannose trimming in concert with one or more EDEM proteins serves as a signal to target folding-incompetent glycoproteins for degradation. The type of glycosidic linkage is depicted by greek letters to the right of the bond.

adding sugar residues. The composition of the N-glycan serves as a reporter for the folding state whose mono-glucosylated form allows interactions of maturing glycoproteins with the lectin chaperones Cnx and Crt upon removal of the two outermost glucose residues by the sequential actions of glucosidase I and II (39-41). Dissociation and further activity of glucosidase II creates the unglucosylated glycan, preventing rebinding to the lectin chaperones. Regeneration of the monoglucosylated glycan moiety resulting in re-entry into a new Cnx/Crt cycle is controlled by the enzyme UDP-glucose: glycoprotein glucosyltransferase (UGGT) (40, 42-44). Proteins of the secretory pathway that successfully terminate their folding in a biologically acceptable time span are rapidly released from a specialized subdomain of the ER named the transitional ER (tER) and transported to the Golgi for further modification and sorting processes (45, 46).

While folding enzymes contribute to smoothing the funnel like energy landscape by accelerating rate-limiting steps, such as the formation and rearrangement of disulfide bonds and the isomerization of peptidyl proline bonds (47, 48), during the folding pathway of a polypeptide towards an energy minimum (49), molecular chaperones represent the key

component of the multitude of folding factors. By definition chaperones do not impart structural information to a polypeptide and do not expedite the folding kinetics or change folding pathways. Chaperones are specialized proteins that promote proper folding of a client protein through cycles of binding and release of the initially unstable polypeptide conformer (50). The selective binding of molecular chaperones to folding or incompletely folded proteins, a hallmark of classical chaperone activity, is based on their ability to recognize non-native determinants such as exposed hydrophobic amino acids that have not been properly buried in the inside of the molecule (51, 52). Thereby chaperones are able to prevent folding intermediates from entering a kinetic folding trap or from proceeding an off-folding pathway to irreversible misfolding and aggregation. This results in an increased folding efficiency (53).

The identification of incompletely or misfolded polypeptides is a critical checkpoint during protein maturation and is ensured by the elaborate ER quality control system. In addition to suppressing aggregation molecular chaperones play an important role in this process by retaining folding polypeptides inside the ER until they reach their native conformation or directing terminally misfolded proteins to the ER associated degradation (ERAD) pathway (54-59).

ERAD

Following identification of folding-defective client proteins, ERAD involves their retrotranslocation into the cytosol, ubiquitination, deglycosylation, and degradation by a cytosolic proteolytic complex, the 26S proteasome (60-62). While the identification of non-glycosylated ERAD substrates by chaperones is poorly understood (63, 64), it is widely accepted that glycoproteins destined for ERAD are recognized by changes in their N-glycan composition through α-mannosidase mediated removal of one or more terminal mannose residues (38, 65-70). The ER degradation enhancing α-mannosidase-like proteins EDEM1-3 (mammals) and Htm1p (yeast) are thought to contribute directly or indirectly to the de-mannosylation process (71-75). Since α-mannosidase I exhibits a much lower rate of enzymatic activity compared to glucosidase II or UGGT, it functions as a “timer” to remove nascent glycoproteins after an extended period of futile cycles of folding attempts from the Cnx/Crt cycle (76-78). Mannose trimming generates the oligosaccharide form that serves as a degradation signal by interacting with putative lectins such as OS-9 and EDEM1 (mammals) (79-82) or Htm1p and Yos9p (yeast) (83-86) which facilitate targeting of glycoproteins to the retrotranslocation channel. Once targeted for degradation, ERAD substrates are probably unfolded and reduced before dislocation from the ER lumen into the cytosol (87, 88). Besides

Sec61 (89-92), additional transmembrane proteins in mammals (Derlin1-3) (82, 93, 94) and in yeast (Der1p) (95) have been identified as potential retrotranslocon components. As soon as ERAD candidates are released into the cytosol, they are decorated with polyubiquitin chains mediated by the concerted action of three types of enzymes termed E1 (ubiquitin-activating enzyme), E2 (ubiquitin-conjugating enzyme), and E3 (ubiquitin ligase) (96). The attachment of multiple copies of the 76 aa ubiquitin as a degradation marker for the proteasome has been well described for cytosolic proteins as well as for ERAD substrates (97). The ubiquitin-conjugated polypeptides are bound by the two 19S regulatory subunits of the proteasome, whose 20S cylindrical subunit displays various proteolytic activities responsible for substrate degradation (61, 98). While N-glycan removal from degradation candidates is thought to facilitate entry into the proteasome, it is not an absolute requirement (99).

1.2 Folding enzymes and molecular chaperones of the endoplasmic reticulum

Although the amino acid sequence of a nascent polypeptide chain already embeds the required information to assume a native structure without assistance (100), the diverse repertoire of ER folding enzymes and chaperones reflects the necessity of assisted folding of client proteins (101). Since the mid-1970s many folding enzymes and chaperones have been identified within the ER (Tab. 1).

Molecular chaperones of the cytosol are classified based on their molecular weight into several families, namely, heat shock protein (Hsp) 100, 90, 70, 60, 40, and small Hsp (sHsp). As indicated by their designation, stress conditions, such as elevated temperatures, generally enhance their transcription (102). ER resident chaperones lack members of the Hsp60 and sHsp families and are typically upregulated in response to cellular stress such as accumulation of unfolded proteins, glucose deprivation, and imbalance in Ca^{2+} or redox homeostasis (103-106). The best known chaperones of the ER are binding protein (BiP) (107, 108), glucose-regulated protein 94 (GRP94) (105), and the lectin chaperones Cnx and Crt (109, 110). These proteins represent the core elements of the two major folding systems in the ER, the BiP/GRP94 and lectin chaperone systems (111). They act in concert with their co-chaperones and the well characterized folding catalysts protein disulfide isomerase (PDI) and endoplasmic reticulum protein 57 (ERp57), respectively, on newly synthesized proteins (112-115).

Tab. 1: Selection of prominent ER resident folding factors.

Family	Mammals	Yeast	Function	Reference
Hsp100	TorsinA	?	Chaperone	(116, 117)
Hsp90	GRP94		Chaperone	(118)
Hsp70	BiP	Kar2p	Chaperone	(107, 119)
Hsp40	Erdj1-5	Sec63p, Sc1p, Jem1p	Cofactors for Hsp70	(120-127)
GrpE-like	BAP	Sls1p	Cofactor for Hsp70	(128, 129)
Lectins	Cnx	Cne1p	Glycoprotein-dedicated chaperone	(130, 131)
	Crt		Glycoprotein-dedicated chaperone	(132)
Glycan-enzymes	α-Glucosidase I	Gls1p	N-glycan trimming	(133, 134)
	α-Glucosidase II	Gls2p	N-glycan trimming	(135, 136)
	α-Mannosidase I	Mns1p	N-glycan trimming	(65, 137)
	EDEM1-3	Htm1p	ER degradation enhancing α-mannosidase-like proteins	(72, 73, 75, 138)
	UGGT	Kre5p	Glucosyltransferase and glycoprotein-dedicated folding sensor	(139, 140)
PDI	PDI	Pdi1p	Thiol oxidoreductase	(141, 142)
	ERp57		Thiol oxidoreductase	(143)
	ERp72		Thiol oxidoreductase	(144)
Cyp	CypB	Cpr5p	Peptidyl prolyl isomerase	(145, 146)
FKBP	FKBP13	Fpr2p	Peptidyl prolyl isomerase	(147, 148)

The detailed mechanisms and functions of these folding enzymes and chaperones will be discussed in the following sections.

1.2.1 PDI

The majority of proteins trafficking through the ER contains disulfide bonds, whose correct formation represents an essential step during the maturation process in this organelle (149). Disulfide bridges are thought to give directionality to the folding pathway of a nascent polypeptide and to stabilize its native state. The oxidation, reduction, and isomerization of disulfide bonds are catalyzed by enzymes known as protein disulfide isomerases (PDIs). Members of the PDI family can be defined by the number and arrangement of thioredoxin-like domains (TLDs) and the sequences of the catalytic active site CXXC motifs (150).

Among the at least 17 PDI family proteins in humans, PDI is the most abundant and thoroughly studied member since its discovery by Goldberger *et al*. in 1964 (151, 152). It consists of four TLDs, the two non-catalytic TLDs are known as **b** and **b'** and they separate the two catalytically active TLDs termed **a** and **a'** (153). Thus the overall domain order of PDI can be described as **a-b-b'-a'-c**, where **c** represents an acidic C-terminal domain which has been shown to bind Ca^{2+} (154).

The crystal structure of yeast PDI revealed that the four TLDs adopt the shape of a "twisted U" (155). The catalytic **a** and **a'** domains are located at opposite ends of the "U" with the two active site CXXC motifs facing each other. The two non-catalytic **b** and **b'** domains form the base of the "U" with hydrophobic residues enriched on the inside surface. The majority of the hydrophobic surface can be attributed to a pocket within the **b'** domain providing the principal peptide-binding site (156, 157). This pocket and additional hydrophobic patches are proposed to hold a substrate within the "U" and position it for reactions with the catalytic **a** and **a'** domains.

To facilitate disulfide bond formation in folding intermediates the cysteines in the catalytically active domains of PDI are present in the oxidized state, forming mixed disulfides with the substrate and leaving the reaction in the reduced state (158). When PDI functions as a reductase, its CXXC motif enters the reaction in the reduced state. Finally, isomerization of disulfide bonds starts and ends with the CXXC motif in the reduced state, either during direct rearrangement of intramolecular disulfide bonds or cycles of reduction and subsequent oxidation (159, 160). Whether PDI functions as an oxidase or reductase is determined by the redox state of Cys residues in the catalytic **a** and **a'** domains which in turn is controlled by its environment and additional proteins, such as the flavoprotein Ero1. This membrane-associated enzyme has been implicated in shuttling oxidizing equivalents from molecular oxygen to PDI so that it can be recycled to fulfill its role again as an oxidizing agent in disulfide bond formation during folding of nascent polypeptides (47).

In an attempt to elucidate domain contributions to the oxidoreductase and isomerase activities of PDI, Darby and Creighton demonstrated that the isolated **a** and **a'** domains of PDI can act as oxidants and reductants, but fail to isomerise disulfide bonds in substrates with non-native disulfide bridges (161). For simple isomerization reactions, a combination of a catalytic domain with the **b'** domain was required and only full-length PDI revealed the capacity to effectively catalyze the isomerization of bovine pancreatic trypsin inhibitor (BPTI) (162). Since PDI has been shown to be essential for viability in *S. cerevisiae* and oxidoreductase deficient mutants with remaining isomerase activity were viable (163, 164), it

was assumed that the essential function of PDI is to catalyze disulfide bond isomerization rather than formation of new disulfide bonds. In contrast to these findings, however, further studies in the same organism indicated that the essentiality of PDI is rather based on its oxidoreductase activity than its isomerase activity (165). Therefore, the relative contribution of oxidoreductase and isomerase activities of PDI to its complete function as a foldase remains to be illuminated.

In addition to its enzymatic activity, PDI revealed the ability to function as a molecular chaperone by preventing the aggregation of misfolded proteins which did not contain any disulfide bridges (166, 167). This chaperone activity, that does not depend on the redox state of the Cys residues of the active site motifs (168, 169), might prevent non-specific interactions during its foldase activity, thereby resulting in more productive folding of nascent proteins (166, 170). While polypeptide binding of PDI is primarily mediated by its **b'** domain, how this binding is regulated is currently not understood. In its folding-assisting role PDI has been suggested to act synergistically together with BiP as shown in a yeast expression system and in an *in vitro* system (113, 171). Therein BiP is proposed to bind to non-native antibody fragments, maintaining the Cys residues accessible for enzymatic activity by PDI.

1.2.2 ERp57

ERp57 is another extensively characterized member of the PDI family. It exhibits a similar overall domain organization compared to PDI with its four thioredoxin-like domains, also labeled **a**, **b**, **b'**, and **a'** (172), but missing the acidic C-terminal domain observed for PDI. The enzymatic activity of ERp57 is mediated through its two active site CXXC motifs residing within the **a** and **a'** domains (173, 174), with a more reducing redox potential compared to PDI (172). ERp57 interacts with a variety of ER proteins via mixed disulfides at the N-terminal Cys residues of its active site motifs, indicative of its role as a foldase in thiol-disulfide exchange reactions (175-178). Findings showing that ERp57 catalyzes disulfide bond formation with a specificity towards glycoproteins and functions more efficiently as an oxidoreductase on monoglucosylated substrates in cooperation with one of the lectin chaperones Cnx and Crt have led to the common view that the recruitment of ERp57 to maturing glycoproteins is always dependent on its association with Cnx or Crt (143, 175, 179-182). Unlike PDI (183), the noncatalytic **b'** domain of ERp57 is not involved in substrate binding or chaperone activity, but possesses a conserved positively charged region mainly responsible for binding to the negatively charged tip of the arm domain of the lectin

chaperones (114, 115, 184, 185). Therefore, the substrate specificity of ERp57 might be defined by Cnx and Crt which bind nascent glycoproteins and allow ERp57 to catalyze disulfide bond formation in close proximity to their folding substrate.

Recent studies examining the biogenesis of major histocompatibility complex (MHC) class I molecules have questioned the exclusive dependency of ERp57 on the lectin chaperones to gain access to their substrates (186, 187). MHC class I molecules bind cytosolically derived antigenic peptides within the ER and present them at the cell surface to cytotoxic T cells. The maturation of MHC class I molecules requires disulfide formation in their heavy chain which, in association with β_2-microglobulin (β_2m), enters the so called peptide loading complex (PLC). This complex consists of Crt, a peptide transporter termed TAP, and tapasin, the latter mediating the interaction between class I heterodimers and TAP. ERp57 has been shown to be essential for efficient catalysis of heavy chain disulfide bond formation at an early stage during MHC class I biogenesis (188) and additionally is suggested to play a structural rather than a catalytical role within the PLC by forming a stable disulfide bridge with tapasin (189, 190). Zhang *et al*. demonstrated that ERp57 can promote disulfide formation in the heavy chain and can be incorporated into the PLC in the absence of interactions with the lectin chaperones Cnx and Crt (187).

Besides MHC class I molecules, influenza hemagglutinin (HA) is the only model glycoprotein so far in metazoan cells to be significantly affected by deletion of ERp57, likely through impaired disulfide bond isomerization during the folding process (180). Along with Crt, ERp57 has been found to be involved in the regulation of SERCA2b Ca^{2+} pumps via cysteines localized within an intralumenal loop of SERCA2b (191). Furthermore, several studies identified ERp57 as a nucleus associated protein (192-195). Although ERp57 carries a putative nuclear localization signal (NLS) close to its C-terminus, it remains unknown how the ER foldase is being transported to the nucleus and what role it plays in this organelle.

1.2.3 Peptidyl prolyl *cis-trans* isomerases

Most peptide bonds are synthesized on the ribosome in the *trans* configuration (196) which is favoured in native proteins over the energetically higher *cis* configuration (197). An exception is peptide bonds prior to prolines where both the *cis* and *trans* configurations are similar in energy (198), resulting in up to 38 % of peptide bridges in the *cis* configuration (199). As refolding experiments have demonstrated, *cis-trans* isomerization of peptidyl prolyl bonds is a rate-limiting step during protein folding (200). This reaction can be catalyzed by a class of

enzymes termed peptidyl prolyl *cis-trans* isomerases (PPI) (201, 202). These enzymes are classified into three families based on their binding of specific inhibitors, namely parvulins, cyclophilins (Cyps), and FK506-binding proteins (FKBPs) (203, 204). In the ER, members of the two latter families have been identified, CypB (145) and up to six FKBPs including FKBP13, 23, and 65 (147, 205, 206). CypB has been described in association with several ER chaperones and is involved in corporation with Hsp47 in the folding of procollagen (207-209). Furthermore, CypB is known to bind to human immunodeficiency virus (HIV) Gag and HIV capsid protein p24 (210, 211). Recent studies showed a regulatory function of ER resident members of the FKBP family on the activity of BiP (205, 212) and their association with client proteins bound to BiP (206).

Although the refolding of denatured proteins was significantly enhanced in the presence of Cyps and FKBPs *in vitro*, their actual contribution to protein maturation in living cells remains poorly understood, since yeast lacking all PPI enzymes was still viable (213).

1.2.4 BiP

BiP, also known as glucose-regulated protein 78 (GRP78) or Kar2p in yeast (214, 215), is a member of the Hsp70 family and is one of the most abundant chaperones in the lumen of the ER (216). The highly conserved Hsp70s participate in protein folding through promiscuous binding to exposed hydrophobic segments in immature or non-native proteins, thereby maintaining their folding-competent state and shielding them from aggregation (217). The preference for hydrophobic peptides by BiP was confirmed by binding studies including affinity panning of a bacteriophage expressed peptide library (218, 219). These experiments revealed a binding specificity in which large hydrophobic amino acids alternate with any other amino acid resulting in the formation of a completely hydrophobic face within a β-strand conformation which promotes BiP binding. The measurements also allowed the development of a binding algorithm based prediction for potential BiP recognition sequences in client proteins (220). An expected binding site once every 36 residues of an average protein underlines the wide spectrum for the chaperone function of BiP during protein maturation.

Like other Hsp70s, BiP consists of a 44 kDa N-terminal ATPase and a 25 kDa C-terminal domain (221). The latter domain has a variable C-terminal region and provides the 15kDa polypeptide-binding domain (222, 223), which assumes a channel configuration with a “hinged lid”. Conformational changes of the polypeptide-binding domain associated with “opening” or “closing” of the “lid” over the channel are controlled by ATP hydrolysis and

ATP to ADP exchange at the ATPase domain (224). The ATP-binding site resides in a cleft of the ATPase domain, formed by two globular subdomains of approximately equal size (225). Peptide binding occurs in the ATP-bound state, facilitated by the open conformation of the "lid" (Fig. 2). ATP hydrolysis leads to closing of the C-terminal "lid" over the substrate and creates a high affinity conformation (226). Subsequent exchange of ADP to ATP results in a low affinity conformation in which the "lid" returns to its open position and the client protein dissociates. Release of ADP from BiP is catalyzed by at least two known nucleotide exchange factors, GRP170 and BiP-associated protein (BAP) (128, 227). BAP has been shown to play a crucial role in regulating the ATPase activity of BiP, as loss of BAP results in

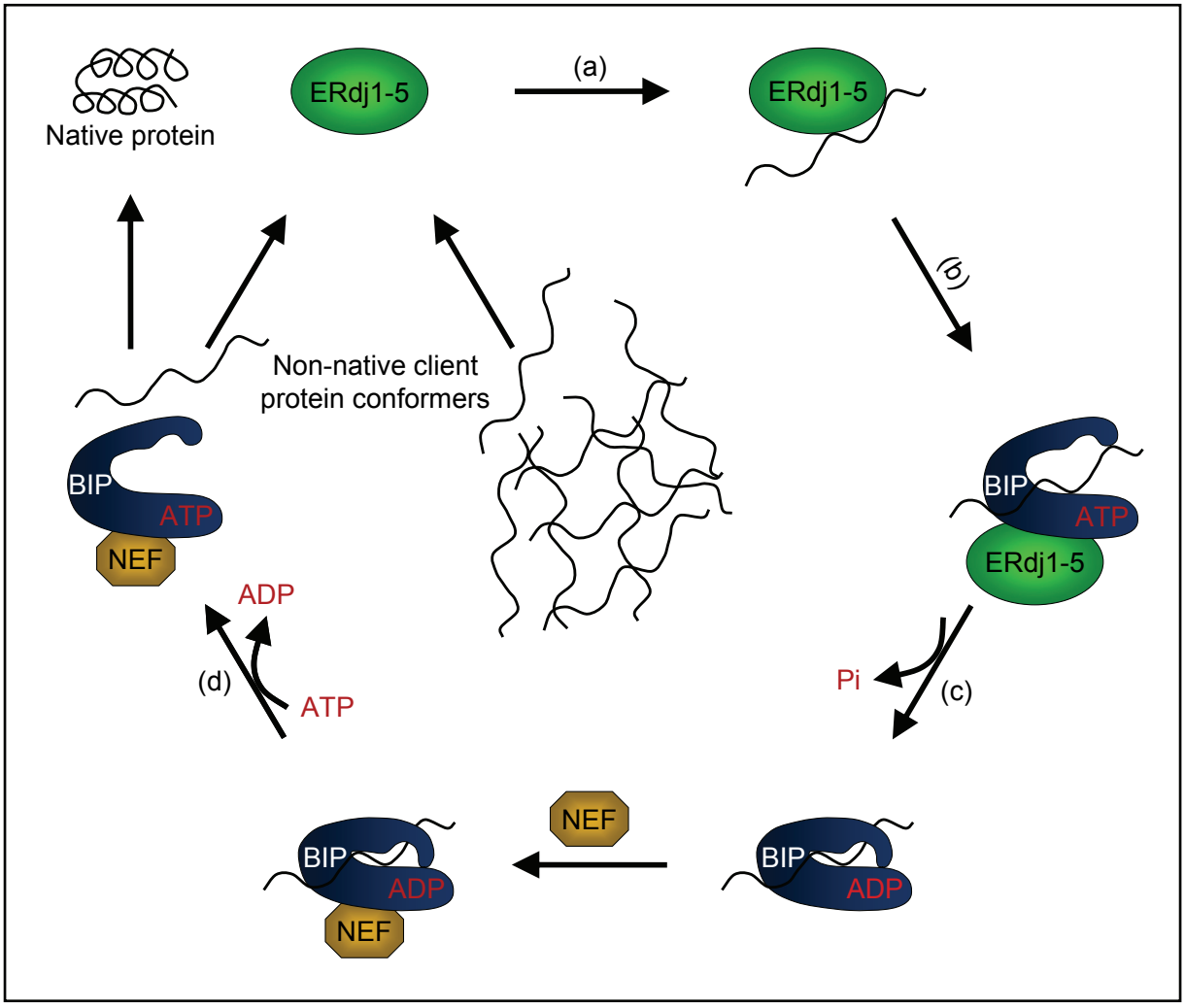

Fig. 2: Model of the BiP chaperone cycle. The cycle starts with initial binding of one of the Hsp40 co-chaperones ERdj1-5 to an unfolded client protein **(a)** which is then delivered to ATP-bound BiP **(b)**. By stimulating the ATPase activity of BiP, the Hsp40 co-chaperones promote locking of an unfolded client protein in an high-affinity complex with BiP **(c)**. At least two known nucleotide exchange factors (NEF), BAP and GRP170, catalyze ADP release and ATP rebinding, resulting in an "open" conformation of BiP and client protein dissociation **(d)**. If folding of the released protein does not occur rapidly, it can reassemble with an ERdj co-chaperone for a new cycle, which prevents aggregation with other non-native protein conformers. Proteins that have achieved a more mature or native conformation in a reasonable period of time are either recognized by further ER chaperones or released into the secretory pathway. Terminally misfolded client proteins are targeted by BiP for the ERAD pathway.

disruption of the ATPase cycle of BiP and accumulation of non-native proteins in the ER (228). In addition, owing to its weak ATPase activity, BiP interacts with further cofactors, of which five have been identified as members of the Hsp40 family, the ER DnaJ-like proteins, ERdj1-5 (120-124). These stimulate the ATPase function of BiP (229, 230). The Hsp40 co-chaperones also contribute to the folding cycle by binding and targeting folding intermediates to BiP and thus broaden the range of client proteins (231).

BiP has been referred to as the master regulator of the ER. This stems from the fact that BiP is involved in several other crucial functions of the ER beside assisting in protein folding (108). Although the X-ray structure analysis of the translocon suggests that intrinsic features serve as the permeability barrier between the ER and cytosol (232), earlier studies indicated the participation of BiP in sealing the translocon pore from the luminal side before and at early stages of translocation (233). Subsequent progressive translocation of a growing polypeptide chain into the ER has also been shown to be facilitated by BiP, either through ATP driven cycles of binding and release to pull nascent chains into the ER lumen or through just binding alone, acting as a "Brownian ratchet" and thereby preventing retrotranslocation (215, 234). Furthermore, BiP contributes to Ca^{2+} homeostasis as one of the most abundant Ca^{2+} buffering proteins in the lumen of the ER (235). It also plays an important role in preparing folding-defective proteins for proteasome mediated disposal and ensures solubility of aggregation prone proteins for their retrotranslocation into the cytosol (112, 236-238). Finally, during accumulation of aberrant proteins upon cell stress, BiP represents the key player of an adaptive signal transduction pathway termed the unfolded protein response (UPR) and is directly involved in the activation of this process (239, 240).

1.2.5 GRP94

GRP94, also known as glycoprotein (gp) 96 or endoplasmin, is the Hsp90 paralog of the ER and is only found in vertebrates (105). Comprising 5-10 % of the total ER protein content, GRP94 represents the most abundant protein in this organelle (241). Since it interacts in some cases with client polypeptides upon their release from BiP, GRP94 has been suggested to be involved in the conformational maturation of more advanced folding intermediates, underscored by its specific binding to immunoglobulin (Ig) chains, thyroglobulins, and apolipoprotein B during their late folding stages (242-246).

As a member of the Hsp90 chaperones, GRP94 shares the same domain organization of this highly conserved family of homodimeric proteins. Each monomer is comprised of an N-

terminal ATP-binding domain (247), connected by an dispensable charged linker sequence to the middle domain, and a C-terminal dimerization domain (248). During chaperone cycles of binding and release, for which both the N- and C-termini are required, Hsp90 acts on client proteins as an opening and closing molecular “clamp” (249, 250). It has been proposed that the chaperone activity is regulated by conformational changes within the N-terminal domain upon ATP binding (251). As a consequence of ATP binding, a short segment of the N-terminal domain closes over the ATP-binding pocket associated with a transiently dimerized N-terminal conformation (252, 253). These N-terminal rearrangements allow the alignment of the catalytic residues from the N-terminal and middle domains and result in hydrolysis of the trapped ATP molecule (254). The different conformational stages during this process are stabilized and regulated by several co-chaperones (255-257), while other co-chaperones such as Hop/Sti1 bind to the C-terminal end of Hsp90 and facilitate client protein transfer from Hsp70 (258, 259).

While the activity of cytosolic Hsp90 is modulated by a multitude of co-chaperones (260), none have been identified so far for GRP94. Recent studies confirmed an ATPase activity for Grp94 that is comparable to yeast Hsp90, although ATP-driven conformational changes adopted by Hsp90 during the ATPase cycle could not be detected for GRP94 (261, 262). Since GRP94 can undergo an open and a closed conformation independent from the nucleotide bound state, it remains to be elucidated which factor is responsible for the regulation of the chaperone cycle.

Recognition of non-native protein conformers through polypeptide based interactions is facilitated by binding sites, presumably localized in all three domains of Hsp90 (263-265). However, the peptide-binding site of GRP94 could be assigned to its N-terminal domain with a rather hydrophilic binding specificity compared to other chaperones such as BiP, thereby indicating a preference for more matured client proteins (118, 266). A further study showed that GRP94 promotes the maturation of only a specific subset of several examined cell surface proteins (267). This suggests GRP94 binding depends on more than just the exposure of hydrophobic patches typically recognized by chaperones. GRP94 also seems to be involved in the maturation process of kinases and other signal transduction proteins (268, 269).

In addition to its protein folding-promoting role GRP94 dually functions as an important Ca^{2+} buffer due to its high Ca^{2+}-binding capacity and has been shown to bind peptides *in vivo* and *in vitro* (266, 270-272). The later ability allows GRP94 to function as an antigen delivery system, thereby inducing MHC class I-restricted T cell responses against a variety of peptides derived from endogenous foreign proteins (273, 274).

1.2.6 Calnexin and calreticulin

In eukaryotes, the Cnx and Crt chaperone system has evolved in close relationship with the N-linked glycosylation system to promote proper folding of nascent glycoproteins in the ER. Cnx, comprised of 573 amino acid residues, is a type I ER membrane protein with a molecular weight of 65.4 kDa and a C-terminal –RKPRRE ER retrieval signal (109). It consists of a 91 aa residue cytoplasmic tail connected via a transmembrane segment to a 461 aa residue domain residing within the lumen of the ER. This luminal portion is similar to Crt, which is a 46 kDa ER-luminal protein of 401 aa residues with a –KDEL ER retrival signal at the C-terminus (110). Interestingly, Cnx and Crt migrate on SDS-PAGE at approximately 90 and 60 kDa, respectively (275) (276). Their high content of negatively charged amino acids, particularly in their C-terminal regions, is responsible for their aberrant migration in gels. No Crt has been identified so far in yeast, and its Cnx homologues termed Cne1p and Cnx1p exhibit shorter cytoplasmic tails in addition to less acidic luminal domains compared to their mammalian family members (277). Neither Cnx nor Crt homologues are expressed in prokaryotic cells.

Since the discovery of Cnx in 1991 several studies demonstrated its transient association with a wide array of newly synthesized glycoproteins traversing the secretory pathway (21, 130, 278). Soon afterwards it was found that Crt revealed a similar capacity to interact with a multitude of nascent glycoproteins (132, 279). The ability of both proteins to bind the majority of glycosylated proteins is mediated by their lectin sites, which specifically recognize glycans of the form $Glc_1Man_9GlcNac_2$ (39, 132). Both chaperones also bind Zn^{2+} (280, 281), Ca^{2+} (281, 282), ATP (283, 284), and the oxidoreductase Erp57 (114, 115). The former three ligands influence their chaperone conformation and their ability to associate with client proteins. While carbohydrate binding by Cnx and Crt was suggested to serve as the crucial determinant in selection of client proteins, they have also been shown to bind to the backbone of non-native protein conformers and suppress the aggregation of non-glycosylated proteins, implying the ability to function as more classical molecular chaperones similar to BiP and GRP94 (283, 284).

1.2.6.1 Structure and binding properties of calnexin and calreticulin

The X-ray crystal structure of the nearly complete ER-luminal portion of Cnx (residues 41-438) revealed the presence of two distinct domains, a compact globular domain and an extended arm domain (Fig. 3b) (282). The arm domain contributes mainly to the characteristic overall structure of Cnx by extending away 140 Å in an elongated hairpin formation from the globular domain. The frequently used term P domain is based on the fact that the arm domain is comprised of two proline-rich repeat motifs, motif 1 [I-DP(D/E)A-KPEDWD(D/E)] and motif 2 [G-W—P-IN-P-Y]. Both motifs are repeated four times in a 11112222 pattern (Fig. 3a). The tandem sequence of motif 1 forms the β-strand extending away from the globular domain, while the tandem sequence of motif 2, making up the antiparallel β-strand, loops back on the motif 1 repeats resulting in four superimposable structural units.

The globular domain of Cnx, which resembles legume lectins (285), consists of a β-sandwich, comprised of a concave six stranded and a convex seven stranded β-sheet and is stabilized by a disulfide bond between residues Cys141 and Cys175. The carbohydrate-binding site resides at the surface of the concave β-sheet, interacting via Tyr145, Lys147, Tyr166, Glu197, Glu406, and Met169 with the terminal glucose of the oligosaccharide. The three underlying mannose residues of the oligosaccharide are also thought to be recognized by the binding site (282, 286). These six residues were confirmed to be essential for the lectin function of Cnx (287).

Since identical oligosaccharide-binding specificities have been determined for Crt (286, 288, 289) and it shares ~39 % amino acid sequence identity (290) and a similar secondary structure composition (281, 291) with Cnx, Crt has been suggested to have a comparable globular domain. Only the structure of the arm domain (residues 188-288) has been determined for Crt by NMR studies (292). In this study, Ellgaard *et al*. demonstrated a close resemblance to the arm domain of Cnx, although only three copies of motif 1 and 2 are present which form a similar but shorter hairpin structure.

Beside yeast two-hybrid and co-immunoisolation experiments, NMR studies also revealed that both Cnx and Crt interact through the tips of their arm domains with the oxidoreductase ERp57 as illustrated in Fig. 3 (114, 115). ERp57 recruitment, presumably to form a ternary complex with a folding glycoprotein bound to Cnx/Crt, results in more efficient disulfide bond formation during the folding process (181). Binding of Zn^{2+} to Cnx and Crt has been associated with their globular domains (280, 293) and results in a structural destabilization in combination with the exposure of a hydrophobic surface in the case for Crt (284, 294).

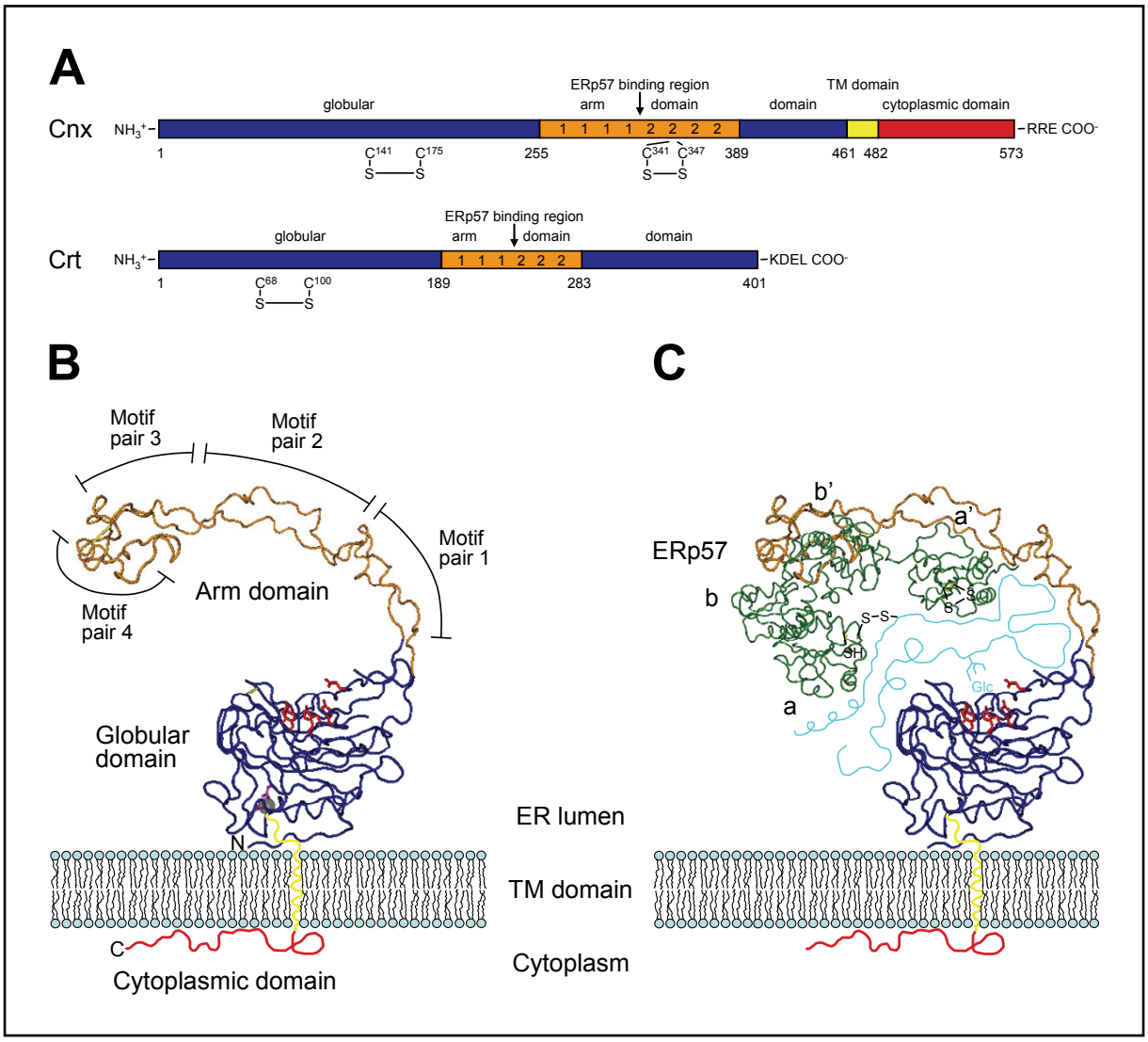

Fig. 3: Structure model of calnexin. (A) Comparison of the linear sequences of dog Cnx and rabbit Crt. Both proteins possess a globular domain (blue box), an arm domain (orange box), and a C-terminal ER retrieval signal. The additional transmembrane (TM) and cytoplasmic domains of Cnx are indicated by yellow and red boxes, respectively. The two repeated sequence motifs are depicted by the numbers 1 and 2. Amino acids forming disulfide bridges are shown and linked with an S-S. The numbers below the sequences represent the amino acid position starting after the signal peptide cleavage sites. **(B)** Crystal structure of the ER-luminal domain of Cnx (282) and theoretical illustration of its transmembrane and cytoplasmic domains at the ER membrane. The globular domain (blue) contains the lectin site that interacts with the terminal glucose residue of monoglucosylated glycans via six amino acids labeled in red. The two aspartates (pink) of the putative Ca^{2+}-binding site coordinate the ion pictured as a dark grey sphere. The elongated arm domain (orange) is comprised of the four repeat motifs 1 and 2 forming four structural units termed motif pair 1-4. Depicted in dark yellow two disulfide bonds of the ER-luminal portion of Cnx. Also illustrated in this cartoon, representations of the transmembrane domain (yellow) followed by the cytoplasmic domain (red). **(C)** Model for the folding-promoting interaction of Cnx with a non-native glycoprotein. Transient binding can occur solely through the lectin site or as well through an additional polypeptide-binding site, resulting in potential sequestration of the client protein (thin cyan line) between the globular and arm domains. Such sequestration is likely to minimize client protein aggregation by removing the protein from the vicinity of other folding intermediates. The efficiency of the folding process may also be enhanced through recruitment of ERp57 (crystal structure of human ERp57 (190) shown in green), whose four thioredoxin-like domains are labeled **a**, **b**, **b'**, and **a'**. Although mediated mainly through the **b'** domain, the **a'** domain along with the positively charged C-terminus are thought to contribute to binding of ERp57 to Cnx. Disulfide bond formation and isomerization reactions can be catalyzed by the two active site CXXC motifs (yellow), placed in close proximity to the folding glycoprotein. TM, transmembrane.

Studies in the early 1990s to elucidate the Ca^{2+}-binding properties of Crt using equilibrium dialysis showed that both the globular and arm domains exhibit the capacity to bind Ca^{2+} (295). In accordance with these findings were overlay experiments two years later by Tjoelker *et al*. demonstrating Ca^{2+} binding to both domains of Cnx, but the more recently solved crystal structure revealed only a single Ca^{2+} ion within the globular domain (282). Ca^{2+} ions are essential for the structure of Cnx and Crt and seem to be involved in modulating their conformational organization, since Ca^{2+} removal is associated with decreased tertiary packing, reduced thermal stability, and increased protease sensitivity (281, 296). The ability of both lectins to bind isolated oligosaccharides and to recognize monoglucosylated glycans of glycoproteins necessitates the presence of Ca^{2+} (286), indicative that Ca^{2+} induced conformational changes affect the functionality of the lectin site.

Although Cnx and Crt do not contain detectable ATPase activity, they appear to be ATP-binding proteins due to the observations that both Cnx and Crt exhibit enhanced capacity to suppress the aggregation of glycosylated and non-glycosylated proteins in the presence of ATP (283, 284). The ability of Cnx and Crt to suppress aggregation in a lectin independent way is suggestive for the presence of a polypeptide-binding site, whose specificity and precise location is not well examined. Deletion mutagenesis of rabbit Crt as well as dog or yeast Cnx indicated that their aggregation suppression function is primarily mediated through their globular domains (280, 297).

Finally, Cnx has been shown to become phosphorylated at multiple serine phosphorylation sites of its cytoplasmic tail by casein kinase 2 (CK2) and extracellular-signal regulated kinase-1 (ERK-1) (298, 299), while Crt can be phosphorylated by various isoforms of protein kinase C (PKC) (300).

1.2.6.2 Biological functions of calnexin and calreticulin

The majority of transmembrane and secretory proteins which interact transiently with Cnx and/or Crt during their folding and assembly process in the ER, are glycosylated (132, 301). The presence of an N-linked glycan within the first ~50 residues of the growing polypeptide chain was found to serve as a determinant that would allow engagement with the Cnx/Crt system, whereas BiP binding was observed in the absence of a glycan (63, 302, 303). Examples for glycosylated client proteins include MHC class I molecules, influenza HA, subunits of the T cell and B cell receptors, transferrin and the insulin receptor (132, 304-308). Treatment of cells with the glucosidase inhibitor castanospermine (CST) revealed that lectin-

mediated interactions required trimming of the initially transferred $Glc_3Man_9GlcNAc_2$ oligosaccharide by the combined actions of glucosidase I and II to the monoglucosylated form as shown for instance for both Cnx and Crt binding to influenza HA (39, 132). Further studies with purified oligosaccharides confirmed that Cnx and Crt function as lectins with identical binding preferences specifically for the monoglucosylated polymannose glycan (41, 286, 309).

Protein folding

The successful application of CST to inhibit glycoprotein binding to Cnx and Crt permitted the opportunity to characterize the functions of both lectins during their interactions with client proteins. Taking into account that processing of the preassembled glycans of all cellular glycoproteins are affected by this approach it can not be concluded that the observed changes in glycoprotein maturation are exclusively a direct consequence of diminished Cnx and/or Crt binding. Despite this caveat, the accumulated data from studies employing glucosidase inhibitors are suggestive of the involvement of Cnx and Crt in the folding and assembly of the majority of nascent glycoproteins (277, 310). For example, CST treatment reduced Crt interaction with early folding intermediates of HIV envelope glycoprotein (311) and completely inhibited Cnx in its folding-promoting role during tyrosinase maturation (312). Furthermore, prevention of N-glycan trimming by CST inhibited binding of Cnx or Crt to the insulin receptor and influenza HA and resulted in increased misfolding and in a decreased overall folding efficiency, respectively (307, 313). For the maturation of influenza HA, a similar outcome examining the functional consequences of the disruption of Cnx/Crt interaction with client glycoproteins was obtained in Cnx- or Crt-deficient cells (314). In the absence of Cnx, influenza HA folding was markedly impaired, while an accelerated export out of the ER with a modest decrease in folding efficiency was particularly associated with Crt depletion. An accelerated but less efficient conformational maturation was also observed for the semliki forest virus glycoprotein in cells lacking Crt (314). However, despite blocking the formation of monoglucosylated oligosaccharides, Cnx and Crt were still detected, albeit at reduced levels, in association with glycoproteins in several cases (315-319), suggesting the capabilities of both lectins also to utilize a glycosylation-independent mode for interactions.

Quality control

Cnx and Crt have been found to distinguish between native and non-native conformers of client proteins. For instance, they both preferentially interact with transferrin, influenza HA, and MHC class I molecules in their incompletely folded/assembled states rather than their native ones (130, 132, 304, 320-322). In addition, Cnx exhibited complex formation with incompletely assembled integrins, as well as with T cell, insulin, and nicotinic acetylcholine receptors (305, 307, 316, 323), and Crt was present in complexes with myeloperoxidase prior to assembly with heme (279). Achievement of fully assembled protein complexes is usually accompanied by dissociation from Cnx and Crt. Their binding preference for incompletely folded client proteins was underscored by further studies revealing an increased affinity towards non-native proteins (324, 325). These findings indicate a chaperone-like function for Cnx and Crt that allowed, in some cases, the prevention of off-pathway folding events *in vivo*. For example, both proteins assist in the maturation of influenza HA in microsomes, where they delay oligomerisation and suppress the degradation of this viral protein (313) and play a similar role in promoting the assembly of MHC class I heavy chains and suppressing their aggregation (310, 326-328). Furthermore, Cnx and Crt were shown to interact for a prolonged period of time with misfolded or incompletely assembled proteins (132, 278, 304, 323). These prolonged interactions with non-native protein conformers, in correlation with their extended residence within the ER, are suggestive that Cnx and Crt are members of the ER quality control system. As such, they function to preserve cellular homeostasis by retaining folding polypeptides in the ER until either their native conformation is attained or degradative processes engage.

Client protein spectrum

Given the identical oligosaccharide-binding specificities of Cnx and Crt it is not surprising that both proteins interact with numerous common glycoproteins, in some cases even simultaneously (301). However, comparison of the overall spectrum of interactions of both lectins chaperones with glycoproteins revealed overlapping but distinct binding pattern (132, 320, 329). Some client proteins such as the nicotinic acetylcholine receptor (330), the vesicular stomatitis virus (VSV) G glycoprotein (132), and the cystic fibrosis transmembrane conductance regulator (CFTR) (331) interact only with Cnx , whereas perforin (332) and PDI (333) solely bind to Crt. Remarkably, temporal differences for Cnx/Crt interactions are exemplified for instance by the biogenesis of MHC class I molecules since free class I heavy chains associate initially exclusively with Cnx, which dissociates at the time of successful

assembly of heavy chain with the β_2m subunit, and is then rapidly replaced by Crt (334, 335). Substrate selection of membrane bound Cnx and soluble Crt has been suggested to be related to their different topologies in the ER. Indeed, converting Cnx and Crt into a soluble and membrane bound ER protein, respectively, resulted in a binding pattern resembling that of the other (320, 327). However, since soluble as well as membrane bound glycoproteins were shown to interact either with Cnx or Crt, the different topologies of both proteins cannot solely account for their divergent binding specificities (301). The observation that a soluble truncated Cnx mutant failed to replace Crt in its role to assist MHC class I molecule biogenesis (328) illustrates that the client protein selection of Cnx and Crt must be influenced by further determinants. Studies by Hebert *et al*. revealed that the number and location of glycosylation sites of a glycoprotein represent one such determinant (336).

Ca^{2+} homeostasis and further cellular processes

In addition to their chaperoning function as part of the quality control system, Cnx and Crt perform an important role in intracellular Ca^{2+} homeostasis and Ca^{2+} storage in the ER. Remarkably, Crt alone binds over 50 % of Ca^{2+} stored in the ER and its overexpression results in a significant enhancement of Ca^{2+} concentration in intracellular stores (337-339). In contrast, Crt deficiency in cells is associated with reduced Ca^{2+} storage capacity (340). Both proteins are involved in Ca^{2+} homeostasis, since they influence Ca^{2+} efflux from the ER via the inositol triphosphate receptor and Ca^{2+} influx through modulation of the SERCA pump activity (340-343). The phosphorylation and dephosphorylation of the cytoplasmic tail of Cnx has been suggested to play an important role in this regulatory function (341). In Crt knockout mice the reduced Ca^{2+}-binding capacity resulted in a lethal phenotype due to the impaired embryonic development of cardiac tissue (344, 345). Furthermore, Crt influence on Ca^{2+} homeostasis has far-reaching impacts on cellular functions, since a multitude of transcription factors are controlled by the Ca^{2+} dependent phosphatase calcineurin, whose activity was dramatically reduced in the absence of Crt (340, 346). Cnx deficient mice are viable but exhibit a reduced life span and suffer severe neurological abnormalities (347).

The different phenotypes in Cnx and Crt deficient mice, and further studies revealing that neither Cnx nor Crt had the capacity to compensate for the loss of each other, underline the unique functions of both proteins (340, 347, 348). The viability of mammalian cell lines lacking either Cnx, Crt or even both (314, 334) and less severe phenotypes in cultured cells are indicative for the involvement of Cnx and Crt in additional cellular processes, for

example, that are essential especially during embryonic development, as they were shown to affect properties such as cell shape, adhesion, and mobility (323, 349-352).

Cnx and Crt have been shown to play a role in several further cellular processes and states including oxidative stress (353, 354), cancer (355, 356), apoptosis (357-360), and phagocytosis (361, 362). While Cnx has been localized exclusively to the ER, various studies over the last 20 years have suggested that Crt resides also outside of the ER in the cytoplasm, the nucleus, secretory granules, and at the cell surface (363-366). The latter site represents the most widely recognized localization, where Crt is thought to inhibit melanoma cell spreading (367), angiogenesis (368), to mediate thrombosspondin induced disassembley of focal contacts (369), and to act as an "eat me" signal for dendritic cells in immunogenic cell death (370, 371).

1.2.6.3 Mechanism of the folding-promoting action of calnexin and calreticulin

The question whether Cnx and Crt assist in client protein folding solely through lectin- or additionally polypeptide-based interactions has spurred an ongoing debate in the literature.

The "lectin-only" model

Helenius and co-workers proposed in the "lectin-only" model (Fig. 4) that transient cycles of binding and release from Cnx and Crt are regulated by the availability of the terminal glucose on Asn-linked oligosaccharide chains (39, 40). Such monoglucosylated oligosaccharides are formed by the sequential action of glucosidase I and II on the preassembled $Glc_3Man_9GlcNac_2$ oligosaccharide and allow initial binding of nascent glycoproteins with micromolar affinities (372). Dissociation of the relatively weakly bound oligosaccharide, in conjunction with the removal of the remaining outermost glucose residue by glucosidase II, prevents rebinding, at which point the glycoprotein may fold and be exported from the ER. If folding does not occur promptly, the glycoprotein becomes a substrate for UGGT, that reattaches the glucose residue only on incompletely folded glycoproteins probably at a glycan likely at least 40 Å away from a non-native surface (44) and thereby facilitates glycoprotein re-entry into the Cnx/Crt cycle (42-44). In this model UGGT sets up a quality control cycle, where it is thought to act as the only folding sensor, whereas Cnx and Crt are thought not to be functioning as classical chaperones by directly binding to hydrophobic segments on glycoprotein folding intermediates. Rather, Cnx and Crt are proposed to promote oxidative folding by recruiting

ERp57 and possible other folding enzymes to the vicinity of the folding glycoprotein (373). It can also be envisioned that, through lectin-based binding, a folding glycoprotein may become sequestered between the arm and globular domains of Cnx and Crt, thereby preventing non-favorable interactions with other aggregation prone folding intermediates (38). In the case of misfolded or mutant glycoproteins, extended cycles of binding and release contribute to retention within the ER until they are further processed by demannosylation, which diverts

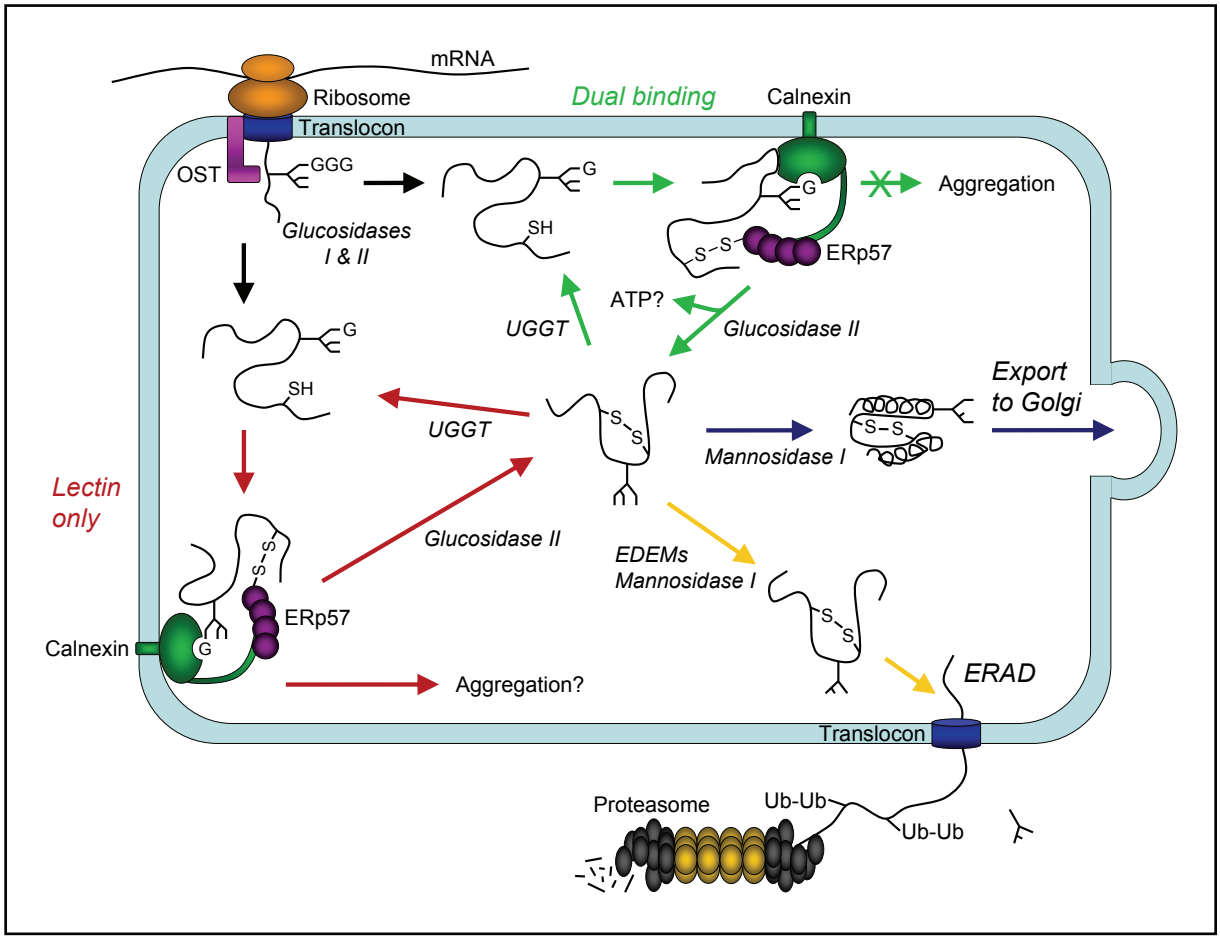

Fig. 4: Proposed model of calnexin and calreticulin action. As a nascent polypeptide chain merges cotranslationally and cotranslocationally into the ER through the translocon pore, it may be glycosylated by OST with one or more preassembled $Glc_3Man_9GlcNAc_2$ oligosaccharides. Removal of the two outermost glucose residues by the sequential action of glucosidase I and II results in the $Glc_1Man_9GlcNAc_2$ oligosaccharide, which allows initial association with Cnx and Crt. In the "lectin-only" model (red arrows), entry and release of a glycoprotein during chaperone cycles are exclusively controlled through de- and reglucosylation of the monoglucosylated glycan species by glucosidase II and UGGT, respectively. UGGT serves as the only folding sensor since it ignores glycoproteins with significant folding defects and only adds back a glucose residue to nearly native folding intermediates. Cycling by the lectin chaperones prevents premature export of folding glycoproteins out of the ER and facilitates disulfide bond formation and isomerization through recruitment of ERp57. In the "dual-binding" model, Cnx and Crt exhibit an additional binding site selective for exposed regions of incompletely folded client proteins. This polypeptide-based interaction is influenced by ATP and contributes to enhanced protein folding by preventing aggregation. In both models, release from the chaperone cycle is obligatory for client proteins whose conformational maturation occurs in the unbound form. Properly folded and assembled proteins are subjected to further glycan trimming and are transported out of the ER to the Golgi. After futile cycling in the chaperone system, mannosidase I in concert with one or more EDEM proteins target folding-incompetent glycoproteins by extensive demannosylation for retrotranslocation to the cytosol and proteasomal disposal. Ub, ubiquitin.

them from the cycle and into the ERAD disposal pathway (38).

Several lines of evidence supporting the "lectin-only" model are based on results from studies with glucosidase-deficient cells or cells treated with glucosidase inhibitors showing dramatically reduced interactions of Cnx and Crt with a variety of glycoproteins (277, 279, 310, 312, 374). In addition, removal of the oligosaccharide chains and/or removal of the glucoses from ribonuclease (RNase) B following complex formation with Cnx or Crt, resulted in dissociation of the complexes (375). In other cases, inhibition of glucosidase II in cells following complex formation impaired complex dissociation, indicating that the activity of glucosidase II is essential for glycoprotein release from Cnx/Crt (40, 308, 376). Furthermore, Cannon and Helenius showed that binding of the VSV G glycoprotein to Cnx was exclusively a lectin-oligosaccharide-based interaction, which was renewed through reglucosylation by UGGT (376). Collectively, these studies demonstrated the importance of cycles of deglucosylation and reglucosylation for proper glycoprotein folding. It also appeared that the association of Crt with MHC class I molecules and binding of Cnx/Crt to RNase B did not depend on their conformational maturation states, challenging a true chaperone function of both lectins (375, 377, 378). Additional evidence strengthening the role of Cnx and Crt in recruiting folding enzymes rather than functioning as classical chaperones was the discovery that Cnx and Crt associate with Erp57 and that its binding to various glycoproteins was affected by treatment with glucosidase inhibitors (379). Based on these observations it has been proposed that the main function of Cnx and Crt is to retain folding glycoproteins in the ER during cycles of quality control and to expose them to ERp57 to promote their oxidative folding.

The "dual-binding" model

In an extended "dual-binding" model (Fig. 4), proposed by Williams and co-workers, Cnx and Crt are thought to possess the capacity to utilize, in addition to their lectin site, a second binding site to promote protein folding via polypeptide-based interactions (283, 284). The recognition of hydrophobic segments exposed on non-native protein conformers would permit Cnx/Crt to function in a manner similar to classical chaperones and to serve as another folding sensor in addition to UGGT during quality control cycles of binding and release. In this model Cnx/Crt binding cycles are controlled by the opposing activities of glucosidase II and UGGT that dictate the carbohydrate composition on maturing glycoproteins, as well as by affinity changes in the polypeptide-binding sites of the lectin chaperones. These changes are possibly regulated by a shift from an ATP-bound to an ATP-unbound state or by other factors. As in

the lectin model, binding of Cnx and Crt serves to prevent premature release of folding intermediates from the ER and promotes proper folding by providing a privileged environment in which associated ERp57 promotes thiol oxidation and isomerization reactions (181, 373) and, additionally, suppresses off-pathway aggregation due to their polypeptide-binding chaperone function.

The concept of a "dual-binding" model is supported by numerous studies *in vivo* and *in vitro*. For example, findings that Cnx and Crt bind to non-glycosylated polypeptides such as the δ subunit of the T cell receptor (TCR), the TM domain 2 of the P-glycoprotein or PDI are suggestive of polypeptide-based interactions (317, 333, 380, 381). Such a mode of binding might also account for the unaffected stability of Cnx complexes with some glycoproteins despite removal of oligosaccharides by Endo H digestion following complex formation (309, 382, 383). Also, association of a wide spectrum of proteins with Cnx has been observed in glucosidase deficient cell lines (384) in accordance with observations showing that the interactions of proteins, including HIV gp160 and MHC class I heavy chain, were not affected following treatment of cells with glucosidase inhibitors (310, 311). These findings contrast with results obtained from similar experiments conducted by proponents of the "lectin-only" model using glucosidase deficient cell lines or glucosidase inhibitors. This discrepancy might stem from differences in cell lysis and immunoisolation conditions, since Danilczyk and Williams demonstrated that polypeptide-based interactions between Cnx/Crt and client proteins survive mild immunoisolation conditions, while almost no co-immunoprecipitated proteins were detected applying higher temperature and harsher detergent (310). It can be argued that the observed glycan-independent interactions are just an artifact due to non-specific formation of aggregates between Cnx/Crt and client proteins. This explanation was excluded in several cases since client proteins appeared to be soluble without any evidence of aggregation as shown by sedimentation studies (310, 385). The apparently conflicting results might also simply reflect the specific recognition of a respective client protein by Cnx and Crt through either their oligosaccharide- or polypeptide-binding sites or even both binding sites during their temporary interaction.

Further evidence supporting the "dual-binding" model, and more relevant in respect to the chaperone function of Cnx/Crt, stems from comprehensive aggregation suppression studies based on assays commonly used to characterize chaperones from the Hsp60, 70, and 90 families (386-388). Therein Cnx and Crt have been shown to be capable of suppressing the aggregation of deglycosylated forms of α-mannosidase, soybean agglutinin (SBA), and chicken immunoglobulin Y (IgY), as well as non-glycosylated client proteins such as citrate

synthase or malate dehydrogenase, and additionally maintaining them in a folding competent conformation (283, 284). Cnx and Crt also bind preferentially to non-native conformers of non-glycosylated proteins, consistent with a classical chaperone function. Furthermore, they suppress aggregation more efficiently in the presence of ATP (283, 284). The latter effect can probably be attributed to the induction of an increase in surface hydrophobicity of both chaperones upon ATP binding. In this context the lack of an obvious hydrophobic polypeptide-binding site in the X-ray crystal structure does not seem surprising, since the crystallization of Cnx was conducted in the absence of ATP (282). Also, a hydrophobic Crt binding peptide was shown to compete with Crt's ability to suppress the thermally induced aggregation of a soluble MHC class I molecule (389), consistent with the presence of a polypeptide-binding site on Cnx and Crt. To characterize the specificity of this site of Crt, Houen and co-workers examined an extensive panel of peptides for their binding to Crt using a competitive ELISA assay (390, 391). Peptide binding required a minimum peptide length of five residues that were hydrophobic in character.

Further support for a lectin-independent chaperone function of Cnx and Crt comes from measurements comparing the ability of wild type Cnx and lectin-deficient Cnx to protect MHC class I molecules from degradation in insect cells (287). Results from this study using pulse chase experiments clearly demonstrate that the lectin site of Cnx is dispensable for its chaperone function in this case. Nevertheless, while Cnx and Crt exhibited the ability to suppress the aggregation of deglycosylated glycoproteins, its aggregation suppression capacity was significantly enhanced in the presence of monoglucosylated glycans on their client proteins (283, 284). Similar experiments were performed in a subsequent study comparing the aggregation suppression potencies of the ER Hsp70 chaperone BiP and Cnx for non-glycoproteins and monoglucosylated glycoproteins (392). Both proteins suppressed the aggregation of non-glycosylated citrate synthase at comparable levels, but Cnx was significantly more efficient than BiP in aggregation suppression assays using monoglucosylated α-mannosidase and chicken IgY. Deglycosylation of those two glycoproteins resulted again in a comparable aggregation suppression potency for Cnx and BiP.

Collectively, these studies are consistent with the "dual-binding" model, wherein Cnx and Crt associate with folding glycoproteins through both lectin- and polypeptide-based interactions, thereby increasing the avidity of the association relative to either interaction alone.

1.3 Rationale of this thesis

At the beginning of this project, accumulating results from various studies led to the suggestion that Cnx and Crt can function as molecular chaperones, specifically since they revealed the ability to suppress the aggregation of deglycosylated and non-glycosylated proteins *in vitro* in a lectin-independent way, similar to classical molecular chaperones.

Because most of the *in vitro* aggregation suppression assays with Cnx and Crt were performed at elevated temperature (42-47°C) to induce the aggregation of the client proteins (283, 284, 389, 393) or involved the removal of Ca^{2+} (389, 393), concerns have been voiced that polypeptide-based interactions are a consequence of an altered chaperone conformation that may not be prevalent under physiological conditions of the ER lumen. Consistent with such a possibility is the finding that Crt has a remarkably low melting temperatures of 46.4°C and 40.2°C in buffer containing 1 mM and 0 mM Ca^{2+} respectively, underlining the role of Ca^{2+} in stabilizing the chaperone structure (281). To overcome this issue an assay system needed to be developed that allowed the examination of the aggregation suppression of a non-glycosylated protein by Cnx or Crt at 37°C, and that permitted an assessment of what impact physiological concentrations of Ca^{2+} and ATP may have on this process. This functional approach, in combination with structural studies, should provide insights into the extent to which the aggregation suppression functions of Cnx or Crt are influenced by environmental parameters prevalent within the lumen of the ER. Such an assay system was developed and characterized for Cnx as described in chapter 3.2 of this thesis.

In contrast to the lectin sites of Cnx and Crt which have been well defined through structural and mutagenesis studies (282, 288, 289), little is known about their polypeptide-binding sites, particularly their locations and polypeptide-binding specificities. Initial deletion mutagenesis studies with Cnx and Crt and more recent peptide binding studies with Crt suggested that the putative polypeptide-binding site, responsible for their ability to suppress the aggregation of non-native proteins, resides within their globular domains (280, 297), with a specificity for peptides hydrophobic in character (390, 391). Since these studies again were conducted under non-physiological conditions that are likely to result in partial unfolding of both chaperones, it cannot be excluded that the observed polypeptide-based interactions are non-specific. Given these limitations and the fact that there have been no reports examining the nature of the polypeptide-binding site of Cnx, it was of great interest to investigate the location and characteristics of Cnx's polypeptide-binding site under physiological conditions of the ER lumen. Therefore, in chapter 3.3 of this thesis, various deletion mutants of Cnx

were tested in the newly established aggregation assay and characterized in terms of their binding to an oligosaccharide and to non-native client polypeptides of increasing size. These studies provided important insights into the polypeptide-binding site and domain contributions to the overall chaperone function of Cnx.

2 Materials and Methods

2.1 Materials

Materials and equipment that are not listed below corresponded to the common laboratory standards.

2.1.1 Chemicals and enzymes

All chemicals and enzymes used in this study were of analytical grade and purchased from the following companies:

Antibiotics: SIGMA-ALDRICH (Oakville, ON, Canada).
Chemicals: BECTON DICKINSON (Le Pont-de-Claix-Cedex, France), BDH CHEMICALS (Toronto, ON, Canada), BIO-RAD LABORATORIES (Hercules, CA, USA), BIOSHOP (Burlington, ON, Canada), CALEDON LABORATORIES (Georgetown, ON, Canada), COMMERCIAL ALCOHOLS (Brampton, ON, Canada), FISHER SCIENTIFIC (Fair Lawn, NJ, USA), ICN BIOMEDICALS (Aurora, OH, USA), INVITROGEN (Eugene, OR, USA), MERCK (Darmstadt, Germany), ROCHE DIAGNOSTICS (Mannheim, Germany), and SIGMA-ALDRICH (Oakville, ON, Canada).
Enzymes: RNase A was purchased from BIOSHOP (Burlington, ON, Canada). Factor Xa protease was ordered from GE HEALTHCARE (Piscataway, NJ, USA). *Pfu*-DNA polymerase, restriction enzymes, and T4-DNA ligase were obtained from MBI FERMENTAS (Burlington, ON, Canada). Recombinant firefly luciferase (FL) was purchased from PROMEGA (Madison, WI, USA). DNase I was from ROCHE (Indianapolis, IN, USA). α-lactalbumin and bovine pancreatic trypsin (type III-S) were ordered from SIGMA-ALDRICH (Oakville, ON, Canada).
Oligosaccharide: The G_1M_3 oligosaccharide (Glcα1-3Manα1-2Manα1-2Man-OH) was purchased from the ALBERTA RESEARCH COUNCIL (Edmonton, AB, Canada).
Peptides: The 6KSGG peptide (KKKKKKSGGSGGSGGSC) with an amidated C-terminus was purchased from GENSCRIPT (Piscataway, NJ, USA). The 6KAAW peptide (KKKKKKAAWAAWAAWAA) and the KHP peptide (KHPYAYLAAAIAAEVAGT-TALKLSK), corresponding to the first transmembrane helix (residues 2-24) of the

Halobacterium salinarum protein Hsmr, were a generous gift from Dr. Charles Deber, SICKKIDS, Toronto. The YSN peptide (YSNENMETM) was synthesized by the ALBERTA PEPTIDE INSTITUTE (Edmonton, AB, Canada). All peptides were purified by reverse-phase HPLC, dissolved in 20 mM Hepes, pH 7.4, 150 mM NaCl, and 0.4 mM $CaCl_2$, aliquoted, and stored at -70°C.

2.1.2 Bacterial strains and plasmids

All bacterial strains, vectors, and plasmids used in this study are listed in Tab. 2.

Tab. 2: Overview of bacterial strains, vectors, and recombinant plasmids used in this study.

Strains	Genotype/Characteristics	Source or reference
E. coli FA113	DHB4 *gor522*. . .mini-Tn10Tc *trxB*::Km *supp*	(394)
E. coli BL21-CodonPlus(DE3)	*E. coli* B F^- *ompT hsdS*(r_B^- m_B^-) *dcm*$^+$ Tet^r *gal* λ(DE3) *endA* Hte [*argU ileY leuW* Cam^r]	STRATAGENE, La Jolla, CA, USA
E. coli XL1-blue *MRF′*	Δ*(mcrA)183* Δ *(mcrCB-hsdSMRmrr) 173 endA1 supE44 thi-1 recA1 gyrA96 relA1 lac* [F‘ *proAB lacIq ZΔM15* Tn*10* (Tet^r) *Amy* Cam^r]	(395)
Vectors		
pGEX-3X	P_{tac} Amp^r pBR322 ori, GST-tag	GE HEALTHCARE
pET15b-TEV	P_{T7} Amp^r ColE1, His-tag	(396)
Recombinant plasmids encoding various constructs of the soluble ER-luminal domain of calnexin (S-Cnx)	(for nomenclature see Fig. 5)	
pGEX-3X-S-Cnx	pGEX-3X with *S-Cnx*-PCR fragment, C-terminal His-tag	(283)
pGEX-3X-glob	pGEX-3X with *glob*-PCR fragment, C-terminal His-tag	(280)
pEtT15b-TEV-S-Cnx	pET15b-TEV with *S-Cnx*-PCR fragment, N-terminal His-tag	this study
pEtT15b-TEV-Δarm1	pET15b-TEV with *Δarm1*-PCR fragment, N-terminal His-tag	this study
pEtT15b-TEV-Δarm2	pET15b-TEV with *Δarm2*-PCR fragment, N-terminal His-tag	this study
pEtT15b-TEV-glob	pET15b-TEV with *glob*-PCR fragment, N-terminal His-tag	this study
pEtT15b-TEV-arm	pET15b-TEV with *arm*-PCR fragment, N-terminal His-tag	this study
pEtT15b-TEV-LD-S-Cnx	pET15b-TEV with *LD-S-Cnx*-PCR fragment, N-terminal His-tag	this study

2.1.3 Oligonucleotides

All oligonucleotides used in this study (Tab. 3) were purchased from SIGMA-ALDRICH (Oakville, ON, Canada). The lyophilized oligonucleotides were dissolved in distilled water with a final concentration of 10 pmol/µl and stored at -20°C.

Tab. 3: Oligonucleotides used in this study. Restriction sites are underlined, stop codons are marked in italics, and introduced codons are highlighted in bold letters.

Primer	Sequence 5' → 3'	Modifications
S-Cnx-forward	atatatatatcatatgcatgaaggacatgatgatgatatg	*Nde*I
S-Cnx-reverse	atatatggatcc*tta*ccacgggcgctcctcagctgcctc	*Bam*HI, Stop
arm-forward	atatatatatcatatgattgaggacccagaagaccagaag	*Nde*I
arm-reverse	atatatggatcc*tta*gaaatccggatttggtatcttcc	*Bam*HI, Stop
Δarm1-forward	gtacctgat**ggtagtgga**cagatcgccaaccctaagtgt	GlySerGly-linker
Δarm1-reverse	ggcgatctg**tccactacc**atcaggtacatattcgggttc	GlySerGly-linker
Δarm2-forward	gatgatgaa**ggtagtgga**ggtgtctggcagcgacctatg	GlySerGly-linker
Δarm2-reverse	ccagacacc**tccactacc**ttcatcatctaaccagccatc	GlySerGly-linker
LD-S-Cnx-forward	caagacccct**gcc**acgatt**gcc**tttggtccagataaatgtggagaagactataagcttcac ttc**gcc**ttccgccacaaaaacccc	Y166A, M169A, *Hin*dIII, I184A
LD-S-Cnx-reverse	gtggcggaa**ggc**gaagtgaagcttatagtcttctccacatttatctggaccaaa**ggc**aatc gt**ggc**aggggtcttgtcgtggaact	I184A, *Hin*dIII, M169A, Y166A

2.1.4 Culture media

LB-medium: 10 g/L tryptone, 5 g/L yeast extract, 10 g/L NaCl

The pH value was adjusted to 7.5 with 2 N NaOH and the medium was autoclaved before use. For making LB-agar plates, 1.5 % (w/v) bacto agar was added to LB-medium before autoclaving. Non heat-resistant additives were sterile filtered using membrane filters with a pore size of 0.2 µm (PALL CORPORATION, Ann Arbor, MI, USA). Liquid and solid media were supplemented with 100 µg/ml ampicillin (Amp) used for selection of Amp resistant *E. coli* strains.

2.2 Methods

2.2.1 Isolation of nucleic acid

Plasmid DNA from *E. coli* was isolated with the "GeneJET™ Plasmid Miniprep Kit" from MBI FERMENTAS (Burlington, ON, Canada) according to the manufacturer's protocol. The method is based on alkaline lysis of bacterial cells and the ability of DNA to bind silica in the presence of high concentrations of chaotropic salts (397-399). DNA was eluted with 50 µl of sterile water and its concentration was determined by absorbance measurement at 260 nm.

2.2.2 Nucleic acid gel electrophoresis

Electrophoretic separation of DNA for its analysis and isolation was conducted in an "i-Mupid Mini Agorose Gel Electrophoresis Apparatus System" (HELIXX TECHNOLOGIES, Toronto, ON, Canada) using 1-2 % (w/v) agarose gels as described by Sambrook *et al*. (400). As electrophoretic buffer 0.5x TBE (89 mM Tris-HCL, pH 8.3, 89 mM boric acid, and 2.5 mM Na_2-EDTA) was used. The separated DNA was visualized in the gel using "SYBR® Safe DNA gel stain" (INVITROGEN, Eugene, OR, USA) via an "UV transilluminator" from ULTRAVIOLETPRODUCTS (Cambridge, UK) and documented with a "Gel Doc 2000" from BIO-RAD (Hercules, CA, USA). To size DNA fragments the "GeneRuler™ DNA Ladder Mix" from MBI FERMENTAS (Burlington, ON, Canada) was used as a molecular weight standard. Extraction of DNA from agarose gels was carried out with the "QIAEX II Gel Extraction Kit" from QIAGEN (Mississauga, ON, Canada) pursuant to the protocol provided.

2.2.3 *In vitro* recombination of DNA

Digestion of DNA with restriction enzymes and ligation of DNA fragments were performed with reaction buffers and enzymes from MBI FERMENTAS (Burlington, ON, Canada) according to Sambrook *et al*. (400) as well as the manufacturer's recommendations.

2.2.4 Transformation of bacteria

2.2.4.1 Chemical transformation of *E. coli*

The $RbCl_2$ method of Hanahan (401) was applied for preparation of transformation competent *E. coli* cells and their transformation with plasmid DNA.

2.2.4.2 Electroporation of *E. coli*

The preparation of electrocompetent bacterial cells and their electrotransformation was performed in accordance with the method of Fiedler and Wirth (402). The electroporation of *E. coli* strains was conducted in an "E. coli Pulser apparatus" from BIO-RAD (Hercules, CA, USA).

2.2.5 Storage of bacteria

Colonies of *E. coli* strains grown on agar plates were kept at 4°C. For long-term storage, 1.5 mL of liquid cell cultures containing 8 % (v/v) DMSO were frozen at -70°C.

2.2.6. Standard polymerase chain reaction (PCR)

Amplification of DNA-fragments was conducted under standard PCR-conditions in a reaction mix containing plasmid-based template (1-25 ng), primer oligonucleotides (50 pmol each), dNTP's (0.2 mM each, ROCHE, Indianapolis, IN, USA), and *Pfu*-Polymerase (2.5 U). The buffer containing $MgSO_4$ was used as recommended by the manufacturer's protocol. Generally, 5 % (v/v) DMSO was added to the reaction mix. Conditions for standard PCR were: 1 x (2 min at 95°C); 35 x (30 s at 95°C; 30 s at 58°C; 30 s up to 4 min at 72°C, depending on the length of target gene), 1 x (7 min at 72°C). The PCR was performed using a "PTC-200 Peltier Thermal Cycler" from MJ RESEARCH (Waltham, MA, USA). The resulting PCR-products were purified by gel extraction using a "QIAEX II Gel Extraction Kit" from QIAGEN (Mississauga, ON, Canada).

2.2.7 Mutagenesis of calnexin cDNA

Amino acid numbering refers to the canine Cnx sequence with residue 1 corresponding to the first residue following signal cleavage. Oligonucleotides used in this study are listed in Tab. 3. The soluble ER-luminal domain of canine calnexin (S-Cnx, residues 1-461) and its globular domain (glob, residues 1-255/390-461) were each amplified in standard PCR reactions with primer pair S-Cnx-forward/S-Cnx-reverse using as templates the previously generated glutathione-S-transferase fusion constructs, pGEX-3X-S-Cnx (283) and pGEX-3X-glob (280), respectively. The latter construct contains a GSGSG linker between residues 255 and 390. The arm domain (arm, residues 256-389) was synthesized in a standard PCR reaction with the primer pair arm-forward/arm-reverse using pET15b-Tev-S-Cnx as the template (see below). To generate two mutants of S-Cnx with a truncated arm domain, Δarm1 (Δaa315-334) and Δarm2 (Δaa309-347), an overlap extension PCR (403) was performed. In both cases, plasmid pET15b-Tev-S-Cnx was used as the template in the first round of PCR reactions. For construct Δarm1, a 975 bp and a 420 bp DNA fragment were amplified with primer pairs S-Cnx-forward/Δarm1-reverse and Δarm1-forward/S-Cnx-reverse, respectively. For construct Δarm2, a 958 bp and a 381 bp DNA fragment were amplified with primer pairs S-Cnx-forward/Δarm2-reverse and Δarm2-forward/S-Cnx-reverse, respectively. After purification, the synthesized DNA fragments were used in equimolar amounts as the template in a second PCR to amplify the complete constructs using the primer pair S-Cnx-forward/S-Cnx-reverse. The mutagenic PCR primers for both the Δarm1 and Δarm2 constructs introduced a GSG linker at the site of truncation (Tab. 3). To generate a lectin-deficient mutant of S-Cnx (LD-S-Cnx), an overlap extension PCR was performed to introduce the amino acid exchanges Y166A, M169A, and I184A into the lectin site of S-Cnx. In the first round of PCR reactions, plasmid pET15b-Tev-S-Cnx was used as the template. A 577 bp and a 919 bp DNA fragment were amplified with primer pairs S-Cnx-forward/LD-S-Cnx-reverse and LD-S-Cnx-forward/S-Cnx-reverse, respectively. After purification, the synthesized DNA fragments were used in equimolar amounts as the template in a second PCR to amplify the complete constructs using the primer pair S-Cnx-forward/S-Cnx-reverse. All generated PCR products were digested with *Nde*I and *Bam*HI and subsequently ligated into the expression vector pET15b-Tev, a modified pET15b vector carrying a tobacco etch virus (TEV) protease cleavage site after the N-terminal His_6-tag. The integrity of each construct (Fig. 5) was confirmed by DNA sequencing.

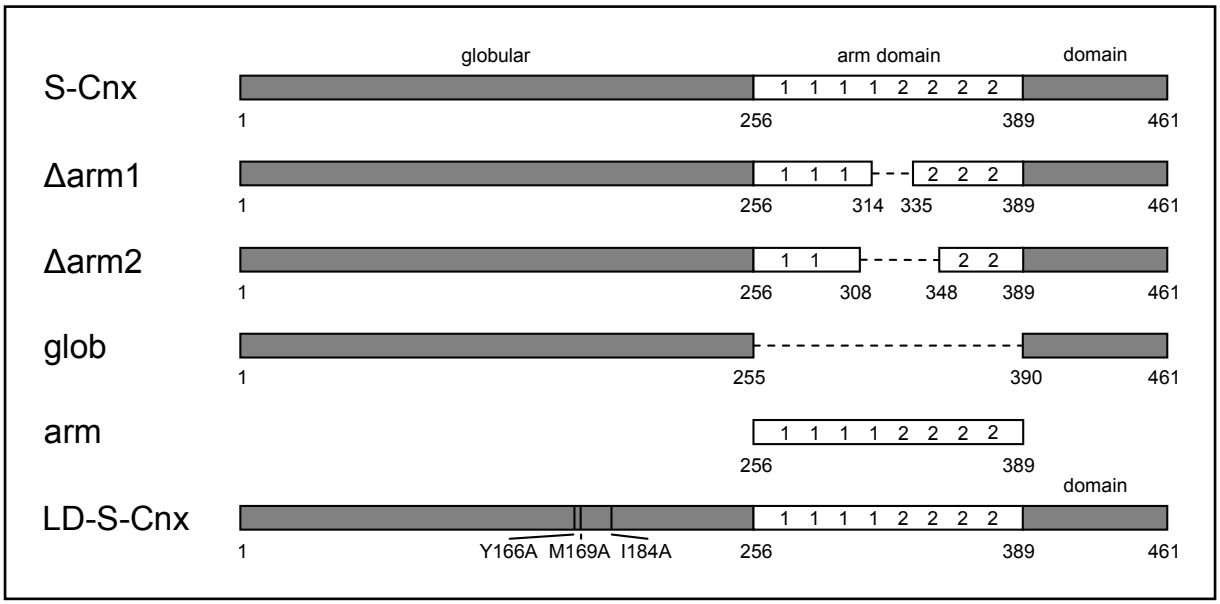

Fig. 5: Illustration of the linear sequences of S-Cnx constructs. The Δarm1 construct represents S-Cnx with an arm domain lacking amino acids 315–334. The Δarm2 mutant is shortened further by removal of amino acids 309–347 and, for the globular domain construct (glob), the complete arm domain (arm) was removed. The three alanine exchanges of the lectin-deficient S-Cnx mutant (LD-S-Cnx) are indicated. Numbers 1 and 2 within the arm domain represent two proline-rich, tandemly repeated sequence motifs. Removed amino acids are shown as dashed lines.

2.2.8 DNA sequencing

All PCR products and DNA constructs were verified via sequencing performed by ACGT CORP. (Toronto, ON, Canada).

2.2.9 Bacterial growth and protein overexpression

Protein overexpressions were performed with the bacterial expression vectors pGEX-3X, encoding C-terminal His_6-tagged S-Cnx, and pET15b-TEV, carrying the various N-terminal His_6-tagged S-Cnx constructs, in *E. coli* strains FA113 and BL21-CodonPlus(DE3), respectively. LB-medium (60 mL) containing Amp as the selection marker (LB/Amp) were inoculated with the respective freshly transformed *E. coli* strain and incubated at 37°C until a cell density (OD_{600}) of 1. This preculture was transferred into 1940 mL prewarmed LB/Amp and grown at 37°C until an OD_{600} of 0.6 was reached. Following induction of overexpression with a final IPTG concentration of 1 mM, *E. coli* FA113 or BL21-CodonPlus(DE3) cultures were shaken for another 16 h at RT or 4 ½ hours at 30°C, respectively. Bacteria were

harvested by centrifugation (30 min, 4 °C, 3500 x g) using a "Sorvall RC-3B" from SORVALL INSTRUMENTS (Newtown, CT, USA).

2.2.10 Cell disruption

To prepare a cell-free lysate for the purification of the various S-Cnx constructs the pelleted cells of the *E. coli* FA113 and BL21-CodonPlus(DE3) strains were resuspended in 30 mL ice-cold 50 mM Tris-HCL, pH 8, 300 mM NaCl, and 3 mM $CaCl_2$, containing DNase I (15 µM), RNase A (22 µM), and protease inhibitors (AEBSF (420 µM), bestatin (48 µM), leupeptin (39 µM), and pepstatin A (24 µM), all from BIOSHOP, Burlington, ON, Canada). Cell lysis was performed by passing the bacterial suspension twice through a precooled "French® Pressure Cell Press" (THERMO SPECTRONIC, Rochester, NY, USA) at 110 MPa. The lysate was centrifuged at 30,000 x g for 60 min at 4°C and the obtained supernatant containing the respective hexahistidine-tagged S-Cnx construct was kept for subsequent purification steps performed, unless stated otherwise, at 4°C.

2.2.11 Protein purification

2.2.11.1 Purification of C-terminal His_6-tagged S-Cnx

C-terminal His_6-tagged S-Cnx fused at the N-terminus to glutathione S-transferase (GST) was purified by nickel-agarose chromatography (Qiagen, Mississauga, ON, Canada) according to the manufacturer's protocol (final elution with 250 mM imidazole). The eluate was dialysed against 50 mM Tris-HCL, pH 8, 150 mM NaCl, and 1 mM $CaCl_2$ before addition of the protease Factor Xa (1 unit/ml) to release S-Cnx from GST. After a 16 h digestion at RT, the $CaCl_2$ concentration was increased to 3 mM and the digest was passed through a glutathione-agarose column (Sigma, St Louis, MO, USA) to remove GST. The S-Cnx-containing flow-through fraction was dialysed against 20 mM Tris-HCL, pH 8, 50 mM NaCl, and 3 mM $CaCl_2$ and S-Cnx was further purified by Mono Q anion exchange FPLC (8 ml column, PHARMACIA BIOTECH, Piscataway, NJ, USA) using a linear, 200 ml 0.05-1 M NaCl gradient in 20 mM Tris-HCL, pH 8, and 3 mM $CaCl_2$. Purified S-Cnx was dialysed against 20 mM Hepes, pH 7.4, 150 mM NaCl, and 1 mM $CaCl_2$ and frozen in aliquots at -20°C. Aliquots were thawed only once, immediately prior to use. Recombinant S-Cnx expressed with a C-

terminal His_6-tag was used in results section 3.2.

2.2.11.2 Purification of N-terminal His_6-tagged S-Cnx constructs

For the purification of the respective S-Cnx constructs with an N-terminal hexahistidine-tag the supernatant fraction (2.2.10) was loaded onto a nickel-NTA-agarose column (QIAGEN, Mississauga, ON, Canada). Subsequent washing steps and the final elution of the recombinant protein with 250 mM imidazole were performed as described in the manufacturer's protocol. The eluate was dialysed against 20 mM Tris-HCL, pH 8, 50 mM NaCl, and 3 mM $CaCl_2$ and subjected to further purification by Mono Q anion exchange chromatography (PHARMACIA BIOTECH, Piscataway, NJ, USA) applying a linear, 200 ml NaCl gradient (0.05-1 M) in 20 mM Tris-HCL, pH 8, and 3 mM $CaCl_2$. After a final dialysis against 20 mM Hepes, pH 7.4, 150 mM NaCl, and 1mM $CaCl_2$, purified proteins were aliquoted and stored at -70 °C. The N-terminal His_6-tagged proteins were studied in results section 3.3.

2.2.12 Determination of protein concentration

Protein concentrations were calculated by reading the optical density at 280 nm at a "BioPhotometer" (EPPENDORF, Hamburg, Germany). The required molar extinction coefficients of the respective S-Cnx constructs were ascertained using the software "ProtParam" provided by the "ExPASy proteomics server" of the SWISS INSTITUTE OF BIOINFORMATICS (http://ca.expasy.org/tools/protparam.html).

2.2.13 SDS-polyacrylamide gel electrophoresis (SDS-PAGE)

Proteins were separated under reducing conditions in the presence of SDS in a discontinuous gel system consisting of a 5 % stacking gel and an either 10 or 16 % separating gel as described by Laemmli (404). Protein samples were mixed with SDS loading buffer (50 mM Tris-HCl, pH 6.8, 4 % (w/v) SDS, 10 % glycerol, 60 mM DTT, and 0.03 % (w/v) bromphenol blue) and denatured at 95°C for 10 min before loading onto the gel. The gel electrophoresis was performed in a "Mini-PROTEAN® II Electrophoresis Cell" from BIO-RAD (Hercules, CA, USA) with a voltage of 150 V and the separated proteins were stained with Coomassie Brilliant Blue R-250.

2.2.14 Adjustment of Ca^{2+} concentration

All experiments were performed using buffer consisting of 20 mM Hepes, pH 7.4, 150 mM NaCl, and 1 mM $CaCl_2$ with various protein or nucleotide additives being prepared in the same buffer. For experiments involving a fixed 1 mM Ca^{2+} concentration, all assay components were simply mixed together. For final Ca^{2+} concentrations other than 1 mM, adjustments were made using two methods. In the first method, samples were prepared by first adding buffer, followed by EDTA to a final concentration of 1 mM, and then sufficient $CaCl_2$ to achieve the desired final free Ca^{2+} concentration. S-Cnx constructs, firefly luciferase, or other components were added last. The Ca^{2+} contributed by these final additions was taken into account when calculating the final Ca^{2+} concentration. In the second method, the respective S-Cnx construct, peptide, and nucleotide were mixed with the appropriate amounts of $CaCl_2$ and calcium-free buffer (20 mM Hepes, pH 7.4, and 150 mM NaCl) to achieve the desired final Ca^{2+} concentration. Final free Ca^{2+} concentrations were confirmed by direct measurement using the Ca^{2+}-specific electrode in a "Radiometer ABL700 Blood Gas Analyzer" (RADIOMETER, Copenhagen, Denmark). S-Cnx constructs were typically equilibrated for 1 h in the final buffer prior to experiment, although preincubations as short as 10 min were sufficient.

2.2.15 Trypsin digestion

S-Cnx (48 µg) was preincubated in 20 mM Hepes, pH 7.4, 150 mM NaCl, and the indicated Ca^{2+} and ATP concentrations for 1 h at RT. All digestions were performed in a final volume of 360 µL at 37°C with 0.48 µg bovine pancreatic trypsin. Aliquots containing 4 µg S-Cnx were removed at each time point, mixed with SDS-PAGE sample buffer, and heated at 95°C for 5 min. Digestion products were analyzed by SDS-PAGE (2.2.13) using 10 % polyacrylamide gels with visualization by Coomassie Brilliant Blue R-250 staining.

2.2.16 Aggregation assay

Recombinant firefly luciferase was dialyzed against 20 mM Hepes, pH 7.4, 150 mM NaCl, 1 mM $CaCl_2$, and 0.5 % glycerol and rapidly frozen in 2.5 µL aliquots at an average concentration of 230 µM. Aliquots were thawed only once, immediately prior to use. S-Cnx

and deletion mutants were equilibrated at their respective concentrations in 20 mM Hepes, pH 7.4, 150 mM NaCl, and the indicated Ca^{2+} and/or nucleotide concentrations with or without peptides (20 µM) or α-lactalbumin (10 µM) for 1 h at RT or 37°C. FL was then diluted into the respective samples to a final concentration of 3 µM in a total volume of 150 µL. Aggregation was monitored immediately at 37°C by measuring light scattering at 360 nm in a "Shimadzu 1601" spectrophotometer (SHIMADZU, Columbia, MD, USA) equipped with a temperature-controlled sample compartment. Absorbance readings were taken every 6 s.

2.2.17 Fluorescence experiments

S-Cnx constructs (0.6 or 0.8 µM) were equilibrated in 150 µL of 20 mM Hepes, pH 7.4, 150 mM NaCl, and the indicated Ca^{2+} and/or ATP concentrations in the presence or absence of various peptides (20 µM) for 1 h at RT or 37°C. For the titration of the various peptides against S-Cnx and Δarm2, samples were allowed to equilibrate for 10 min between the respective titration steps. Intrinsic fluorescence of S-Cnx constructs was measured with an excitation wavelength of 280 nm, if not stated otherwise. For measurements of the interaction between the hydrophobic fluorescent probe 1,1'-bis(4-anilino)naphthalene-5,5'-disulfonic acid (bis-ANS) and S-Cnx, 1 µM S-Cnx was preincubated in 20 mM Hepes, pH 7.4, and 150 mM NaCl at the indicated Ca^{2+} and/or nucleotide concentrations for 1 h at RT. Subsequently, bis-ANS was added to each sample to a final concentration of 6 µM. Bis-ANS fluorescence was monitored with an excitation wavelength of 395 nm. All fluorescence measurements were recorded at 37°C with the indicated emission wavelengths using a "Photon Technology International QM-1" fluorescence spectrofluorometer (excitation slit width: 2 nm; emission slit width: 5 nm). The measured fluorescence data were corrected for the contribution of the respective additives to fluorescence intensity or the absorption of ATP at 290 nm excitation (405).

2.2.18 Circular dichroism measurements

Reaction mixtures for circular dichroism (CD) measurements contained S-Cnx or its deletion/lectin-deficient mutants (1.81 µM) in 2.5 or 5 mM Hepes, pH 7.4, 150 mM NaCl, and the indicated Ca^{2+} or ATP concentrations in the presence or absence of various peptides (20 µM). Samples were allowed to equilibrate for 1 h at RT or 37°C prior to measuring

spectra between 200-260 nm at 37°C.

For thermal denaturation experiments, S-Cnx or its deletion/lectin-deficient mutants (7.24 µM) were equilibrated in 20 mM Hepes, pH 7.4, and 150 mM NaCl at the indicated Ca^{2+} or ATP concentrations in the presence or absence of G_1M_3 oligosaccharide (20 µM) for 1 h at RT or 37°C. Thermal denaturation curves were recorded from 20 up to 80 °C at 228 or 231 nm with a scan rate of 2°C/min. To determine the particular T_m values (transition midpoint temperature of thermal unfolding) the measured thermal denaturation curves were fit to a standard equation describing a two-state transition process by nonlinear least-squares regression using the software SigmaPlot 2004 version 9.0. All CD experiments were measured on a "Jasco J-810" spectropolarimeter equipped with a "Jasco PTC-423S" temperature controlling unit (JASCO, Easton, MD, USA) in a 1 mm path length cuvette. The results are expressed as mean residue ellipticity [Θ] (λ) in units of deg·cm^2·dmol^{-1}, given by:

$$[\Theta](\lambda) = 100\frac{\Theta(\lambda)}{c \cdot n \cdot l}$$

Where Θ (λ) is the recorded ellipticity at wavelength λ in mdeg, *c* is the concentration in mM, *n* is the number of amino acid residues in S-Cnx constructs, and *l* is the path length of the cuvette in cm. In the case of samples containing both S-Cnx construct and peptide, the obtained spectra were corrected by subtracting the contribution of the peptide alone.

2.2.19 Peptide radioiodination

KHP peptide was radioiodinated by adding 173 µM KHP-peptide to 1 mCi $Na^{125}I$ (PERKINELMER, Billerica, MA, USA) and 110 µM chloramine T in 0.2 M sodium phosphate buffer, pH 7.4, in a final volume of 90 µL. The sample was mixed for 15 s at RT and the reaction was stopped by the addition of 110 µL of 36 mM $Na_2S_2O_5$ and 16.4 mM KI in 0.2 M sodium phosphate buffer, pH 7.4. Thin layer chromatography and gamma counting of separated peptide revealed 61 % of input radioactivity incorporated into the peptide resulting in a specific activity of 39.7 mCi/µmol peptide. The radioiodination mixture was loaded onto a C_{18} Sep-Pak column (MILLIPORE, Billerica, MA, USA) and was washed with 25 mL 0.05 % trifluoroacetic acid (TFA) and subsequently with 10 mL 0.05 % TFA and 5 % acetonitrile to remove unbound $Na^{123}I$. The radioiodinated peptide was eluted with 2 ml 0.05 % TFA and 50 % acetonitrile, vacuum dried, and resuspended in 20 mM Hepes, pH 7.4, 150 mM NaCl, and 0.4 mM $CaCl_2$.

2.2.20 Peptide binding competition experiments

To analyze the interaction between S-Cnx and KHP peptide, the various His_6-tagged S-Cnx constructs (5 µM) and the ^{125}I-KHP-peptide (1 µM) were incubated in 20 mM Hepes, pH 7.4, 150 mM NaCl, and 0.4 mM $CaCl_2$ in the presence or absence of unlabeled KHP peptide (20 µM) or G_1M_3 oligosaccharide (20 µM) in an 80 µL reaction volume for 1 h at 37°C. The samples were then applied to Mini-Spin Columns (PIERCE, Rockford, IL, USA) containing 15 µL of nickel-agarose beads (QIAGEN, Mississauga, ON, Canada) equilibrated in 20 mM Hepes, pH 7.4, 150 mM NaCl, and 0.4 mM $CaCl_2$. Proteins were allowed to bind to the beads for 1 h at 37°C before removing unbound peptides by centrifugation for 30 s at 730 x g. The beads were washed twice rapidly with 300 µL of 20 mM Hepes, pH 7.4, 150 mM NaCl, and 0.4 mM $CaCl_2$ and bound proteins were eluted with 200 µL of 20 mM Hepes, pH 7.4, 150 mM NaCl, 0.4 mM $CaCl_2$, and 250 mM imidazole. The amount of radioiodinated KHP peptide that remained bound to the various S-Cnx constructs in the eluates was quantified using a "1470 Automatic Gamma Counter" (PERKINELMER, Billerica, MA, USA). To control for non-specific peptide binding to nickel-agarose beads, separate incubations lacking S-Cnx were performed and radioactive peptide eluted from the beads was subtracted from the values obtained with the complete incubations. Typically, ~130,000 cpm of peptide was specifically bound to S-Cnx.

2.2.21 Reduction and carboxymethylation of α-lactalbumin

Bovine α-lactalbumin was reduced and carboxymethylated according to a modified protocol described previously by Bosl *et al*. (406). Reduction of α-lactalbumin (500 µM) was performed in 0.2 M Tris-HCL, pH 8.7, 2 mM EDTA, and 20 mM dithiothreitol for 90 min at RT. All free thiols of the reduced protein were blocked by 0.1 M iodoacetic acid for 20 min in the dark. Subsequently the alkylation reaction was quenched with an excess of reduced glutathione in 0.2 M Tris-HCL, pH 7.5. The reduced, carboxymethylated α-lactalbumin (R-CMLA) was excessively dialyzed against 20 mM Hepes, pH 7.4, 150 mM NaCl, and 1 mM $CaCl_2$, aliquoted, and stored at -70 °C.

2.2.22 Surface plasmon resonance assays

Real time binding between S-Cnx and non-native protein conformers was analysed by surface plasmon resonance (SPR) spectroscopy using a "Biacore X instrument" (BIACORE AB CORPORATION, Uppsala, Sweden). Recombinant firefly luciferase or reduced, carboxymethylated α-lactalbumin were covalently immobilized to the activated dextran surface of a "Sensor Chip CM5" (BIACORE INC., Piscataway, NJ, USA) in 10 mM sodium acetate buffer at one pH unit below the pI of the respective protein according to the standard amine coupling procedure recommended by the manufacturer. While the first flow cell was used as the control surface, immobilization of FL or R-CMLA in the second flow cell resulted in approximately 4500 and 830 resonance units (RU), respectively. Binding of S-Cnx and deletion mutants to FL (30°C) and R-CMLA (25°C) was conducted at a flow rate of 20 µL/min. Prior to the experiment, S-Cnx constructs were equilibrated in 20 mM Hepes, pH 7.4, 150 mM NaCl, 1 mM EDTA, 1.4 mM $CaCl_2$, and 0.005 % surfactant P20 (BIACORE INC., Piscataway, NJ, USA) for 1 h at the respective temperature. Complex association was monitored for 1 min followed by a 2 min dissociation phase in the same buffer before the surface was regenerated with 50 % ethylene glycol, pH 8.5.

3 Results

3.1 Expression and purification of S-Cnx constructs

During the course of this thesis the initially applied expression system for S-Cnx was altered, in combination with a modified purification protocol, to increase the yield of S-Cnx and mutant constructs for following studies in results section 3.3.

For expression of S-Cnx, examined in early experiments (3.2) the bacterial expression vector pGEX-3X, encoding glutathione S-transferase fused to the N-terminus of the soluble ER-luminal domain of Cnx followed by a His_6 sequence (283), was transformed into the *E. coli* strain FA113. This strain, lacking thioredoxin reductase and glutathione reductase, possesses an oxidizing cytosol which supports efficient expression of disulfide bonded proteins (394). The fusion protein-expressing bacteria were cultured in IPTG-containing medium for 16 h at RT. Upon cell harvest and cell disruption, GST-S-Cnx was purified using a Ni-NTA agarose column. Following Factor Xa protease digestion to release GST, S-Cnx was further purified by glutathione-agarose chromatography to remove GST and by Mono Q anion exchange chromatography. S-Cnx eluted typically from the Mono Q FPLC column at 0.43 M NaCl. From 2 L of bacterial culture about 7 mg of S-Cnx could be obtained with a purity in excess of 95 % as assessed by SDS-PAGE and Coomassie Brilliant Blue R-250 staining (Fig. 6).

To improve the expression of S-Cnx and its deletion/lectin-deficient mutants, the corresponding cDNAs were cloned (2.2.7) into pET15b-TEV vectors resulting in an in frame fusion of the His_6 sequence to the N-terminus of the various S-Cnx constructs. The generated plasmids were transformed into *E. coli* BL21-CodonPlus(DE3) cells, which supply additional copies of the rare *argU, ileY,* and *leuW* tRNA genes to facilitate heterologous protein expression in *E. coli* hosts. Transformants were incubated for 4 h at 30°C following induction of protein overexpression with IPTG. Purification of the various constructs was performed by Ni-NTA agarose chromatography and subsequent Mono Q anion exchange chromatography. Elution of S-Cnx and mutants from the Mono Q anion exchange column was usually observed between 0.35-0.5 M NaCl. The purity of the proteins was judged to be greater than 95 % by SDS-PAGE and Coomassie Brilliant Blue R-250 staining (Fig. 6). The following average yields were obtained for the various S-Cnx constructs from 2 L of bacterial culture: S-Cnx: 20 mg; Δarm1: 22 mg; Δarm2: 19 mg; glob: 5 mg; arm: 34 mg; LD-S-Cnx: 20 mg.

Thus, changing from the tac (pGEX-3X) to the T7 (pET15b-TEV) promotor controlled protein expression with a shortened 4 h time period in *E. coli* BL21-CodonPlus(DE3) cells and using a modified purification procedure resulted in a ~3 fold enhanced yield for S-Cnx. This resembles previous studies, showing higher expression levels with the T7 promotor when compared to those obtained with the tac promotor (407).

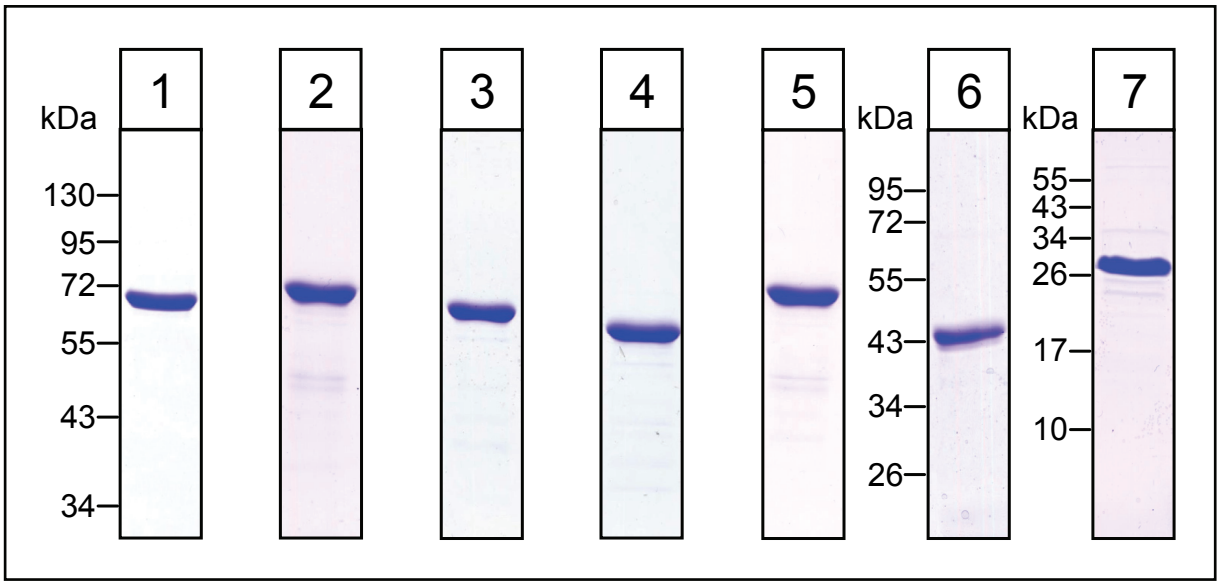

Fig. 6: SDS-PAGE analysis of purified S-Cnx, deletion mutants, and lectin-deficient S-Cnx. C-terminal His_6-tagged S-Cnx is shown in lane 1. N-terminal His_6-tagged S-Cnx constructs are depicted in lane 2-7. Lane 2: S-Cnx; lane 3: Δarm1; lane 4: Δarm2; lane 5: LD-S-Cnx; lane 6: glob; lane 7: arm. For every S-Cnx construct 4 µg were loaded onto a 10 % polyacrylamide gel with the exception of the arm domain, which was analyzed by a 16 % polyacrylamide gel. Gels were stained with Coomassie Blue R-250.

3.2 Characterization of the chaperone function of calnexin under conditions prevalent within the lumen of the endoplasmic reticulum

3.2.1 Effect of Ca^{2+} concentration on the aggregation suppression function of S-Cnx

To evaluate the lectin-independent aggregation suppression function of S-Cnx at physiological temperature, a client protein was sought that would aggregate at 37°C. Firefly luciferase (FL) is a thermolabile protein that is frequently used *in vitro* as a substrate in chaperone-mediated refolding or aggregation suppression assays, usually at temperatures greater than 37°C or following dilution from a denaturant (226, 408). It is also a non-glycosylated protein, and thus, any interaction with S-Cnx cannot be lectin-mediated. As

shown in Fig. 7, FL in 20 mM Hepes buffer at pH 7.4 containing 150 mM NaCl aggregated at 37°C following a lag period of 7-8 min. This behavior was unchanged in the presence of 1 mM Ca^{2+}. The addition of S-Cnx (3-fold molar excess) at the 1 mM Ca^{2+} concentration previously used in aggregation suppression assays involving S-Cnx or Crt (283, 284) had only a small inhibitory effect on FL aggregation.

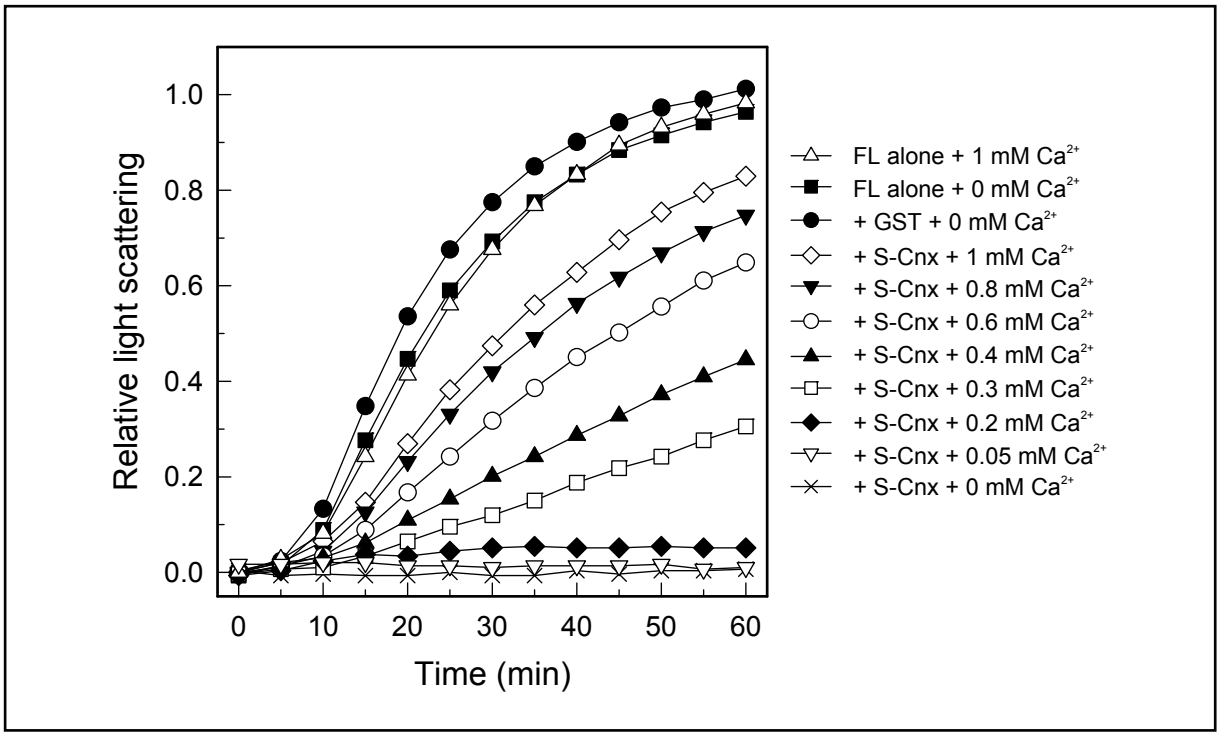

Fig. 7: Ca^{2+} influences the aggregation suppression function of S-Cnx. S-Cnx (or GST) (9 µM) was equilibrated in 20 mM Hepes, pH 7.4, 150 mM NaCl, and the indicated free [Ca^{2+}] for 1 h at RT. FL was diluted into the various S-Cnx samples to a final concentration of 3 µM, and its aggregation was monitored by measuring light scattering at 360 nm and 37°C. Data points were measured every 6 s and plotted every 5 min.

The Ca^{2+} concentration was then reduced to assess the potency of S-Cnx's aggregation suppression function under conditions that reflect the free ER Ca^{2+} store in its resting or filled state or following Ca^{2+} mobilization (empty state). Reducing the Ca^{2+} concentration resulted in a marked enhancement of the ability of S-Cnx to suppress FL aggregation (Fig. 7). Specifically, when Ca^{2+} was reduced to the 0.4 mM level reflective of the resting ER-luminal Ca^{2+} concentration (31, 34, 409), S-Cnx inhibited the aggregation of FL by 55 %. Furthermore, reduction of Ca^{2+} to the 50 µM level typically observed following mobilization of the ER Ca^{2+} store (34, 410) completely suppressed FL aggregation. This aggregation suppression by S-Cnx was specific because the addition of a control protein, glutathione S-transferase (GST), in the absence of added Ca^{2+} had no effect on FL aggregation (Fig. 7).

3.2.2 Conformation of S-Cnx is influenced by Ca^{2+} concentration

To understand the basis for the enhanced aggregation suppression function exhibited by S-Cnx as the Ca^{2+} concentration is reduced, the conformational consequences of altering the Ca^{2+} concentration were assessed using several approaches. Initially, the far-UV circular dichroism spectrum of S-Cnx in the presence or absence of Ca^{2+} was examined.

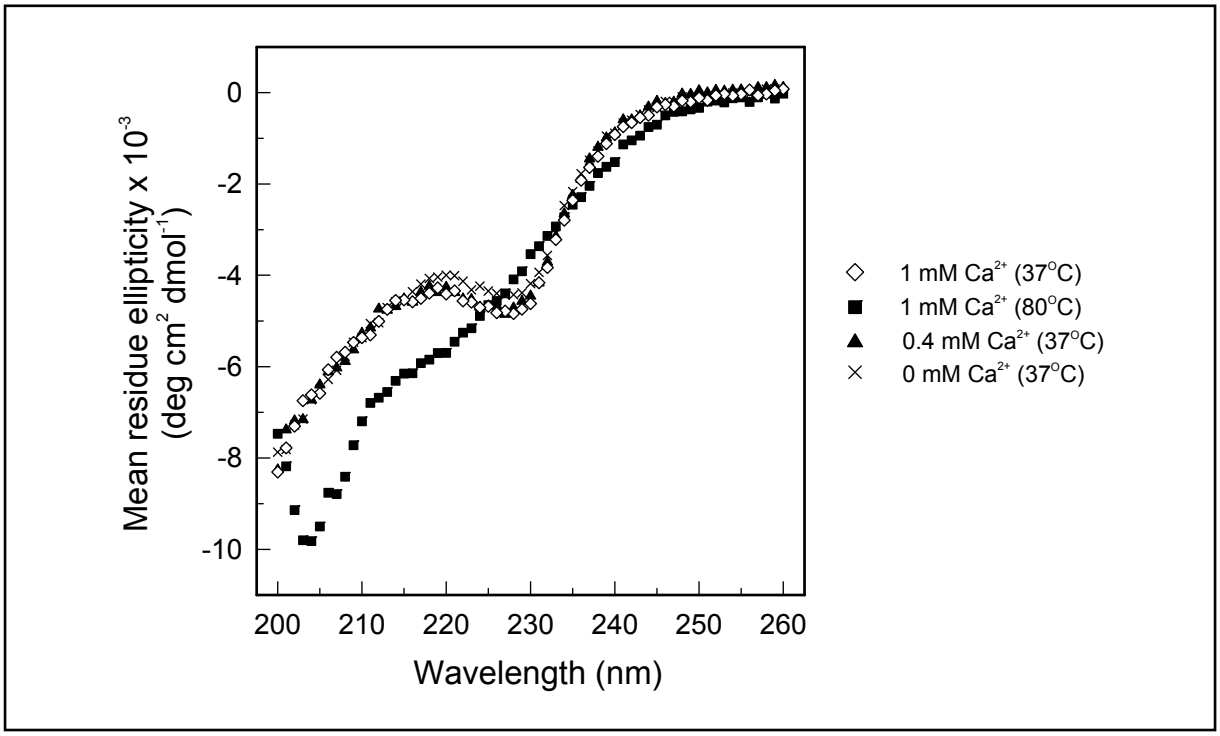

Fig. 8: Far-UV circular dichroism spectra of S-Cnx. S-Cnx (1.81 µM) was equilibrated in 5 mM Hepes, pH 7.4, 150 mM NaCl, and the indicated free [Ca^{2+}] for 1 h at RT before recording the CD spectra (200-260 nm) at the indicated temperatures.

As shown in Fig. 8, the CD spectrum of S-Cnx in the presence of 1 mM Ca^{2+} was characterized by a negative CD band at 228 nm but lacked secondary structure spectral features typical of proteins with a substantial content of β-sheets or α-helices. Rather, the spectrum appeared to be dominated by short wavelength aromatic CD transitions, which reflects the relatively high content of aromatic residues in the ER-luminal domain of Cnx (9.5 % of total residues). Similar observations have been made previously for Crt (411). No difference in the CD spectrum was observed upon reduction of the Ca^{2+} concentration to 0.4 mM, and only a minor decrease in mean residue ellipticity was associated with the complete absence of Ca^{2+}. However, the CD spectrum of S-Cnx denatured by heating at 80°C was sufficiently distinct to permit an examination of the thermal stability of S-Cnx at various Ca^{2+} concentrations. The thermal denaturation curve of S-Cnx in 1 mM Ca^{2+} recorded at 228 nm

shows that the protein denatures via a well-defined cooperative transition having a T_m of 49.5°C (Fig. 9). This was unaltered when the Ca^{2+} concentration was reduced to the resting ER level of ~0.4 mM. However, further reduction led to a progressive loss of thermal stability such that at a Ca^{2+} concentration of 50 µM, typical of the empty ER, the T_m was reduced to 42.4°C.

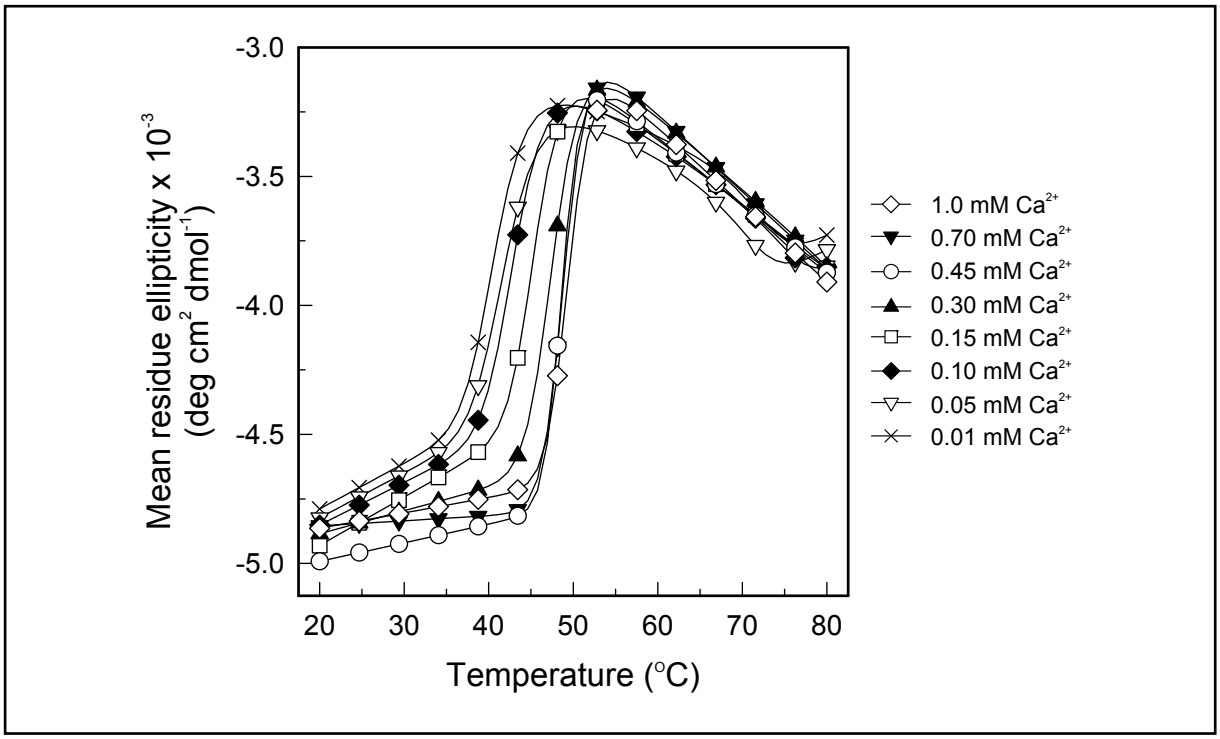

Fig. 9: Effect of Ca^{2+} on melting curves of S-Cnx. S-Cnx (7.24 µM) was equilibrated in 20 mM Hepes, pH 7.4, 150 mM NaCl, and the indicated free [Ca^{2+}] for 1 h at RT. Thermal denaturation curves (20-80°C) were obtained by measuring the mean residue ellipticity by CD at 228 nm. For clarity, not all recorded melting curves are shown. Data points were acquired every 2°C and plotted every 5°C.

These values resemble those reported for Crt at 1 mM Ca^{2+} (T_m = 46.4°C) and at 50 µM Ca^{2+} (T_m = 44.3°C) (281). Thus, Ca^{2+} ions have a stabilizing effect on both S-Cnx and Crt.

These Ca^{2+}-dependent changes in thermal stability were also used to estimate the affinity of Ca^{2+} binding to S-Cnx, which has not been reported previously. As shown in Fig. 10, a plot of T_m versus Ca^{2+} concentration could be fit to an equation describing single site binding with a dissociation constant (K_d) of 125 µM.

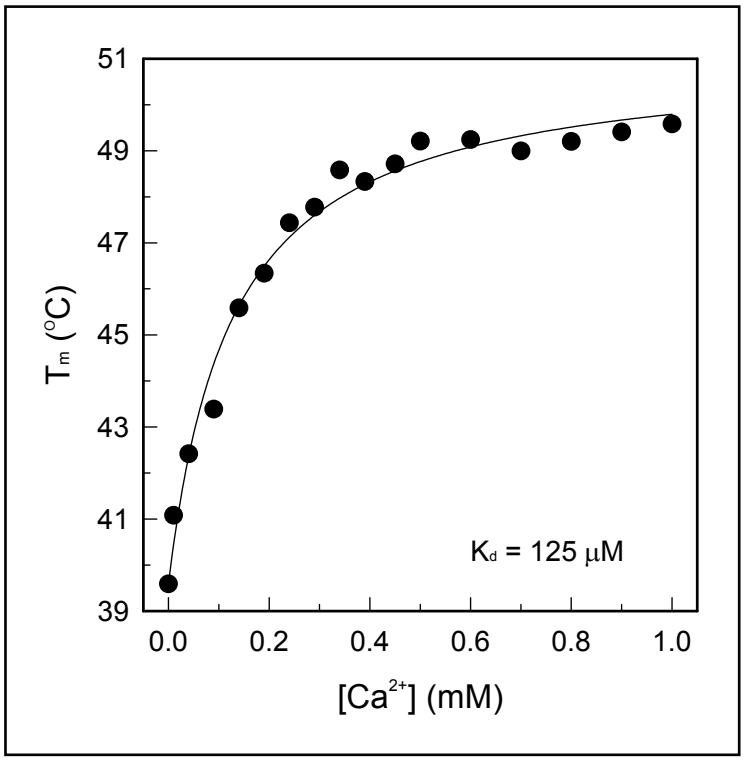

Fig. 10: Thermal stability of S-Cnx is influenced by Ca^{2+}. Calculated T_m values of the thermal denaturation curves from Fig. 9 were plotted against [Ca^{2+}] and fit to an equation describing single site binding using SigmaPlot. The indicated K_d value represents the average of three independent measurements with a standard deviation of 15 %.

Next, the accessibility of S-Cnx to proteolytic digestion over a range of Ca^{2+} concentrations was examined. Fig. 11 shows that at 1 mM Ca^{2+} and at 37°C, S-Cnx is relatively resistant to trypsin digestion with only slight shifts in electrophoretic mobility observed between 5 and 60 min of digestion. This has been observed previously and reflects clipping at both the N- and

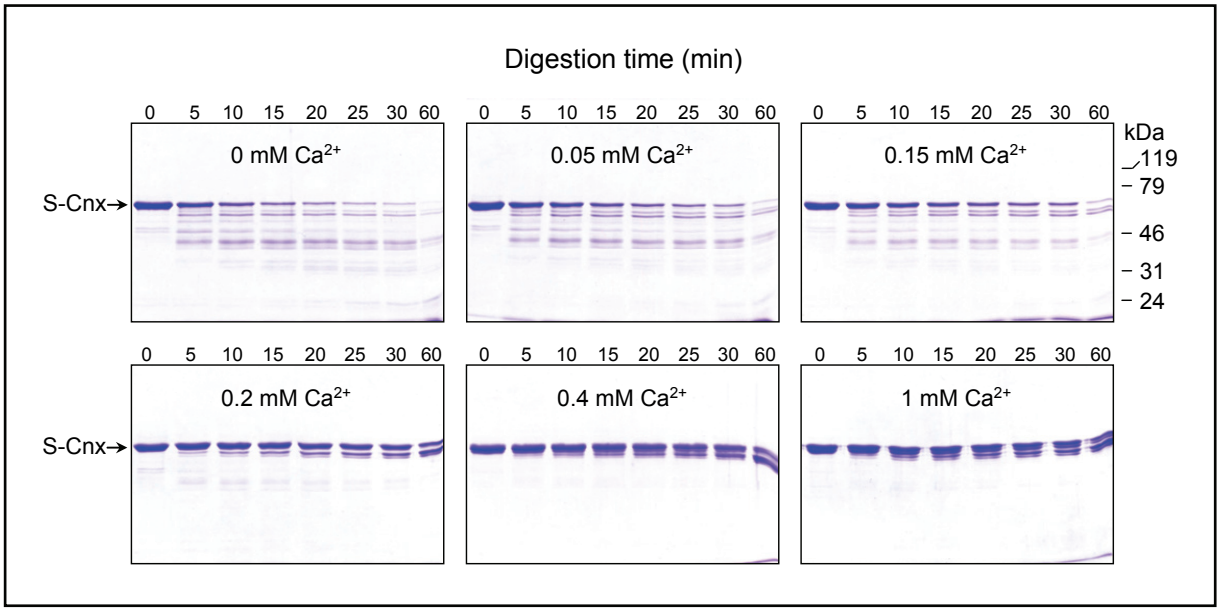

Fig. 11: Effect of Ca^{2+} on the protease sensitivity of S-Cnx. S-Cnx was preincubated in 20 mM Hepes, pH 7.4, 150 mM NaCl, and the indicated free [Ca^{2+}] for 1 h at RT. All digestions were carried out at 37°C with a S-Cnx/trypsin ratio of 100:1 (w/w). Aliquots containing 4 µg of S-Cnx were removed at each time point and analyzed by SDS-PAGE using 10 % polyacrylamide gels followed by Coomassie Brilliant Blue R-250 staining. The arrow indicates the S-Cnx band migrating at 68 kDa.

C-termini of ~68 kDa S-Cnx to give rise to a ~60 kDa protease-resistant core (412). No significant change was observed in the digestion pattern or kinetics when the Ca^{2+} concentration was reduced to the resting ER level of 0.4 mM. However, further reduction in Ca^{2+} concentration led to a progressive increase in sensitivity to trypsin digestion, closely reflecting the loss of stability observed by CD spectroscopy (compare Fig. 11 with Fig. 10). These findings are consistent with the loss of a tightly folded conformation of S-Cnx at Ca^{2+} concentrations below that of the resting ER.

Changes in the intrinsic (predominantly tryptophan) fluorescent emission spectrum of S-Cnx were also measured as a means to assess the nature of conformational changes in response to reductions in Ca^{2+} concentration. As illustrated in Fig. 12.A, the complete removal of Ca^{2+} ions from S-Cnx resulted in a major reduction in fluorescence emission intensity along with a shift of the spectrum to longer wavelengths. This is indicative of the

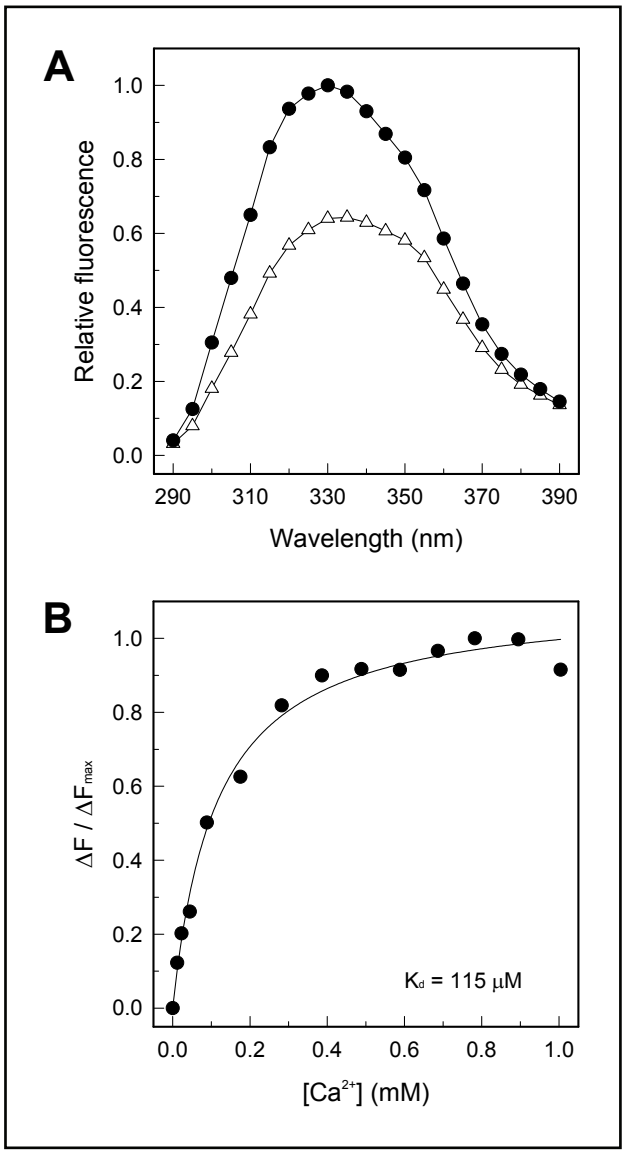

Fig. 12: Effect of Ca^{2+} on the intrinsic fluorescence of S-Cnx. (A) Intrinsic fluorescence spectra of S-Cnx. S-Cnx (0.6 µM) was equilibrated in 20 mM Hepes, pH 7.4, 150 mM NaCl, and a free [Ca^{2+}] of either 1 mM or 0 mM for 1 h at RT. The emission spectra (290-390 nm) were monitored at 37°C with an excitation wavelength of 280 nm: (—●—) 1 mM Ca^{2+}; (—△—) 0 mM Ca^{2+}. Data points were measured every 1 nm and shown every 5 nm. **(B)** Intrinsic fluorescence changes as a function of Ca^{2+} concentration. S-Cnx (0.6 µM) was preincubated in 20 mM Hepes, pH 7.4, 150 mM NaCl, and the indicated free [Ca^{2+}] for 1 h at RT, and the intrinsic fluorescence was measured at 37°C (excitation wavelength: 280 nm; emission wavelength: 333 nm). The results were plotted as the change in fluorescence (ΔF) divided by the maximum change in fluorescence between 1 and 0 mM Ca^{2+} (ΔF_{max}). The titration curve was fit to an equation describing single site binding using SigmaPlot. The K_d value was derived by calculating the average of three independent experiments with a standard deviation of 20 %.

transfer of one or more of the 13 tryptophan residues of S-Cnx from a hydrophobic environment to one that is more polar, probably exposed to solvent. Upon repeating this experiment at a variety of Ca^{2+} concentrations, it was observed that little change in the fluorescence emission intensity occurred upon lowering Ca^{2+} to the level of the resting ER (0.4 mM), but progressive quenching of fluorescence occurred at lower Ca^{2+} concentrations (Fig. 12.B). Fitting these data to a single site-binding model resulted in a K_d for Ca^{2+} binding to S-Cnx of 115 µM, quite similar to the K_d determined by measuring thermal stability as a function of Ca^{2+} concentration (Fig. 10).

Finally, binding of the hydrophobic fluorescent probe bis-ANS was monitored as a measure of the surface hydrophobicity of S-Cnx. As shown in Fig. 13.A, when the emission spectra of bis-ANS alone or in the presence of S-Cnx (1 mM Ca^{2+}) were compared, bis-ANS exhibited the increase in fluorescence and the shift to shorter wavelength expected for its

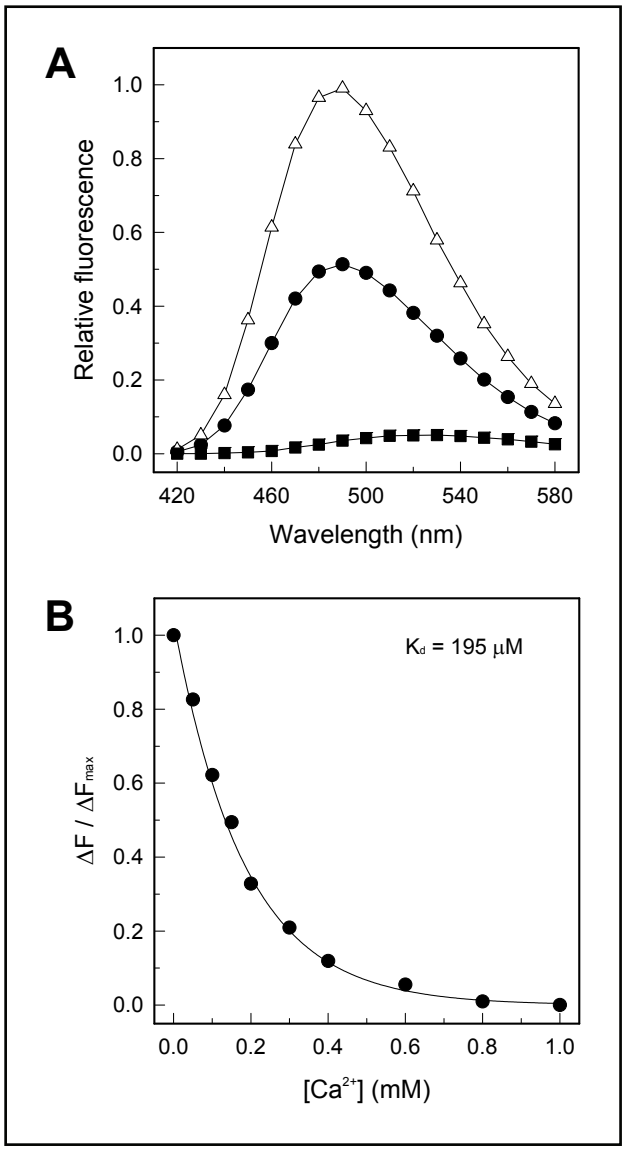

Fig. 13: Bis-ANS binding by S-Cnx is influenced by Ca^{2+}. (A) Bis-ANS binding by S-Cnx. S-Cnx (1 µM) was equilibrated in 20 mM Hepes, pH 7.4, 150 mM NaCl with or without a free [Ca^{2+}] of 1 mM for 1 h at RT and mixed with 6 µM bis-ANS. Bis-ANS fluorescence spectra were recorded between 420 and 580 nm at 37°C with an excitation wavelength of 395 nm: (—■—) bis-ANS in 1 mM Ca^{2+}; (—●—) bis-ANS + S-Cnx + 1 mM Ca^{2+}; (—△—) bis-ANS + S-Cnx + 0 mM Ca^{2+}. Data points were measured every 1 nm and shown every 10 nm. **(B)** Bis-ANS fluorescence changes as a function of Ca^{2+} concentration. S-Cnx (1 µM) was preincubated in 20 mM Hepes, pH 7.4, 150 mM NaCl, and the indicated free [Ca^{2+}] for 1 h at RT before the addition of 6 µM bis-ANS. Bis-ANS fluorescence was measured at 37°C (excitation wavelength: 395 nm; emission wavelength: 490 nm). The results were plotted as the change in fluorescence (ΔF) divided by the maximum change in fluorescence between 0 and 1 mM Ca^{2+} (ΔF_{max}). The data were fit to an equation describing single site binding using SigmaPlot. The depicted K_d value is the average of three independent measurements with a standard deviation of 11 %.

transfer from water to a hydrophobic environment. This confirms previous observations that S-Cnx at 1 mM Ca^{2+} possesses significant surface hydrophobicity (283). Upon the complete removal of Ca^{2+}, a further increase in bis-ANS fluorescence was observed, indicative of the increased exposure of hydrophobic sites (Fig. 13.A). Again, only a small portion of this Ca^{2+}-dependent hydrophobic exposure occurred when Ca^{2+} was reduced to the level of the resting ER (0.4 mM) with progressively more exposure resulting from further decreases in Ca^{2+} concentration (Fig. 13.B). These data could be fit to a single site equation for Ca^{2+} binding with a K_d = 195 μM, in good agreement with the values obtained by CD and intrinsic fluorescence changes (Fig. 10 and Fig. 12B).

Collectively, these assessments of S-Cnx conformation are consistent with a minor structural change associated with increased surface hydrophobicity when the Ca^{2+} concentration is reduced to the resting ER level. Further reductions in Ca^{2+} concentration are associated with a loss of stability and a less tightly packed conformation with likely exposure of the hydrophobic core.

3.2.3 Effect of nucleotides on the structure and aggregation suppression function of S-Cnx

It was shown previously that 1 mM ATP has a modest enhancing effect on the ability of S-Cnx to suppress the aggregation of citrate synthase at 45°C (283). Fig. 14 shows that this is also true for the suppression of FL aggregation at 37°C in the presence of 1 mM Ca^{2+}. Furthermore, 2 mM ATP enhanced aggregation suppression by S-Cnx even more, and in the presence of 3 mM ATP, the aggregation of FL was completely suppressed. The possibility was considered that these effects might be indirect because of a substantial drop in free Ca^{2+} concentration through chelation to the added nucleotide. However, direct measurement of free Ca^{2+} (see 2.2.14) revealed that the addition of 1 and 3 mM ATP reduced the free Ca^{2+} concentration from 1 to 0.9 and 0.7 mM, respectively. As shown in Fig. 7, such reductions in Ca^{2+} concentration are associated with only slight enhancements in the aggregation suppression function of S-Cnx (relative to 1 mM Ca^{2+}). It was also considered that the reduced aggregation observed upon addition of ATP might be due to its binding to and stabilization of FL. However, 3 mM ATP had only minimal effects on FL aggregation when added in the absence of S-Cnx (not shown) or in the presence of GST (Fig. 14). The addition of 1 mM Mg^{2+} did not influence the effect of ATP on the aggregation suppression function of S-Cnx nor did it alter the outcome of subsequent conformational studies (data not shown).

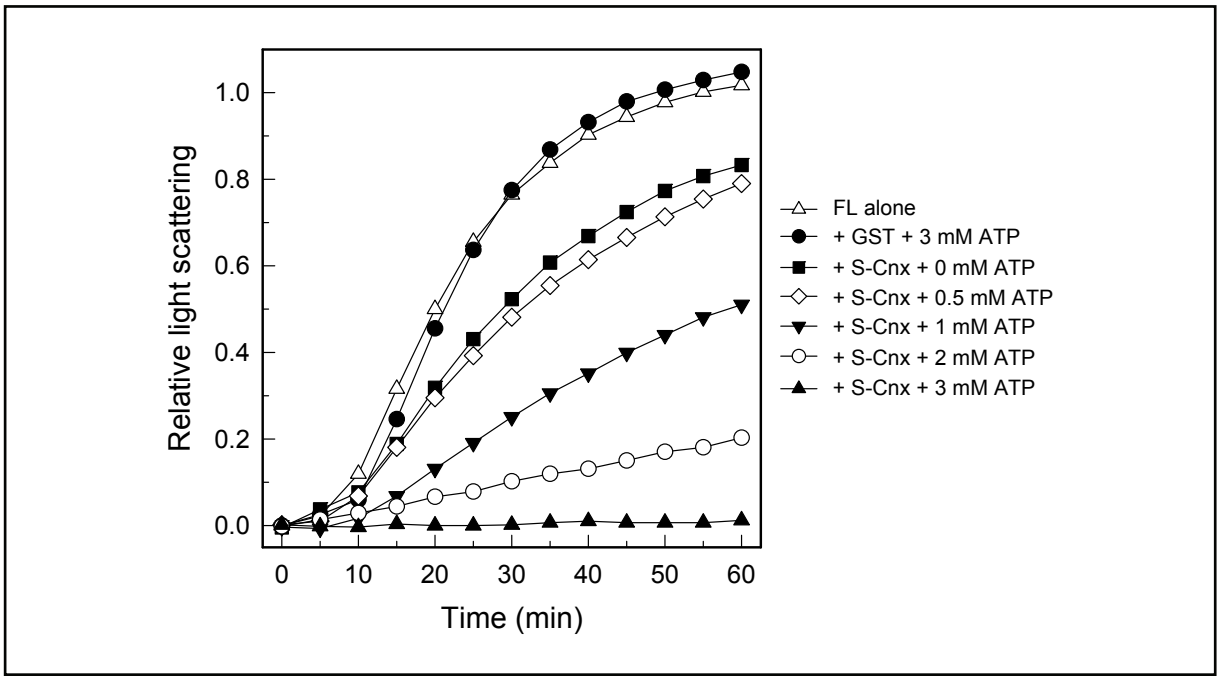

Fig. 14: ATP enhances the aggregation suppression function of S-Cnx. Following equilibration of S-Cnx or GST (9 µM) for 1 h at RT in 20 mM Hepes, pH 7.4, 150 mM NaCl, 1 mM $CaCl_2$, and the indicated [ATP], 3 µM FL was added, and aggregation was monitored at 37°C by light scattering at 360 nm. Data points were measured every 6 s but, for clarity, are shown every 5 min.

To determine the structural basis for the enhanced aggregation suppression by S-Cnx in the presence of ATP, far-UV CD spectra for S-Cnx were collected at various ATP concentrations. As was the case for Ca^{2+}, only minimal changes in the spectra were observed (data not shown). Consequently, CD was used to monitor the thermal stability of S-Cnx as a function of ATP concentration. As shown in Fig. 15, the addition of up to 3 mM ATP had

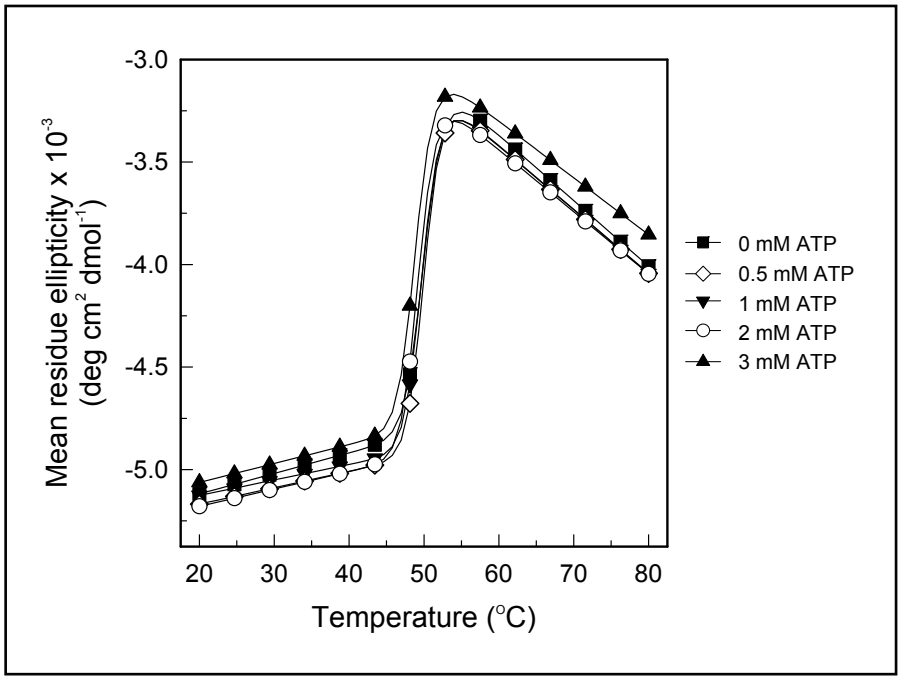

Fig. 15: Effect of ATP on the thermal stability of S-Cnx. S-Cnx (7.24 µM) was equilibrated in 20 mM Hepes, pH 7.4, 150 mM NaCl, 1 mM $CaCl_2$, and the indicated [ATP] for 1 h at RT. Thermal denaturation curves were recorded by measuring mean residue ellipticity by CD at 228 nm as the temperature was increased from 20 to 80°C. Data points were measured every 2°C and shown every 5°C.

little effect on S-Cnx stability. The melting temperature decreased only 1°C over the range of 0.5-3 mM ATP.

Similarly, no alteration in S-Cnx conformation in response to ATP could be detected by proteolytic digestion. Fig. 16 shows that S-Cnx remained largely resistant to digestion by trypsin at 37°C (1 mM Ca^{2+}) either in the absence or presence of 5 mM ATP.

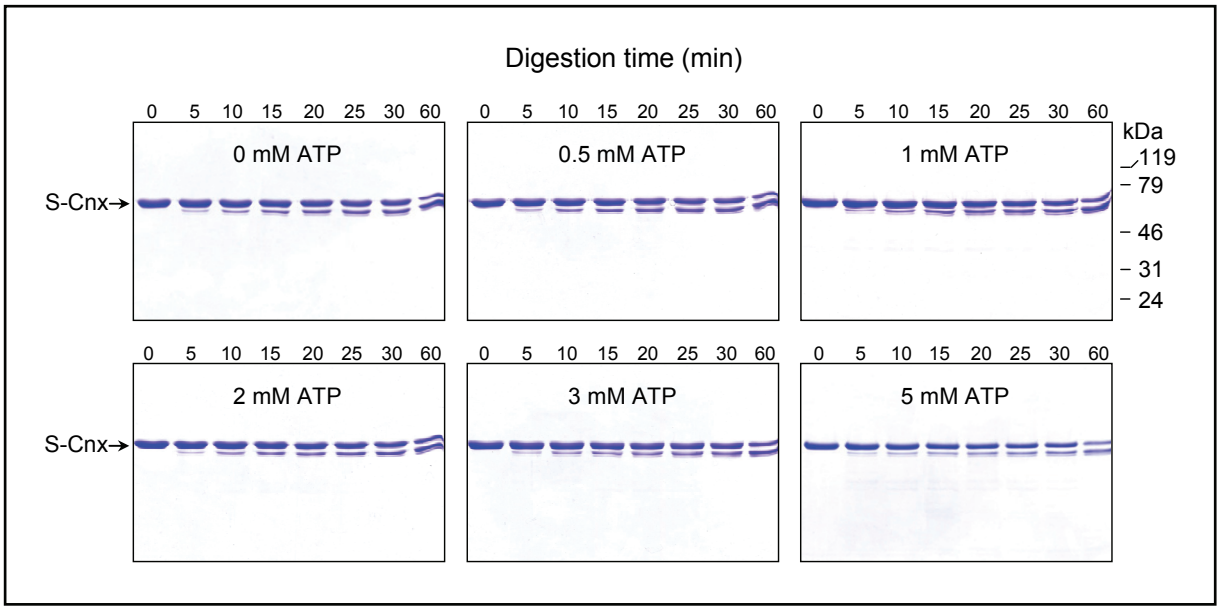

Fig. 16: Effect of ATP on the trypsin susceptibility of S-Cnx. S-Cnx was incubated in 20 mM Hepes, pH 7.4, 150 mM NaCl, 1 mM $CaCl_2$, and the indicated [ATP] for 1 h at RT. Digestions were performed at 37°C using a S-Cnx/trypsin ratio of 100:1 (w/w), and aliquots containing 4 µg of S-Cnx were taken at the indicated time points. Digestion products were separated by SDS-PAGE using 10 % polyacrylamide gels with visualization by Coomassie Brilliant Blue R-250 staining. The arrow indicates the 68-kDa band of S-Cnx.

To examine if minor structural changes of S-Cnx upon ATP binding could be detected by intrinsic fluorescence measurements, fluorescence spectra of S-Cnx with and without 5 mM ATP were compared. In contrast to Ca^{2+}-induced conformational changes of S-Cnx characterized by a significant increase in fluorescence intensity (Fig. 12), ATP caused no change in the emission spectrum (Fig. 17).

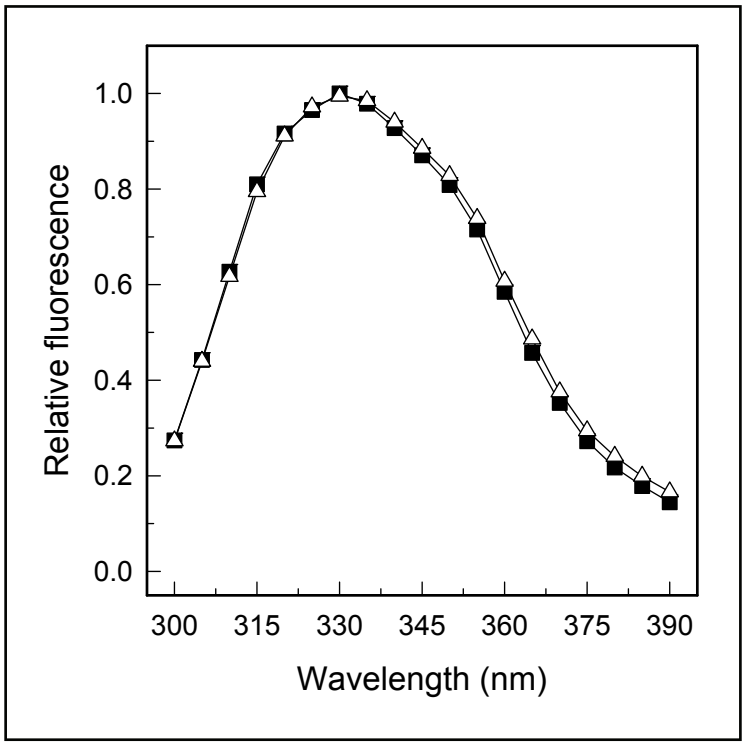

Fig. 17: Effect of ATP on the intrinsic fluorescence of S-Cnx. S-Cnx (0.6 µM) was preincubated in 20 mM Hepes, pH 7.4, 150 mM NaCl, and 1 mM $CaCl_2$ in the presence or absence of 5 mM ATP for 1 h at RT before recording the emission spectra (300-390 nm) at 37°C with an excitation wavelength of 290 nm: (—△—) 5 mM ATP; (—■—) 0 mM ATP. Data points were measured every 1 nm and plotted every 5 nm.

However, a substantial increase in bis-ANS fluorescence was observed upon addition of ATP (Fig. 18). This was detectable at 0.5 mM ATP and reached a maximum near 5 mM ATP (Fig. 19).

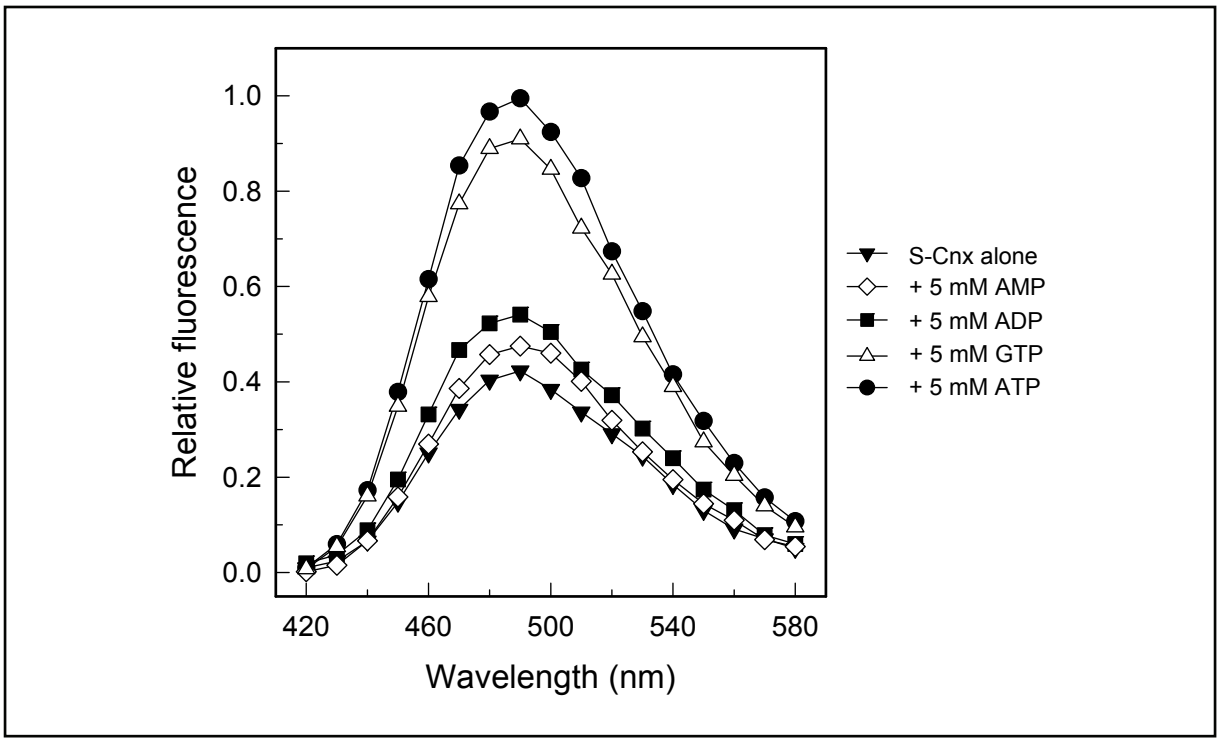

Fig. 18: Bis-ANS binding by S-Cnx is influenced by nucleotides. S-Cnx (1 µM) was equilibrated in 20 mM Hepes, pH 7.4, 150 mM NaCl, 1 mM $CaCl_2$, and 5 mM of the indicated nucleotides for 1 h at RT and then mixed with 6 µM bis-ANS. Bis-ANS fluorescence spectra (420-580 nm) were monitored with an excitation wavelength of 395 nm at 37°C. Data points were measured every 1 nm and shown every 10 nm.

These data could be fit to a single site-binding model with a K_d for ATP binding to S-Cnx of 2.9 mM. The marked increase in bis-ANS fluorescence coupled with the minimal changes in thermal stability and protease sensitivity are consistent with ATP inducing the exposure of a localized hydrophobic site on S-Cnx.

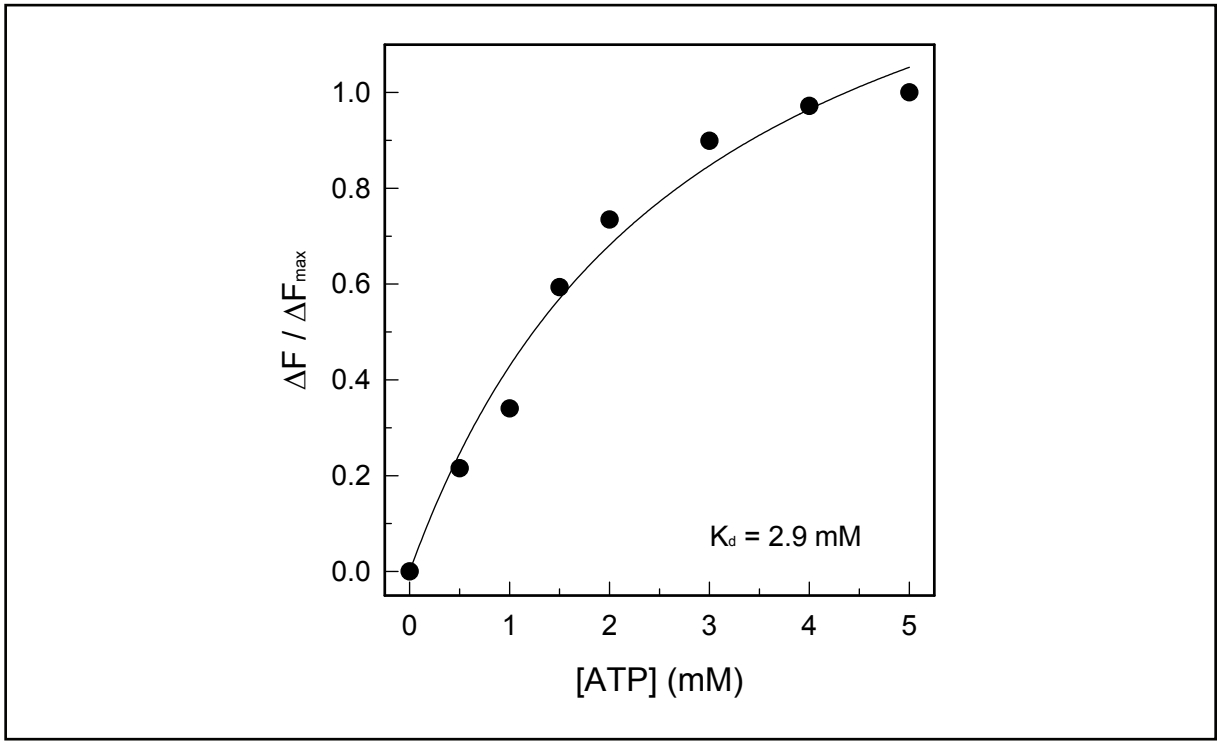

Fig. 19: Bis-ANS fluorescence as a function of ATP concentration. S-Cnx (1 µM) was preincubated in 20 mM Hepes, pH 7.4, 150 mM NaCl, and 1 mM $CaCl_2$ with various concentrations of ATP for 1 h at RT before the addition of 6 µM bis-ANS. Bis-ANS fluorescence was measured at 37°C with excitation and emission wavelengths of 395 and 490 nm, respectively. The results were plotted as the change in fluorescence (ΔF) divided by the maximum change in fluorescence between 0 and 5 mM ATP (ΔF_{max}). The titration curve was fit to an equation describing single site binding using SigmaPlot. The shown K_d value represents the average of three independent measurements with a standard deviation of 8 %.

An examination of nucleotide specificity revealed that ATP was substantially more potent than either ADP or AMP in enhancing the aggregation suppression function of S-Cnx (Fig. 20). In contrast, GTP was almost as potent as ATP, although this is unlikely to be physiologically relevant because there is no detectable GTP transporter activity within ER membranes (413). The ability of S-Cnx to bind all of these nucleotides has been documented previously (412). Consistent with their effects on aggregation suppression, the addition of GTP to S-Cnx increased bis-ANS fluorescence emission to almost the same extent as ATP, whereas ADP and AMP had only modest effects (Fig. 18). Thus, there is a direct correlation between nucleotide-regulated increases in surface hydrophobicity and the capacity of S-Cnx to suppress FL aggregation.

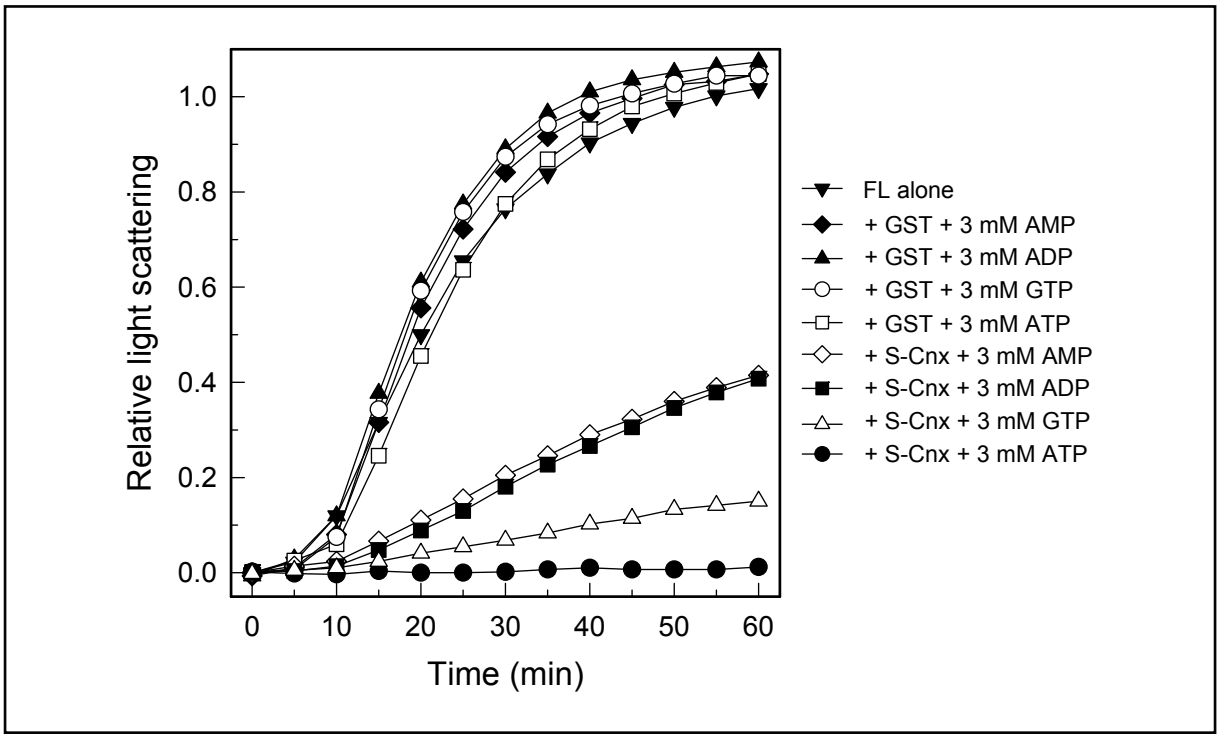

Fig. 20: Nucleotides influence the aggregation suppression function of S-Cnx. S-Cnx (9 µM) was equilibrated in 20 mM Hepes, pH 7.4, 150 mM NaCl, 1 mM $CaCl_2$, and 3 mM of the indicated nucleotides for 1 h at RT. FL (3 µM) was pipetted into the various S-Cnx samples, and light scattering measurements were recorded at 360 nm at 37°C. For clarity, data points were measured every 6 s, but are plotted at 5 min intervals.

3.2.4 Resting ER Ca^{2+} concentration potentiates the effect of ATP on the aggregation suppression function of S-Cnx

Because the lowering of Ca^{2+} concentration to the normal ER-luminal level and the addition of 1-3 mM ATP independently enhanced the aggregation suppression function of S-Cnx, it was of interest to examine the combined effects of these treatments. As shown in Fig. 21, the addition of S-Cnx in the presence of 1 mM Ca^{2+} caused a modest suppression of FL aggregation. This was only slightly enhanced by the addition of 0.5 mM ATP (compare + S-Cnx + 1 mM Ca^{2+} and + S-Cnx + 1 mM Ca^{2+} + 0.5 mM ATP traces). Lowering the Ca^{2+} concentration to 0.4 mM in the absence of ATP substantially increased the potency of aggregation suppression, as was observed previously (Fig. 7). However, in contrast to the situation at 1 mM Ca^{2+}, the addition of 0.5 mM ATP strongly potentiated aggregation suppression such that only a small degree of FL aggregation occurred (Fig. 21; compare + S-Cnx + 0.4 mM Ca^{2+} and + S-Cnx + 0.4 mM Ca^{2+} + 0.5 mM ATP traces). It appears that the reduction in Ca^{2+} concentration and the addition of ATP act synergistically to enhance the aggregation suppression function of S-Cnx. Again, this was not an indirect effect of ATP

chelating Ca^{2+} because the direct measurement of free Ca^{2+} revealed that its concentration was reduced only slightly from 0.4 to 0.36 mM in the presence of 0.5 mM ATP. Furthermore, the effects were not due to altered FL stability because the addition of GST in the presence of 0.4 mM Ca^{2+} and 0.5 mM ATP did not alter the extent or kinetics of FL aggregation (Fig. 21).

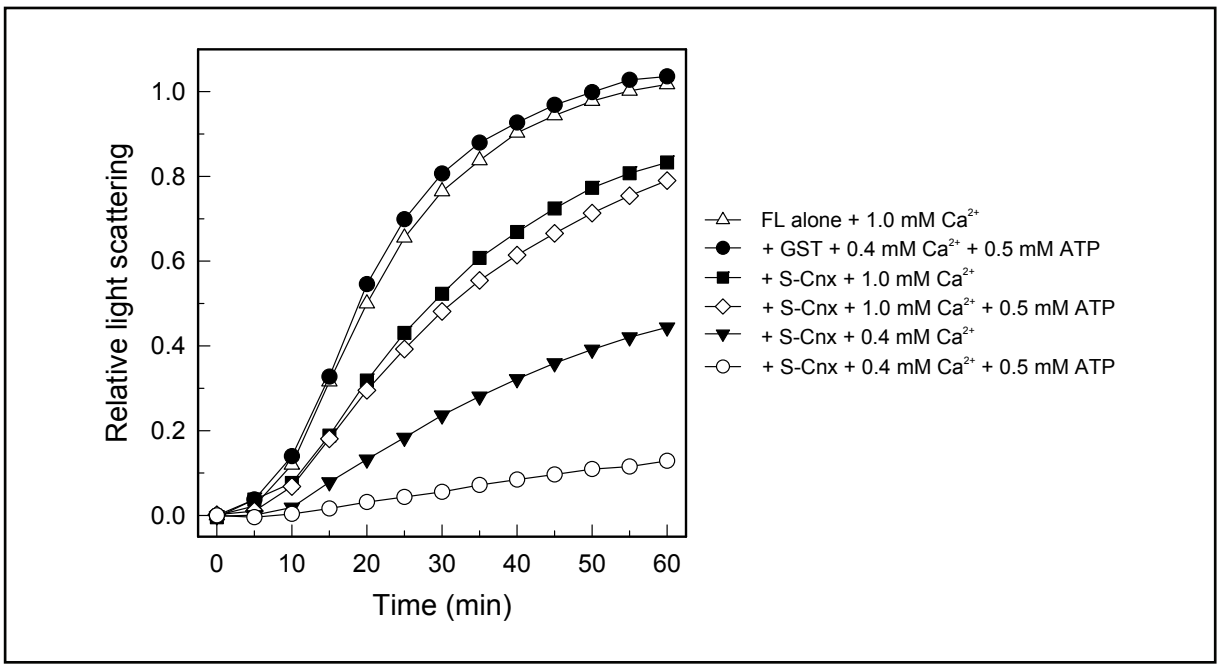

Fig. 21: Ca^{2+} and ATP enhance synergistically the aggregation suppression function of S-Cnx. S-Cnx (9 µM) was equilibrated in 20 mM Hepes, pH 7.4, 150 mM NaCl, and the indicated [Ca^{2+}] and [ATP] for 1 h at RT. FL was added to the various S-Cnx samples at a final concentration of 3 µM, and its aggregation at 37°C was monitored by measuring light scattering at 360 nm. Data points were measured every 6 s, shown every 5 min.

Far-UV CD spectra revealed no significant differences between S-Cnx in the presence of either 1 mM Ca^{2+}, 0.4 mM Ca^{2+}, or 1 mM Ca^{2+} + 0.5 mM ATP (Fig. 22.A). However, in the presence of 0.4 mM Ca^{2+} + 0.5 mM ATP, a significant decrease in mean residue ellipticity was observed, consistent with conformational changes in the chaperone. These changes were not associated with a decrease in thermal stability or an increase in protease susceptibility (data not shown). Rather, an increase in the affinity of ATP binding to S-Cnx was observed. Whereas the K_d for ATP binding was 2.9 mM in the presence of 1 mM Ca^{2+} (Fig. 19), it decreased to 0.7 mM in the presence of 0.4 mM Ca^{2+} (Fig. 22.B), both assessed by monitoring ATP-associated changes in bis-ANS fluorescence emission. Thus, the resting ER-luminal Ca^{2+} concentration of 0.4 mM exerts a significant impact on the ATP-binding site of S-Cnx, lowering the ATP concentration required to trigger exposure of a hydrophobic site that appears to be involved in suppressing the aggregation of non-glycosylated client polypeptides.

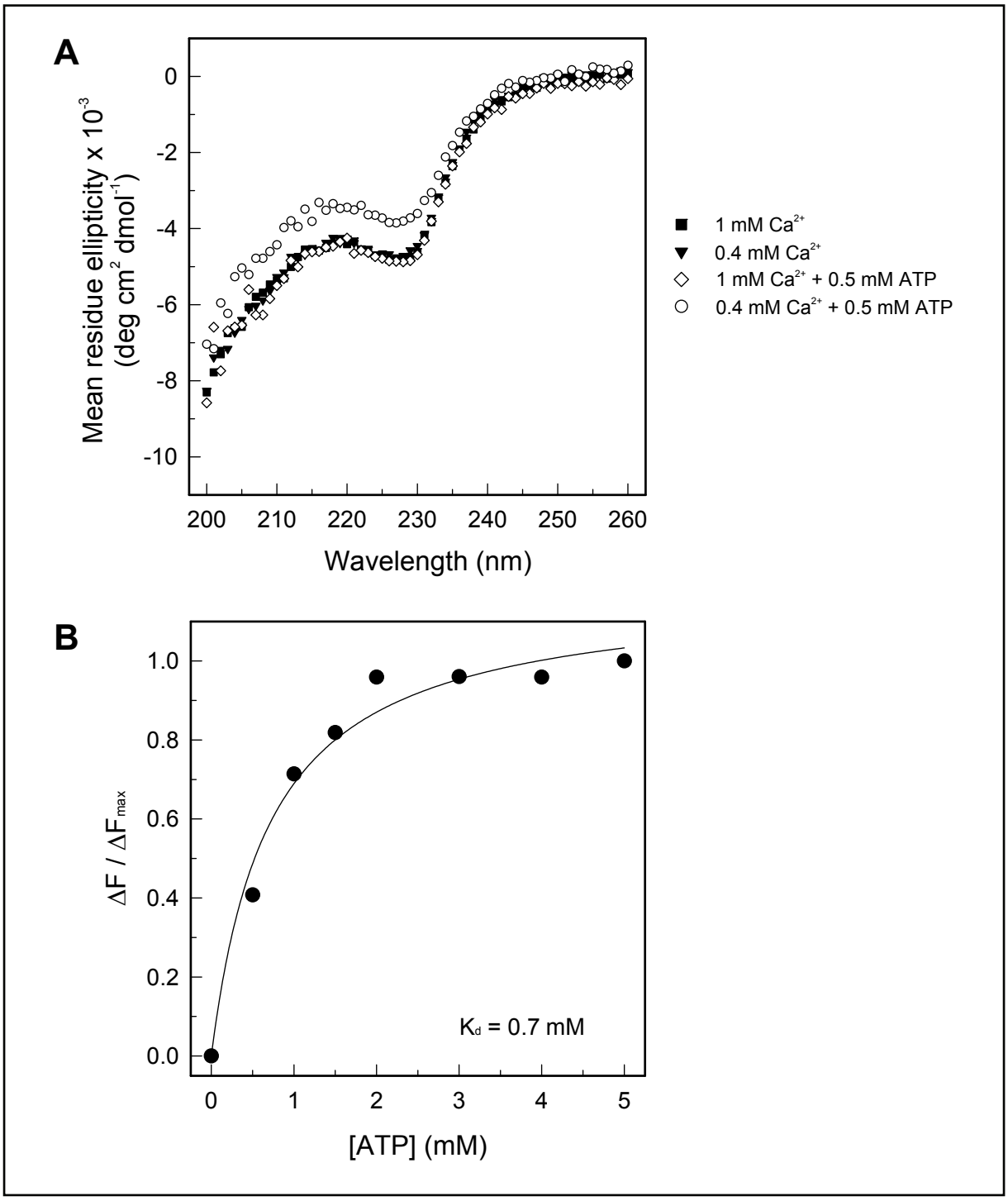

Fig. 22: Synergistic effects of Ca^{2+} and ATP on the structure of S-Cnx. (A) Far-UV CD spectra of S-Cnx. S-Cnx (1.81 µM) was equilibrated in 5 mM Hepes, pH 7.4, 150 mM NaCl, and various concentrations of Ca^{2+} and ATP for 1 h at RT. CD spectra were recorded from 200 to 260 nm at 37°C. (**B**) Bis-ANS binding to S-Cnx. S-Cnx (1 µM) was preincubated in 20 mM Hepes, pH 7.4, 150 mM NaCl, 0.4 mM $CaCl_2$, and the indicated [ATP] for 1 h at RT and mixed with 6 µM bis-ANS. Bis-ANS fluorescence was measured at 37°C with excitation and emission wavelengths of 390 and 490 nm, respectively. Results were plotted as the change in fluorescence (ΔF) divided by the maximum change in fluorescence between 0 mM and 5 mM ATP (ΔF_{max}). The data were fit to an equation describing single site binding using SigmaPlot. The K_d value is calculated as the average of three independent measurements with a standard deviation of 19 %.

3.3 Characterizing the contributions of the lectin and arm domains of calnexin to its molecular chaperone function

3.3.1 Domain contributions to the aggregation suppression function of S-Cnx

To localize the polypeptide-binding site of S-Cnx within the context of its arm and globular domains, the various deletion mutants depicted in Fig. 23 were generated and compared for their abilities to suppress the aggregation of FL under physiological conditions of the ER lumen.

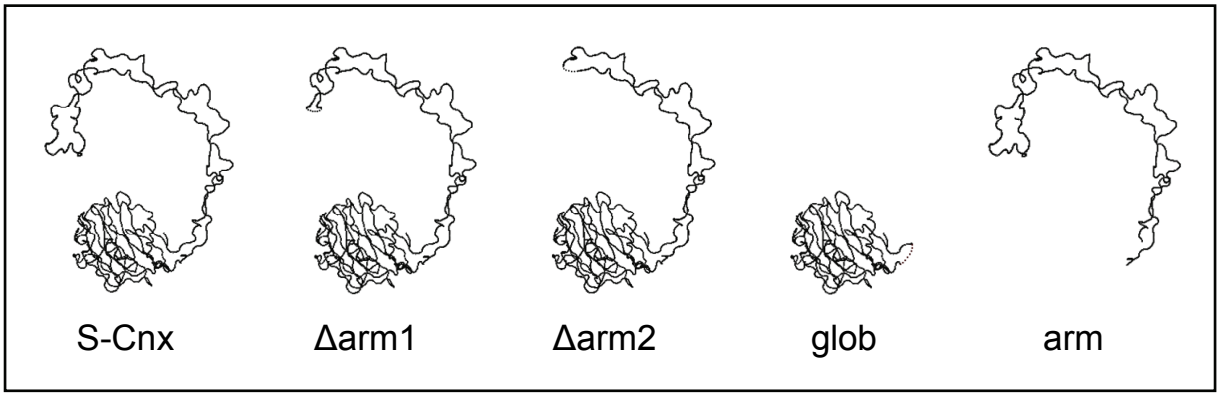

Fig. 23: Deletion mutants of S-Cnx used in this study. Crystal structure of S-Cnx (282) and theoretical depiction of deletion mutants as rendered by "Cn3D Viewer" (www.ncbi.nlm.nih.gov/Structure/CN3D/cn3d.shtml). Note that deleted residues were replaced by a GSG linker in the case of the Δarm1 and Δarm2 constructs and by a GSGSG linker in the case of the globular domain construct. For more details see Fig. 5 showing the linear sequences of the S-Cnx constructs.

Before undertaking the aggregation suppression assays, the structural integrity of the various constructs was assessed by far-UV CD and by measuring their thermal stabilities. In agreement with CD measurements described under result section 3.2.2 (Fig. 8), the CD spectrum of S-Cnx shown in Fig. 24.A exhibited a negative band at ~226 nm and a strong increase in signal intensity below 213 nm. Again, although the secondary structure of S-Cnx consists mainly of β-sheet with a minor α-helical component (282) , it has a high tryptophan content (2.9 % versus 1.7 % for an average protein (414)) which results in a CD spectrum that is dominated by the influence of tryptophan residues rather than expressing typical secondary structure characteristics (415). Aromatic side chains likely contribute as well to the distinct far-UV spectrum of the arm domain (Fig. 24.B), with a negative band at 230 nm, intercepting

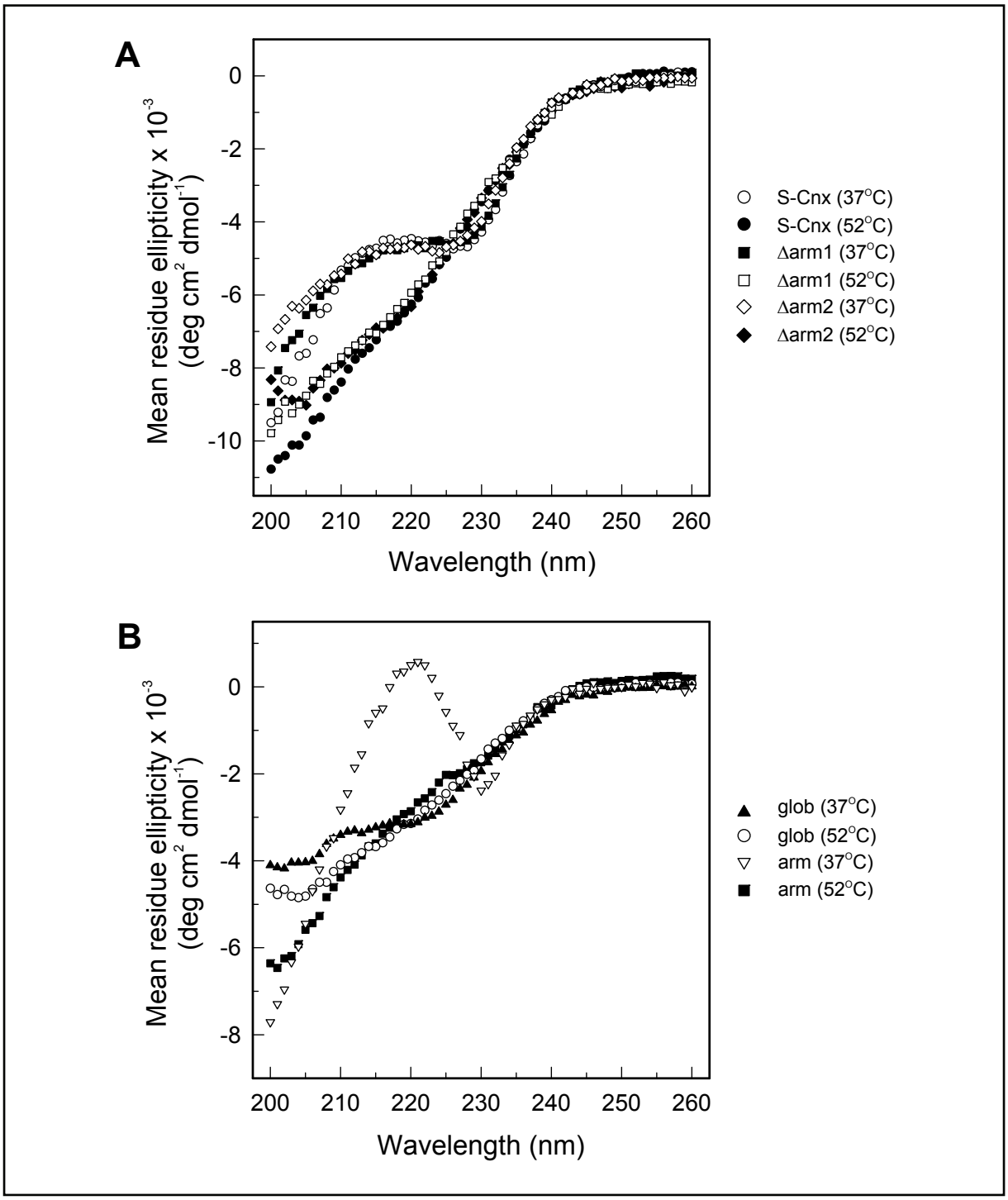

Fig. 24: Far-UV circular dichroism spectra of S-Cnx and its deletion mutants. The CD spectra of **(A)** S-Cnx, **(A)** Δarm1, **(A)** Δarm2, **(B)** arm, and **(B)** glob (1.81 µM each) in 2.5 mM Hepes, pH 7.4, 150 mM NaCl, and a free [Ca^{2+}] of 0.4 mM were monitored at the indicated temperatures after a preincubation period of 1 h at 37°C.

the baseline with a pronounced positive maximum at 222 nm. This closely resembles the reported far-UV CD spectrum of the arm domain of Crt (294). The CD spectra of the Δarm1 and Δarm2 constructs in Fig. 24.A were essentially superimposable with that of S-Cnx except for a minor decrease in intensity in the 200-209 nm region, correlating with the extent of the

truncation. By contrast, the CD spectrum of the globular domain had a comparatively low intensity (Fig. 24.B), a characteristic also reported for the globular domain of Crt (281, 294). In addition a negative band at 220 nm and a modest increase in signal intensity below 210 nm were observed. The individual globular and arm domains of S-Cnx have previously been shown to exhibit native functionality as assessed by retention of oligosaccharide and ERp57 binding, respectively (280).

Changes in the CD spectrum following unfolding at 52°C were distinct enough for both S-Cnx, similar to denaturation experiments shown before (Fig. 8), and for the various deletion mutants (Fig. 24.A: S-Cnx, Δarm1, Δarm2; Fig. 24.B: glob, arm) to compare their stabilities by recording thermal denaturation curves at 231 nm (Fig. 25.A: S-Cnx, Δarm1, Δarm2; Fig. 25.B: glob, arm). A T_m value of 48.6°C was calculated from the well-defined

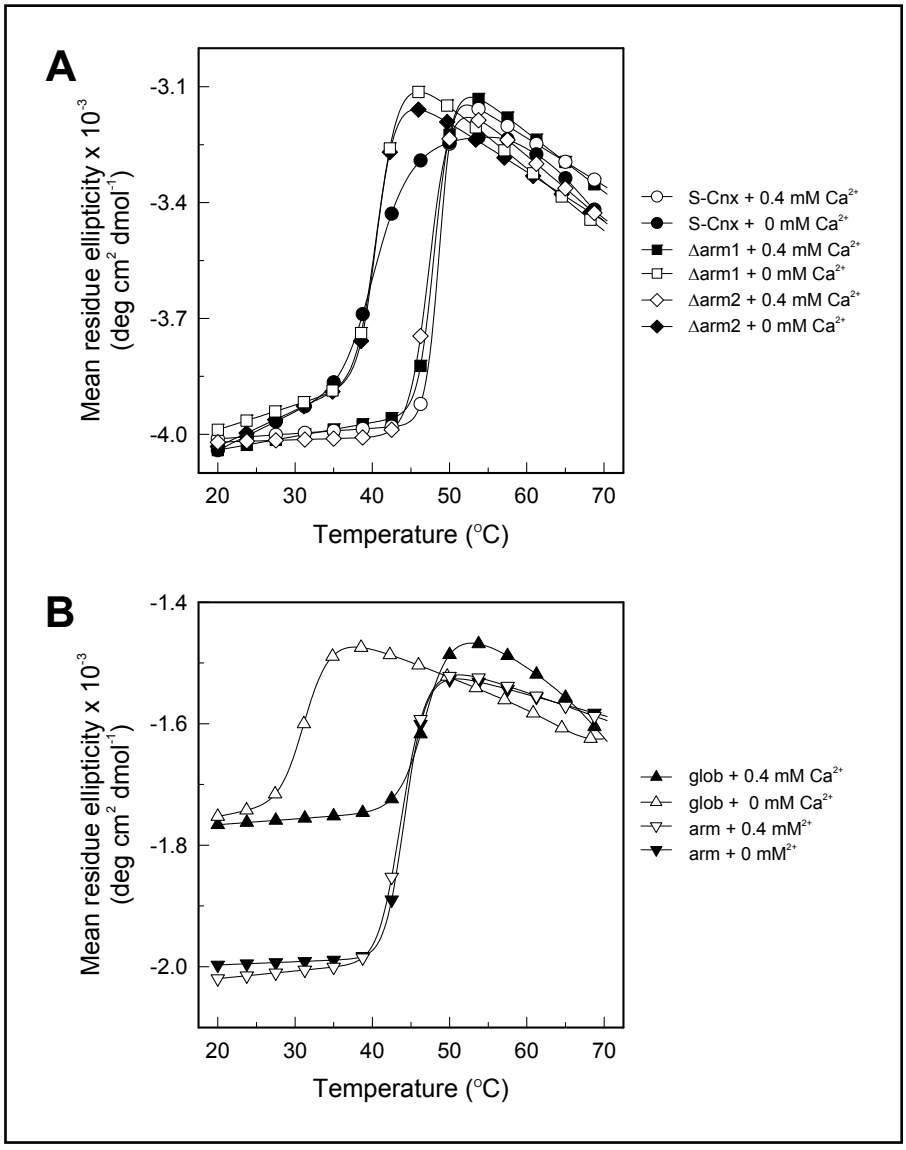

Fig. 25: Thermal stabilities and Ca^{2+}-binding properties of S-Cnx constructs. (A) S-Cnx, **(A)** Δarm1, **(A)** Δarm2, **(B)** arm, and **(B)** glob (7.24 µM each) were equilibrated in 20 mM Hepes, pH 7.4, 150 mM NaCl, and the indicated free [Ca^{2+}] for 1 h at 37°C and thermal denaturation curves (20-70°C) were obtained by recording the change in CD signal at 231 nm.

thermal transition curve of S-Cnx. Partial or complete truncation of the arm domain did not result in a significant destabilization of the proteins (Tab. 4); only the arm domain appeared to be less stable with a T_m value of 44.2°C. Importantly, no evidence of denaturation was observed for any of the mutants at the 37°C temperature used in subsequent aggregation suppression assays.

As shown in result section 3.2.2, reducing the Ca^{2+} concentration below the 0.4 mM level of the resting ER was associated with a marked decrease in thermal stability of S-Cnx (Fig. 10). To assess the Ca^{2+}-binding properties of the various mutants, the thermal denaturation experiments were repeated in the absence of Ca^{2+}. As shown in Tab. 4, the removal of Ca^{2+} resulted in decreased thermal stability for S-Cnx and all mutants (Fig. 25), with the exception of the arm domain, for which the T_m value remained the same.

Tab. 4: Comparison of T_m values of S-Cnx constructs. T_m values were calculated by fitting the thermal denaturation curves (Fig. 25) to an equation describing a two-state denaturation process using SigmaPlot. Values represent averages obtained from three different measurements with a standard deviation below 2.4 %.

$[Ca^{2+}]$	0.4 mM	0 mM
	T_m (°C)	
S-Cnx	48.6	41.1
Δarm1	48.3	40.9
Δarm2	47.5	40.8
glob	47.6	31.7
arm	44.2	44.4

Ca^{2+} binding analysis of S-Cnx domains was also performed by measuring changes in intrinsic fluorescence given that this method already allowed the characterization of Ca^{2+} binding to S-Cnx depicted in Fig. 12. Truncation and complete removal of the arm domain with its 8 tryptophan residues was accompanied by a correlative decrease in fluorescence intensity compared to the emission spectrum of S-Cnx (Fig. 26). However, in addition, intrinsic fluorescence of all S-Cnx constructs containing the globular domain was reduced in average by ~40 % upon Ca^{2+} removal. Only for the arm domain was no Ca^{2+} dependent change in the emission spectrum detectable.

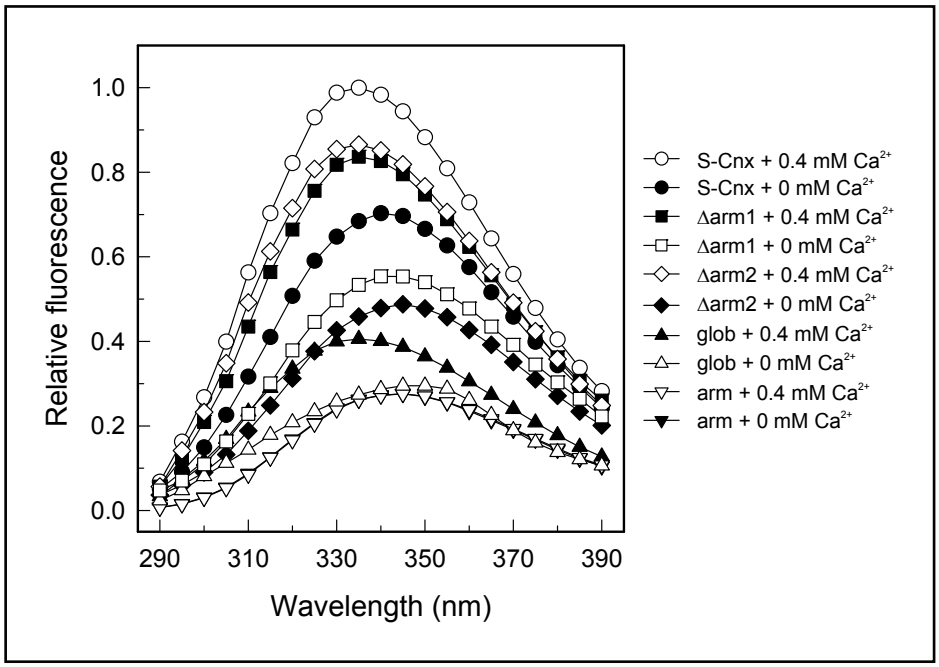

Fig. 26: Effect of Ca^{2+} on the intrinsic fluorescence of S-Cnx constructs. S-Cnx and deletion mutants (0.8 μM) were incubated in 20 mM Hepes, pH 7.4, 150 mM NaCl, and the indicated free [Ca^{2+}] for 1 h at 37°C and the fluorescence spectra were measured from 290 to 390 nm at 37°C with an excitation wavelength of 280 nm. Emission values were recorded every 1 nm, but for clarity plotted every 5 nm.

These findings demonstrate that all mutants possessing the globular domain retain the ability to bind Ca^{2+}, and further, that the observed Ca^{2+}-dependent changes in S-Cnx structure are mediated by the globular domain rather than by the arm domain.

The various deletion mutants were next compared for their capacities to suppress the aggregation of FL. As demonstrated before (Fig. 7), FL is an ideal client protein for these assays because, being non-glycosylated, aggregation suppression is mediated solely through polypeptide-based interactions. Furthermore, since FL unfolds and aggregates at 37ºC in the presence of 0.4 mM Ca^{2+}, suppression of aggregation by S-Cnx can be examined under physiological conditions of the ER lumen. Fig. 27 shows the comparison between the concentrations of S-Cnx and the various deletion mutants required to suppress the aggregation of 3 μM FL to ~ 40 % of the level observed with FL alone. This is a more sensitive assay than the complete suppression of FL aggregation and, in the case of S-Cnx, a 4 μM concentration suppressed FL aggregation to 40 %. Progressive truncation of the arm domain resulted in a corresponding increase in chaperone concentration required to suppress aggregation to the same level. By comparing these concentrations, Δarm1, Δarm2, and the globular domain were 2.5-fold, 3.25-fold, and 3.75-fold less potent than S-Cnx, respectively. Although this suggested that a polypeptide-based interaction site may reside within the arm domain, the arm domain itself did not reveal any capacity to suppress FL aggregation at a 10-fold molar excess. Thus, the polypeptide-binding site of S-Cnx appears to reside within its globular domain but the arm domain is required to effect maximal aggregation suppression.

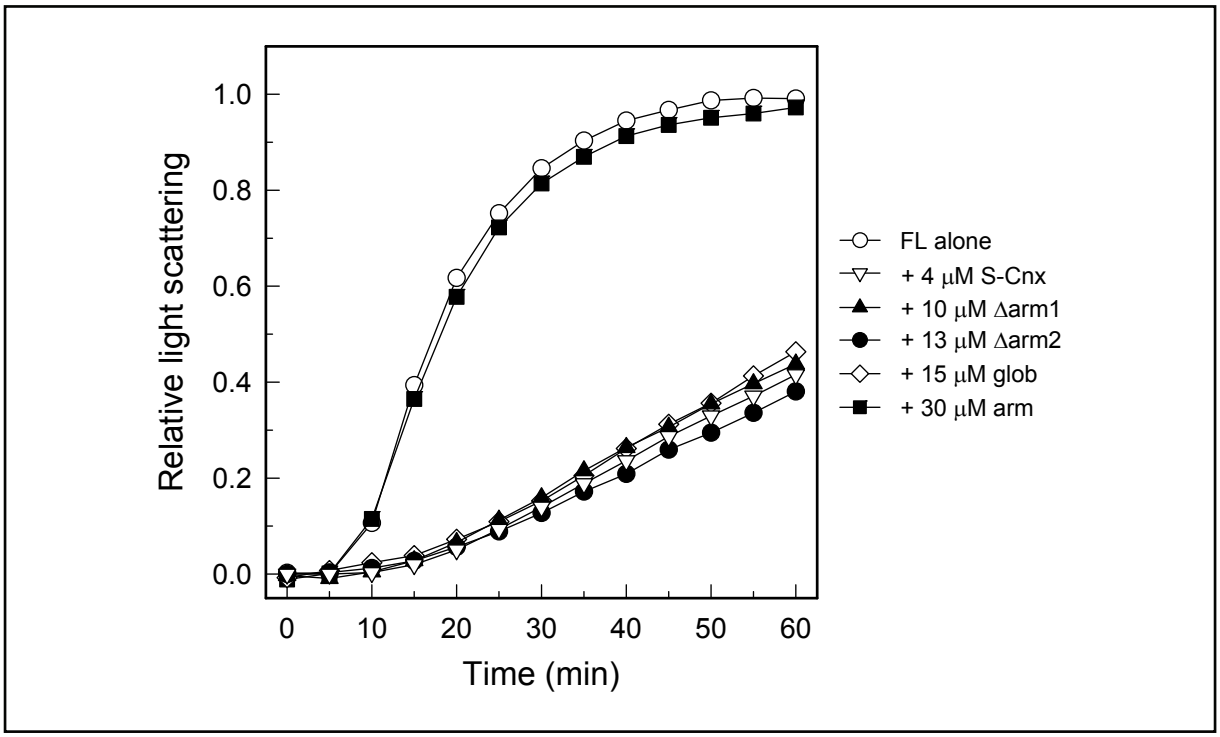

Fig. 27: Contributions of S-Cnx's domains to its aggregation suppression function. S-Cnx constructs were equilibrated at the indicated concentrations in 20 mM Hepes, pH 7.4, 150 mM NaCl, and 0.4 mM $CaCl_2$ for 1 h at 37°C. Upon addition of FL (3 μM) to the various samples aggregation was monitored at 37°C every 6 s by measuring light scattering at 360 nm. For clarity, data points are shown every 5 min.

3.3.2 Hydrophobic peptides compete with S-Cnx in the suppression of FL aggregation

Small peptides have been used as client protein mimetics to report on the location and characteristics of client protein-binding sites on a variety of molecular chaperones (218, 416-422). In most cases, effective peptides exhibit substantial hydrophobicity.

To determine if this approach could be applied to S-Cnx, it was first tested whether peptides with hydrophobic character could compete with S-Cnx to suppress FL aggregation. Again, the S-Cnx:FL ratio was chosen to provide partial aggregation suppression as a sensitive readout of the effects of additives (Fig. 28A). The three peptides tested did not affect the aggregation of FL by themselves (Fig. 28.A). However, when S-Cnx was preincubated for 1 h with peptide 6KAAW (KKKKKKAAWAAWAAWAA), the ability of S-Cnx to subsequently suppress FL aggregation was lost. To exclude the possibility that the inhibitory effect of the 6KAAW peptide was due to the positively charged hexa-lysine segment, the more hydrophilic peptide 6KSGG (KKKKKKSGGSGGSGGSC) was tested and found that it had no significant effect on the aggregation suppression function of S-Cnx (Fig. 28.A). Also,

another largely hydrophobic peptide was examined representing the first transmembrane segment of the Hsmr protein from *Halobacterium salinarum*, for which just two lysines flanking the C- and N-termini were sufficient to confer water solubility. This KHP peptide (KHPYAYLAAAIAAEVAGTTALKLSK) also blocked the ability of S-Cnx to suppress FL aggregation, although somewhat less potently than 6KAAW. The experiments were repeated with the arm domain truncation mutants, Δarm1 and Δarm2, as well as with the globular domain with similar results (Fig. 28.B-D).

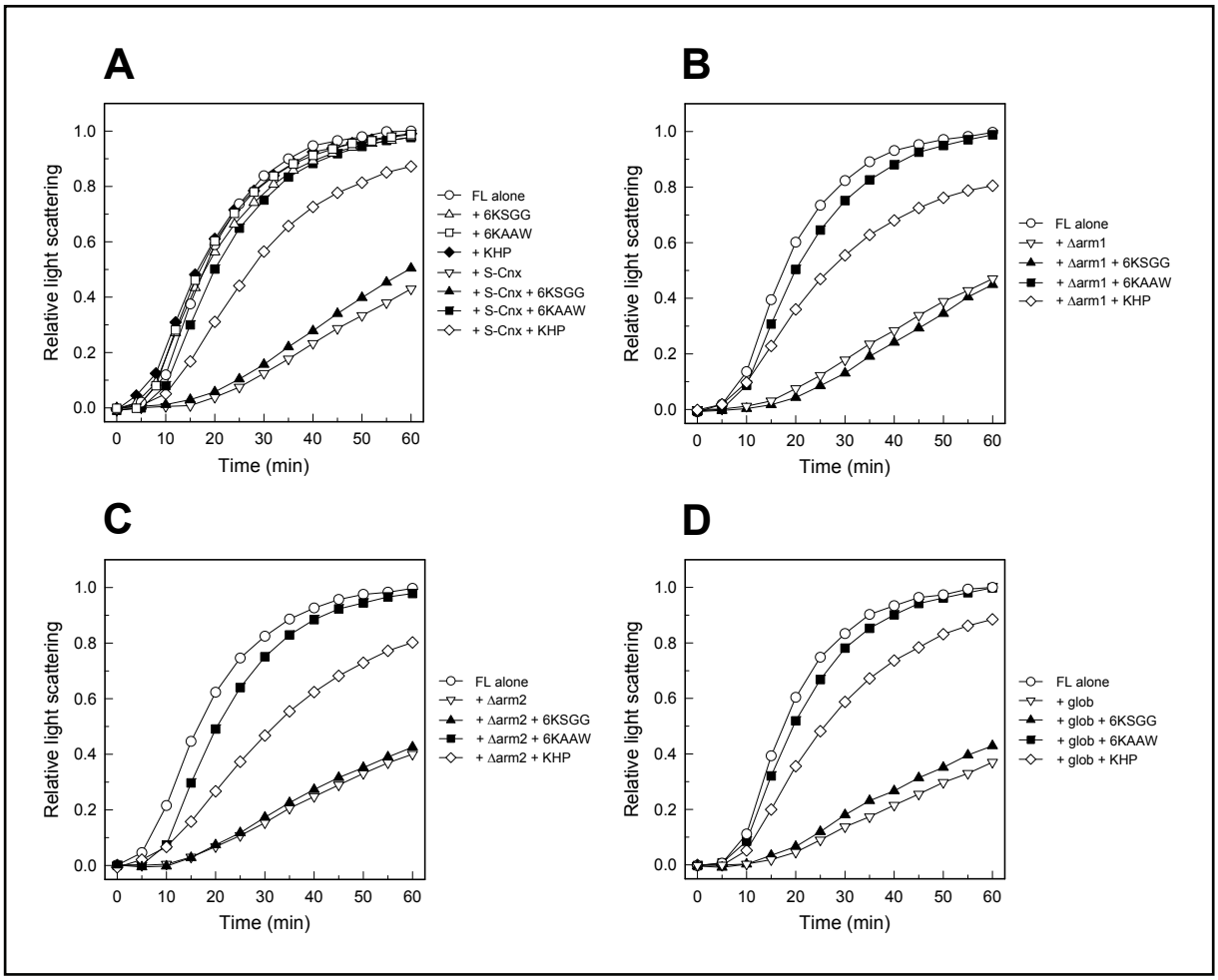

Fig. 28: Hydrophobic peptides influence the aggregation suppression function of S-Cnx and deletion mutants. Prior to aggregation measurements, the indicated peptides (20 µM) were incubated with S-Cnx constructs (**(A)** S-Cnx, 4 µM; **(B)** Δarm1, 10 µM; **(C)** Δarm2, 13 µM; **(D)** glob, 15 µM) in 20 mM Hepes, pH 7.4, 150 mM NaCl, and 0.4 mM $CaCl_2$ for 1 h at 37°C. Subsequently, FL was added at a final concentration of 3 µM and light scattering was monitored at 360 nm for 1 h at 37°C. Data points were measured every 6 s and plotted every 5 min.

3.3.3 The globular domain of S-Cnx binds hydrophobic peptides

To confirm that the ability of hydrophobic peptides to compete in the aggregation suppression assay was due to their binding to one or more sites on S-Cnx, peptide interactions with S-Cnx and its mutants were examined using two direct binding assays.

As mentioned previously, the far-UV CD spectrum of a protein is influenced by structural elements other than secondary structure. Disulfide bonds (423, 424), the length and regularity of structural elements (425), as well as aromatic amino acid side chains (especially tryptophans) in combination with a low content of α-helix contribute to far-UV CD spectra (415, 426). Consequently, the far-UV CD spectrum can detect changes in an asymmetric environment upon ligand binding. Thus, in the first assay, the far-UV spectra of S-Cnx with and without the largely hydrophobic 6KAAW peptide were compared and a decrease in the magnitude of the mean residue ellipticity values below 237 nm was observed in the presence of peptide, indicative of interaction (Fig. 29). These changes were also observed upon

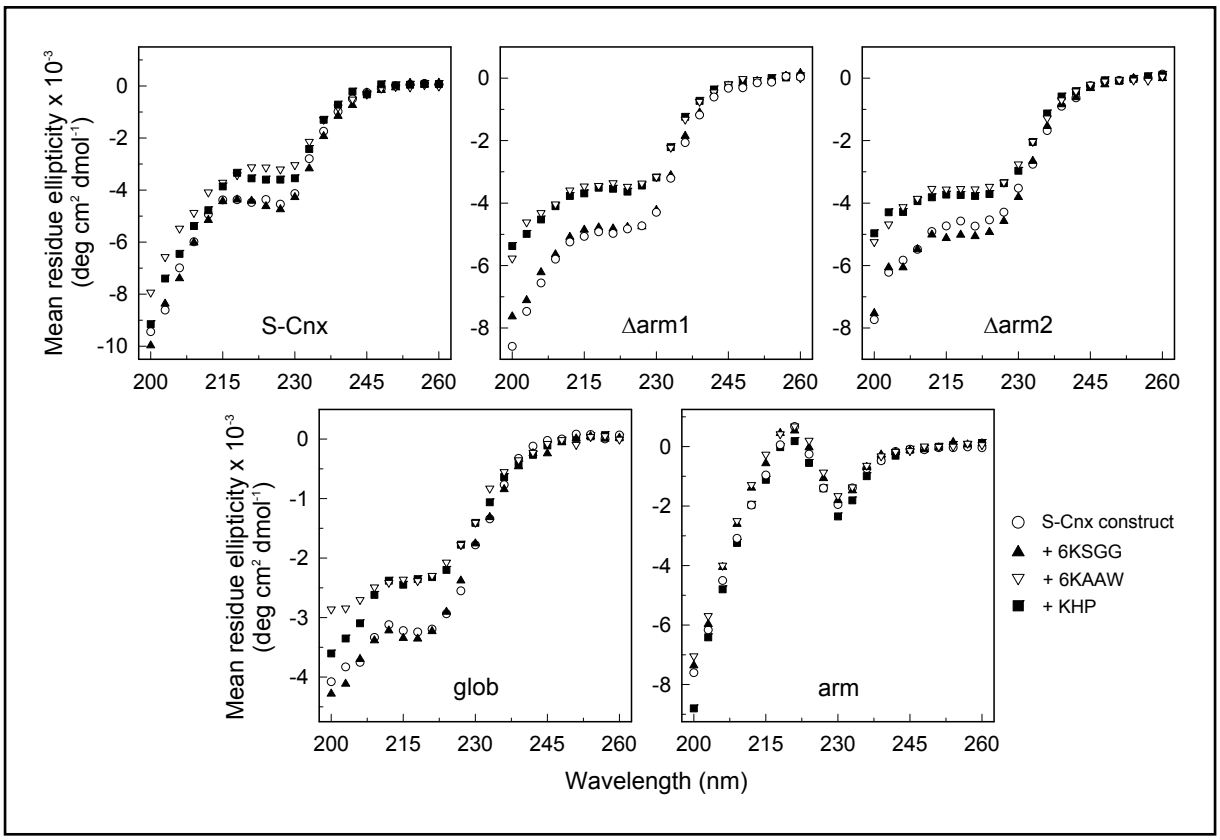

Fig. 29: Peptide binding to S-Cnx and deletion mutants as assessed by far-UV circular dichroism. S-Cnx or mutants (1.81 µM) were preincubated in the presence or absence of the indicated peptides (20 µM) in 2.5 mM Hepes, pH 7.4, 150 mM NaCl, and a free [Ca^{2+}] of 0.4 mM for 1 h at 37°C. Far-UV CD spectra were scanned from 200 to 260 nm at 37°C. The obtained spectra were corrected by subtracting the contribution of the respective peptide alone.

incubation of S-Cnx with the hydrophobic KHP peptide. By contrast, the more hydrophilic 6KSGG peptide had no detectable effect on the CD spectrum of S-Cnx. Similar intensity shifts in mean residue ellipticity below 237 nm were measured for Δarm1, Δarm2, and the globular domain in the presence of the hydrophobic peptides but not with the 6KSGG peptide (Fig. 29). Notably, none of the peptides caused any significant change in the far-UV spectra of the arm domain. The data are consistent with peptide binding only to the globular domain of S-Cnx since observed intensity changes in mean residue ellipticity were independent of the length or presence of the arm domain and no spectral changes were detected upon incubation of peptide with the arm domain. Furthermore, these findings are in good agreement with the aggregation suppression experiments, where only the hydrophobic 6KAAW and KHP peptides were able to compete with the various S-Cnx constructs to suppress FL aggregation.

To further localize the site of peptide binding to S-Cnx, the KHP peptide was radioiodinated and incubated with the various His_6-tagged S-Cnx constructs. Following collection of ^{125}I-peptide-S-Cnx complexes on nickel-agarose beads, complexes were eluted and radioactivity quantified by gamma counting. As shown in Fig. 30, all deletion mutants with the exception of the arm domain exhibited similar ability to bind radioiodinated

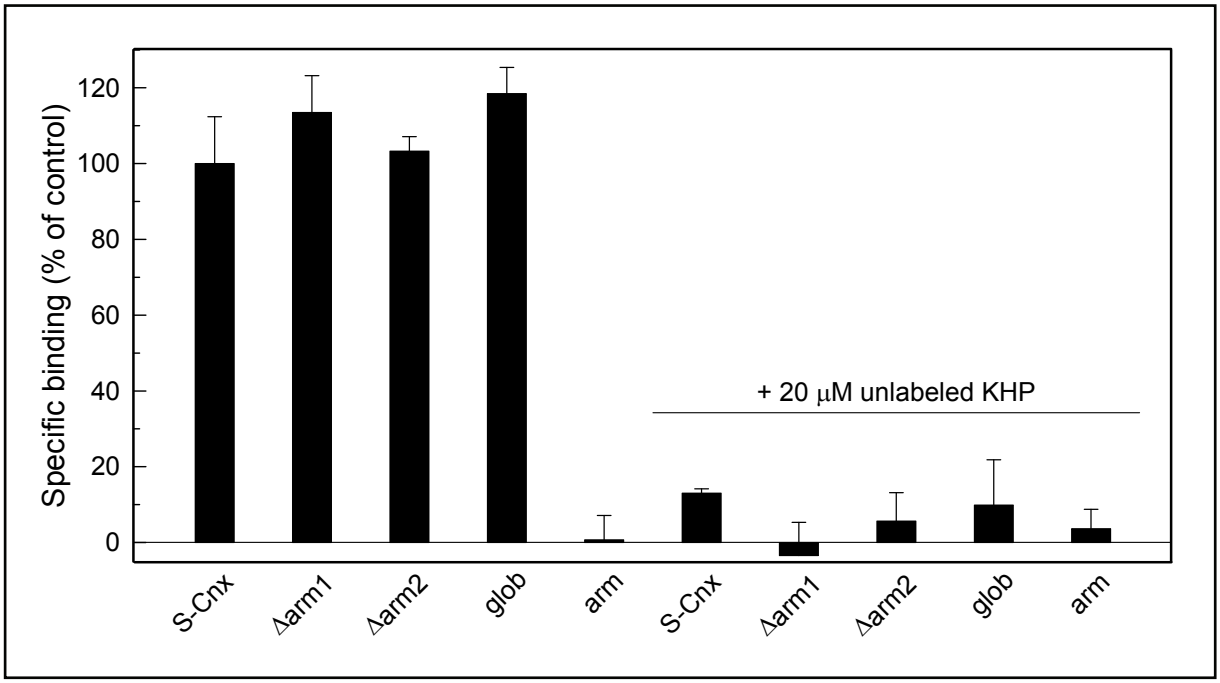

Fig 30: Binding of radioiodinated KHP peptide to S-Cnx and deletion mutants. The various S-Cnx constructs (5 μM) were incubated with 1 μM ^{125}I-KHP-peptide in 20 mM Hepes, pH 7.4, 150 mM NaCl, and 0.4 mM $CaCl_2$ for 1 h at 37°C in the presence or absence of 20 μM unlabeled KHP peptide as indicated. The His_6-tagged proteins were then recovered by incubation with nickel-agarose beads and, after washing and elution with buffer containing 250 mM imidazole, radioactivity in the eluates was quantified by gamma counting. Radioiodinated KHP peptide bound to the deletion mutants was expressed as a percentage of ^{125}I-KHP-peptide bound to intact S-Cnx (~132,000 cpm). Error bars represent the standard deviation of three replicate experiments.

KHP peptide. Binding was specific as evidenced by the lack of arm domain binding as well as by the ability of a 20-fold excess of unlabeled KHP peptide to compete with radiolabeled peptide in the assay. These results confirm the suggestion from the CD-based binding assay that the peptide-binding site resides solely within the globular domain of S-Cnx.

3.3.4 Hydrophobic peptides bind to the globular domain of S-Cnx at a location distinct from the lectin site

Analysis of the X-ray structure of the ER-luminal domain of Cnx upon co-crystallization with α-D-glucose (282) allowed the localization of the carbohydrate molecule on the concave β-sheet of the lectin domain. The terminal glucose of the natural $Glc_1Man_9GlcNAc_2$ oligosaccharide presumably rests on the side chain of Met169, while the hydroxyl groups form hydrogen bonds to Tyr145, Lys147, Tyr166, Glu197, and Glu406 (Fig. 31). Site directed mutagenesis studies with those six residues confirmed their essential role for the lectin function as the loss of even a single hydrogen bonding residue abolished oligosaccharide binding (287). Since the lectin site of S-Cnx possesses significant hydrophobic character conferred by the two tyrosine residues and one methionine residue it was a candidate for the site of hydrophobic peptide binding.

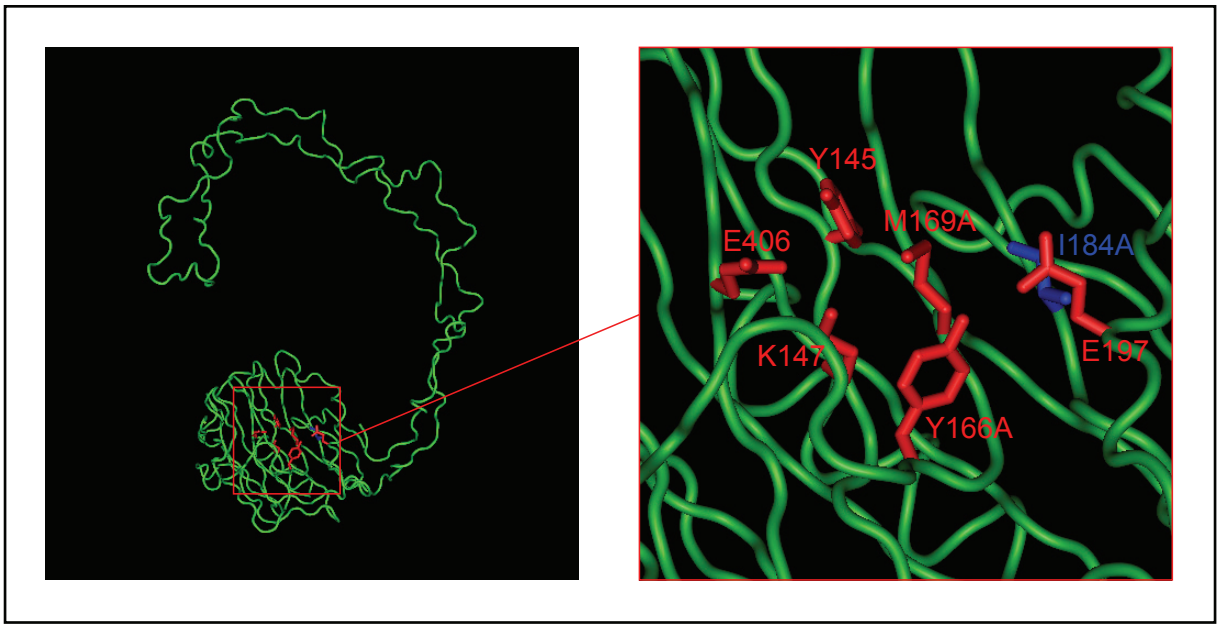

Fig. 31: Oligosaccharide-binding site of the ER-luminal domain of calnexin. (A) Location and **(B)** close-up of the lectin site in the X-ray crystal structure of S-Cnx (282) illustrated by "Cn3D Viewer" (www.ncbi.nlm.nih.gov/Structure/CN3D/cn3d.shtml). The six amino acid residues that displayed contacts to co-crystallized glucose are shown in red stick representation and are labeled. Labels also indicate the positions of the three alanine exchanges of amino acids Y166, M169, and I184 (blue) in lectin-deficient S-Cnx.

This possibility was evaluated in two ways using the ^{125}I-KHP peptide binding assay (2.2.20).

In the first approach, three hydrophobic residues within the lectin site were mutated to alanine (Y166A, M169A, and I184A) in an effort to generate a lectin-deficient mutant of S-Cnx (LD-S-Cnx). To ensure that the structural integrity of S-Cnx was not severely affected by the three point mutations, far-UV CD spectra of this lectin-deficient triple mutant and S-Cnx were compared as shown in Fig. 32.

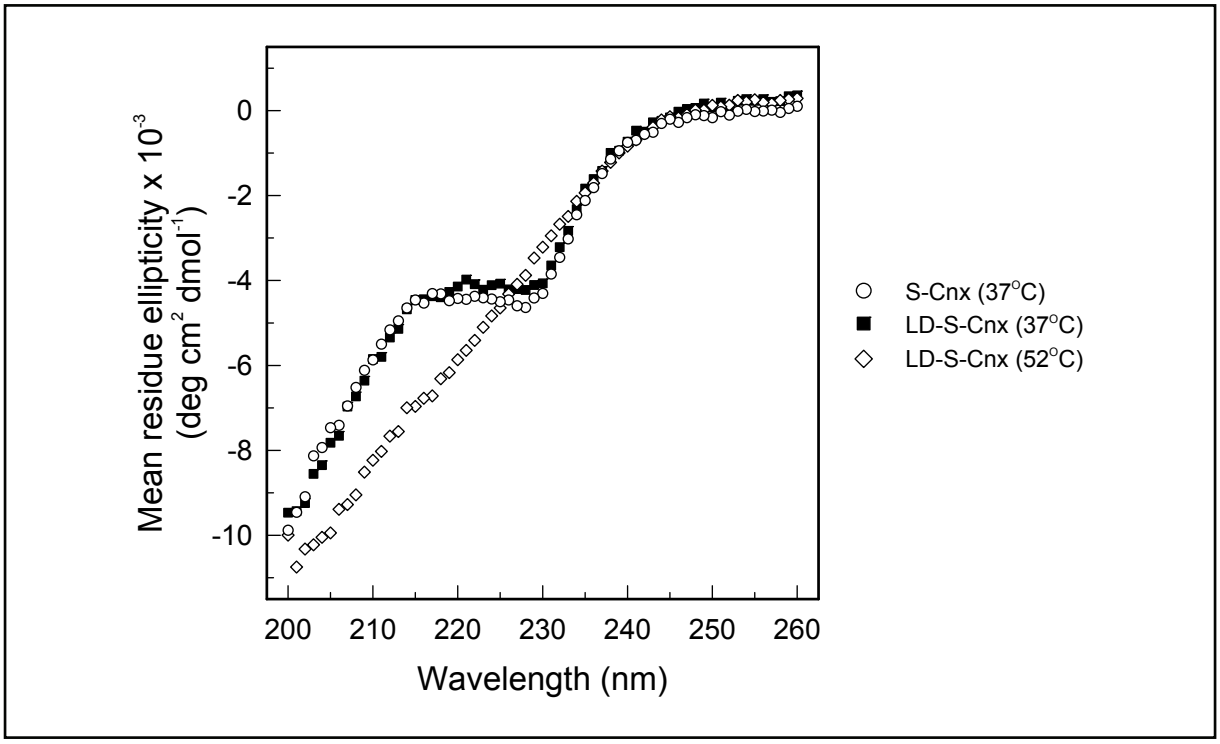

Fig. 32: Structural integrity assessment of lectin-deficient S-Cnx by far-UV circular dichroism. Prior to recording the CD spectra of S-Cnx and its lectin-deficient mutant at the indicated temperatures, proteins (1.81 µM) were preincubated in 2.5 mM Hepes, pH 7.4, 150 mM NaCl, and a free [Ca^{2+}] of 0.4 mM for 1 h at 37°C.

The recorded CD spectra displayed the same characteristics and were basically superimposable, indicative that the mutations did not cause any significant distortion of the structure. Yet, the triple mutant appeared to be slightly less stable, since its thermal denaturation curve exhibited a T_m value 1.9°C below the T_m value of S-Cnx of 48.5°C (Fig. 33 and Tab. 5), but, importantly, there was no sign of unfolding at 37°C. In addition, the thermal stability of LD-S-Cnx was measured in the absence of Ca^{2+} to test if the mutant retained the ability to respond with Ca^{2+} induced conformational changes. As was the case for S-Cnx and deletion mutants (Fig. 25 and Tab. 4), Ca^{2+} removal yielded a substantial destabilization of the molecule evidenced by a reduced T_m value of 39.7°C. Thermal stability measurements by CD were next performed to confirm the oligosaccharide-binding deficiency of the triple mutant. S-Cnx revealed a 3°C increase in T_m upon the addition of the

tetrasaccharide G_1M_3 (Fig. 33), which binds to S-Cnx or Crt with similar affinity as the full length oligosaccharide (K_d = 1-2 µM; (372, 427)). In contrast, LD-S-Cnx exhibited nearly unaltered T_m values of 46.3 and 46.6°C in the presence or absence of G_1M_3, respectively, demonstrating the successful inactivation of the lectin site by introduction of the three point mutations.

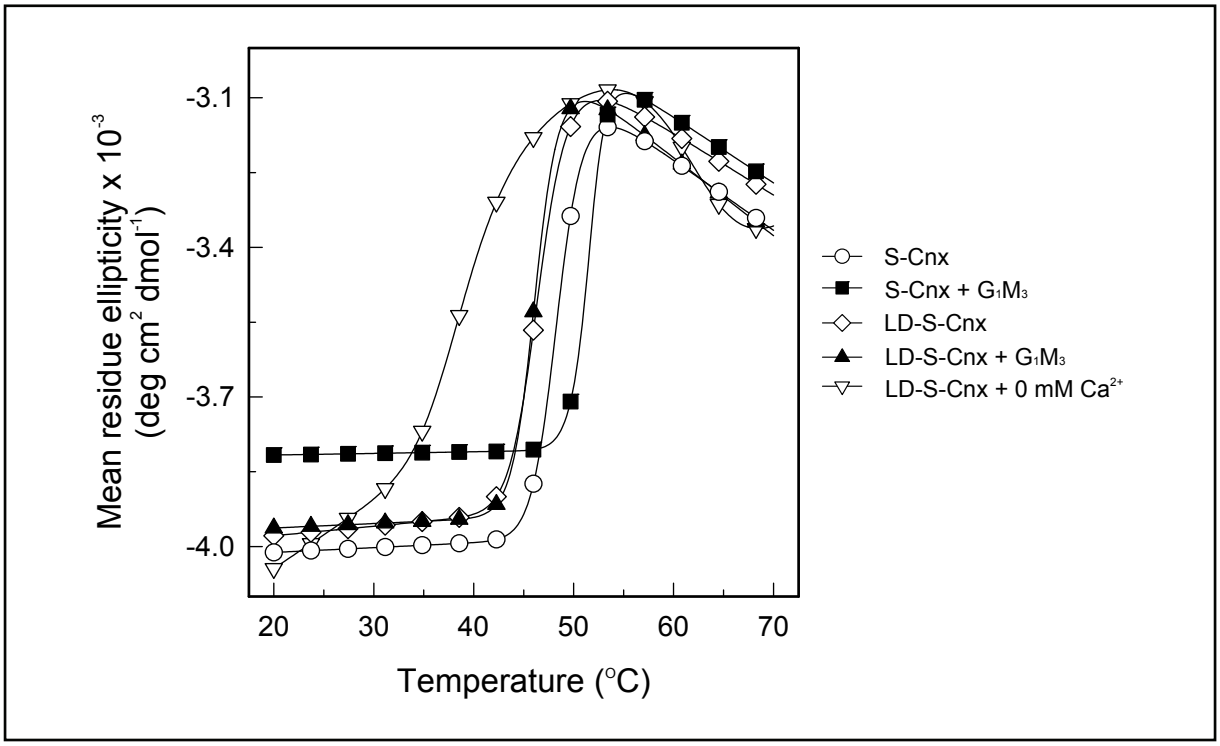

Fig. 33: Ca^{2+}- and oligosaccharide-binding properties of lectin-deficient S-Cnx. S-Cnx or LD-S-Cnx (7.24 µM) were incubated in 20 mM Hepes, pH 7.4, 150 mM NaCl, and the indicated free [Ca^{2+}] with or without G_1M_3 oligosaccharide (20 µM) for 1 h at 37°C and changes in CD signal at 231 nm were recorded from 20-70°C. T_m values were determined by fitting the thermal denaturation curves to an equation describing a two-state denaturation process using SigmaPlot.

Tab. 5: Effect of Ca^{2+} and oligosaccharide on the thermal stability of lectin-deficient S-Cnx. T_m values were determined by fitting the thermal denaturation data (Fig. 33) to an equation describing a two-state denaturation process using SigmaPlot. Results are average values from three different experiments with a standard deviation below 1 %.

[Ca^{2+}]	0 mM	0.4 mM	0.4 mM
[G_1M_3]	0 µM	0 µM	20 µM
		T_m (°C)	
S-Cnx		48.5	51.5
LD-S-Cnx	39.7	46.6	46.3

To address the possibility that the triple amino acid exchange within the lectin site could have impaired S-Cnx's chaperone function, the potency of LD-S-Cnx in suppressing the thermal aggregation of FL was examined. As illustrated in Fig. 34, FL aggregation was comparably

reduced in the presence of S-Cnx or equimolar concentrations of the lectin deficient mutant. Also the ability of hydrophobic peptides to compete with S-Cnx in aggregation suppression of FL upon disruption of the lectin site was still observed.

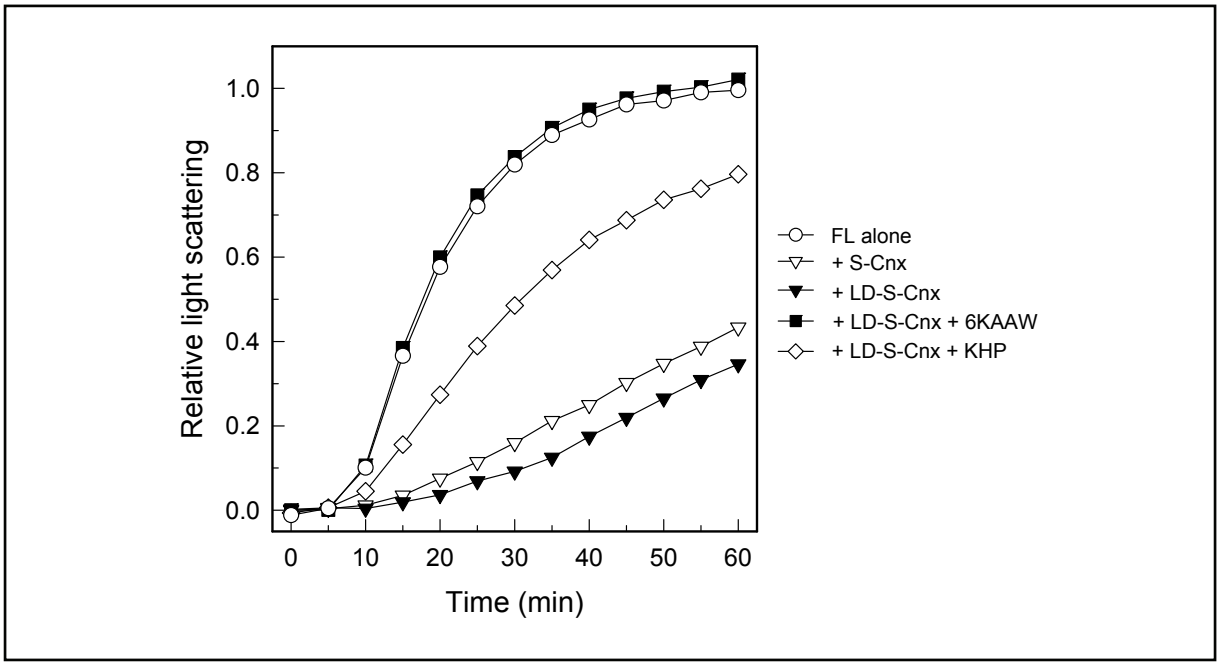

Fig. 34: Aggregation suppression potency of lectin-deficient S-Cnx. S-Cnx constructs were equilibrated in 20 mM Hepes, pH 7.4, 150 mM NaCl, and 0.4 mM $CaCl_2$ in the presence or absence of the indicated peptides (20 μM) for 1 h at 37°C. FL was diluted into the various samples to a final concentration of 3 μM and its aggregation at 37°C was monitored by light scattering measurements at 360 nm for 1 h. Data points were measured every 6 s, but plotted at 5 min intervals.

Thus, having shown the structural integrity of the triple mutant and its unaltered aggregation suppression function independent of the lectin site, the ability of LD-S-Cnx to bind radioiodinated KHP peptide was tested. Upon incubation of lectin-deficient S-Cnx with ^{125}I-KHP peptide, LD-S-Cnx displayed full capability of binding to ^{125}I-KHP peptide (Fig. 35).

In the second approach, the tetrasaccharide G_1M_3, was tested as a potential competitor of the S-Cnx-KHP peptide interaction. As depicted in Fig. 35, binding of this oligosaccharide to the lectin site of S-Cnx at a concentration 20-fold greater than that of the KHP peptide, had no effect on the formation of the S-Cnx-^{125}I-KHP complex.

Collectively, these findings demonstrate that the peptide-binding site of S-Cnx is distinct from the lectin site.

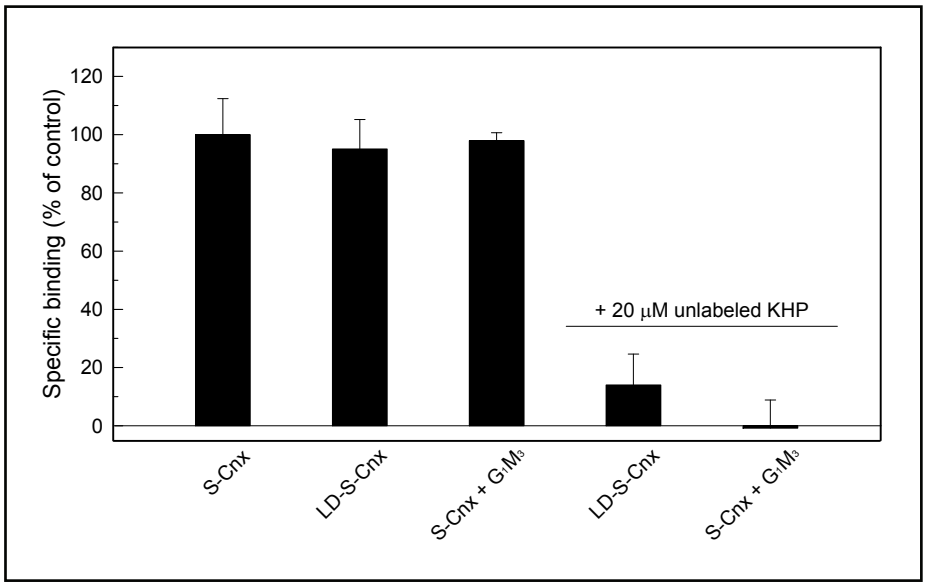

Fig 35: Lectin-independent binding of S-Cnx to radioiodinated KHP peptide. S-Cnx or LD-S-Cnx (5 μM) were equilibrated with 1 μM ^{125}I-KHP-peptide in 20 mM Hepes, pH 7.4, 150 mM NaCl, and 0.4 mM $CaCl_2$ for 1 h at 37°C with or without 20 μM unlabeled KHP peptide or 20 μM G_1M_3 oligosaccharide as indicated. After recovery of the His_6-tagged constructs on nickel-agarose beads, proteins were washed and eluted with buffer containing 250 mM imidazole. Radioactivity in the eluates was determined by gamma counting and was expressed as a percentage of ^{125}I-KHP-peptide bound to intact S-Cnx (~132,000 cpm). All samples were measured in triplicates with a standard deviation indicated by error bars.

3.3.5 Characteristics of hydrophobic peptide binding to S-Cnx

As a means to investigate the affinity and stoichiometry of peptide binding to S-Cnx, the intrinsic fluorescence spectra of S-Cnx upon incubation with KHP peptide, YSN peptide (YSNENMETM) and 6KSGG peptide were compared. The YSN peptide was included as a control because it contains a single tyrosine and exhibits weak intrinsic fluorescence, as does the KHP peptide which possesses two tyrosine residues. Furthermore, like 6KSGG, the YSN peptide did not compete with S-Cnx in the aggregation suppression assay with FL and was not expected to bind to S-Cnx (data not shown). Fig. 36.A shows that, following subtraction of the weak peptide emission spectrum, neither the YSN peptide nor the 6KSGG altered the fluorescent emission spectra of S-Cnx. By contrast, S-Cnx fluorescence was enhanced significantly in the presence of the KHP peptide, indicative of a conformational change associated with complex formation.

The change in fluorescent emission at the peak wavelength of 333 nm was used to produce titration profiles with increasing peptide concentration as shown in Fig. 36.B. For the KHP peptide, saturable binding to S-Cnx was observed. By contrast, the non-hydrophobic 6KSGG and YSN peptides did not exhibit any binding to S-Cnx over the entire concentration range, confirming the specificity of the assay. Drawing two lines of best fit through the initial linear and saturation portions of the KHP peptide binding isotherm allowed the determination of the equivalence point (428, 429), resulting in a stoichiometry of 1.6 μmol of KHP peptide bound

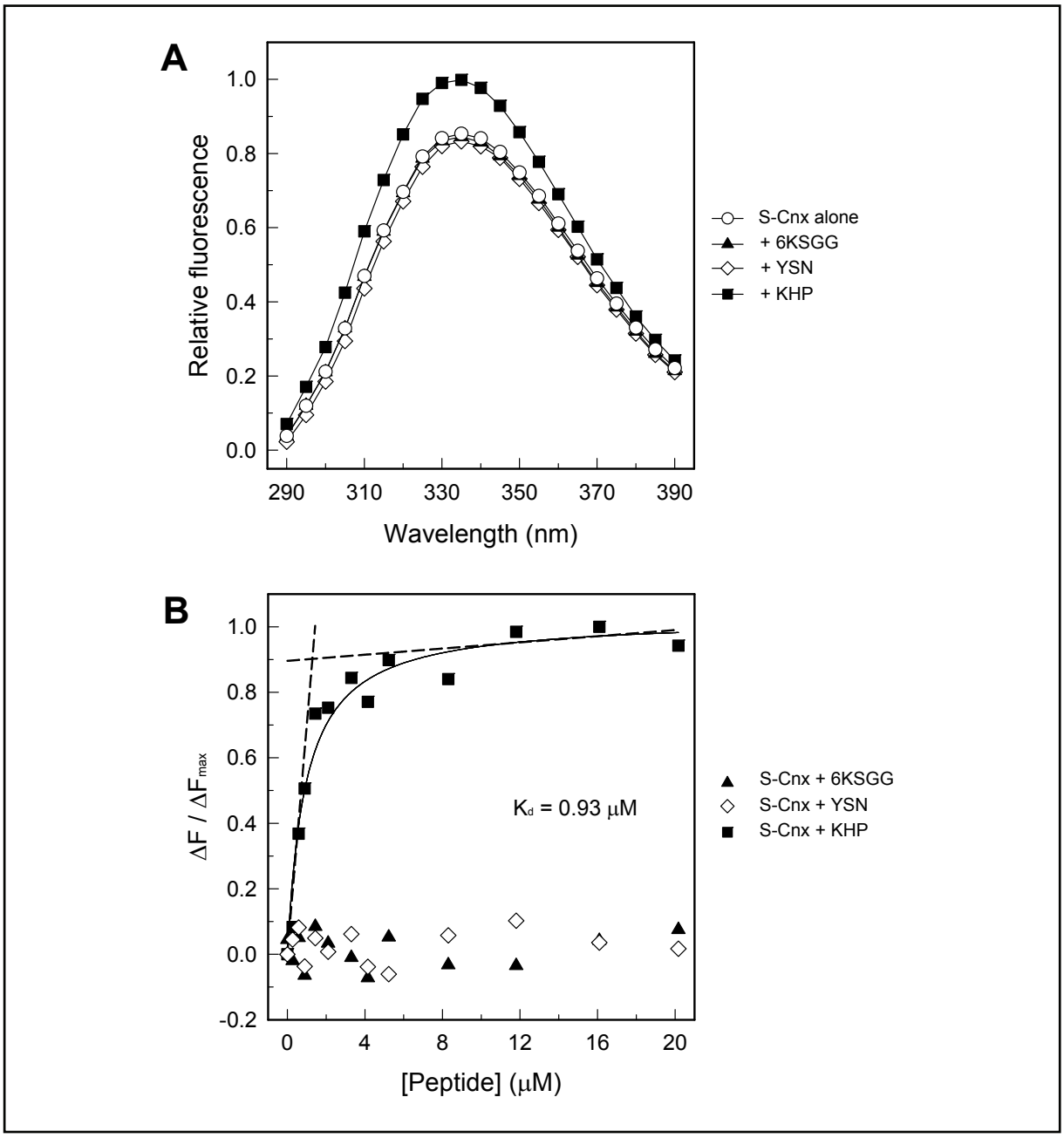

Fig. 36: Interaction of peptides with S-Cnx as assessed by intrinsic fluorescence. (A) Intrinsic fluorescence emission spectra of S-Cnx. Various peptides (20 μM) were incubated with S-Cnx (0.8 μM) in 20 mM Hepes, pH 7.4, 150 mM NaCl, and 0.4 mM $CaCl_2$ for 1 h at 37°C. The excitation wavelength was set to 280 nm and the intrinsic fluorescence was measured every 1 nm from 290 to 390 nm at 37°C. For clarity, emission values were plotted every 5 nm. All fluorescence measurements were corrected by subtracting the contribution of the respective peptide to fluorescence intensity. **(B)** Titration of S-Cnx with various peptides. S-Cnx (0.8 μM) was equilibrated in 20 mM Hepes, pH 7.4, 150 mM NaCl, and 0.4 mM $CaCl_2$ for 1 h at 37°C prior to the addition of peptides. Further 10 min equilibration periods were applied between each titration step at 37°C. Changes in intrinsic fluorescence were recorded at 333 nm with an excitation wavelength of 280 nm. Results were expressed as the change in fluorescence (ΔF) divided by the maximum change in fluorescence between 0 μM and 20 μM KHP peptide (ΔF_{max}). The data were fitted to an equation describing single site binding using SigmaPlot. The indicated K_d value represents the average of three independent measurements with a standard deviation of 18 %. Dashed lines represent lines of best fit used for determination of KHP peptide binding stoichiometry to S-Cnx (equivalence point = 1.3 μM KHP peptide; stoichiometry = 1.6:1).

per µmol of S-Cnx. Furthermore, the data could be readily fit to an equation describing single site binding with a K_d of 0.93 µM for KHP peptide binding to S-Cnx.

Collectively, these binding experiments with hydrophobic peptides that inhibit S-Cnx's aggregation suppression function strongly suggest that the capacity of S-Cnx to suppress the aggregation of non-glycosylated client proteins resides within its globular domain at a probable single site distinct from the site of oligosaccharide binding.

3.3.6 The arm domain of S-Cnx influences interactions with large client proteins

Given that the polypeptide-binding site of S-Cnx resides within its globular domain, it could be speculated that the observed influence of the extended arm domain on the suppression of FL aggregation (Fig. 27) might be due to steric effects on the client protein. To investigate this possibility, the influence of the arm domain on the binding affinity of S-Cnx for client polypeptides of differing size was examed. For a small client peptide, the 2.6 kDa KHP peptide was used. As a client polypeptide of intermediate size, the 14 kDa reduced and carboxymethylated α-lactalbumin (R-CMLA) was employed, which remains soluble despite assuming a non-native, extended conformation with limited secondary structure (430). It competes with S-Cnx in suppressing the aggregation of FL and thus was considered likely to interact with the chaperone (Fig. 37).

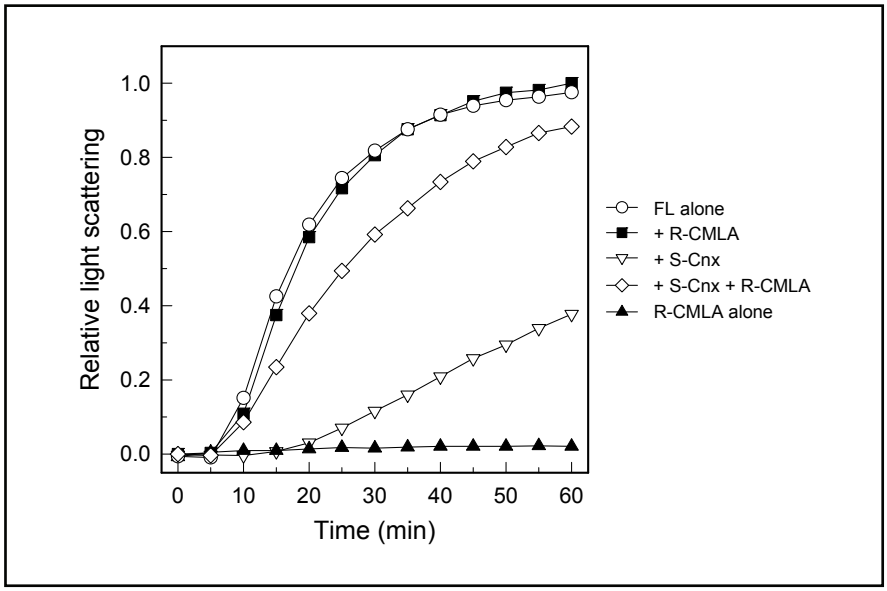

Fig. 37: Non-native α-lactalbumin influences the aggregation suppression function of S-Cnx. After a 1 h incubation of S-Cnx (4 µM) in 20 mM Hepes, pH 7.4, 150 mM NaCl, and 0.4 mM $CaCl_2$ in the presence or absence of R-CMLA (10 µM) at 37°C, FL (3 µM) was added to the respective samples and light scattering was monitored at 360 nm for 1 h at 37°C. Data points were recorded every 6 s and shown every 5 min.

For a large client polypeptide, the thermally unfolded FL (61 kDa) was used.

Initially, the binding affinity of S-Cnx and the truncated Δarm2 mutant for the small KHP peptide was compared. The Δarm2 construct was used rather than the globular domain because it was easier to purify in large quantities from *E. coli* and it exhibited almost the same reduction in potency, relative to S-Cnx, as the globular domain in the suppression of FL aggregation (Fig. 27).

As shown in Fig. 38, incubation of the hydrophobic KHP peptide with the Δarm2 mutant resulted in an enhancement in the fluorescence emission spectrum and a titration curve closely resembling the results from fluorescence experiments of S-Cnx with the peptide (Fig. 36). The calculated K_d for KHP binding to the Δarm2 mutant (0.7 μM) indicates an affinity very similar to the one measured for the S-Cnx-KHP interaction (0.93 μM). This is consistent with the radioactive peptide binding assay in which the ^{125}I-KHP peptide bound equally well to all globular domain-containing S-Cnx constructs regardless of the length of the arm domain (Fig. 30).

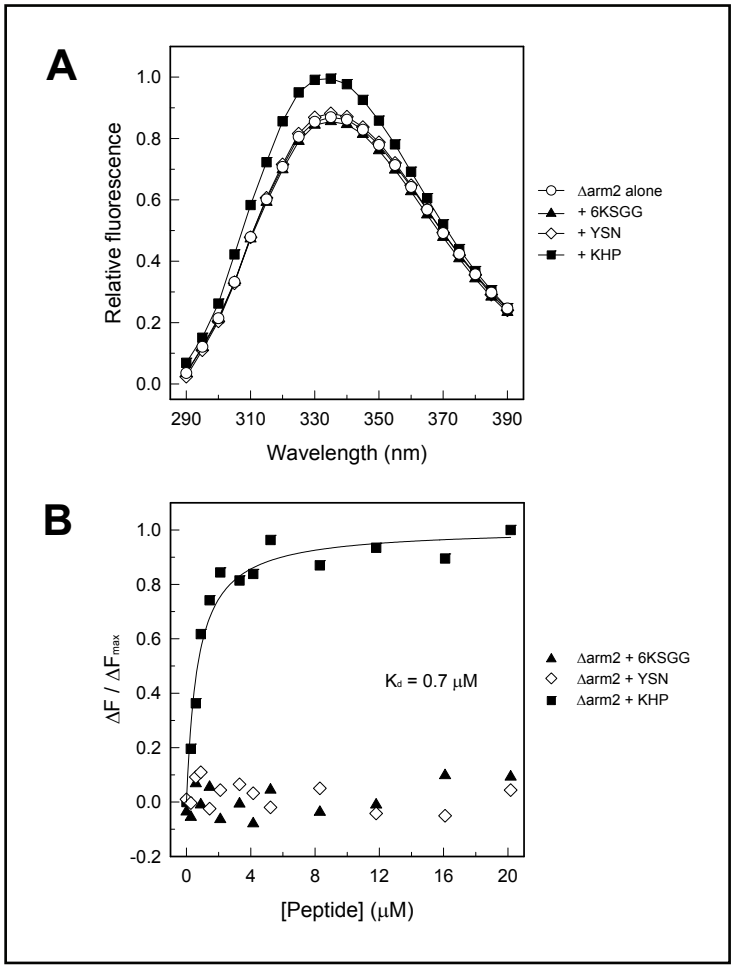

Fig. 38: Interaction of peptides with Δarm2 as assessed by intrinsic fluorescence. (A) Intrinsic fluorescence emission spectra of Δarm2. Δarm2 (0.8 μM) was equilibrated with various peptides (20 μM) in 20 mM Hepes, pH 7.4, 150 mM NaCl, and 0.4 mM $CaCl_2$ for 1 h at 37°C. Changes in intrinsic fluorescence were measured with an excitation wavelength of 280 nm from 290 to 390 nm at 37°C. Data points were recorded at 1 nm intervals but plotted every 5 nm. All fluorescence contributions of the various peptides were taken into account when the respective fluorescence spectra were corrected for background intensities. **(B)** Titration of Δarm2 with various peptides. Δarm2 (0.8 μM) was preincubated in 20 mM Hepes, pH 7.4, 150 mM NaCl, and 0.4 mM $CaCl_2$ for 1 h at 37°C. Subsequently peptide titration was performed at 37°C where a 10 min equilibration period was allowed at each titration step. Intrinsic fluorescence was monitored at 333 nm with an excitation wavelength of 280 nm. Results were plotted as the change in fluorescence (ΔF) divided by the maximum change in fluorescence between 0 μM and 20 μM KHP peptide (ΔF_{max}). The titration curve was fit to an equation describing single site binding using SigmaPlot. The K_d value was derived by calculating the average of three independent experiments with a standard deviation of 24 %.

To examine the binding of R-CMLA and FL to S-Cnx and its truncated arm mutants, surface plasmon resonance (SPR) was employed using sensor chips derivatized with the client proteins and S-Cnx constructs as the injected analytes. In the case of FL, experiments were performed at 30°C, a temperature where it undergoes slow unfolding as assessed by light scattering measurements (data not shown). Fig. 39.A shows sensorgrams obtained when various concentrations of S-Cnx were injected over immobilized R-CMLA, the intermediate sized client protein. Binding was readily detected and could be fit to an equation describing

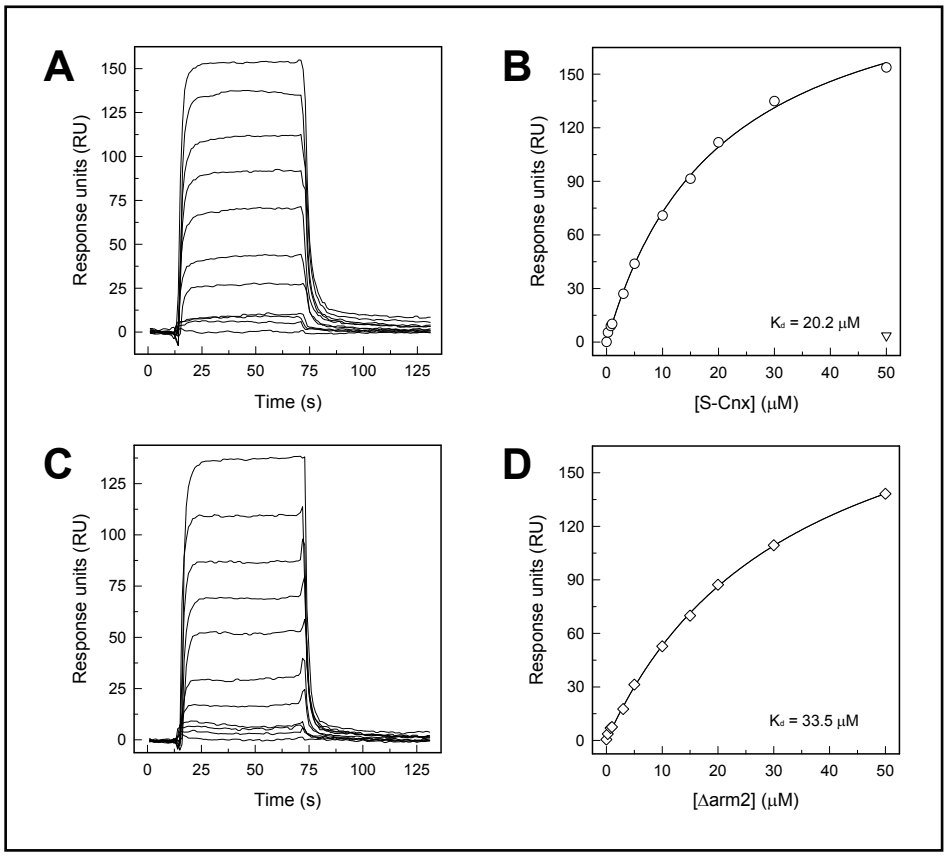

Fig. 39: Binding of S-Cnx and Δarm2 deletion mutant to reduced and carboxymethylated α-lactalbumin measured by surface plasmon resonance. Sensorgram overlay for the binding of **(A)** S-Cnx or **(C)** Δarm2 to immobilized R-CMLA. S-Cnx and the Δarm2 deletion mutant were equilibrated in 20 mM Hepes, pH 7.4, 150 mM NaCl, and a free $[Ca^{2+}]$ of 0.4 mM for 1 h at 25°C and then injected at the same temperature over the surface of a R-CMLA-conjugated sensor chip at increasing concentrations (0, 0.25, 0.75, 1, 3, 5, 10, 15, 20, 30, 50 μM, bottom to top). Binding isotherms for the interaction of **(B)** S-Cnx and **(D)** Δarm2 with R-CMLA. Changes in RU at 68 s of the sensorgram overlays were plotted against the respective S-Cnx construct concentrations. The data were fit to an equation describing single site binding using SigmaPlot. The depicted K_d values are averages derived from three different measurements with a standard deviation below 7 %. For comparison, the change in RU observed with the isolated arm domain (white triangle) at 50 μM is included in panel B.

single site binding with a K_d = 20.2 μM (Fig. 39.B). Interestingly, when the experiment was repeated with the truncated Δarm2 mutant of S-Cnx, a 1.7-fold reduction in binding affinity was observed (K_d = 33.5 μM, Fig. 39.D and Tab. 6). No binding of the isolated arm domain to R-CMLA could be detected (Fig. 39.B). The reduction in binding affinity accompanying truncation of the arm domain became even more pronounced when the large FL client protein

was examined. For these experiments, the complete set of S-Cnx mutants was tested. As shown in Fig. 40.A and B, binding of S-Cnx to FL was observed with a K_d of 1.6 µM.

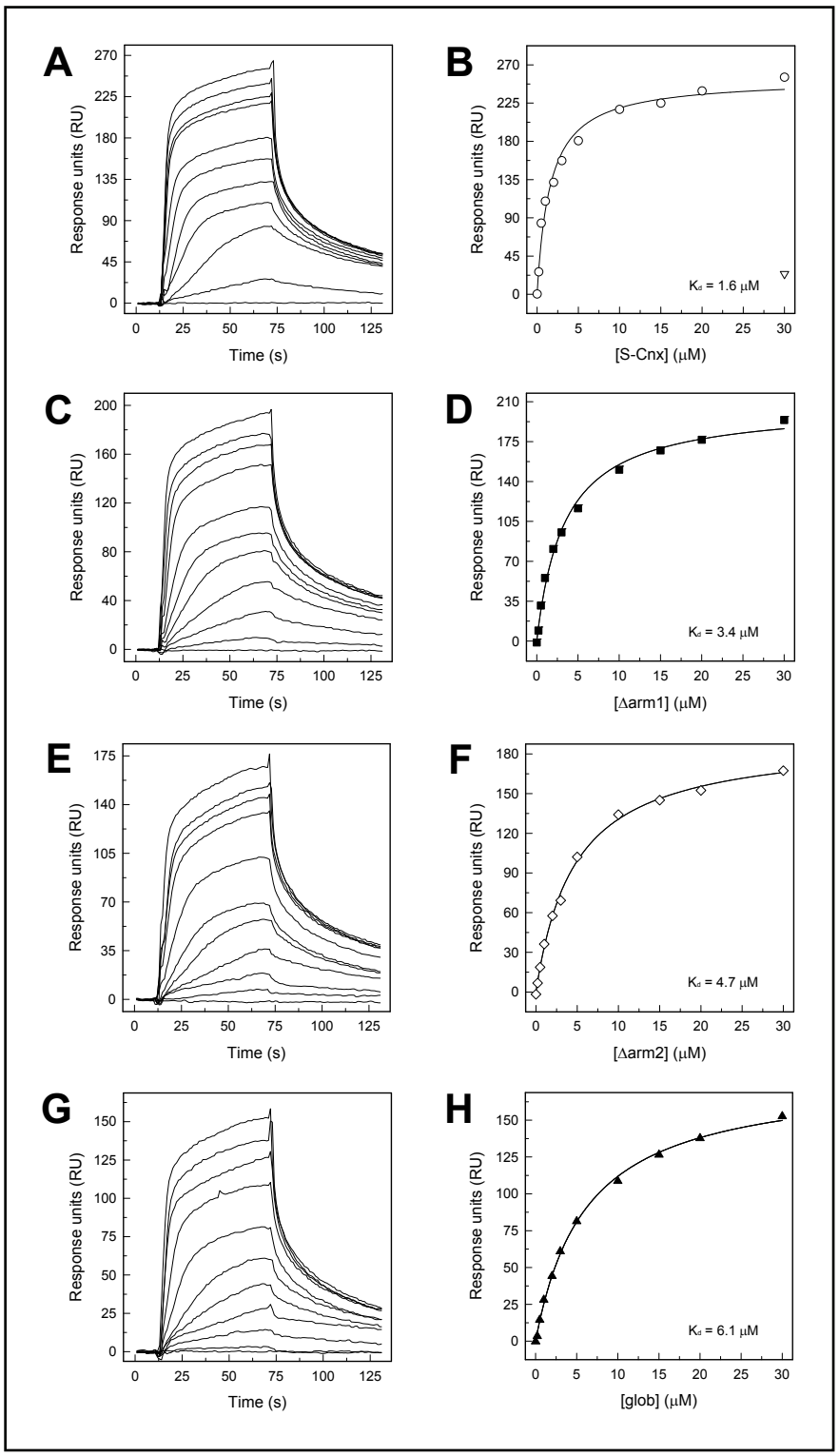

Fig. 40: Binding of S-Cnx and deletion mutants to non-native firefly luciferase measured by surface plasmon resonance. Sensorgram overlays for the interaction of **(A)** S-Cnx, **(C)** Δarm1, **(E)** Δarm2, and **(G)** glob with immobilized FL. S-Cnx constructs were incubated in 20 mM Hepes, pH 7.4, 150 mM NaCl, and a free [Ca^{2+}] of 0.4 mM for 1 h at 30°C and then injected at the same temperature over a FL-derivatized sensor chip at increasing concentrations (0, 0.2, 0.5, 1, 2, 3, 5, 10, 15, 20, 30 µM, bottom to top). Binding isotherms for the interaction of **(B)** S-Cnx, **(D)** Δarm1, **(F)** Δarm2, and **(H)** glob with FL. Changes in RU at 68 s were derived from the sensorgram overlays of the respective S-Cnx constructs and plotted against the concentrations of the injected proteins. The titration curves were fit to an equation describing single site binding using SigmaPlot. The shown K_d values represent averages obtained from three different measurements with a standard deviation below 13 %. For comparison, results with the isolated arm domain (white triangle) at 30 µM are included in panel B.

However, further SPR experiments with S-Cnx deletion mutants, depicted in Fig. 40.C-H and summarized in Tab. 6, revealed a progressive loss of binding affinity occurring as the arm domain was increasingly truncated from 15 % (Δarm1; K_d = 3.4 µM), to 30 % (Δarm2; K_d = 4.7 µM), to 100 % (glob; K_d = 6.1 µM).

Tab. 6: Dissociation constants (µM) for binding of S-Cnx constructs to various client polypeptides.

	KHP[a]	R-CMLA[b]	FL[b]
S-Cnx	0.93	20.2	1.6
Δarm1			3.4
Δarm2	0.7	33.5	4.7
glob			6.1

[a] K_d values were obtained from fluorescence experiments.
[b] K_d values were determined by SPR measurements.

This trend closely mirrored the progressive reduction in potency of the mutants in the aggregation suppression assay (Fig. 27). Again, no specific binding to the isolated arm domain was detected (Fig. 40.B); the low signal observed was non-specific, exhibiting no evidence of saturation up to 160 µM (not shown).

Importantly, the magnitude of the reduction in binding affinity when comparing S-Cnx with the Δarm2 mutant correlated with the size of the client polypeptide tested (Tab. 6). There was no loss in binding affinity with the small KHP peptide, a 1.7-fold reduction with the intermediate-sized R-CMLA client protein and a 3-fold reduction with the large FL client protein. Since there was no specific binding of any of the client polypeptides to the isolated arm domain, the results are consistent with the arm domain contributing to S-Cnx binding affinity through steric constraint of the larger client proteins. Such a mechanism should also be detectable by changes in client protein dissociation rate constants obtained from the surface plasmon resonance data. However, it was not possible to fit the dissociation component of the binding curves to obtain these rate constants, presumably due to the multiple conformational states of the non-native substrates immobilized on the sensor chips.

4 Discussion

In general, molecular chaperones distinguish correctly folded from incompletely folded client proteins during their maturation process through binding to hydrophobic polypeptide segments that are exposed in non-native conformational states. This transient interaction, through regulated cycles of binding and release, stabilizes folding intermediates, prevents their aggregation, and thereby promotes more efficient folding (52). This concept is well described for the Hsp60 and Hsp70 chaperones (221), especially for the ER resident protein BiP as a member of the latter family (431).

Among the remaining ER chaperones that participate in the folding and quality control of nascent proteins, Cnx and Crt form one of the most exhaustively studied chaperone systems. They are characterized by a unique mode of client protein recognition via their lectin sites. Since inhibition of lectin-oligosaccharide interactions resulted in a reduced and/or abolished association of Cnx with many glycoproteins (277), it has been concluded that this membrane-bound chaperone functions solely as a lectin. This view is supported for example by findings that binding between Cnx and monoglucosylated RNase B is based only on lectin-oligosaccharide interactions independent of the conformational state of RNase B (375, 377).

Alternatively, other studies have suggested that Cnx may possess a polypeptide-binding site, in addition to its lectin site, that confers the ability to recognize non-native protein conformations in a manner similar to classical chaperones. Early support for this view came from observations demonstrating interactions between Cnx and proteins completely lacking Asn-linked oligosaccharides (244, 310, 380, 432, 433). Subsequent support for a dual mode of binding stems from assays revealing the potency of Cnx to suppress the aggregation of non-glycosylated client proteins (283, 393). However, utilization of a polypeptide-binding site during Cnx's folding-promoting role has been somewhat controversial, since aggregation assays were typically performed under non-physiological conditions, likely to alter the structural integrity of Cnx.

Therefore, as the first objective of this thesis work, an aggregation assay needed to be developed, that would allow the elucidation of the lectin-independent aggregation suppression function of Cnx under conditions prevalent within the lumen of the endoplasmic reticulum. The outcome of this newly established aggregation assay, in combination with further biochemical and biophysical studies, gave new insights into how the aggregation suppression function of Cnx is influenced by Ca^{2+} and ATP and provided strong evidence that Cnx displays a significant non-glycoprotein chaperone function.

While progress has been made in characterizing the lectin site of Cnx, the nature of its polypeptide-binding site has not been determined. Elucidation of this site would provide important insights into how this chaperone discriminates between native and non-native client proteins. Early studies assigned the aggregation suppression function of Cnx to its globular domain, although this activity may have been compromised by partial unfolding under non-physiological experimental conditions. Consequently a second objective of this thesis work was to better localize the polypeptide-binding site and to understand how the globular and arm domains of Cnx contribute to its overall chaperone function.

To achieve this objective, several deletion mutants were created during the further course of this work. After establishing their structural integrity, the mutants were tested for their role in aggregation suppression of a non-glycosylated client protein under physiological conditions of the ER. For the first time several peptides were effectively used as competitors of Cnx in an aggregation suppression assay thereby strengthening the specificity of this newly established assay system. Furthermore, binding experiments with peptides and non-native proteins of increasing size allowed new insights concerning the location and further characteristics of the polypeptide-binding site and revealed how the arm domain of Cnx contributes to its aggregation suppression function.

4.1 Potent lectin-independent chaperone function of calnexin under physiological conditions of the ER

4.1.1 The new FL aggregation assay

Since abnormal conformations of proteins, such as misfolding, misassembly, and aggregation, have been determined as the main cause in the genesis and progression of several human diseases including Alzheimer's disease (434, 435), Parkinson's disease (436), Creutzfeld-Jacob disease (437), amyotrophic lateral sclerosis (ALS) (438), and cystic fibrosis (439), there is a great need to develop assay systems that allow the identification and characterization of agents promoting the folding of proteins, stabilizing their native conformation, and suppressing their aggregation. In this context, aggregation suppression assays have been widely used to examine the chaperone activity of a multitude of proteins (386-388, 440-442). Herein, the aggregation of a client protein can be induced by several factors including the action of elevated temperatures, the application of reducing agents, and the acidification of the

protein solution. Alternatively, induction of aggregation of denatured proteins can be observed through reduction of the concentration of the denaturing agent by rapid dilution.

First evidence supporting the concept that Cnx can utilize a polypeptide-binding site to select for exposed hydrophobic sites on incompletely folded proteins and suppress their aggregation, a hallmark of every molecular chaperone, stemmed from work by Ihara *et al*. (283). In this study, Cnx revealed the ability to prevent the aggregation of an unfolded protein as shown for denatured SBA lacking monoglucosylated oligosaccharides. It also appeared to function as a bona fide molecular chaperone by protecting citrate synthase (CS) and malate dehydrogenase (MDH), both mitochondrial proteins lacking Asn-linked oligosaccharides, against thermal denaturation. Subsequently, similar findings were also obtained for Crt (284). Aggregation of all three client proteins required induction by elevated temperatures and experiments were therefore performed at the non-physiological temperature of 45°C. Consequently, the validity of the obtained results have been questioned considering the low melting temperature of Crt of 46.4°C in the presence of 1 mM Ca^{2+} (281). Further studies, strengthening a polypeptide-based mode of interaction for Cnx by suppressing the aggregation of model proteins such as CS, MDH, and, HLA-A2 heavy chains (Tab. 7), also suffered from the drawback of a potential altered conformation of Cnx through the applied elevated temperatures (45-47°C) or depletion of Ca^{2+} (280, 297, 393).

It was therefore highly desirous to establish an aggregation assay wherein the model protein would aggregate under physiological conditions prevalent within the lumen of the ER without affecting the structural integrity of Cnx. The thermolabile, non-glycosylated protein firefly luciferase appeared to be a promising candidate. FL is a structurally (443) and biochemically (444-446) well characterized enzyme that catalyzes the oxidation of firefly luciferin in the presence of Mg-ATP and molecular oxygen, resulting in an electronically excited oxyluciferin species accompanied by light emission upon the return to the ground state.

Besides its wide utility in biotechnological and molecularbiological applications due to its ability to generate bioluminescence, FL has been frequently used in aggregation or refolding assays (408, 447-454). Herein, aggregation of FL has been induced by dilution from a denaturant or by thermal induction at temperatures greater than 37°C (Tab. 7).

Tab. 7: Commonly used model proteins in thermal aggregation suppression assays.

Protein	Buffer conditions	Temperature	Reference
Alcohol dehydrogenase (yeast)	25 mM Tris/HCl, pH 7.4	42°C	(455)
Carbonic anhydrase B (bovine erythrocytes)	50 mM Tris-sulfate, pH 7.5	63°C	(456)
Catalase (bovine liver)	50 mM Na phosphate, pH 7.0	55°C	(457)
Citrate synthase* (porcine heart mitochondria)	10 mM Tris, pH 7.2, 150 mM NaCl, 2-5 mM $CaCl_2$ or 10-40 mM Hepes, pH 7.5, with or without 150mMNaCl, 5 mM CaCl	40-45°C	(280, 283, 297, 392, 440)
Coat protein (tobacco mosaic virus)	50-100 mM phosphate buffer, pH 7.0-8.0	42-52°C	(458, 459)
βL-Crystallin (lenses of rats)	50 mM phosphate buffer, pH 7.2	65°C	(460)
γ-Crystallin (lenses of rats)	50 mM phosphate buffer, pH 7.2	65°C	(460)
HLA-A2 heavy chain* (soluble, human)	10 mM Tris, pH 7.2, 150 mM NaCl, 5 mM $CaCl_2$	47°C	(393)
Malate dehydrogenase* (porcine hear mitochondria)	10 mM Tris, pH 7.2, 150 mM NaCl, 2 mM $CaCl_2$, or 10-50 mM Hepes, pH 7.5, with or without 150 mM NaCl, 5 mM $CaCl_2$	45°C	(280, 283, 461)
Firefly luciferase (North American firefly)	25 mM Tris, pH 7.8, 50 mM KCl, 2 mM MgATP, 1mM DTT or 28-40 mM Hepes, pH 7.5-7.6 with or without 120 mM K acetate, 1.2 mM Mg acetate, 2.2 mM DTT, 1 mM ATP, 8.8 mM creatine phosphate, 3.5 units/ml creatine kinase	42-43°C	(388, 454, 462)

* Client protein used to characterize the aggregation suppression function of Cnx.

In the present studies, the aggregation behavior of FL was tested under the physiological temperature of 37°C. Not surprisingly, given its low thermal stability (T_m = 34.4°C) (463), FL revealed a distinct aggregation profile with a characteristic lag period of 7-8 min (Fig. 7). These observations are in good agreement with thermal aggregation curves of FL at 42°C (442), where kinetic analysis indicated that this aggregation occurred by a nucleation-dependent mechanism. In this mechanism, aggregates possess the ability to seed and propagate aggregation of further molecules. The known instability of FL can prove challenging as it often compromises precision in analytical applications (463), but the storage and handling conditions designed herein (2.2.16) permitted the establishment of a stable user-friendly aggregation assay. Since aggregation of FL alone was unaffected by several additives such as Ca^{2+}, nucleotides, and various peptides, this new assay offered the opportunity to characterize the lectin-independent aggregation suppression function of S-Cnx under physiological conditions of the ER. Thus, potential unfolding of S-Cnx through elevated temperatures or aggregation inducing agents could be avoided, a feature which might also be beneficial for the characterization of other chaperones in the future.

4.1.2 The aggregation suppression function of S-Cnx is influenced by Ca^{2+}

During efforts to test the capacity of S-Cnx to suppress the aggregation of the non-glycosylated client protein FL under physiological temperature and Ca^{2+} concentrations of the ER lumen, important novel insights were obtained. First of all, S-Cnx is fully capable of suppressing the aggregation of thermally denatured FL through lectin-independent interactions at 37°C (Fig. 7). Therefore, this is an intrinsic property of S-Cnx and not merely a consequence of thermally induced unfolding of S-Cnx at the 43-45 °C temperatures used in previous aggregation suppression studies (280, 283, 392). In fact, in this thesis work, no evidence for thermally induced conformational changes in S-Cnx could be detected by CD at temperatures from 20°C up to 45°C (Fig. 9, 1 mM Ca^{2+}). Furthermore, the aggregation suppression function of S-Cnx at 37°C is influenced by Ca^{2+} concentration. Whereas most previous studies employed Ca^{2+} concentrations in the range of 1-2 mM (283, 393), it was observed that aggregation suppression is significantly enhanced at the 0.4 mM concentration typical of the resting ER lumen and further enhanced at lower concentrations.

The importance of Ca^{2+} in maintaining the structural integrity of both S-Cnx and Crt has been well documented. Crt possesses a single high affinity Ca^{2+}-binding site (K_d = 11 μM) and as many as 17 low affinity sites (K_d = 2 mM) (295). In the case of S-Cnx, the crystal structure revealed a single binding site for Ca^{2+} (282). Presumably, it is this site that is shown in the present study that binds Ca^{2+} with a K_d = 0.1-0.2 mM. For both chaperones, complete chelation of Ca^{2+} results in a marked increase in protease susceptibility ((281, 296, 412) and Fig. 11) and a loss of lectin function (286). Moreover, the removal of Ca^{2+} results in destabilization of Crt with a decrease in melting temperature from 46.4 to 40.2°C (281). A similar destabilization is shown for S-Cnx in the absence of Ca^{2+}, with a decrease in melting temperature from 49.5 to 39.5°C (Fig. 10). This was accompanied by a quenching of tryptophan fluorescence (Fig. 12) and an increase in hydrophobic exposure as measured by bis-ANS binding (Fig. 13). Collectively, these findings indicate a loss of native structure for both S-Cnx and Crt upon Ca^{2+} removal, with an increase in conformational flexibility and likely exposure of the hydrophobic core.

In contrast, the reduction of Ca^{2+} to the 0.4 mM level typical of the resting ER had barely detectable conformational consequences on S-Cnx. Compared to 1 mM Ca^{2+}, there was no discernible change in thermal stability or susceptibility to protease digestion. Only a slight quenching of intrinsic fluorescence (Fig. 12.B) and increase in surface hydrophobicity (Fig. 13.B) could be detected. Nevertheless, a substantial enhancement of the ability of S-Cnx to

suppress the aggregation of FL was observed as the Ca^{2+} concentration was reduced from 1.0 to 0.4 mM (Fig. 7). These findings support the view that the aggregation suppression function of S-Cnx is associated with the native conformations it is likely to assume within the lumen of the resting ER.

The relevance of lower Ca^{2+} concentrations to Cnx function is less clear. Although the ability of S-Cnx to suppress FL aggregation increases continuously as Ca^{2+} is reduced from 0.4 mM down to the 50 μM level typical of the empty ER (Fig. 7), the associated loss of native structure and likely exposure of the hydrophobic interior suggest that the increased aggregation suppression may merely be a consequence of interactions arising from such exposure.

Are low Ca^{2+}-induced structural changes in S-Cnx and enhanced interactions with folding glycoproteins likely to occur under physiological conditions? Most studies examining stimulus-induced changes in intracellular Ca^{2+} utilize Ca^{2+}-free medium or SERCA pump blockers to facilitate the detection of changes in ER Ca^{2+} levels (31). Under such conditions, reductions in free ER Ca^{2+} from 0.3-0.5 mM to 50-100 μM are commonly observed with ~30 s required to empty or refill ER stores. This suggests that there is ample opportunity for Cnx to undergo low Ca^{2+}-induced structural changes because it was observed *in vitro* that only a few seconds are required to completely dissociate Ca^{2+} from this chaperone (data not shown). However, more recent experiments examining sarcoplasmic reticulum Ca^{2+} dynamics during muscle contraction in living mice have shown that Ca^{2+} levels fall by only 50 μM following nerve stimulation or by ~100 μM following combined nerve and β-adrenergic stimulation. Also, cycles of Ca^{2+} release and recovery are extremely fast, on the order of 0.1 s (464). It is unlikely that such transient and modest fluctuations would have substantial impact on Cnx structure. However, until more *in vivo* experiments are performed on a variety of cell types under normal and pathological situations, the potential regulatory impacts of ER Ca^{2+} on Cnx structure remains an open question.

4.1.3 ATP induces the exposure of enhanced surface hydrophobicity of S-Cnx and increases its aggregation suppression potency

The ability of both S-Cnx and Crt to bind ATP is well established, although neither chaperone possesses ATPase activity (283, 284, 296, 412). Using photo cross-linking, Ou *et al*. demonstrated the binding of ATP, ADP, AMP, and GTP to S-Cnx and the fact that these interactions require Mg^{2+} (412). They also reported an increased sensitivity to protease digestion in the presence of ATP, although Vassilakos *et al*. were unable to reproduce this finding previously (286).

In the present study, it was found that ATP is capable of binding to S-Cnx in the presence of 1 mM Ca^{2+} with a K_d = 2.9 mM (Fig. 19) and that this interaction does not require Mg^{2+} ions. It is not clear what form of ATP is binding to S-Cnx in the conducted experiments shown in chapter 3.2.3 and 3.2.4, but given the dissociation constants for metal binding to ATP (465, 466) and the composition of the buffers used, Ca-ATP, Na-ATP, and free ATP are all candidates.

Whatever the form of ATP that binds, it had no significant impact on the thermal stability of S-Cnx or in its maintenance of a tightly folded conformation (Figs. 15-17). Rather, it was associated with a substantial increase in surface hydrophobicity (Fig. 18 and Fig. 19), an effect that correlated with a strong potentiation in the ability of S-Cnx to suppress FL aggregation (Fig. 14). These findings suggest that ATP binding regulates the exposure of a localized hydrophobic polypeptide-binding site on S-Cnx.

Remarkably, ATP-binding affinity was increased 4-fold to a K_d of 0.7 mM when Ca^{2+} was reduced to the luminal ER concentration of 0.4 mM (Fig. 22.B). This reduced the concentration of ATP required to obtain the suppression of FL aggregation such that near maximal suppression could be achieved at 0.5 mM rather than 2 mM ATP (Fig. 14 and Fig. 21). Although this appears to be a very high effective concentration of ATP, it is likely that the ER lumen contains ATP in the millimolar range similar to that of the cytosol. ER membranes contain a robust ATP transporter (413), and several ER proteins are known ATPases, including the chaperones BiP and Grp94. It is noteworthy that Grp94 also exhibits very weak ATP binding (467, 468) with a K_d likely to be in the 0.1-0.5 mM range (Christopher Nicchitta, personal communication), as observed for its cytosolic homologue, Hsp90 (469, 470).

Collectively, these findings suggest that S-Cnx is a highly effective chaperone capable of suppressing client protein aggregation through non-lectin interactions under conditions

prevalent in the ER. They also suggest that under various stress conditions when ATP levels fall (471), the efficacy of Cnx in suppressing glycoprotein aggregation may be reduced. This could be a contributing factor to the induction of the ER unfolded protein response (472).

4.2 Distict contributions of the lectin and arm domains of calnexin to its molecular chaperone function

Based on the findings that S-Cnx successfully suppressed the aggregation of non-glycosylated FL in a lectin-independent manner, likely through ATP-regulated polypeptide-based interactions (Fig. 21), further attention was focused on the characterization of the putative polypeptide-binding site and of domain contributions to the aggregation suppression function. Several deletion mutants of S-Cnx (Fig. 23) were generated that consist of its arm or globular domains alone as well as mutants that lack the distal 15 % (Δarm1) or 30 % (Δarm2) of the arm domain. These were tested for their binding and aggregation suppression properties.

4.2.1 Structural integrity of S-Cnx deletion mutants

Before usage of the deletion mutants of S-Cnx in results section 3.3 of this thesis, their structural integrity was assessed by CD measurements (Fig. 24 and Fig. 25). The far-UV CD spectra and melting temperatures for the Δarm1 and Δarm2 mutants were similar to those of S-Cnx, indicating that truncation of as much as 30 % of the arm domain does not significantly affect the secondary structure or stability of the chaperone. Not surprisingly, the individual arm and globular domains exhibited far-UV CD spectra different from that of S-Cnx, with the arm domain closely resembling that of the isolated arm domain of Crt (294). The thermal stability of the globular domain was not significantly different from that of S-Cnx, whereas the arm domain exhibited a melting temperature ~4°C less than that of S-Cnx. Notably, none of the mutants exhibited any evidence of thermal denaturation at 37°C, the temperature employed in subsequent aggregation suppression and peptide binding assays.

These findings contrast with those described previously for Crt where the isolated globular and arm domains exhibited a 7.5°C drop and an 11.6°C drop, respectively, in melting temperature relative to the intact molecule (281, 294). This suggests that excision of individual domains from Crt has a greater destabilizing effect than for Cnx. Coupled with previous demonstrations that the individual arm and globular domains of S-Cnx retain ERp57

and oligosaccharide binding function, respectively (280), it can be concluded that the various deletion mutants examined in this study retain a high degree of structural and functional integrity.

4.2.2 The globular domain of S-Cnx mediates Ca^{2+}-induced conformational changes

The biophysical studies described above also provided the opportunity to examine which domain of S-Cnx is responsible for the structural stabilization that accompanies Ca^{2+} binding, detected as an increase in thermal stability (Fig. 9 and Fig. 10), increased resistance to exogenous proteases (Fig. 11), enhanced intrinsic fluorescence (Fig. 12), and reduced binding of the hydrophobic probe bis-ANS (Fig. 13) in chapter 3.2. There is some uncertainty concerning the site(s) of Ca^{2+} binding in Cnx with an early report documenting high affinity binding to the arm domain with lower affinity binding within the globular domain (473). By contrast, the crystal structure revealed only a single putative binding site within the globular domain (282).

The thermal melting curves of the various deletion mutants of S-Cnx in the presence and absence of Ca^{2+} were compared (Fig. 25), and it was observed that all constructs containing the globular domain exhibited a marked decrease in thermal stability upon complete removal of Ca^{2+} (Tab. 5). However, the thermal stability of the arm domain was unaffected, which stands in accordance with intrinsic fluorescence measurements, where Ca^{2+}-induced intensity changes were detected for all S-Cnx constructs with exception of the arm domain (Fig. 26). These findings cannot rule out Ca^{2+} binding to the arm domain, but they do demonstrate that the structural stabilization that accompanies Ca^{2+} binding is an exclusive property of the globular domain.

These findings are consistent with the identification of a putative Ca^{2+}-binding site within the globular domain of the S-Cnx crystal structure (282) and also with the findings of Bouvier and co-workers (294) who localized the Ca^{2+}-responsive region of Crt to its globular domain.

4.2.3 The polypeptide-binding site of S-Cnx resides in the globular domain at a location distinct from the lectin site

Examination of the various deletion mutants for their abilities to suppress the aggregation of non-glycosylated FL under physiological ER conditions revealed that the arm domain itself possessed no aggregation suppression capacity (Fig. 27). However, shortening or complete removal of the arm domain resulted in a progressive impairment of chaperone function such that the globular domain alone exhibited about 25 % aggregation suppression potency relative to intact S-Cnx. These findings indicate that the region primarily responsible for the chaperone function of S-Cnx resides within its globular domain with the extended arm domain somehow contributing to optimal aggregation suppression.

To clarify the role of the arm domain in the polypeptide-based chaperone function of S-Cnx, hydrophobic peptides were used as client protein mimetics to localize and characterize the unfolded polypeptide-binding site(s) on S-Cnx. These peptides were effective competitors in the aggregation suppression assay (Fig. 28), indicating that they were reporting on the relevant function of S-Cnx.

Subsequent peptide binding experiments, using assays based on CD spectral changes (Fig. 29) or the recovery of radioiodinated peptide-S-Cnx complexes (Fig. 30), revealed that peptides bound equally well to S-Cnx constructs regardless of the length or even the presence of the arm domain. Indeed, no binding to the isolated arm domain could be detected. This demonstrates that the site through which S-Cnx exerts its aggregation suppression function resides exclusively within the globular domain and, because peptide binding could not be competed with mono-glucosylated oligosaccharide and was unaffected by lectin-inactivating mutations (Fig. 35), that this site is at a location distinct from the lectin site. Further analysis of the peptide binding isotherm revealed a probable single binding site with a K_d of 0.9 μM for peptide KHPYAYLAAAIAAEVAGTTALKLSK (Fig. 36).

4.2.4 The arm domain of S-Cnx contributes to its chaperone function by physical sequestration of a client protein

If the arm domain does not possess a binding site for non-native polypeptides, how does it enhance by as much as 4-fold the aggregation suppression potency of S-Cnx? Using direct binding assays with client polypeptides ranging in size from a 2.3-kDa peptide to 14-kDa R-

CMLA to 61-kDa FL, it was shown that the arm domain increasingly contributes to S-Cnx binding affinity as a function of client polypeptide size (Tab. 6). Furthermore, with the large FL client protein, binding affinity also increased as a function of arm length. However, the isolated arm domain itself exhibited no specific binding to any of these client proteins suggesting that its contribution to binding affinity occurs through steric constraint of the larger client proteins (Fig. 41). It can be envisioned that as a glycoprotein folding intermediate interacts with both lectin and polypeptide-based binding sites on the globular domain of S-Cnx, it enters the cavity between the arm and globular domains.

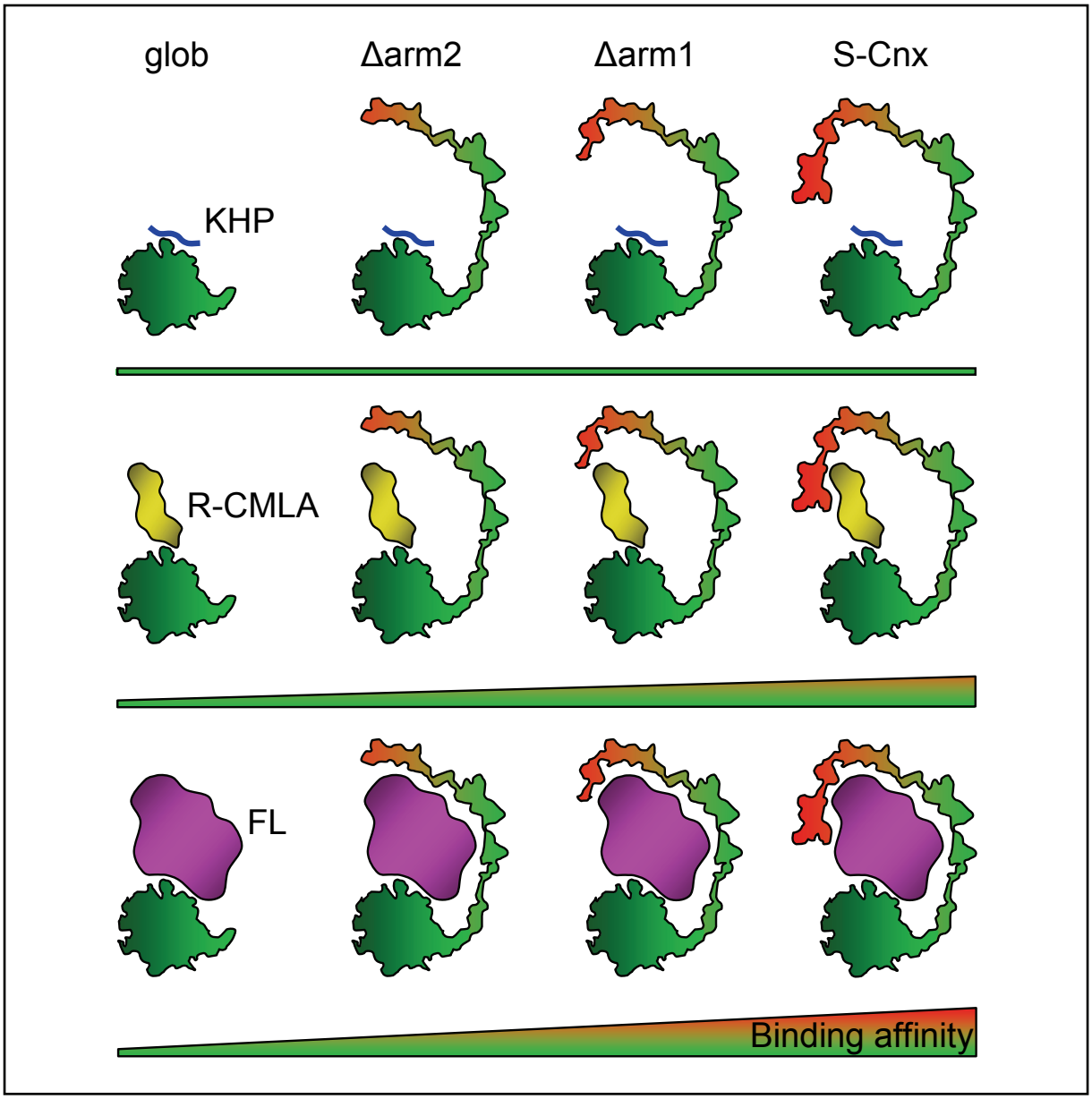

Fig. 41: Model for the contribution of the arm domain of S-Cnx to its binding affinity. The binding affinity of S-Cnx to a small client polypeptide as exemplified by the KHP peptide is unaffected by the length of the arm domain. Following binding to the globular domain, larger client proteins (R-CMLA, FL) can be physically sequestered by the arm domain, thereby allowing this conformationally flexible domain to enhance the binding affinity of S-Cnx as a function of client protein size.

Electron microscopic studies have revealed that the arm domain appears to be highly flexible, adopting a variety of curved shapes (294). Furthermore, in the S-Cnx crystal structure, the arm domain of each molecule within the crystal lattice is wrapped around the globular domain of an adjacent molecule (282). Consequently, the arm domain could enhance the aggregation suppression function of S-Cnx by physically sequestering a folding glycoprotein. This may have the combined effect of increasing the binding affinity as well as removing the folding glycoprotein from the vicinity of other aggregation-prone folding intermediates. Thus, aggregation suppression of client proteins would occur by a combination of direct binding of S-Cnx to exposed hydrophobic patches as well as physical sequestration. That such physical sequestration may be important for client protein interaction in living cells is supported by recent findings from Zhang *et al*., indicating that partial truncation of the arm domain of Crt prevented its interaction with MHC class I molecules, despite the continued presence of its lectin and polypeptide-binding sites (187).

4.3 Working model for the molecular chaperone mechanism of calnexin

The emerging picture from this thesis work on S-Cnx and recent work on Crt is that, despite being unique among chaperones in utilizing oligosaccharide recognition as a mode of substrate interaction, they share important features in common with other classical chaperone families.

It is well established that chaperones of the Hsp70, Hsp60, Hsp40, and small heat shock protein families recognize hydrophobic segments of incompletely folded client proteins and that this interaction can be modeled with client mimetic peptides that are largely hydrophobic in character (218, 416-422, 474). The current peptide binding studies presented in chapter 3.3 demonstrate that the globular domain of S-Cnx also possesses a site capable of binding hydrophobic peptides with micromolar K_d, an affinity that is similar to that exhibited by the Hsp70 chaperones BiP and DnaK (422, 475). In the case of Crt, this binding specificity was elaborated further by Houen and co-workers (390) who showed that Crt prefers peptides composed mainly of hydrophobic residues and a minimum length of five amino acids.

In addition, both the Hsp70 and Hsp60 chaperones employ strategies to either partially or completely sequester client proteins from other folding proteins. Upon ATP hydrolysis, the α-helical lid of Hsp70 chaperones closes over bound client protein and reduces the client protein dissociation rate by 200-fold (223, 476). For Hsp60 chaperones, client proteins enter a

chamber that, in another ATP-dependent reaction, is enclosed by the Hsp10 co-chaperone "lid", thus completely sequestering the folding protein (221).

This study provides the first evidence that the arm domain of S-Cnx, and presumably that of Crt as well, plays an analogous role in client protein sequestration that enhances the overall aggregation suppression function of these chaperones. Since protein folding takes place in the unbound form upon dissociation from the chaperone, ATP regulated client protein binding represents a common feature of chaperones including members of the Hsp60 and Hsp70 families mentioned above (477), whose ATPase activity is essential for a functional binding-release cycle. Considering that no ATPase activity has been detected so far for Cnx (283), it can be questioned how polypeptide-based interactions can be integrated into a folding-promoting chaperone cycle? Also contrary to the Hsp60 and Hsp70 chaperones is the finding that increased binding to a client protein occurs in an ATP-bound state, a characteristic that Cnx only shares with Hsp90 (478). While the relatively weak ATPase activity of Hsp90 is stimulated by unfolded client proteins or peptides (479), a similar stimulatory effect has not been observed yet for Cnx by any client protein or other ligands. Furthermore, despite extensive attempts using pull-down experiments to identify a possible co-chaperone, of which several have been shown to promote ATPase activity or nucleotide exchange/dissociation in classical chaperone cycles, none of the consistently recovered proteins appeared to be a promising candidate to function in the expected co-chaperone capacity (Y. Noguchi and D. B. Williams, unpublished). However, given the extremely weak ATP-binding affinity (K_d = 0.7 mM) under physiological Ca^{2+} conditions of the ER measured in this study (Fig. 22.B) coupled with a high ER-luminal ATP concentration, it is likely that Cnx is in equilibrium between ATP-occupied and ATP-unoccupied states. Since ATP binding exposes a hydrophobic binding site on S-Cnx (Fig. 18 and Fig. 19) and potentiates its aggregation suppression potency (Fig. 14), it can be proposed that the ATP-bound state of Cnx is the predominant form that mediates client protein association. Furthermore, the enhancing effect of ATP dominates over the inhibitory effect of occupying the lectin site with monoglucosylated oligosaccharide in aggregation suppression assays with non-glycosylated client proteins (283). Thus, this evidence collectively suggests a chaperone mechanism of Cnx, where both lectin and polypeptide-binding sites can be engaged during interaction with a folding glycoprotein (Fig. 42). Dissociation of ATP is accompanied by a shift of the polypeptide-binding site to a lower affinity state and continued occupancy of the lectin site results in further destabilization and eventually disruption of polypeptide binding.

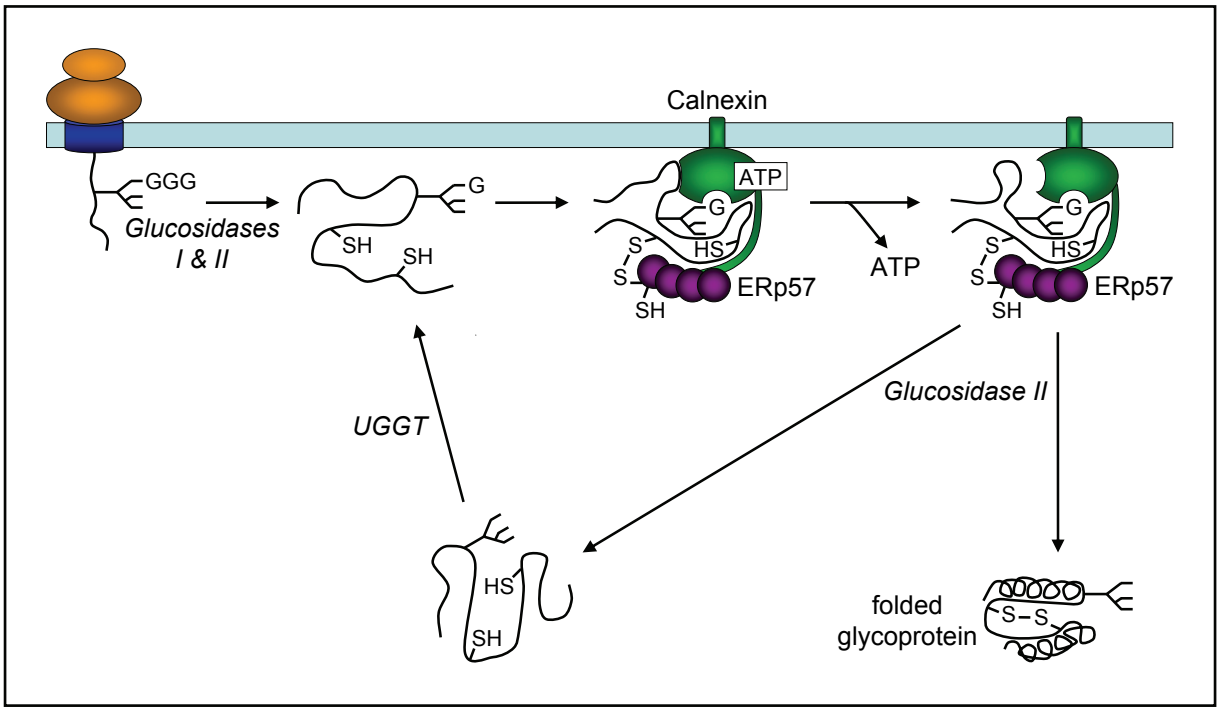

Fig. 42: Model for the dual-binding mode of calnexin during chaperone cycles with a folding glycoprotein. In this revised "dual-binding" model, Cnx functions as a lectin and as a classical chaperone similar to the mechanism described for BiP in Fig. 2. While lectin-based interactions are controlled by the concerted activity of glucosidase II and UGGT, polypeptide-based interactions are regulated by a low affinity ATP-binding site, whose occupied and unoccupied forms are in equilibrium. ATP binding to Cnx leads to a shift of its polypeptide-binding site to a high affinity state, promoting association with non-native polypeptide segments. Dissociation of ATP causes the polypeptide-binding site to assume a low affinity conformation. Further destabilization of polypeptide binding by continued lectin-oligosaccharide engagement and the relatively low affinity of the latter interaction permits release of the folding glycoprotein. Cycles of binding and release occur until a native conformation is attained. Besides recruitment of ERp57, productive glycoprotein folding is promoted through off-pathway aggregation suppression, which is achieved by binding of Cnx to hydrophobic non-native areas via its polypeptide-binding site as well as physical sequestration by the arm domain.

The remaining lectin-based association is also probably weak with respect to the low K_d of 1-2 μM in the case of Crt (480) and leads finally to complete dissociation of the chaperone/client protein complex. If folding and subunit assembly is not achieved rapidly, the presence of non-native features allows UGGT to act on the folding glycoprotein and promotes rebinding to the high affinity ATP state of Cnx. Such cycles of binding and release continue until all recognition sites for UGGT and Cnx are buried in the native conformation of a completely folded client protein. To what degree cyclic lectin- and polypeptide-based interactions appear in a synchronized or sequential manner might largely depend on whether the folding sensors, UGGT and Cnx, exhibit a binding preference to similar or different folding states of a client protein.

Having demonstrated the capacity of S-Cnx to mediate classical chaperone functions by utilizing a polypeptide-binding site during interaction and physical sequestration of a client protein, one might wonder why Cnx assisted protein folding necessitates lectin function at all?

One reason is that, in concert with polypeptide-based interactions, lectin-oligosaccharide interactions may enhance the overall binding avidity for glycoproteins, as S-Cnx suppressed significantly more effectively the aggregation of monoglucosylated SBA compared to its deglucosylated form (283). This effect can also account for the observations that S-Cnx's performance in suppressing the aggregation of a client glycoprotein was much more efficient compared to BiP's, an advantage that was lost when confronted with a non-glycosylated client protein (392). Whether the binding to a glycoprotein solely through its lectin site and additional sequestration by the arm domain of Cnx are sufficient to suppress aggregation is unclear. As another reason, lectin function may be also beneficial by allowing Cnx to interact more flexibly with a wider spectrum of client proteins. For example, in the case of RNase B, lacking nearly any recognizable hydrophobic polypeptide determinants, binding to Cnx relies exclusively on lectin-oligosaccharide interactions and contributes to assisted folding by recruiting ERp57 (375, 377). It is also conceivable that the addition of relatively large glycan moieties to certain well conserved areas of a nascent glycoprotein facilitates its initial interaction with Cnx and places less accessible hydrophobic segments during later stages of the folding process in close proximity to the polypeptide-binding site.

The results of several studies are indicative of the organization of ER chaperones and folding enzymes into subsets of low affinity complexes (481, 482), probably to allow them to collaborate more efficiently. Herein, it is possible that the unique mode of client protein recognition through a lectin site, in addition to a classical polypeptide-binding site, helps to orchestrate the activity of Cnx relative to those of other chaperones in the lumen of the ER. For example, monoglucosylated oligosaccharides are generated with a half time of approximitly 5 min (483). Considering this, it can be envisioned that the lectin site, whose engagement is associated with a marked increase in overall binding affinity of Cnx, ensures binding to glycoproteins during later stages of their folding process. Thereby, competition with BiP, which might bind to earlier folding stages during its initial interactions with nascent polypeptides, can be prevented.

However, it is noteworthy that significant variability in the aggregation suppression potency of BiP and S-Cnx was shown with various de- and non-glycosylated client proteins (392). The findings demonstrate inherent differences in the intrinsic properties of Cnx's and BiP's polypeptide-binding sites which are expected to contribute to their capacity to cooperate in protein folding by flexibly interacting with the different types of non-native determinants exposed on the multitude of client proteins. In fact, sequential as well as simultaneous association with several client proteins have been documented *in vivo* for Cnx and BiP (63,

244, 302, 304, 306, 319). Furthermore these chaperones have been identified in an heterogeneous network of weakly associated ER chaperones including GRP94 and Crt by pulse-chase and chemical cross-linking experiments (484). This feature of several molecular chaperones cooperating to promote protein folding was also demonstrated for Cnx *in vitro*. S-Cnx was found to be essential to maintain monoglucosylated α-mannosidase or non-glycosylated CS in a folding competent state during their thermal denaturation, whereas subsequent ATP-dependent refolding required the participation of BiP and the Sec63p J domain (392).

The *in vitro* experiments presented in this thesis work clearly demonstrate that the chaperone function of S-Cnx under physiological conditions of the ER lumen employs a dual mode of client protein recognition that allows Cnx, and probably Crt as well, to occupy a unique niche within the complex quality control system of the ER.

4.4 Future perspectives

Results obtained during the course of this thesis work provide compelling evidence that S-Cnx utilizes polypeptide-based interactions, in addition to lectin-mediated interactions, to suppress client protein aggregation under physiological conditions of the ER.

Since aggregation suppression and peptide binding experiments with various deletion mutants of S-Cnx allowed the localization of polypeptide binding to the globular domain at a site distinct from the lectin site, it would be of particular interest to determine the exact localization of the polypeptide-binding site. This could be achieved by using the hydrophobic KHP peptide, which revealed specific binding to S-Cnx with a K_d of 0.9 μM (Fig. 36). One possibility would first require the successful cross-linking of the KHP peptide to the globular domain of S-Cnx before identification of modified protein segments by tryptic digestion and subsequent sequence analysis by mass spectrometry to reveal which portion of S-Cnx contributes to peptide binding. Solving the structure of a complex between the KHP peptide and the globular domain of S-Cnx by NMR spectroscopy or X-ray crystallography represents an alternative approach that might facilitate precise mapping and a more detailed characterization of the polypeptide-binding site. Furthermore, residues within the putative polypeptide-binding site could be mutated and the resulting mutants, if exhibiting structural integrity as assessed by CD, examined for their aggregation suppression and peptide-binding capacities.

Having shown a preference of the polypeptide-binding site of S-Cnx for peptides hydrophobic in character, additional determinants in the polypeptide sequence for specific binding might exist that are crucial for the mechanism by which Cnx discriminates between native and non-native client proteins. This also appears to be an interesting aspect in the light of differing client protein selection of Cnx and Crt beyond their different topologies (301, 320, 327). To determine such binding motifs, solid-phase peptide arrays can be employed that allow one to scan through libraries of up to ~13 residue immobilized peptides derived from the complete sequence of Cnx and Crt client proteins. Incubation of a peptide array with S-Cnx or Crt and subsequent detection of interaction by Western Blotting should permit a consensus motif specific for S-Cnx and Crt to be determined after comprehensive screening of peptide libraries and additional variants of positive peptides. This technique has allowed the successful identification of the peptide-binding specificity in the case of the bacterial DnaK (Hsp70), DnaJ (Hsp40), and SecB molecular chaperones (422, 485, 486). Similar solid-phase binding assays have also been used by Houen and co-workers to characterize the polypeptide-binding site of Crt (390, 391). However, the observed polypeptide-based interactions of Crt are suspect since its structural integrity might have been affected by the applied non-physiological conditions. Extensive screening of over 4000 peptides during past attempts of the Williams laboratory to elucidate the peptide-binding specificities of S-Cnx and Crt were generally compromised by problems associated with an apparent non-specific dominance of electrostatic interactions. Considering that those experiments were conducted under non-optimal conditions (1 mM Ca^{2+}, 22°C), and bis-ANS binding experiments (Fig. 22) demonstrated a marked increase of the exposure of S-Cnx's polypeptide-binding site at 0.4 mM Ca^{2+}, 37°C, and in the presence of ATP, further studies under the newly established conditions might allow the delineation of specific binding motifs for S-Cnx and Crt. The validity of this method could be tested by using high affinity peptides as direct competitors in the FL aggregation assay.

Although no ATPase activity has been detected for Cnx and Crt and there are no obvious nucleotide-binding motifs in their sequences, their aggregation suppression potencies were significantly enhanced by ATP (283, 284) in agreement with Fig. 14 of this thesis. In addition, the establishment of the first direct binding assay for ATP to S-Cnx using changes in surface hydrophobicity as a readout (Fig. 19 and Fig. 22.B) revealed a weak but saturable interaction, indicative of the existence of an ATP-binding site. The assignment of this site to the arm or globular domains of S-Cnx using the direct binding assay should not present tremendous difficulty since the required domain constructs are already created. For further

identification of residues involved in ATP binding photo-crosslinking of the positive tested domain to [γ-^{32}P]-8-azido ATP could serve as a promising tool. This technique has already been used successfully for S-Cnx by Ou *et al*. (412) and for Crt by the Williams laboratory (unpublished results) despite problems such as low crosslinking affinity and incipiently non-specific crosslinking to multiple sites in the protein. Subsequently, residues crosslinked to [γ-^{32}P]-8-azido ATP could be determined by the combination of proteolytic digestion and mass spectrometry as already described for peptide binding above. Identified residues could be mutated and their contribution to ATP binding assessed by testing respective S-Cnx mutants in aggregation suppression and direct binding assays.

Bearing in mind that the aggregation suppression ability of S-Cnx is influenced by Ca^{2+} and ATP binding as well as by physical sequestration of a client protein between the arm and globular domains, it is conceivable that ligand binding also affects the chaperone function by modulating the alignment of the two domains relative to each other. Such conformational changes could be described as a closing and opening of the arm domain over the client protein and this mechanism could be detected by examining the distance between the arm and globular domains in the presence and absence of various ligands. A technique that offers considerable promise in elucidating molecular distances is Förster resonance energy transfer (FRET), a very useful type of fluorescence spectroscopy (487-489). FRET represents a radiationless transfer of energy and only occurs between a donor and acceptor fluorophor when their separating distance is less than 10 nm (490), resulting in reduced and enhanced emission intensity of the donor and acceptor, respectively. In many cases FRET has been successfully applied to analyze protein interactions (491-495), protein folding (496-498), and to measure changes in inter- and intramolecular distances during ligand induced conformational changes as shown for the small HdeA chaperone and the large GroEL-GroES chaperone complex in bacteria (499, 500). The incorporation of fluorophores at appropriately chosen positions in the arm and globular domains of S-Cnx may also provide ligand dependent distance information and exciting insights into a putative open and closing mechanism of the arm domain.

To shed further light into the ongoing debate concerning the relative contributions of the lectin site, the polypeptide-binding site, ATP binding, client protein sequestration, and ERp57 recruitment to the molecular chaperone and quality control function of Cnx, it would be of particular interest to compare the functional consequences of various mutants selectively deficient in these respective properties in living cells. Therefore, the previously described *Drosophila* SC2 cells should serve as a promising *in vivo* system (326, 501). Although these

cells comprise all the necessary compounds for lectin-based Cnx and Crt cycles (502-504) endogenous Cnx and Crt do not interact with heterologous mouse class I molecules (501). Consequently, SC2 cells allow the examination of MHC class I biogenesis in an operationally Cnx- and Crt-deficient environment, as shown in initial studies with canine wild type Cnx (326, 501). There are four aspects of MHC class I biogenesis that are promoted by Cnx; folding of free H chain, assembly of H chain with β_2m, ER retention of H chain-β_2m complexes, and stabilization of folded free H chains. Considering a significant enhancement of these processes by Cnx (326, 327, 501), it is conceivable that this system is sensitive enough to evaluate the impact of the respective mutations alone or in combination on the chaperone function of Cnx during MHC class I biogenesis. Experiments with lectin-deficient Cnx have already been conducted and revealed unimpaired interactions with MHC class I H chains, indicative of the utilization of a polypeptide-binding site in living cells (287).

The existence of several binding sites on Cnx raises the question of how regulatory effects of ligand binding might contribute in detail to chaperone cycles of binding and release involving both lectin- and polypeptide-based interactions. The latter interactions were clearly enhanced in the presence of ATP as shown in aggregation suppression experiments (Fig. 14) of this thesis, whereby such interactions were attenuated following occupancy of the lectin site with Glc_1Man_3 under non-physiological conditions (283, 284). In the presence of both ligands, the enhancing effect of ATP appeared to be dominant. Also, resting ER Ca^{2+} concentrations were found to potentiate the ATP effect in aggregation suppression assays (Fig. 21) in accordance with direct binding experiments revealing an increased binding affinity of S-Cnx for ATP following reduction of the Ca^{2+} concentration to the resting ER level (Fig. 22.B). Besides the establishment of direct binding assays for Ca^{2+}, ATP and peptides in this thesis, further development of similar assays for oligosaccharides and ERp57 would be extremely valuable to systematically evaluate the effect of each ligand on the binding affinities of each other ligands towards S-Cnx.

Based on such experiments giving new insights into how the various ligands might modulate client protein interactions through either the lectin or polypeptide-binding site, it might be possible to reconstitute functional chaperone cycles for S-Cnx *in vitro*. While in a classical aggregation suppression assay there is no need for a chaperone to dissociate from the client protein, the achievement of the native state requires folding in an unbound form and therefore cycles of binding and release. To assess the ability of S-Cnx to promote client protein folding to its mature conformation, three different client proteins could be used that would constitute binding and release cycles of increasing complexity.

In initial experiments S-Cnx could be confronted with a non-glycosylated client protein, to focus only on polypeptide-based interactions and to gain important information concerning its function to act as a classical chaperone. This could be attained by dilution of chemically denatured FL into solution with or without S-Cnx under physiological Ca^{2+} concentrations and following analysis of FL activity at different time points. The refolding efficiency could then be tested in the presence of different ligands using various combinations to evaluate their regulatory role in functional cycles of binding and release.

Next, cycling of a non-glycosylated client protein with S-Cnx could be examined in the more complex context of oxidative folding. Here, it would be of particular interest if S-Cnx is capable of enhancing the oxidative folding process of a client protein through its recruitment via the polypeptide-binding site and the simultaneous recruitment of ERp57 via the arm domain. Hen egg white lysozyme contains four disulfides and might be a suitable candidate for these experiments (170). Refolding can be assessed by monitoring a gain in enzyme activity and refolding rates could be compared in the presence or absence of ERp57 and appropriate ligands under physiological Ca^{2+} concentrations and a mildly oxidizing environment.

The ultimate goal would be the reconstitution of an S-Cnx cycle that facilitates refolding of an unfolded monoglucosylated client protein through both lectin and polypeptide-mediaded interactions. Such a system should probably consist of S-Cnx, glucosidase II, UGGT, ERp57, reduced:oxidized glutathione, UDP-glucose, physiological Ca^{2+} concentrations and ATP. Since jack bean α-mannosidase exposes a single monoglucosylated oligosaccharide and forms at least one disulfide bond, it represents an ideal client protein. In addition, S-Cnx has been shown to suppress α-mannosidase aggregation following chemical denaturation/reduction in a lectin- as well as polypeptide-dependent manner (287, 392). If S-Cnx also exhibited the capacity to successfully refold this enzyme when allowed to act in a cyclic fashion, this would be a superb system to assess in detail the contributions of the individual components to the molecular chaperone function.

5 Summary

Calnexin is a membrane-bound chaperone of the endoplasmic reticulum (ER) that participates in the folding and quality control of newly synthesized glycoproteins. Binding to glycoproteins occurs through a lectin site with specificity for $Glc_1Man_9GlcNAc_2$ oligosaccharides as well as through a polypeptide-binding site that recognizes non-native protein conformations. The latter interaction is somewhat controversial because it is based on observations that calnexin can suppress the aggregation of non-glycosylated client proteins at elevated temperature or at low calcium concentrations, conditions that may affect the structural integrity of calnexin. This thesis focuses on the ability of calnexin to interact with client proteins in a lectin-independent manner under physiological conditions of the ER lumen and provides new mechanistic insights into its molecular chaperone function.

(1) The successful development of a new aggregation suppression assay using the thermolabile enzyme firefly luciferase permitted the demonstration that the soluble ER-luminal domain of calnexin (S-Cnx) can indeed suppress the aggregation of a non-glycosylated client protein at physiological temperature and at the normal resting ER Ca^{2+} concentration of 0.4 mM. However, gradual reduction of Ca^{2+} below the resting level resulted in an increased aggregation suppression potency but was accompanied by a progressive loss of native S-Cnx structure as assessed by thermal stability, protease sensitivity, intrinsic fluorescence, and bis-ANS binding. These assays permitted the characterization of a single Ca^{2+}-binding site on S-Cnx with a dissociation constant (K_d) of 0.15 ± 0.05 mM.

(2) Furthermore it was shown that the suppression of firefly luciferase aggregation by S-Cnx is strongly enhanced in the presence of millimolar concentrations of ATP and that the K_d for ATP binding to S-Cnx in the presence of 0.4 mM Ca^{2+} is 0.7 mM. In contrast to Ca^{2+}, ATP did not alter the overall stability of S-Cnx but instead triggered the localized exposure of a hydrophobic site on the chaperone. These findings exemplify that calnexin can act as a potent molecular chaperone that is capable of suppressing the aggregation of client proteins through polypeptide-based interactions under conditions that exist within the ER lumen.

(3) Since the luminal portion of calnexin consists of two domains, a globular domain, which comprises the lectin site, and an extended arm domain, it was of great interest to understand the function of these domains during interactions of calnexin with non-native protein conformers. For this reason the aggregation suppression abilities of various deletion mutants of S-Cnx were tested in the newly established aggregation assay with non-glycosylated firefly luciferase. The arm domain alone showed no capacity to suppress aggregation. However, stepwise truncation of the arm domain in S-Cnx resulted in a progressive reduction in aggregation suppression potency to the point where the globular domain alone exhibited 25 % potency. Thus aggregation suppression appears to be primarily mediated by the globular domain, but the arm domain is required for maximal function.

(4) To characterize the putative polypeptide-binding site, hydrophobic peptides were used that were effective competitors of the ability of S-Cnx to suppress firefly luciferase aggregation. Direct binding experiments revealed a single site of peptide binding in the globular domain (K_d = 0.9 μM) at a location distinct from the lectin site.

(5) Progressive truncation of the arm domain in S-Cnx had no effect on the binding of small peptides but reduced the binding affinity of S-Cnx for large, non-native client proteins. Because client proteins/peptides exhibited no binding to the isolated arm domain, the findings support a model in which calnexin suppresses aggregation through a polypeptide-binding site in its globular domain, with the arm domain enhancing aggregation suppression by sterically constraining large client proteins.

6 Zusammenfassung

Calnexin ist ein membranegebundenes Chaperon des endoplasmatischen Retikulums (ER), welches maßgeblich an der Faltung und Qualitätskontrolle von neu synthetisierten Glykoproteinen beteiligt ist. Die Interaktion mit Glykoproteinen erfolgt sowohl über eine Lektin-Bindestelle, die eine hohe Spezifität für $Glc_1Man_9GlcNAc_2$-Oligosaccharide aufweist, als auch durch eine Polypeptid-Bindestelle, welche die Erkennung nicht-nativer Proteinkonformationen ermöglicht. Die Existenz der besagten Polypeptid-Bindestelle gilt jedoch als kontrovers. Ihr Nachweis beruht vornehmlich auf Untersuchungen, durch die die Unterdrückung der Aggregation von nicht-glykosylierten Klienten-Proteinen durch Calnexin unter unphysiologisch hohen Temperaturen beziehungsweise niedrigen Calcium-Konzentrationen gezeigt werden konnte, Bedingungen, die die strukturelle Integrität von Calnexin beeinträchtigt haben könnten. Aus diesem Grund stand die Charakterisierung des putativen Lektin-unabhängigen Bindungsmodus von Calnexin mit Klienten-Proteinen unter physiologischen Bedingungen des ER im Vordergrund dieser Arbeit und erlaubte neue Einblicke in den Mechanismus der molekularen Chaperonfunktion.

(1) Aufgrund der erfolgreichen Entwicklung eines neuen Aggregations-Suppressions-Assays unter Verwendung des thermolabilen Enzyms Luziferase der nord-amerikanischen Feuerfliege konnte gezeigt werden, dass die lösliche ER-luminale Domäne von Calnexin (S-Cnx) tatsächlich die Aggregation eines nicht-glykosilierten Klienten-Proteins unter physiologischen Bedingungen des ruhenden ER-Lumens (37°C, 0,4 mM Ca^{2+}) unterdrücken kann. Die graduelle Reduktion von Ca^{2+} unterhalb von 0,4 mM resultierte in einer erhöhten Potenz zur Supression der Aggregation. Allerdings war diese Steigerung mit einem zuhnehmenden Verlust der nativen Struktur von S-Cnx verbunden, was durch Messungen der thermalen Stabilität, Protease-Sensitivität, intrinsischer Fluoreszenz und bis-ANS-Bindung beobachtet werden konnte. Anhand dieser Experimente konnte eine singuläre Ca^{2+}-Bindestelle für S-Cnx mit einer Dissoziationskonstanten (K_d) von 0,15 ± 0,05 mM beschrieben werden.

(2) Desweiteren konnte eine deutlich effizientere Unterdrückung der Luziferase-Aggregation durch S-Cnx in Gegenwart von millimolarem ATP nachgewiesen werden, wobei für die Interaktion zwischen ATP und S-Cnx bei einer Ca^{2+}-

Konzentration von 0,4 mM ein K_d-Wert von 0,7 mM mittels bis-ANS-Bindungsstudien bestimmt werden konnte. Im Gegensatz zu Ca^{2+} führte die Bindung von ATP zwar nicht zu einer nennenwerten Destabilisierung von S-Cnx, hatte jedoch die lokale Exposition einer ansonsten größtenteils verborgenen hydrophoben Region zur Folge. Somit konnte gezeigt werden, dass Calnexin durchaus ähnlich wie ein klassisches molekulares Chaperon fungieren kann, indem es die Aggregation von Klienten-Proteinen durch Polypeptid-vermittelte Interaktionen unter physiologischen Bedingungen des ER-Lumens unterdrücken kann.

(3) In Anbetracht der Tatsache, dass das ER-luminale Segment von Calnexin aus zwei Domänen besteht, einer globulären Lektin- und einer länglichen Arm-Domäne, war es von großem Interesse, die Funktion der beiden Domänen während der Interaktion von Calnexin mit nicht-nativen Klienten-Proteinen zu verstehen. Aus diesem Grund wurde das Potential zur Aggregations-Suppression von verschiedenen Deletionsmutanten von S-Cnx in dem neu entwickelten Aggregations-Assay mit nicht-glykosylierter Luziferase getestet. Während die Arm-Domäne alleine nicht in der Lage war, die Aggregation zu unterdrücken, resultierte die schrittweise Verkürzung der Arm-Domäne von S-Cnx in einer progressiven Reduktion seiner Eigenschaft als Aggregations-Suppressor zu agieren. So konnte nach vollständiger Entfernung der Arm-Domäne für die verbleibende globuläre Domäne lediglich 25 % des ursprünglichen Aggregations-Suppressions-Potentials verzeichnet werden. Somit scheint die Unterdrückung der Aggregation primär durch die globuläre Domäne vermittelt zu werden, wobei die Arm-Domäne für eine optimale Funktionsweise erforderlich ist.

(4) Um die putative Polypeptid-Bindestelle zu charakterisieren, konnten hydrophobe Peptide verwendet werden, welche sich als effektive Kompetitoren im Aggregations-Suppressions-Assay mit S-Cnx erwiesen. Durch direkte Bindungsexperimente ließ sich eine singuläre Peptid-Bindestelle in der globuläre Domäne (K_d = 0,9 µM) lokalisieren, bei der es sich nicht um die Lektin-Bindestelle handelt.

(5) Die sukzessive Verkürzung der Arm-Domäne von S-Cnx hatte keinen Einfluss auf die Bindung von kleinen Peptiden, wohingegen eine verringerte Bindungsaffinität zwischen S-Cnx und größeren nicht-nativen Klienten-Proteinen festgestellt werden

konnte. Da für die isolierte Arm-Domäne keine Interaktion mit Klienten-Proteinen/Peptiden nachgewiesen werden konnte, ließ sich ein Modell erstellen, wonach Calnexin Proteinaggregation durch seine Polypeptid-Bindestelle in der globulären Domäne unterdrückt. Dabei erfolgt eine Potenzierung des Suppressionsmechanismus durch die Arm-Domäne, indem diese größere Klienten-Proteine sterisch sequestriert und vor unspezifischen intermolekularen Wechselwirkungen schützt.

7 References

1. **Pfeffer, S.** 2003. Membrane domains in the secretory and endocytic pathways. Cell **112:**507-17.

2. **van Meer, G., and H. Sprong.** 2004. Membrane lipids and vesicular traffic. Curr Opin Cell Biol **16:**373-8.

3. **Geuze, H. J., J. L. Murk, A. K. Stroobants, J. M. Griffith, M. J. Kleijmeer, A. J. Koster, A. J. Verkleij, B. Distel, and H. F. Tabak.** 2003. Involvement of the endoplasmic reticulum in peroxisome formation. Mol Biol Cell **14:**2900-7.

4. **Papp, S., E. Dziak, M. Michalak, and M. Opas.** 2003. Is all of the endoplasmic reticulum created equal? The effects of the heterogeneous distribution of endoplasmic reticulum Ca2+-handling proteins. J Cell Biol **160:**475-9.

5. **Bollini, R., and M. J. Chrispeels.** 1979. The Rough Endoplasmic Reticulum Is the Site of Reserve-Protein Synthesis in Developing Phaseolus vulgaris Cotyledons. Planta **146:**487-501.

6. **Chrispeels, M. J., T. J. Higgins, S. Craig, and D. Spencer.** 1982. Role of the endoplasmic reticulum in the synthesis of reserve proteins and the kinetics of their transport to protein bodies in developing pea cotyledons. J Cell Biol **93:**5-14.

7. **Redman, C. M.** 1969. Biosynthesis of serum proteins and ferritin by free and attached ribosomes of rat liver. J Biol Chem **244:**4308-15.

8. **Palade, G.** 1975. Intracellular aspects of the process of protein synthesis. Science **189:**347-58.

9. **Walter, P., and G. Blobel.** 1983. Signal recognition particle: a ribonucleoprotein required for cotranslational translocation of proteins, isolation and properties. Methods Enzymol **96:**682-91.

10. **Krieg, U. C., P. Walter, and A. E. Johnson.** 1986. Photocrosslinking of the signal sequence of nascent preprolactin to the 54-kilodalton polypeptide of the signal recognition particle. Proc Natl Acad Sci U S A **83:**8604-8.

11. **Keenan, R. J., D. M. Freymann, R. M. Stroud, and P. Walter.** 2001. The signal recognition particle. Annu Rev Biochem **70:**755-75.

12. **Sipos, L., and G. von Heijne.** 1993. Predicting the topology of eukaryotic membrane proteins. Eur J Biochem **213:**1333-40.

13. **von Heijne, G.** 1986. Towards a comparative anatomy of N-terminal topogenic protein sequences. J Mol Biol **189:**239-42.

14. **Hartmann, E., T. A. Rapoport, and H. F. Lodish.** 1989. Predicting the orientation of eukaryotic membrane-spanning proteins. Proc Natl Acad Sci U S A **86:**5786-90.

15. **Blobel, G.** 1980. Intracellular protein topogenesis. Proc Natl Acad Sci U S A **77:**1496-500.

16. **Nunnari, J., and P. Walter.** 1992. Protein targeting to and translocation across the membrane of the endoplasmic reticulum. Curr Opin Cell Biol **4:**573-80.

17. **Johnson, A. E., and M. A. van Waes.** 1999. The translocon: a dynamic gateway at the ER membrane. Annu Rev Cell Dev Biol **15:**799-842.

18. **Meacock, S. L., J. J. Greenfield, and S. High.** 2000. Protein targeting and translocation at the endoplasmic reticulum membrane--through the eye of a needle? Essays Biochem **36:**1-13.

19. **Nicola, A. V., W. Chen, and A. Helenius.** 1999. Co-translational folding of an alphavirus capsid protein in the cytosol of living cells. Nat Cell Biol **1:**341-5.

20. **Kleizen, B., T. van Vlijmen, H. R. de Jonge, and I. Braakman.** 2005. Folding of CFTR is predominantly cotranslational. Mol Cell **20:**277-87.

21. **Chen, W., J. Helenius, I. Braakman, and A. Helenius.** 1995. Cotranslational folding and calnexin binding during glycoprotein synthesis. Proc Natl Acad Sci U S A **92:**6229-33.

22. **Stevens, F. J., and Y. Argon.** 1999. Protein folding in the ER. Semin Cell Dev Biol **10:**443-54.

23. **Hwang, C., A. J. Sinskey, and H. F. Lodish.** 1992. Oxidized redox state of glutathione in the endoplasmic reticulum. Science **257:**1496-502.

24. **Fahey, R. C., J. S. Hunt, and G. C. Windham.** 1977. On the cysteine and cystine content of proteins. Differences between intracellular and extracellular proteins. J Mol Evol **10:**155-60.

25. **Freedman, R.** 1984. Native disulphide bond formation in protein biosynthesis: Evidence for the role of protein disulfide isomerase. Trends Biochem Sci **9:**438-441.

26. **Berridge, M. J., M. D. Bootman, and P. Lipp.** 1998. Calcium--a life and death signal. Nature **395:**645-8.

27. **Lodish, H. F., N. Kong, and L. Wikstrom.** 1992. Calcium is required for folding of newly made subunits of the asialoglycoprotein receptor within the endoplasmic reticulum. J Biol Chem **267:**12753-60.

28. **Kuznetsov, G., M. A. Brostrom, and C. O. Brostrom.** 1992. Demonstration of a calcium requirement for secretory protein processing and export. Differential effects of calcium and dithiothreitol. J Biol Chem **267:**3932-9.

29. **Lee, A. S.** 1987. Coordinated regulation of a set of genes by glucose and calcium ionophores in mammalian cells. Trends Biochem Sci **12:**20-23.

30. **MacLennan, D. H.** 2000. Ca2+ signalling and muscle disease. Eur J Biochem **267:**5291-7.

31. **Meldolesi, J., and T. Pozzan.** 1998. The endoplasmic reticulum Ca2+ store: a view from the lumen. Trends Biochem Sci **23:**10-4.

32. **Fliegel, L., K. Burns, K. Wlasichuk, and M. Michalak.** 1989. Peripheral membrane proteins of sarcoplasmic and endoplasmic reticulum. Comparison of carboxyl-terminal amino acid sequences. Biochem Cell Biol **67:**696-702.

33. **Corbett, E. F., and M. Michalak.** 2000. Calcium, a signaling molecule in the endoplasmic reticulum? Trends Biochem Sci **25:**307-11.

34. **Miyawaki, A., J. Llopis, R. Heim, J. M. McCaffery, J. A. Adams, M. Ikura, and R. Y. Tsien.** 1997. Fluorescent indicators for Ca2+ based on green fluorescent proteins and calmodulin. Nature **388:**882-7.

35. **Kornfeld, R., and S. Kornfeld.** 1985. Assembly of asparagine-linked oligosaccharides. Annu Rev Biochem **54:**631-64.

36. **Parodi, A. J., N. H. Behrens, L. F. Leloir, and H. Carminatti.** 1972. The role of polyprenol-bound saccharides as intermediates in glycoprotein synthesis in liver. Proc Natl Acad Sci U S A **69:**3268-72.

37. **Popov, M., L. Y. Tam, J. Li, and R. A. Reithmeier.** 1997. Mapping the ends of transmembrane segments in a polytopic membrane protein. Scanning N-glycosylation mutagenesis of extracytosolic loops in the anion exchanger, band 3. J Biol Chem **272:**18325-32.

38. **Helenius, A., and M. Aebi.** 2004. Roles of N-linked glycans in the endoplasmic reticulum. Annu Rev Biochem **73:**1019-49.

39. **Hammond, C., I. Braakman, and A. Helenius.** 1994. Role of N-linked oligosaccharide recognition, glucose trimming, and calnexin in glycoprotein folding and quality control. Proc Natl Acad Sci U S A **91:**913-7.

40. **Hebert, D. N., B. Foellmer, and A. Helenius.** 1995. Glucose trimming and reglucosylation determine glycoprotein association with calnexin in the endoplasmic reticulum. Cell **81:**425-33.

41. **Spiro, R. G., Q. Zhu, V. Bhoyroo, and H. D. Soling.** 1996. Definition of the lectin-like properties of the molecular chaperone, calreticulin, and demonstration of its copurification with endomannosidase from rat liver Golgi. J Biol Chem **271:**11588-94.

42. **Caramelo, J. J., O. A. Castro, G. de Prat-Gay, and A. J. Parodi.** 2004. The endoplasmic reticulum glucosyltransferase recognizes nearly native glycoprotein folding intermediates. J Biol Chem **279:**46280-5.

43. **Ritter, C., K. Quirin, M. Kowarik, and A. Helenius.** 2005. Minor folding defects trigger local modification of glycoproteins by the ER folding sensor GT. Embo J **24:**1730-8.

44. **Taylor, S. C., A. D. Ferguson, J. J. Bergeron, and D. Y. Thomas.** 2004. The ER protein folding sensor UDP-glucose glycoprotein-glucosyltransferase modifies substrates distant to local changes in glycoprotein conformation. Nat Struct Mol Biol **11:**128-34.

45. **LaPointe, P., C. Gurkan, and W. E. Balch.** 2004. Mise en place-this bud's for the Golgi. Mol Cell **14:**413-4.

46. **Antonny, B., and R. Schekman.** 2001. ER export: public transportation by the COPII coach. Curr Opin Cell Biol **13:**438-43.

47. **Tu, B. P., and J. S. Weissman.** 2004. Oxidative protein folding in eukaryotes: mechanisms and consequences. J Cell Biol **164:**341-6.

48. **Fanghanel, J., and G. Fischer.** 2004. Insights into the catalytic mechanism of peptidyl prolyl cis/trans isomerases. Front Biosci **9:**3453-78.

49. **Dobson, C. M.** 2004. Principles of protein folding, misfolding and aggregation. Semin Cell Dev Biol **15:**3-16.

50. **Hendrick, J. P., and F. U. Hartl.** 1993. Molecular chaperone functions of heat-shock proteins. Annu Rev Biochem **62:**349-84.

51. **Ellis, J.** 1987. Proteins as molecular chaperones. Nature **328:**378-9.

52. **Hartl, F. U.** 1996. Molecular chaperones in cellular protein folding. Nature **381:**571-9.

53. **Brinker, A., G. Pfeifer, M. J. Kerner, D. J. Naylor, F. U. Hartl, and M. Hayer-Hartl.** 2001. Dual function of protein confinement in chaperonin-assisted protein folding. Cell **107:**223-33.

54. **Bonifacino, J. S., P. Cosson, and R. D. Klausner.** 1990. Colocalized transmembrane determinants for ER degradation and subunit assembly explain the intracellular fate of TCR chains. Cell **63:**503-13.

55. **Brodsky, J. L., and R. J. Wojcikiewicz.** 2009. Substrate-specific mediators of ER associated degradation (ERAD). Curr Opin Cell Biol **24:**516-21.

56. **Meusser, B., C. Hirsch, E. Jarosch, and T. Sommer.** 2005. ERAD: the long road to destruction. Nat Cell Biol **7:**766-72.

57. **Sayeed, A., and D. T. Ng.** 2005. Search and destroy: ER quality control and ER-associated protein degradation. Crit Rev Biochem Mol Biol **40:**75-91.

58. **Kostova, Z., and D. H. Wolf.** 2003. For whom the bell tolls: protein quality control of the endoplasmic reticulum and the ubiquitin-proteasome connection. Embo J **22:**2309-17.

59. **Romisch, K.** 2005. Endoplasmic reticulum-associated degradation. Annu Rev Cell Dev Biol **21:**435-56.

60. **Ellgaard, L., M. Molinari, and A. Helenius.** 1999. Setting the standards: quality control in the secretory pathway. Science **286:**1882-8.

61. **Voges, D., P. Zwickl, and W. Baumeister.** 1999. The 26S proteasome: a molecular machine designed for controlled proteolysis. Annu Rev Biochem **68:**1015-68.

62. **Jung, T., B. Catalgol, and T. Grune.** 2009. The proteasomal system. Mol Aspects Med **30:**191-296.

63. **Molinari, M., and A. Helenius.** 2000. Chaperone selection during glycoprotein translocation into the endoplasmic reticulum. Science **288:**331-3.

64. **Gillece, P., J. M. Luz, W. J. Lennarz, F. J. de La Cruz, and K. Romisch.** 1999. Export of a cysteine-free misfolded secretory protein from the endoplasmic reticulum for degradation requires interaction with protein disulfide isomerase. J Cell Biol **147:**1443-56.

65. **Moremen, K. W.** 2000. Alpha-mannosidases in asparagine-linked oligosaccharide processing and catabolism, p. 81-117. *In* B. Ernst, G. Hart, and P. Sinay (ed.), Oligosaccharides in chemistry and biology: a comprehensive handbook, vol. 2. Wiley, New York.

66. **Cabral, C. M., Y. Liu, and R. N. Sifers.** 2001. Dissecting glycoprotein quality control in the secretory pathway. Trends Biochem Sci **26:**619-24.

67. **Helenius, A.** 1994. How N-linked oligosaccharides affect glycoprotein folding in the endoplasmic reticulum. Mol Biol Cell **5:**253-65.

68. **Herscovics, A., P. A. Romero, and L. O. Tremblay.** 2002. The specificity of the yeast and human class I ER alpha 1,2-mannosidases involved in ER quality control is not as strict previously reported. Glycobiology **12:**14G-15G.

69. **Hebert, D. N., S. C. Garman, and M. Molinari.** 2005. The glycan code of the endoplasmic reticulum: asparagine-linked carbohydrates as protein maturation and quality-control tags. Trends Cell Biol **15:**364-70.

70. **Herscovics, A.** 2001. Structure and function of Class I alpha 1,2-mannosidases involved in glycoprotein synthesis and endoplasmic reticulum quality control. Biochimie **83:**757-62.

71. **Hosokawa, N., I. Wada, K. Hasegawa, T. Yorihuzi, L. O. Tremblay, A. Herscovics, and K. Nagata.** 2001. A novel ER alpha-mannosidase-like protein accelerates ER-associated degradation. EMBO Rep **2:**415-22.

72. **Mast, S. W., K. Diekman, K. Karaveg, A. Davis, R. N. Sifers, and K. W. Moremen.** 2005. Human EDEM2, a novel homolog of family 47 glycosidases, is involved in ER-associated degradation of glycoproteins. Glycobiology **15:**421-36.

73. **Hirao, K., Y. Natsuka, T. Tamura, I. Wada, D. Morito, S. Natsuka, P. Romero, B. Sleno, L. O. Tremblay, A. Herscovics, K. Nagata, and N. Hosokawa.** 2006. EDEM3, a soluble EDEM homolog, enhances glycoprotein endoplasmic reticulum-associated degradation and mannose trimming. J Biol Chem **281:**9650-8.

74. **Clerc, S., C. Hirsch, D. M. Oggier, P. Deprez, C. Jakob, T. Sommer, and M. Aebi.** 2009. Htm1 protein generates the N-glycan signal for glycoprotein degradation in the endoplasmic reticulum. J Cell Biol **184:**159-72.

75. **Olivari, S., T. Cali, K. E. Salo, P. Paganetti, L. W. Ruddock, and M. Molinari.** 2006. EDEM1 regulates ER-associated degradation by accelerating de-mannosylation of folding-defective polypeptides and by inhibiting their covalent aggregation. Biochem Biophys Res Commun **349:**1278-84.

76. **Ellgaard, L., and A. Helenius.** 2001. ER quality control: towards an understanding at the molecular level. Curr Opin Cell Biol **13:**431-7.

77. **Liu, Y., P. Choudhury, C. M. Cabral, and R. N. Sifers.** 1999. Oligosaccharide modification in the early secretory pathway directs the selection of a misfolded glycoprotein for degradation by the proteasome. J Biol Chem **274:**5861-7.

78. **Lederkremer, G. Z., and M. H. Glickman.** 2005. A window of opportunity: timing protein degradation by trimming of sugars and ubiquitins. Trends Biochem Sci **30:**297-303.

79. **Molinari, M., V. Calanca, C. Galli, P. Lucca, and P. Paganetti.** 2003. Role of EDEM in the release of misfolded glycoproteins from the calnexin cycle. Science **299:**1397-400.

80. **Christianson, J. C., T. A. Shaler, R. E. Tyler, and R. R. Kopito.** 2008. OS-9 and GRP94 deliver mutant alpha1-antitrypsin to the Hrd1-SEL1L ubiquitin ligase complex for ERAD. Nat Cell Biol **10:**272-82.

81. **Oda, Y., N. Hosokawa, I. Wada, and K. Nagata.** 2003. EDEM as an acceptor of terminally misfolded glycoproteins released from calnexin. Science **299:**1394-7.

82. **Oda, Y., T. Okada, H. Yoshida, R. J. Kaufman, K. Nagata, and K. Mori.** 2006. Derlin-2 and Derlin-3 are regulated by the mammalian unfolded protein response and are required for ER-associated degradation. J Cell Biol **172:**383-93.

83. **Gnann, A., J. R. Riordan, and D. H. Wolf.** 2004. Cystic fibrosis transmembrane conductance regulator degradation depends on the lectins Htm1p/EDEM and the Cdc48 protein complex in yeast. Mol Biol Cell **15:**4125-35.

84. **Kim, W., E. D. Spear, and D. T. Ng.** 2005. Yos9p detects and targets misfolded

glycoproteins for ER-associated degradation. Mol Cell **19:**753-64.

85. **Szathmary, R., R. Bielmann, M. Nita-Lazar, P. Burda, and C. A. Jakob.** 2005. Yos9 protein is essential for degradation of misfolded glycoproteins and may function as lectin in ERAD. Mol Cell **19:**765-75.

86. **Denic, V., E. M. Quan, and J. S. Weissman.** 2006. A luminal surveillance complex that selects misfolded glycoproteins for ER-associated degradation. Cell **126:**349-59.

87. **Tortorella, D., C. M. Story, J. B. Huppa, E. J. Wiertz, T. R. Jones, I. Bacik, J. R. Bennink, J. W. Yewdell, and H. L. Ploegh.** 1998. Dislocation of type I membrane proteins from the ER to the cytosol is sensitive to changes in redox potential. J Cell Biol **142:**365-76.

88. **Fagioli, C., A. Mezghrani, and R. Sitia.** 2001. Reduction of interchain disulfide bonds precedes the dislocation of Ig-mu chains from the endoplasmic reticulum to the cytosol for proteasomal degradation. J Biol Chem **276:**40962-7.

89. **Ng, W., T. Sergeyenko, N. Zeng, J. D. Brown, and K. Romisch.** 2007. Characterization of the proteasome interaction with the Sec61 channel in the endoplasmic reticulum. J Cell Sci **120:**682-91.

90. **Gillece, P., M. Pilon, and K. Romisch.** 2000. The protein translocation channel mediates glycopeptide export across the endoplasmic reticulum membrane. Proc Natl Acad Sci U S A **97:**4609-14.

91. **Jarosch, E., R. Geiss-Friedlander, B. Meusser, J. Walter, and T. Sommer.** 2002. Protein dislocation from the endoplasmic reticulum--pulling out the suspect. Traffic **3:**530-6.

92. **Clemons, W. M., Jr., J. F. Menetret, C. W. Akey, and T. A. Rapoport.** 2004. Structural insight into the protein translocation channel. Curr Opin Struct Biol **14:**390-6.

93. **Lilley, B. N., and H. L. Ploegh.** 2004. A membrane protein required for dislocation of misfolded proteins from the ER. Nature **429:**834-40.

94. **Ye, Y., Y. Shibata, C. Yun, D. Ron, and T. A. Rapoport.** 2004. A membrane protein complex mediates retro-translocation from the ER lumen into the cytosol. Nature **429:**841-7.

95. **Knop, M., A. Finger, T. Braun, K. Hellmuth, and D. H. Wolf.** 1996. Der1, a novel protein specifically required for endoplasmic reticulum degradation in yeast. Embo J **15:**753-63.

96. **Hershko, A., A. Ciechanover, and A. Varshavsky.** 2000. Basic Medical Research Award. The ubiquitin system. Nat Med **6:**1073-81.

97. **McCracken, A. A., and J. L. Brodsky.** 2003. Evolving questions and paradigm shifts in endoplasmic-reticulum-associated degradation (ERAD). Bioessays **25:**868-77.

98. **Glickman, M. H., D. M. Rubin, O. Coux, I. Wefes, G. Pfeifer, Z. Cjeka, W. Baumeister, V. A. Fried, and D. Finley.** 1998. A subcomplex of the proteasome regulatory particle required for ubiquitin-conjugate degradation and related to the COP9-signalosome and eIF3. Cell **94:**615-23.

99. **Misaghi, S., M. E. Pacold, D. Blom, H. L. Ploegh, and G. A. Korbel.** 2004. Using a small molecule inhibitor of peptide: N-glycanase to probe its role in glycoprotein turnover. Chem Biol **11:**1677-87.

100. **Anfinsen, C. B., E. Haber, M. Sela, and F. H. White, Jr.** 1961. The kinetics of formation of native ribonuclease during oxidation of the reduced polypeptide chain. Proc Natl Acad Sci U S A **47:**1309-14.

101. **Marquardt, T., D. N. Hebert, and A. Helenius.** 1993. Post-translational folding of influenza hemagglutinin in isolated endoplasmic reticulum-derived microsomes. J Biol Chem **268:**19618-25.

102. **Wu, C.** 1995. Heat shock transcription factors: structure and regulation. Annu Rev Cell Dev Biol **11:**441-69.

103. **Shen, X., K. Zhang, and R. J. Kaufman.** 2004. The unfolded protein response--a stress signaling pathway of the endoplasmic reticulum. J Chem Neuroanat **28:**79-92.

104. **Gething, M. J., and J. Sambrook.** 1992. Protein folding in the cell. Nature **355:**33-45.

105. **Lee, A. S.** 2001. The glucose-regulated proteins: stress induction and clinical applications. Trends Biochem Sci **26:**504-10.

106. **Shiu, R. P., J. Pouyssegur, and I. Pastan.** 1977. Glucose depletion accounts for the induction of two transformation-sensitive membrane proteinsin Rous sarcoma virus-transformed chick embryo fibroblasts. Proc Natl Acad Sci U S A **74:**3840-4.

107. **Haas, I. G., and M. Wabl.** 1983. Immunoglobulin heavy chain binding protein. Nature **306:**387-9.

108. **Hendershot, L. M.** 2004. The ER function BiP is a master regulator of ER function. Mt Sinai J Med **71:**289-97.

109. **Wada, I., D. Rindress, P. H. Cameron, W. J. Ou, J. J. Doherty, 2nd, D. Louvard, A. W. Bell, D. Dignard, D. Y. Thomas, and J. J. Bergeron.** 1991. SSR alpha and associated calnexin are major calcium binding proteins of the endoplasmic reticulum membrane. J Biol Chem **266:**19599-610.

110. **Fliegel, L., K. Burns, D. H. MacLennan, R. A. Reithmeier, and M. Michalak.** 1989. Molecular cloning of the high affinity calcium-binding protein (calreticulin) of skeletal muscle sarcoplasmic reticulum. J Biol Chem **264:**21522-8.

111. **Ma, Y., and L. M. Hendershot.** 2004. ER chaperone functions during normal and stress conditions. J Chem Neuroanat **28:**51-65.

112. **Molinari, M., C. Galli, V. Piccaluga, M. Pieren, and P. Paganetti.** 2002. Sequential assistance of molecular chaperones and transient formation of covalent complexes during protein degradation from the ER. J Cell Biol **158:**247-57.

113. **Mayer, M., U. Kies, R. Kammermeier, and J. Buchner.** 2000. BiP and PDI cooperate in the oxidative folding of antibodies in vitro. J Biol Chem **275:**29421-5.

114. **Frickel, E. M., R. Riek, I. Jelesarov, A. Helenius, K. Wuthrich, and L. Ellgaard.** 2002. TROSY-NMR reveals interaction between ERp57 and the tip of the calreticulin P-domain. Proc Natl Acad Sci U S A **99:**1954-9.

115. **Pollock, S., G. Kozlov, M. F. Pelletier, J. F. Trempe, G. Jansen, D. Sitnikov, J. J. Bergeron, K. Gehring, I. Ekiel, and D. Y. Thomas.** 2004. Specific interaction of ERp57 and calnexin determined by NMR spectroscopy and an ER two-hybrid system. Embo J **23:**1020-9.

116. **Breakefield, X. O., C. Kamm, and P. I. Hanson.** 2001. TorsinA: movement at many levels. Neuron **31:**9-12.

117. **McLean, P. J., H. Kawamata, S. Shariff, J. Hewett, N. Sharma, K. Ueda, X. O. Breakefield, and B. T. Hyman.** 2002. TorsinA and heat shock proteins act as molecular chaperones: suppression of alpha-synuclein aggregation. J Neurochem **83:**846-54.

118. **Argon, Y., and B. B. Simen.** 1999. GRP94, an ER chaperone with protein and peptide binding properties. Semin Cell Dev Biol **10:**495-505.

119. **Rose, M. D., L. M. Misra, and J. P. Vogel.** 1989. KAR2, a karyogamy gene, is the yeast homolog of the mammalian BiP/GRP78 gene. Cell **57:**1211-21.

120. **Chevalier, M., H. Rhee, E. C. Elguindi, and S. Y. Blond.** 2000. Interaction of murine BiP/GRP78 with the DnaJ homologue MTJ1. J Biol Chem **275:**19620-7.

121. **Skowronek, M. H., M. Rotter, and I. G. Haas.** 1999. Molecular characterization of a novel mammalian DnaJ-like Sec63p homolog. Biol Chem **380:**1133-8.

122. **Bies, C., R. Blum, J. Dudek, W. Nastainczyk, S. Oberhauser, M. Jung, and R. Zimmermann.** 2004. Characterization of pancreatic ERj3p, a homolog of yeast DnaJ-like protein Scj1p. Biol Chem **385:**389-95.

123. **Shen, Y., L. Meunier, and L. M. Hendershot.** 2002. Identification and characterization of a novel endoplasmic reticulum (ER) DnaJ homologue, which stimulates ATPase activity of BiP in vitro and is induced by ER stress. J Biol Chem **277:**15947-56.

124. **Cunnea, P. M., A. Miranda-Vizuete, G. Bertoli, T. Simmen, A. E. Damdimopoulos, S. Hermann, S. Leinonen, M. P. Huikko, J. A. Gustafsson, R. Sitia, and G. Spyrou.**

2003. ERdj5, an endoplasmic reticulum (ER)-resident protein containing DnaJ and thioredoxin domains, is expressed in secretory cells or following ER stress. J Biol Chem **278:**1059-66.

125. **Feldheim, D., J. Rothblatt, and R. Schekman.** 1992. Topology and functional domains of Sec63p, an endoplasmic reticulum membrane protein required for secretory protein translocation. Mol Cell Biol **12:**3288-96.

126. **Schlenstedt, G., S. Harris, B. Risse, R. Lill, and P. A. Silver.** 1995. A yeast DnaJ homologue, Scj1p, can function in the endoplasmic reticulum with BiP/Kar2p via a conserved domain that specifies interactions with Hsp70s. J Cell Biol **129:**979-88.

127. **Nishikawa, S., and T. Endo.** 1997. The yeast JEM1p is a DnaJ-like protein of the endoplasmic reticulum membrane required for nuclear fusion. J Biol Chem **272:**12889-92.

128. **Chung, K. T., Y. Shen, and L. M. Hendershot.** 2002. BAP, a mammalian BiP-associated protein, is a nucleotide exchange factor that regulates the ATPase activity of BiP. J Biol Chem **277:**47557-63.

129. **Boisrame, A., M. Kabani, J. M. Beckerich, E. Hartmann, and C. Gaillardin.** 1998. Interaction of Kar2p and Sls1p is required for efficient co-translational translocation of secreted proteins in the yeast Yarrowia lipolytica. J Biol Chem **273:**30903-8.

130. **Ou, W. J., P. H. Cameron, D. Y. Thomas, and J. J. Bergeron.** 1993. Association of folding intermediates of glycoproteins with calnexin during protein maturation. Nature **364:**771-6.

131. **Parlati, F., M. Dominguez, J. J. Bergeron, and D. Y. Thomas.** 1995. Saccharomyces cerevisiae CNE1 encodes an endoplasmic reticulum (ER) membrane protein with sequence similarity to calnexin and calreticulin and functions as a constituent of the ER quality control apparatus. J Biol Chem **270:**244-53.

132. **Peterson, J. R., A. Ora, P. N. Van, and A. Helenius.** 1995. Transient, lectin-like association of calreticulin with folding intermediates of cellular and viral glycoproteins. Mol Biol Cell **6:**1173-84.

133. **Herscovics, A.** 1999. Importance of glycosidases in mammalian glycoprotein biosynthesis. Biochim Biophys Acta **1473:**96-107.

134. **Kilker, R. D., Jr., B. Saunier, J. S. Tkacz, and A. Herscovics.** 1981. Partial purification from Saccharomyces cerevisiae of a soluble glucosidase which removes the terminal glucose from the oligosaccharide Glc3Man9GlcNAc2. J Biol Chem **256:**5299-5303.

135. **Deprez, P., M. Gautschi, and A. Helenius.** 2005. More than one glycan is needed for ER glucosidase II to allow entry of glycoproteins into the calnexin/calreticulin cycle. Mol Cell **19:**183-95.

136. **Trombetta, E. S., J. F. Simons, and A. Helenius.** 1996. Endoplasmic reticulum glucosidase II is composed of a catalytic subunit, conserved from yeast to mammals, and a tightly bound noncatalytic HDEL-containing subunit. J Biol Chem **271:**27509-16.

137. **Jakob, C. A., P. Burda, J. Roth, and M. Aebi.** 1998. Degradation of misfolded endoplasmic reticulum glycoproteins in Saccharomyces cerevisiae is determined by a specific oligosaccharide structure. J Cell Biol **142:**1223-33.

138. **Jakob, C. A., D. Bodmer, U. Spirig, P. Battig, A. Marcil, D. Dignard, J. J. Bergeron, D. Y. Thomas, and M. Aebi.** 2001. Htm1p, a mannosidase-like protein, is involved in glycoprotein degradation in yeast. EMBO Rep **2:**423-30.

139. **Caramelo, J. J., O. A. Castro, L. G. Alonso, G. De Prat-Gay, and A. J. Parodi.** 2003. UDP-Glc:glycoprotein glucosyltransferase recognizes structured and solvent accessible hydrophobic patches in molten globule-like folding intermediates. Proc Natl Acad Sci U S A **100:**86-91.

140. **Levinson, J. N., S. Shahinian, A. M. Sdicu, D. C. Tessier, and H. Bussey.** 2002. Functional, comparative and cell biological analysis of Saccharomyces cerevisiae Kre5p. Yeast **19:**1243-59.

141. **Creighton, T. E., D. A. Hillson, and R. B. Freedman.** 1980. Catalysis by protein-disulphide isomerase of the unfolding and

refolding of proteins with disulphide bonds. J Mol Biol **142:**43-62.

142. **Mizunaga, T., Y. Katakura, T. Miura, and Y. Maruyama.** 1990. Purification and characterization of yeast protein disulfide isomerase. J Biochem **108:**846-51.

143. **Oliver, J. D., H. L. Roderick, D. H. Llewellyn, and S. High.** 1999. ERp57 functions as a subunit of specific complexes formed with the ER lectins calreticulin and calnexin. Mol Biol Cell **10:**2573-82.

144. **Satoh, M., A. Shimada, H. Keino, A. Kashiwai, N. Nagai, S. Saga, and M. Hosokawa.** 2005. Functional characterization of 3 thioredoxin homology domains of ERp72. Cell Stress Chaperones **10:**278-84.

145. **Bose, S., M. Mucke, and R. B. Freedman.** 1994. The characterization of a cyclophilin-type peptidyl prolyl cis-trans-isomerase from the endoplasmic-reticulum lumen. Biochem J **300 (Pt 3):**871-5.

146. **Frigerio, G., and H. R. Pelham.** 1993. A Saccharomyces cerevisiae cyclophilin resident in the endoplasmic reticulum. J Mol Biol **233:**183-8.

147. **Bush, K. T., B. A. Hendrickson, and S. K. Nigam.** 1994. Induction of the FK506-binding protein, FKBP13, under conditions which misfold proteins in the endoplasmic reticulum. Biochem J **303 (Pt 3):**705-8.

148. **Nielsen, J. B., F. Foor, J. J. Siekierka, M. J. Hsu, N. Ramadan, N. Morin, A. Shafiee, A. M. Dahl, L. Brizuela, G. Chrebet, and et al.** 1992. Yeast FKBP-13 is a membrane-associated FK506-binding protein encoded by the nonessential gene FKB2. Proc Natl Acad Sci U S A **89:**7471-5.

149. **Braakman, I., J. Helenius, and A. Helenius.** 1992. Manipulating disulfide bond formation and protein folding in the endoplasmic reticulum. Embo J **11:**1717-22.

150. **Ellgaard, L., and L. W. Ruddock.** 2005. The human protein disulphide isomerase family: substrate interactions and functional properties. EMBO Rep **6:**28-32.

151. **Bies, C., S. Guth, K. Janoschek, W. Nastainczyk, J. Volkmer, and R. Zimmermann.** 1999. A Scj1p homolog and folding catalysts present in dog pancreas microsomes. Biol Chem **380:**1175-82.

152. **Goldberger, R. F., C. J. Epstein, and C. B. Anfinsen.** 1964. Purification and Properties of a Microsomal Enzyme System Catalyzing the Reactivation of Reduced Ribonuclease and Lysozyme. J Biol Chem **239:**1406-10.

153. **Alanen, H. I., K. E. Salo, M. Pekkala, H. M. Siekkinen, A. Pirneskoski, and L. W. Ruddock.** 2003. Defining the domain boundaries of the human protein disulfide isomerases. Antioxid Redox Signal **5:**367-74.

154. **Macer, D. R., and G. L. Koch.** 1988. Identification of a set of calcium-binding proteins in reticuloplasm, the luminal content of the endoplasmic reticulum. J Cell Sci **91 (Pt 1):**61-70.

155. **Tian, G., S. Xiang, R. Noiva, W. J. Lennarz, and H. Schindelin.** 2006. The crystal structure of yeast protein disulfide isomerase suggests cooperativity between its active sites. Cell **124:**61-73.

156. **Klappa, P., L. W. Ruddock, N. J. Darby, and R. B. Freedman.** 1998. The b' domain provides the principal peptide-binding site of protein disulfide isomerase but all domains contribute to binding of misfolded proteins. Embo J **17:**927-35.

157. **Denisov, A. Y., P. Maattanen, C. Dabrowski, G. Kozlov, D. Y. Thomas, and K. Gehring.** 2009. Solution structure of the bb' domains of human protein disulfide isomerase. Febs J **276:**1440-9.

158. **Frand, A. R., and C. A. Kaiser.** 1999. Ero1p oxidizes protein disulfide isomerase in a pathway for disulfide bond formation in the endoplasmic reticulum. Mol Cell **4:**469-77.

159. **Kersteen, E. A., S. R. Barrows, and R. T. Raines.** 2005. Catalysis of protein disulfide bond isomerization in a homogeneous substrate. Biochemistry **44:**12168-78.

160. **Schwaller, M., B. Wilkinson, and H. F. Gilbert.** 2003. Reduction-reoxidation cycles contribute to catalysis of disulfide isomerization by protein-disulfide isomerase. J Biol Chem **278:**7154-9.

161. **Darby, N. J., and T. E. Creighton.** 1995. Functional properties of the individual thioredoxin-like domains of protein disulfide isomerase. Biochemistry **34:**11725-35.

162. **Darby, N. J., E. Penka, and R. Vincentelli.** 1998. The multi-domain structure of protein disulfide isomerase is essential for high catalytic efficiency. J Mol Biol **276:**239-47.

163. **LaMantia, M. L., and W. J. Lennarz.** 1993. The essential function of yeast protein disulfide isomerase does not reside in its isomerase activity. Cell **74:**899-908.

164. **Laboissiere, M. C., S. L. Sturley, and R. T. Raines.** 1997. Protein disulfide isomerase in spore germination and cell division. Biol Chem **378:**431-7.

165. **Solovyov, A., R. Xiao, and H. F. Gilbert.** 2004. Sulfhydryl oxidation, not disulfide isomerization, is the principal function of protein disulfide isomerase in yeast Saccharomyces cerevisiae. J Biol Chem **279:**34095-100.

166. **Cai, H., C. C. Wang, and C. L. Tsou.** 1994. Chaperone-like activity of protein disulfide isomerase in the refolding of a protein with no disulfide bonds. J Biol Chem **269:**24550-2.

167. **Song, J. L., and C. C. Wang.** 1995. Chaperone-like activity of protein disulfide-isomerase in the refolding of rhodanese. Eur J Biochem **231:**312-6.

168. **Quan, H., G. Fan, and C. C. Wang.** 1995. Independence of the chaperone activity of protein disulfide isomerase from its thioredoxin-like active site. J Biol Chem **270:**17078-80.

169. **Lumb, R. A., and N. J. Bulleid.** 2002. Is protein disulfide isomerase a redox-dependent molecular chaperone? Embo J **21:**6763-70.

170. **Puig, A., and H. F. Gilbert.** 1994. Protein disulfide isomerase exhibits chaperone and anti-chaperone activity in the oxidative refolding of lysozyme. J Biol Chem **269:**7764-71.

171. **Shusta, E. V., R. T. Raines, A. Pluckthun, and K. D. Wittrup.** 1998. Increasing the secretory capacity of Saccharomyces cerevisiae for production of single-chain antibody fragments. Nat Biotechnol **16:**773-7.

172. **Ferrari, D. M., and H. D. Soling.** 1999. The protein disulphide-isomerase family: unravelling a string of folds. Biochem J **339 (Pt 1):**1-10.

173. **Antoniou, A. N., S. Ford, M. Alphey, A. Osborne, T. Elliott, and S. J. Powis.** 2002. The oxidoreductase ERp57 efficiently reduces partially folded in preference to fully folded MHC class I molecules. Embo J **21:**2655-63.

174. **Frickel, E. M., P. Frei, M. Bouvier, W. F. Stafford, A. Helenius, R. Glockshuber, and L. Ellgaard.** 2004. ERp57 is a multifunctional thiol-disulfide oxidoreductase. J Biol Chem **279:**18277-87.

175. **Oliver, J. D., F. J. van der Wal, N. J. Bulleid, and S. High.** 1997. Interaction of the thiol-dependent reductase ERp57 with nascent glycoproteins. Science **275:**86-8.

176. **Bourdi, M., D. Demady, J. L. Martin, S. K. Jabbour, B. M. Martin, J. W. George, and L. R. Pohl.** 1995. cDNA cloning and baculovirus expression of the human liver endoplasmic reticulum P58: characterization as a protein disulfide isomerase isoform, but not as a protease or a carnitine acyltransferase. Arch Biochem Biophys **323:**397-403.

177. **Hirano, N., F. Shibasaki, R. Sakai, T. Tanaka, J. Nishida, Y. Yazaki, T. Takenawa, and H. Hirai.** 1995. Molecular cloning of the human glucose-regulated protein ERp57/GRP58, a thiol-dependent reductase. Identification of its secretory form and inducible expression by the oncogenic transformation. Eur J Biochem **234:**336-42.

178. **Srivastava, S. P., N. Q. Chen, Y. X. Liu, and J. L. Holtzman.** 1991. Purification and characterization of a new isozyme of thiol:protein-disulfide oxidoreductase from rat hepatic microsomes. Relationship of this isozyme to cytosolic phosphatidylinositol-specific phospholipase C form 1A. J Biol Chem **266:**20337-44.

179. **Jessop, C. E., S. Chakravarthi, N. Garbi, G. J. Hammerling, S. Lovell, and N. J. Bulleid.** 2007. ERp57 is essential for efficient folding of glycoproteins sharing

common structural domains. Embo J **26:**28-40.

180. **Solda, T., N. Garbi, G. J. Hammerling, and M. Molinari.** 2006. Consequences of ERp57 deletion on oxidative folding of obligate and facultative clients of the calnexin cycle. J Biol Chem **281:**6219-26.

181. **Zapun, A., N. J. Darby, D. C. Tessier, M. Michalak, J. J. Bergeron, and D. Y. Thomas.** 1998. Enhanced catalysis of ribonuclease B folding by the interaction of calnexin or calreticulin with ERp57. J Biol Chem **273:**6009-12.

182. **Jessop, C. E., T. J. Tavender, R. H. Watkins, J. E. Chambers, and N. J. Bulleid.** 2009. Substrate specificity of the oxidoreductase ERp57 is determined primarily by its interaction with calnexin and calreticulin. J Biol Chem **284:**2194-202.

183. **Pirneskoski, A., P. Klappa, M. Lobell, R. A. Williamson, L. Byrne, H. I. Alanen, K. E. Salo, K. I. Kivirikko, R. B. Freedman, and L. W. Ruddock.** 2004. Molecular characterization of the principal substrate binding site of the ubiquitous folding catalyst protein disulfide isomerase. J Biol Chem **279:**10374-81.

184. **Kozlov, G., P. Maattanen, J. D. Schrag, S. Pollock, M. Cygler, B. Nagar, D. Y. Thomas, and K. Gehring.** 2006. Crystal structure of the bb' domains of the protein disulfide isomerase ERp57. Structure **14:**1331-9.

185. **Russell, S. J., L. W. Ruddock, K. E. Salo, J. D. Oliver, Q. P. Roebuck, D. H. Llewellyn, H. L. Roderick, P. Koivunen, J. Myllyharju, and S. High.** 2004. The primary substrate binding site in the b' domain of ERp57 is adapted for endoplasmic reticulum lectin association. J Biol Chem **279:**18861-9.

186. **Peaper, D. R., P. A. Wearsch, and P. Cresswell.** 2005. Tapasin and ERp57 form a stable disulfide-linked dimer within the MHC class I peptide-loading complex. Embo J **24:**3613-23.

187. **Zhang, Y., G. Kozlov, C. L. Pocanschi, U. Brockmeier, B. S. Ireland, P. Maattanen, C. Howe, T. Elliott, K. Gehring, and D. B. Williams.** 2009. ERp57 does not require interactions with calnexin and calreticulin to promote assembly of class I histocompatibility molecules and it enhances peptide loading independently of its redox activity. J Biol Chem **284:**10160-73.

188. **Zhang, Y., E. Baig, and D. B. Williams.** 2006. Functions of ERp57 in the folding and assembly of major histocompatibility complex class I molecules. J Biol Chem **281:**14622-31.

189. **Dick, T. P., N. Bangia, D. R. Peaper, and P. Cresswell.** 2002. Disulfide bond isomerization and the assembly of MHC class I-peptide complexes. Immunity **16:**87-98.

190. **Dong, G., P. A. Wearsch, D. R. Peaper, P. Cresswell, and K. M. Reinisch.** 2009. Insights into MHC class I peptide loading from the structure of the tapasin-ERp57 thiol oxidoreductase heterodimer. Immunity **30:**21-32.

191. **Li, Y., and P. Camacho.** 2004. Ca2+-dependent redox modulation of SERCA 2b by ERp57. J Cell Biol **164:**35-46.

192. **Altieri, F., B. Maras, M. Eufemi, A. Ferraro, and C. Turano.** 1993. Purification of a 57kDa nuclear matrix protein associated with thiol:protein-disulfide oxidoreductase and phospholipase C activities. Biochem Biophys Res Commun **194:**992-1000.

193. **Gerner, C., K. Holzmann, M. Meissner, J. Gotzmann, R. Grimm, and G. Sauermann.** 1999. Reassembling proteins and chaperones in human nuclear matrix protein fractions. J Cell Biochem **74:**145-51.

194. **Ohtani, H., H. Wakui, T. Ishino, A. Komatsuda, and A. B. Miura.** 1993. An isoform of protein disulfide isomerase is expressed in the developing acrosome of spermatids during rat spermiogenesis and is transported into the nucleus of mature spermatids and epididymal spermatozoa. Histochemistry **100:**423-9.

195. **Coppari, S., F. Altieri, A. Ferraro, S. Chichiarelli, M. Eufemi, and C. Turano.** 2002. Nuclear localization and DNA interaction of protein disulfide isomerase ERp57 in mammalian cells. J Cell Biochem **85:**325-33.

196. **Lim, V. I., and A. S. Spirin.** 1986. Stereochemical analysis of ribosomal

transpeptidation. Conformation of nascent peptide. J Mol Biol **188:**565-74.

197. **Scherer, G., M. L. Kramer, M. Schutkowski, U. Reimer, and G. Fischer.** 1998. Barriers to rotation of secondary amide peptide bonds. J Am Chem Soc **120:**5568-5574.

198. **Stein, R. L.** 1993. Mechanism of enzymatic and nonenzymatic prolyl cis-trans isomerization. Adv Protein Chem **44:**1-24.

199. **Reimer, U., G. Scherer, M. Drewello, S. Kruber, M. Schutkowski, and G. Fischer.** 1998. Side-chain effects on peptidyl-prolyl cis/trans isomerisation. J Mol Biol **279:**449-60.

200. **Kiefhaber, T., R. Quaas, U. Hahn, and F. X. Schmid.** 1990. Folding of ribonuclease T1. 2. Kinetic models for the folding and unfolding reactions. Biochemistry **29:**3061-70.

201. **Fischer, G., H. Bang, and C. Mech.** 1984. [Determination of enzymatic catalysis for the cis-trans-isomerization of peptide binding in proline-containing peptides]. Biomed Biochim Acta **43:**1101-11.

202. **Fischer, G., B. Wittmann-Liebold, K. Lang, T. Kiefhaber, and F. X. Schmid.** 1989. Cyclophilin and peptidyl-prolyl cis-trans isomerase are probably identical proteins. Nature **337:**476-8.

203. **Gothel, S. F., and M. A. Marahiel.** 1999. Peptidyl-prolyl cis-trans isomerases, a superfamily of ubiquitous folding catalysts. Cell Mol Life Sci **55:**423-36.

204. **Schiene-Fischer, C., and C. Yu.** 2001. Receptor accessory folding helper enzymes: the functional role of peptidyl prolyl cis/trans isomerases. FEBS Lett **495:**1-6.

205. **Zhang, X., Y. Wang, H. Li, W. Zhang, D. Wu, and H. Mi.** 2004. The mouse FKBP23 binds to BiP in ER and the binding of C-terminal domain is interrelated with Ca2+ concentration. FEBS Lett **559:**57-60.

206. **Davis, E. C., T. J. Broekelmann, Y. Ozawa, and R. P. Mecham.** 1998. Identification of tropoelastin as a ligand for the 65-kD FK506-binding protein, FKBP65, in the secretory pathway. J Cell Biol **140:**295-303.

207. **Meunier, L., Y. K. Usherwood, K. T. Chung, and L. M. Hendershot.** 2002. A subset of chaperones and folding enzymes form multiprotein complexes in endoplasmic reticulum to bind nascent proteins. Mol Biol Cell **13:**4456-69.

208. **Zhang, J., and H. Herscovitz.** 2003. Nascent lipidated apolipoprotein B is transported to the Golgi as an incompletely folded intermediate as probed by its association with network of endoplasmic reticulum molecular chaperones, GRP94, ERp72, BiP, calreticulin, and cyclophilin B. J Biol Chem **278:**7459-68.

209. **Smith, T., L. R. Ferreira, C. Hebert, K. Norris, and J. J. Sauk.** 1995. Hsp47 and cyclophilin B traverse the endoplasmic reticulum with procollagen into pre-Golgi intermediate vesicles. A role for Hsp47 and cyclophilin B in the export of procollagen from the endoplasmic reticulum. J Biol Chem **270:**18323-8.

210. **Endrich, M. M., P. Gehrig, and H. Gehring.** 1999. Maturation-induced conformational changes of HIV-1 capsid protein and identification of two high affinity sites for cyclophilins in the C-terminal domain. J Biol Chem **274:**5326-32.

211. **Luban, J., K. L. Bossolt, E. K. Franke, G. V. Kalpana, and S. P. Goff.** 1993. Human immunodeficiency virus type 1 Gag protein binds to cyclophilins A and B. Cell **73:**1067-78.

212. **Wang, Y., R. Han, D. Wu, J. Li, C. Chen, H. Ma, and H. Mi.** 2007. The binding of FKBP23 to BiP modulates BiP's ATPase activity with its PPIase activity. Biochem Biophys Res Commun **354:**315-20.

213. **Dolinski, K., S. Muir, M. Cardenas, and J. Heitman.** 1997. All cyclophilins and FK506 binding proteins are, individually and collectively, dispensable for viability in Saccharomyces cerevisiae. Proc Natl Acad Sci U S A **94:**13093-8.

214. **Haas, I. G., and T. Meo.** 1988. cDNA cloning of the immunoglobulin heavy chain binding protein. Proc Natl Acad Sci U S A **85:**2250-4.

215. **Simons, J. F., S. Ferro-Novick, M. D. Rose, and A. Helenius.** 1995. BiP/Kar2p serves as a molecular chaperone during

carboxypeptidase Y folding in yeast. J Cell Biol **130:**41-9.

216. **Munro, S., and H. R. Pelham.** 1986. An Hsp70-like protein in the ER: identity with the 78 kd glucose-regulated protein and immunoglobulin heavy chain binding protein. Cell **46:**291-300.

217. **Bukau, B., J. Weissman, and A. Horwich.** 2006. Molecular chaperones and protein quality control. Cell **125:**443-51.

218. **Flynn, G. C., J. Pohl, M. T. Flocco, and J. E. Rothman.** 1991. Peptide-binding specificity of the molecular chaperone BiP. Nature **353:**726-30.

219. **Blond-Elguindi, S., S. E. Cwirla, W. J. Dower, R. J. Lipshutz, S. R. Sprang, J. F. Sambrook, and M. J. Gething.** 1993. Affinity panning of a library of peptides displayed on bacteriophages reveals the binding specificity of BiP. Cell **75:**717-28.

220. **Rudiger, S., A. Buchberger, and B. Bukau.** 1997. Interaction of Hsp70 chaperones with substrates. Nat Struct Biol **4:**342-9.

221. **Bukau, B., and A. L. Horwich.** 1998. The Hsp70 and Hsp60 chaperone machines. Cell **92:**351-66.

222. **Morshauser, R. C., H. Wang, G. C. Flynn, and E. R. Zuiderweg.** 1995. The peptide-binding domain of the chaperone protein Hsc70 has an unusual secondary structure topology. Biochemistry **34:**6261-6.

223. **Zhu, X., X. Zhao, W. F. Burkholder, A. Gragerov, C. M. Ogata, M. E. Gottesman, and W. A. Hendrickson.** 1996. Structural analysis of substrate binding by the molecular chaperone DnaK. Science **272:**1606-14.

224. **McCarty, J. S., A. Buchberger, J. Reinstein, and B. Bukau.** 1995. The role of ATP in the functional cycle of the DnaK chaperone system. J Mol Biol **249:**126-37.

225. **Flaherty, K. M., C. DeLuca-Flaherty, and D. B. McKay.** 1990. Three-dimensional structure of the ATPase fragment of a 70K heat-shock cognate protein. Nature **346:**623-8.

226. **Szabo, A., T. Langer, H. Schroder, J. Flanagan, B. Bukau, and F. U. Hartl.** 1994. The ATP hydrolysis-dependent reaction cycle of the Escherichia coli Hsp70 system DnaK, DnaJ, and GrpE. Proc Natl Acad Sci U S A **91:**10345-9.

227. **Weitzmann, A., J. Volkmer, and R. Zimmermann.** 2006. The nucleotide exchange factor activity of Grp170 may explain the non-lethal phenotype of loss of Sil1 function in man and mouse. FEBS Lett **580:**5237-40.

228. **Zhao, L., C. Longo-Guess, B. S. Harris, J. W. Lee, and S. L. Ackerman.** 2005. Protein accumulation and neurodegeneration in the woozy mutant mouse is caused by disruption of SIL1, a cochaperone of BiP. Nat Genet **37:**974-9.

229. **Awad, W., I. Estrada, Y. Shen, and L. M. Hendershot.** 2008. BiP mutants that are unable to interact with endoplasmic reticulum DnaJ proteins provide insights into interdomain interactions in BiP. Proc Natl Acad Sci U S A **105:**1164-9.

230. **Cheetham, M. E., and A. J. Caplan.** 1998. Structure, function and evolution of DnaJ: conservation and adaptation of chaperone function. Cell Stress Chaperones **3:**28-36.

231. **Misselwitz, B., O. Staeck, and T. A. Rapoport.** 1998. J proteins catalytically activate Hsp70 molecules to trap a wide range of peptide sequences. Mol Cell **2:**593-603.

232. **Van den Berg, B., W. M. Clemons, Jr., I. Collinson, Y. Modis, E. Hartmann, S. C. Harrison, and T. A. Rapoport.** 2004. X-ray structure of a protein-conducting channel. Nature **427:**36-44.

233. **Hamman, B. D., L. M. Hendershot, and A. E. Johnson.** 1998. BiP maintains the permeability barrier of the ER membrane by sealing the lumenal end of the translocon pore before and early in translocation. Cell **92:**747-58.

234. **Corsi, A. K., and R. Schekman.** 1997. The lumenal domain of Sec63p stimulates the ATPase activity of BiP and mediates BiP recruitment to the translocon in Saccharomyces cerevisiae. J Cell Biol **137:**1483-93.

235. **Lievremont, J. P., R. Rizzuto, L. Hendershot, and J. Meldolesi.** 1997. BiP, a major chaperone protein of the

endoplasmic reticulum lumen, plays a direct and important role in the storage of the rapidly exchanging pool of Ca2+. J Biol Chem **272:**30873-9.

236. **Cabral, C. M., Y. Liu, K. W. Moremen, and R. N. Sifers.** 2002. Organizational diversity among distinct glycoprotein endoplasmic reticulum-associated degradation programs. Mol Biol Cell **13:**2639-50.

237. **Kabani, M., S. S. Kelley, M. W. Morrow, D. L. Montgomery, R. Sivendran, M. D. Rose, L. M. Gierasch, and J. L. Brodsky.** 2003. Dependence of endoplasmic reticulum-associated degradation on the peptide binding domain and concentration of BiP. Mol Biol Cell **14:**3437-48.

238. **Sorgjerd, K., B. Ghafouri, B. H. Jonsson, J. W. Kelly, S. Y. Blond, and P. Hammarstrom.** 2006. Retention of misfolded mutant transthyretin by the chaperone BiP/GRP78 mitigates amyloidogenesis. J Mol Biol **356:**469-82.

239. **Luo, S., C. Mao, B. Lee, and A. S. Lee.** 2006. GRP78/BiP is required for cell proliferation and protecting the inner cell mass from apoptosis during early mouse embryonic development. Mol Cell Biol **26:**5688-97.

240. **Schroder, M., and R. J. Kaufman.** 2005. The mammalian unfolded protein response. Annu Rev Biochem **74:**739-89.

241. **Koch, G., M. Smith, D. Macer, P. Webster, and R. Mortara.** 1986. Endoplasmic reticulum contains a common, abundant calcium-binding glycoprotein, endoplasmin. J Cell Sci **86:**217-32.

242. **Melnick, J., J. L. Dul, and Y. Argon.** 1994. Sequential interaction of the chaperones BiP and GRP94 with immunoglobulin chains in the endoplasmic reticulum. Nature **370:**373-5.

243. **Schaiff, W. T., K. A. Hruska, Jr., D. W. McCourt, M. Green, and B. D. Schwartz.** 1992. HLA-DR associates with specific stress proteins and is retained in the endoplasmic reticulum in invariant chain negative cells. J Exp Med **176:**657-66.

244. **Kim, P. S., and P. Arvan.** 1995. Calnexin and BiP act as sequential molecular chaperones during thyroglobulin folding in the endoplasmic reticulum. J Cell Biol **128:**29-38.

245. **Muresan, Z., and P. Arvan.** 1997. Thyroglobulin transport along the secretory pathway. Investigation of the role of molecular chaperone, GRP94, in protein export from the endoplasmic reticulum. J Biol Chem **272:**26095-102.

246. **Ferreira, L. R., K. Norris, T. Smith, C. Hebert, and J. J. Sauk.** 1994. Association of Hsp47, Grp78, and Grp94 with procollagen supports the successive or coupled action of molecular chaperones. J Cell Biochem **56:**518-26.

247. **Soldano, K. L., A. Jivan, C. V. Nicchitta, and D. T. Gewirth.** 2003. Structure of the N-terminal domain of GRP94. Basis for ligand specificity and regulation. J Biol Chem **278:**48330-8.

248. **Yamada, S., T. Ono, A. Mizuno, and T. K. Nemoto.** 2003. A hydrophobic segment within the C-terminal domain is essential for both client-binding and dimer formation of the HSP90-family molecular chaperone. Eur J Biochem **270:**146-54.

249. **Prodromou, C., S. M. Roe, R. O'Brien, J. E. Ladbury, P. W. Piper, and L. H. Pearl.** 1997. Identification and structural characterization of the ATP/ADP-binding site in the Hsp90 molecular chaperone. Cell **90:**65-75.

250. **Richter, K., P. Muschler, O. Hainzl, and J. Buchner.** 2001. Coordinated ATP hydrolysis by the Hsp90 dimer. J Biol Chem **276:**33689-96.

251. **Panaretou, B., C. Prodromou, S. M. Roe, R. O'Brien, J. E. Ladbury, P. W. Piper, and L. H. Pearl.** 1998. ATP binding and hydrolysis are essential to the function of the Hsp90 molecular chaperone in vivo. Embo J **17:**4829-36.

252. **Ali, M. M., S. M. Roe, C. K. Vaughan, P. Meyer, B. Panaretou, P. W. Piper, C. Prodromou, and L. H. Pearl.** 2006. Crystal structure of an Hsp90-nucleotide-p23/Sba1 closed chaperone complex. Nature **440:**1013-7.

253. **Richter, K., S. Moser, F. Hagn, R. Friedrich, O. Hainzl, M. Heller, S. Schlee, H. Kessler, J. Reinstein, and J. Buchner.** 2006. Intrinsic inhibition of the

Hsp90 ATPase activity. J Biol Chem **281:**11301-11.

254. **Weikl, T., P. Muschler, K. Richter, T. Veit, J. Reinstein, and J. Buchner.** 2000. C-terminal regions of Hsp90 are important for trapping the nucleotide during the ATPase cycle. J Mol Biol **303:**583-92.

255. **Richter, K., S. Walter, and J. Buchner.** 2004. The Co-chaperone Sba1 connects the ATPase reaction of Hsp90 to the progression of the chaperone cycle. J Mol Biol **342:**1403-13.

256. **Meyer, P., C. Prodromou, C. Liao, B. Hu, S. M. Roe, C. K. Vaughan, I. Vlasic, B. Panaretou, P. W. Piper, and L. H. Pearl.** 2004. Structural basis for recruitment of the ATPase activator Aha1 to the Hsp90 chaperone machinery. Embo J **23:**1402-10.

257. **Siligardi, G., B. Panaretou, P. Meyer, S. Singh, D. N. Woolfson, P. W. Piper, L. H. Pearl, and C. Prodromou.** 2002. Regulation of Hsp90 ATPase activity by the co-chaperone Cdc37p/p50cdc37. J Biol Chem **277:**20151-9.

258. **Scheufler, C., A. Brinker, G. Bourenkov, S. Pegoraro, L. Moroder, H. Bartunik, F. U. Hartl, and I. Moarefi.** 2000. Structure of TPR domain-peptide complexes: critical elements in the assembly of the Hsp70-Hsp90 multichaperone machine. Cell **101:**199-210.

259. **Smith, D. F., W. P. Sullivan, T. N. Marion, K. Zaitsu, B. Madden, D. J. McCormick, and D. O. Toft.** 1993. Identification of a 60-kilodalton stress-related protein, p60, which interacts with hsp90 and hsp70. Mol Cell Biol **13:**869-76.

260. **Richter, K., B. Meinlschmidt, and J. Buchner.** 2005. p. 768-829. *In* J. Buchner and T. Kiefhaber (ed.), Protein Folding Handbook Wiley-VCH Verlag GmbH & Co., Weinheim, Germany.

261. **Dollins, D. E., J. J. Warren, R. M. Immormino, and D. T. Gewirth.** 2007. Structures of GRP94-nucleotide complexes reveal mechanistic differences between the hsp90 chaperones. Mol Cell **28:**41-56.

262. **Frey, S., A. Leskovar, J. Reinstein, and J. Buchner.** 2007. The ATPase cycle of the endoplasmic chaperone Grp94. J Biol Chem **282:**35612-20.

263. **Scheibel, T., T. Weikl, and J. Buchner.** 1998. Two chaperone sites in Hsp90 differing in substrate specificity and ATP dependence. Proc Natl Acad Sci U S A **95:**1495-9.

264. **Young, J. C., C. Schneider, and F. U. Hartl.** 1997. In vitro evidence that hsp90 contains two independent chaperone sites. FEBS Lett **418:**139-43.

265. **Vaughan, C. K., U. Gohlke, F. Sobott, V. M. Good, M. M. Ali, C. Prodromou, C. V. Robinson, H. R. Saibil, and L. H. Pearl.** 2006. Structure of an Hsp90-Cdc37-Cdk4 complex. Mol Cell **23:**697-707.

266. **Gidalevitz, T., C. Biswas, H. Ding, D. Schneidman-Duhovny, H. J. Wolfson, F. Stevens, S. Radford, and Y. Argon.** 2004. Identification of the N-terminal peptide binding site of glucose-regulated protein 94. J Biol Chem **279:**16543-52.

267. **Randow, F., and B. Seed.** 2001. Endoplasmic reticulum chaperone gp96 is required for innate immunity but not cell viability. Nat Cell Biol **3:**891-6.

268. **Schulte, T. W., S. Akinaga, T. Murakata, T. Agatsuma, S. Sugimoto, H. Nakano, Y. S. Lee, B. B. Simen, Y. Argon, S. Felts, D. O. Toft, L. M. Neckers, and S. V. Sharma.** 1999. Interaction of radicicol with members of the heat shock protein 90 family of molecular chaperones. Mol Endocrinol **13:**1435-48.

269. **Stancato, L. F., Y. H. Chow, K. A. Hutchison, G. H. Perdew, R. Jove, and W. B. Pratt.** 1993. Raf exists in a native heterocomplex with hsp90 and p50 that can be reconstituted in a cell-free system. J Biol Chem **268:**21711-6.

270. **Van, P. N., F. Peter, and H. D. Soling.** 1989. Four intracisternal calcium-binding glycoproteins from rat liver microsomes with high affinity for calcium. No indication for calsequestrin-like proteins in inositol 1,4,5-trisphosphate-sensitive calcium sequestering rat liver vesicles. J Biol Chem **264:**17494-501.

271. **Nieland, T. J., M. C. Tan, M. Monne-van Muijen, F. Koning, A. M. Kruisbeek, and G. M. van Bleek.** 1996. Isolation of an immunodominant viral peptide that is endogenously bound to the stress protein GP96/GRP94. Proc Natl Acad Sci U S A **93:**6135-9.

272. **Vogen, S., T. Gidalevitz, C. Biswas, B. B. Simen, E. Stein, F. Gulmen, and Y. Argon.** 2002. Radicicol-sensitive peptide binding to the N-terminal portion of GRP94. J Biol Chem **277:**40742-50.

273. **Li, Z., and P. K. Srivastava.** 1993. Tumor rejection antigen gp96/grp94 is an ATPase: implications for protein folding and antigen presentation. Embo J **12:**3143-51.

274. **Arnold, D., S. Faath, H. Rammensee, and H. Schild.** 1995. Cross-priming of minor histocompatibility antigen-specific cytotoxic T cells upon immunization with the heat shock protein gp96. J Exp Med **182:**885-9.

275. **Ahluwalia, N., J. J. Bergeron, I. Wada, E. Degen, and D. B. Williams.** 1992. The p88 molecular chaperone is identical to the endoplasmic reticulum membrane protein, calnexin. J Biol Chem **267:**10914-8.

276. **Milner, R. E., S. Baksh, C. Shemanko, M. R. Carpenter, L. Smillie, J. E. Vance, M. Opas, and M. Michalak.** 1991. Calreticulin, and not calsequestrin, is the major calcium binding protein of smooth muscle sarcoplasmic reticulum and liver endoplasmic reticulum. J Biol Chem **266:**7155-65.

277. **Parodi, A. J.** 2000. Role of N-oligosaccharide endoplasmic reticulum processing reactions in glycoprotein folding and degradation. Biochem J **348 Pt 1:**1-13.

278. **David, V., F. Hochstenbach, S. Rajagopalan, and M. B. Brenner.** 1993. Interaction with newly synthesized and retained proteins in the endoplasmic reticulum suggests a chaperone function for human integral membrane protein IP90 (calnexin). J Biol Chem **268:**9585-92.

279. **Nauseef, W. M., S. J. McCormick, and R. A. Clark.** 1995. Calreticulin functions as a molecular chaperone in the biosynthesis of myeloperoxidase. J Biol Chem **270:**4741-7.

280. **Leach, M. R., M. F. Cohen-Doyle, D. Y. Thomas, and D. B. Williams.** 2002. Localization of the lectin, ERp57 binding, and polypeptide binding sites of calnexin and calreticulin. J Biol Chem **277:**29686-97.

281. **Li, Z., W. F. Stafford, and M. Bouvier.** 2001. The metal ion binding properties of calreticulin modulate its conformational flexibility and thermal stability. Biochemistry **40:**11193-201.

282. **Schrag, J. D., J. J. Bergeron, Y. Li, S. Borisova, M. Hahn, D. Y. Thomas, and M. Cygler.** 2001. The Structure of calnexin, an ER chaperone involved in quality control of protein folding. Mol Cell **8:**633-44.

283. **Ihara, Y., M. F. Cohen-Doyle, Y. Saito, and D. B. Williams.** 1999. Calnexin discriminates between protein conformational states and functions as a molecular chaperone in vitro. Mol Cell **4:**331-41.

284. **Saito, Y., Y. Ihara, M. R. Leach, M. F. Cohen-Doyle, and D. B. Williams.** 1999. Calreticulin functions in vitro as a molecular chaperone for both glycosylated and non-glycosylated proteins. Embo J **18:**6718-29.

285. **Rudenko, G., E. Hohenester, and Y. A. Muller.** 2001. LG/LNS domains: multiple functions -- one business end? Trends Biochem Sci **26:**363-8.

286. **Vassilakos, A., M. Michalak, M. A. Lehrman, and D. B. Williams.** 1998. Oligosaccharide binding characteristics of the molecular chaperones calnexin and calreticulin. Biochemistry **37:**3480-90.

287. **Leach, M. R., and D. B. Williams.** 2004. Lectin-deficient calnexin is capable of binding class I histocompatibility molecules in vivo and preventing their degradation. J Biol Chem **279:**9072-9.

288. **Kapoor, M., L. Ellgaard, J. Gopalakrishnapai, C. Schirra, E. Gemma, S. Oscarson, A. Helenius, and A. Surolia.** 2004. Mutational analysis provides molecular insight into the carbohydrate-binding region of calreticulin: pivotal roles of tyrosine-109 and aspartate-135 in carbohydrate recognition. Biochemistry **43:**97-106.

289. **Thomson, S. P., and D. B. Williams.** 2005. Delineation of the lectin site of the molecular chaperone calreticulin. Cell Stress Chaperones **10:**242-51.

290. **Coppolino, M. G., and S. Dedhar.** 1998. Calreticulin. Int J Biochem Cell Biol **30:**553-8.

291. **Guo, L., J. Groenendyk, S. Papp, M. Dabrowska, B. Knoblach, C. Kay, J. M. Parker, M. Opas, and M. Michalak.** 2003. Identification of an N-domain histidine essential for chaperone function in calreticulin. J Biol Chem **278:**50645-53.

292. **Ellgaard, L., R. Riek, T. Herrmann, P. Guntert, D. Braun, A. Helenius, and K. Wuthrich.** 2001. NMR structure of the calreticulin P-domain. Proc Natl Acad Sci U S A **98:**3133-8.

293. **Baksh, S., C. Spamer, C. Heilmann, and M. Michalak.** 1995. Identification of the Zn2+ binding region in calreticulin. FEBS Lett **376:**53-7.

294. **Tan, Y., M. Chen, Z. Li, K. Mabuchi, and M. Bouvier.** 2006. The calcium- and zinc-responsive regions of calreticulin reside strictly in the N-/C-domain. Biochim Biophys Acta **1760:**745-53.

295. **Baksh, S., and M. Michalak.** 1991. Expression of calreticulin in Escherichia coli and identification of its Ca2+ binding domains. J Biol Chem **266:**21458-65.

296. **Corbett, E. F., K. M. Michalak, K. Oikawa, S. Johnson, I. D. Campbell, P. Eggleton, C. Kay, and M. Michalak.** 2000. The conformation of calreticulin is influenced by the endoplasmic reticulum luminal environment. J Biol Chem **275:**27177-85.

297. **Xu, X., H. Azakami, and A. Kato.** 2004. P-domain and lectin site are involved in the chaperone function of Saccharomyces cerevisiae calnexin homologue. FEBS Lett **570:**155-60.

298. **Wong, H. N., M. A. Ward, A. W. Bell, E. Chevet, S. Bains, W. P. Blackstock, R. Solari, D. Y. Thomas, and J. J. Bergeron.** 1998. Conserved in vivo phosphorylation of calnexin at casein kinase II sites as well as a protein kinase C/proline-directed kinase site. J Biol Chem **273:**17227-35.

299. **Chevet, E., H. N. Wong, D. Gerber, C. Cochet, A. Fazel, P. H. Cameron, J. N. Gushue, D. Y. Thomas, and J. J. Bergeron.** 1999. Phosphorylation by CK2 and MAPK enhances calnexin association with ribosomes. Embo J **18:**3655-66.

300. **Rendon-Huerta, E., G. Mendoza-Hernandez, and M. Robles-Flores.** 1999. Characterization of calreticulin as a protein interacting with protein kinase C. Biochem J **344 Pt 2:**469-75.

301. **Helenius, A., E. S. Trombetta, D. N. Herbert, and J. F. Simons.** 1997. Calnexin, calreticulin and the folding of glycoproteins. Trends Cell Biol. **7:**193-200.

302. **Hammond, C., and A. Helenius.** 1994. Folding of VSV G protein: sequential interaction with BiP and calnexin. Science **266:**456-8.

303. **Wang, N., R. Daniels, and D. N. Hebert.** 2005. The cotranslational maturation of the type I membrane glycoprotein tyrosinase: the heat shock protein 70 system hands off to the lectin-based chaperone system. Mol Biol Cell **16:**3740-52.

304. **Degen, E., M. F. Cohen-Doyle, and D. B. Williams.** 1992. Efficient dissociation of the p88 chaperone from major histocompatibility complex class I molecules requires both beta 2-microglobulin and peptide. J Exp Med **175:**1653-61.

305. **Hochstenbach, F., V. David, S. Watkins, and M. B. Brenner.** 1992. Endoplasmic reticulum resident protein of 90 kilodaltons associates with the T- and B-cell antigen receptors and major histocompatibility complex antigens during their assembly. Proc Natl Acad Sci U S A **89:**4734-8.

306. **Tatu, U., C. Hammond, and A. Helenius.** 1995. Folding and oligomerization of influenza hemagglutinin in the ER and the intermediate compartment. Embo J **14:**1340-8.

307. **Bass, J., G. Chiu, Y. Argon, and D. F. Steiner.** 1998. Folding of insulin receptor monomers is facilitated by the molecular chaperones calnexin and calreticulin and impaired by rapid dimerization. J Cell Biol **141:**637-46.

308. **Wada, I., M. Kai, S. Imai, F. Sakane, and H. Kanoh.** 1997. Promotion of transferrin folding by cyclic interactions with calnexin and calreticulin. Embo J **16:**5420-32.

309. **Ware, F. E., A. Vassilakos, P. A. Peterson, M. R. Jackson, M. A. Lehrman, and D. B. Williams.** 1995. The molecular chaperone calnexin binds Glc1Man9GlcNAc2 oligosaccharide as an initial step in recognizing unfolded glycoproteins. J Biol Chem **270:**4697-704.

310. **Danilczyk, U. G., and D. B. Williams.** 2001. The lectin chaperone calnexin utilizes polypeptide-based interactions to associate with many of its substrates in vivo. J Biol Chem **276:**25532-40.

311. **Otteken, A., and B. Moss.** 1996. Calreticulin interacts with newly synthesized human immunodeficiency virus type 1 envelope glycoprotein, suggesting a chaperone function similar to that of calnexin. J Biol Chem **271:**97-103.

312. **Toyofuku, K., I. Wada, K. Hirosaki, J. S. Park, Y. Hori, and K. Jimbow.** 1999. Promotion of tyrosinase folding in COS 7 cells by calnexin. J Biochem **125:**82-9.

313. **Hebert, D. N., B. Foellmer, and A. Helenius.** 1996. Calnexin and calreticulin promote folding, delay oligomerization and suppress degradation of influenza hemagglutinin in microsomes. Embo J **15:**2961-8.

314. **Molinari, M., K. K. Eriksson, V. Calanca, C. Galli, P. Cresswell, M. Michalak, and A. Helenius.** 2004. Contrasting functions of calreticulin and calnexin in glycoprotein folding and ER quality control. Mol Cell **13:**125-35.

315. **Zhang, Q., and R. D. Salter.** 1998. Distinct patterns of folding and interactions with calnexin and calreticulin in human class I MHC proteins with altered N-glycosylation. J Immunol **160:**831-7.

316. **Keller, S. H., J. Lindstrom, and P. Taylor.** 1998. Inhibition of glucose trimming with castanospermine reduces calnexin association and promotes proteasome degradation of the alpha-subunit of the nicotinic acetylcholine receptor. J Biol Chem **273:**17064-72.

317. **van Leeuwen, J. E., and K. P. Kearse.** 1996. Calnexin associates exclusively with individual CD3 delta and T cell antigen receptor (TCR) alpha proteins containing incompletely trimmed glycans that are not assembled into multisubunit TCR complexes. J Biol Chem **271:**9660-5.

318. **Pipe, S. W., J. A. Morris, J. Shah, and R. J. Kaufman.** 1998. Differential interaction of coagulation factor VIII and factor V with protein chaperones calnexin and calreticulin. J Biol Chem **273:**8537-44.

319. **Jannatipour, M., M. Callejo, A. J. Parodi, J. Armstrong, and L. A. Rokeach.** 1998. Calnexin and BiP interact with acid phosphatase independently of glucose trimming and reglucosylation in Schizosaccharomyces pombe. Biochemistry **37:**17253-61.

320. **Wada, I., S. Imai, M. Kai, F. Sakane, and H. Kanoh.** 1995. Chaperone function of calreticulin when expressed in the endoplasmic reticulum as the membrane-anchored and soluble forms. J Biol Chem **270:**20298-304.

321. **Harris, M. R., Y. Y. Yu, C. S. Kindle, T. H. Hansen, and J. C. Solheim.** 1998. Calreticulin and calnexin interact with different protein and glycan determinants during the assembly of MHC class I. J Immunol **160:**5404-9.

322. **Peterson, J. R., and A. Helenius.** 1999. In vitro reconstitution of calreticulin-substrate interactions. J Cell Sci **112 (Pt 16):**2775-84.

323. **Lenter, M., and D. Vestweber.** 1994. The integrin chains beta 1 and alpha 6 associate with the chaperone calnexin prior to integrin assembly. J Biol Chem **269:**12263-8.

324. **Swanton, E., S. High, and P. Woodman.** 2003. Role of calnexin in the glycan-independent quality control of proteolipid protein. Embo J **22:**2948-58.

325. **Jorgensen, C. S., N. H. Heegaard, A. Holm, P. Hojrup, and G. Houen.** 2000. Polypeptide binding properties of the chaperone calreticulin. Eur J Biochem **267:**2945-54.

326. **Vassilakos, A., M. F. Cohen-Doyle, P. A. Peterson, M. R. Jackson, and D. B. Williams.** 1996. The molecular chaperone calnexin facilitates folding and assembly of class I histocompatibility molecules. Embo J **15:**1495-506.

327. **Danilczyk, U. G., M. F. Cohen-Doyle, and D. B. Williams.** 2000. Functional relationship between calreticulin, calnexin, and the endoplasmic reticulum luminal domain of calnexin. J Biol Chem **275:**13089-97.

328. **Gao, B., R. Adhikari, M. Howarth, K. Nakamura, M. C. Gold, A. B. Hill, R. Knee, M. Michalak, and T. Elliott.** 2002.

Assembly and antigen-presenting function of MHC class I molecules in cells lacking the ER chaperone calreticulin. Immunity **16:**99-109.

329. **Van Leeuwen, J. E., and K. P. Kearse.** 1996. The related molecular chaperones calnexin and calreticulin differentially associate with nascent T cell antigen receptor proteins within the endoplasmic reticulum. J Biol Chem **271:**25345-9.

330. **Chang, W., M. S. Gelman, and J. M. Prives.** 1997. Calnexin-dependent enhancement of nicotinic acetylcholine receptor assembly and surface expression. J Biol Chem **272:**28925-32.

331. **Pind, S., J. R. Riordan, and D. B. Williams.** 1994. Participation of the endoplasmic reticulum chaperone calnexin (p88, IP90) in the biogenesis of the cystic fibrosis transmembrane conductance regulator. J Biol Chem **269:**12784-8.

332. **Fraser, S. A., R. Karimi, M. Michalak, and D. Hudig.** 2000. Perforin lytic activity is controlled by calreticulin. J Immunol **164:**4150-5.

333. **Corbett, E. F., K. Oikawa, P. Francois, D. C. Tessier, C. Kay, J. J. Bergeron, D. Y. Thomas, K. H. Krause, and M. Michalak.** 1999. Ca2+ regulation of interactions between endoplasmic reticulum chaperones. J Biol Chem **274:**6203-11.

334. **Sadasivan, B., P. J. Lehner, B. Ortmann, T. Spies, and P. Cresswell.** 1996. Roles for calreticulin and a novel glycoprotein, tapasin, in the interaction of MHC class I molecules with TAP. Immunity **5:**103-14.

335. **Solheim, J. C., M. R. Harris, C. S. Kindle, and T. H. Hansen.** 1997. Prominence of beta 2-microglobulin, class I heavy chain conformation, and tapasin in the interactions of class I heavy chain with calreticulin and the transporter associated with antigen processing. J Immunol **158:**2236-41.

336. **Hebert, D. N., J. X. Zhang, W. Chen, B. Foellmer, and A. Helenius.** 1997. The number and location of glycans on influenza hemagglutinin determine folding and association with calnexin and calreticulin. J Cell Biol **139:**613-23.

337. **Bastianutto, C., E. Clementi, F. Codazzi, P. Podini, F. De Giorgi, R. Rizzuto, J. Meldolesi, and T. Pozzan.** 1995. Overexpression of calreticulin increases the Ca2+ capacity of rapidly exchanging Ca2+ stores and reveals aspects of their lumenal microenvironment and function. J Cell Biol **130:**847-55.

338. **Mery, L., N. Mesaeli, M. Michalak, M. Opas, D. P. Lew, and K. H. Krause.** 1996. Overexpression of calreticulin increases intracellular Ca2+ storage and decreases store-operated Ca2+ influx. J Biol Chem **271:**9332-9.

339. **Arnaudeau, S., M. Frieden, K. Nakamura, C. Castelbou, M. Michalak, and N. Demaurex.** 2002. Calreticulin differentially modulates calcium uptake and release in the endoplasmic reticulum and mitochondria. J Biol Chem **277:**46696-705.

340. **Mesaeli, N., K. Nakamura, E. Zvaritch, P. Dickie, E. Dziak, K. H. Krause, M. Opas, D. H. MacLennan, and M. Michalak.** 1999. Calreticulin is essential for cardiac development. J Cell Biol **144:**857-68.

341. **Roderick, H. L., J. D. Lechleiter, and P. Camacho.** 2000. Cytosolic phosphorylation of calnexin controls intracellular Ca(2+) oscillations via an interaction with SERCA2b. J Cell Biol **149:**1235-48.

342. **John, L. M., J. D. Lechleiter, and P. Camacho.** 1998. Differential modulation of SERCA2 isoforms by calreticulin. J Cell Biol **142:**963-73.

343. **Xu, W., F. J. Longo, M. R. Wintermantel, X. Jiang, R. A. Clark, and S. DeLisle.** 2000. Calreticulin modulates capacitative Ca2+ influx by controlling the extent of inositol 1,4,5-trisphosphate-induced Ca2+ store depletion. J Biol Chem **275:**36676-82.

344. **Michalak, M., J. Lynch, J. Groenendyk, L. Guo, J. M. Robert Parker, and M. Opas.** 2002. Calreticulin in cardiac development and pathology. Biochim Biophys Acta **1600:**32-7.

345. **Guo, L., K. Nakamura, J. Lynch, M. Opas, E. N. Olson, L. B. Agellon, and M. Michalak.** 2002. Cardiac-specific expression of calcineurin reverses embryonic lethality in calreticulin-deficient mouse. J Biol Chem **277:**50776-9.

346. **Lynch, J., and M. Michalak.** 2003. Calreticulin is an upstream regulator of calcineurin. Biochem Biophys Res Commun **311:**1173-9.

347. **Denzel, A., M. Molinari, C. Trigueros, J. E. Martin, S. Velmurgan, S. Brown, G. Stamp, and M. J. Owen.** 2002. Early postnatal death and motor disorders in mice congenitally deficient in calnexin expression. Mol Cell Biol **22:**7398-404.

348. **Nakamura, K., A. Zuppini, S. Arnaudeau, J. Lynch, I. Ahsan, R. Krause, S. Papp, H. De Smedt, J. B. Parys, W. Muller-Esterl, D. P. Lew, K. H. Krause, N. Demaurex, M. Opas, and M. Michalak.** 2001. Functional specialization of calreticulin domains. J Cell Biol **154:**961-72.

349. **Fadel, M. P., E. Dziak, C. M. Lo, J. Ferrier, N. Mesaeli, M. Michalak, and M. Opas.** 1999. Calreticulin affects focal contact-dependent but not close contact-dependent cell-substratum adhesion. J Biol Chem **274:**15085-94.

350. **Opas, M., M. Szewczenko-Pawlikowski, G. K. Jass, N. Mesaeli, and M. Michalak.** 1996. Calreticulin modulates cell adhesiveness via regulation of vinculin expression. J Cell Biol **135:**1913-23.

351. **Fadel, M. P., M. Szewczenko-Pawlikowski, P. Leclerc, E. Dziak, J. M. Symonds, O. Blaschuk, M. Michalak, and M. Opas.** 2001. Calreticulin affects beta-catenin-associated pathways. J Biol Chem **276:**27083-9.

352. **Coppolino, M. G., M. J. Woodside, N. Demaurex, S. Grinstein, R. St-Arnaud, and S. Dedhar.** 1997. Calreticulin is essential for integrin-mediated calcium signalling and cell adhesion. Nature **386:**843-7.

353. **Merad-Boudia, M., A. Nicole, D. Santiard-Baron, C. Saille, and I. Ceballos-Picot.** 1998. Mitochondrial impairment as an early event in the process of apoptosis induced by glutathione depletion in neuronal cells: relevance to Parkinson's disease. Biochem Pharmacol **56:**645-55.

354. **Halaban, R., S. Svedine, E. Cheng, Y. Smicun, R. Aron, and D. N. Hebert.** 2000. Endoplasmic reticulum retention is a common defect associated with tyrosinase-negative albinism. Proc Natl Acad Sci U S A **97:**5889-94.

355. **Yeates, L. C., and G. Powis.** 1997. The expression of the molecular chaperone calnexin is decreased in cancer cells grown as colonies compared to monolayer. Biochem Biophys Res Commun **238:**66-70.

356. **Brunagel, G., U. Shah, R. E. Schoen, and R. H. Getzenberg.** 2003. Identification of calreticulin as a nuclear matrix protein associated with human colon cancer. J Cell Biochem **89:**238-43.

357. **Mesaeli, N., and C. Phillipson.** 2004. Impaired p53 expression, function, and nuclear localization in calreticulin-deficient cells. Mol Biol Cell **15:**1862-70.

358. **Groenendyk, J., A. Zuppini, G. Shore, M. Opas, R. C. Bleackley, and M. Michalak.** 2006. Caspase 12 in calnexin-deficient cells. Biochemistry **45:**13219-26.

359. **Mohan, C., and G. M. Lee.** 2009. Calnexin overexpression sensitizes recombinant CHO cells to apoptosis induced by sodium butyrate treatment. Cell Stress Chaperones **14:**49-60.

360. **Lim, S., W. Chang, B. K. Lee, H. Song, J. H. Hong, S. Lee, B. W. Song, H. J. Kim, M. J. Cha, Y. Jang, N. Chung, S. Y. Choi, and K. C. Hwang.** 2008. Enhanced calreticulin expression promotes calcium-dependent apoptosis in postnatal cardiomyocytes. Mol Cells **25:**390-6.

361. **Jimbow, K., H. Chen, J. S. Park, and P. D. Thomas.** 2001. Increased sensitivity of melanocytes to oxidative stress and abnormal expression of tyrosinase-related protein in vitiligo. Br J Dermatol **144:**55-65.

362. **Kuraishi, T., J. Manaka, M. Kono, H. Ishii, N. Yamamoto, K. Koizumi, A. Shiratsuchi, B. L. Lee, H. Higashida, and Y. Nakanishi.** 2007. Identification of calreticulin as a marker for phagocytosis of apoptotic cells in Drosophila. Exp Cell Res **313:**500-10.

363. **Roderick, H. L., A. K. Campbell, and D. H. Llewellyn.** 1997. Nuclear localisation of calreticulin in vivo is enhanced by its interaction with glucocorticoid receptors. FEBS Lett **405:**181-5.

364. **Holaska, J. M., B. E. Black, F. Rastinejad, and B. M. Paschal.** 2002. Ca2+-dependent nuclear export mediated by calreticulin. Mol Cell Biol **22:**6286-97.

365. **Dupuis, M., E. Schaerer, K. H. Krause, and J. Tschopp.** 1993. The calcium-binding protein calreticulin is a major constituent of lytic granules in cytolytic T lymphocytes. J Exp Med **177:**1-7.

366. **White, T. K., Q. Zhu, and M. L. Tanzer.** 1995. Cell surface calreticulin is a putative mannoside lectin which triggers mouse melanoma cell spreading. J Biol Chem **270:**15926-9.

367. **Zhu, Q., P. Zelinka, T. White, and M. L. Tanzer.** 1997. Calreticulin-integrin bidirectional signaling complex. Biochem Biophys Res Commun **232:**354-8.

368. **Pike, S. E., L. Yao, K. D. Jones, B. Cherney, E. Appella, K. Sakaguchi, H. Nakhasi, J. Teruya-Feldstein, P. Wirth, G. Gupta, and G. Tosato.** 1998. Vasostatin, a calreticulin fragment, inhibits angiogenesis and suppresses tumor growth. J Exp Med **188:**2349-56.

369. **Goicoechea, S., A. W. Orr, M. A. Pallero, P. Eggleton, and J. E. Murphy-Ullrich.** 2000. Thrombospondin mediates focal adhesion disassembly through interactions with cell surface calreticulin. J Biol Chem **275:**36358-68.

370. **Madeo, F., M. Durchschlag, O. Kepp, T. Panaretakis, L. Zitvogel, K. U. Frohlich, and G. Kroemer.** 2009. Phylogenetic conservation of the preapoptotic calreticulin exposure pathway from yeast to mammals. Cell Cycle **8:**639-42.

371. **Panaretakis, T., O. Kepp, U. Brockmeier, A. Tesniere, A. C. Bjorklund, D. C. Chapman, M. Durchschlag, N. Joza, G. Pierron, P. van Endert, J. Yuan, L. Zitvogel, F. Madeo, D. B. Williams, and G. Kroemer.** 2009. Mechanisms of pre-apoptotic calreticulin exposure in immunogenic cell death. Embo J **28:**578-90.

372. **Kapoor, M., H. Srinivas, E. Kandiah, E. Gemma, L. Ellgaard, S. Oscarson, A. Helenius, and A. Surolia.** 2003. Interactions of substrate with calreticulin, an endoplasmic reticulum chaperone. J Biol Chem **278:**6194-200.

373. **High, S., F. J. Lecomte, S. J. Russell, B. M. Abell, and J. D. Oliver.** 2000. Glycoprotein folding in the endoplasmic reticulum: a tale of three chaperones? FEBS Lett **476:**38-41.

374. **Petrescu, S. M., A. J. Petrescu, H. N. Titu, R. A. Dwek, and F. M. Platt.** 1997. Inhibition of N-glycan processing in B16 melanoma cells results in inactivation of tyrosinase but does not prevent its transport to the melanosome. J Biol Chem **272:**15796-803.

375. **Rodan, A. R., J. F. Simons, E. S. Trombetta, and A. Helenius.** 1996. N-linked oligosaccharides are necessary and sufficient for association of glycosylated forms of bovine RNase with calnexin and calreticulin. Embo J **15:**6921-30.

376. **Cannon, K. S., and A. Helenius.** 1999. Trimming and readdition of glucose to N-linked oligosaccharides determines calnexin association of a substrate glycoprotein in living cells. J Biol Chem **274:**7537-44.

377. **Zapun, A., S. M. Petrescu, P. M. Rudd, R. A. Dwek, D. Y. Thomas, and J. J. Bergeron.** 1997. Conformation-independent binding of monoglucosylated ribonuclease B to calnexin. Cell **88:**29-38.

378. **Wearsch, P. A., C. A. Jakob, A. Vallin, R. A. Dwek, P. M. Rudd, and P. Cresswell.** 2004. Major histocompatibility complex class I molecules expressed with monoglucosylated N-linked glycans bind calreticulin independently of their assembly status. J Biol Chem **279:**25112-21.

379. **Molinari, M., and A. Helenius.** 1999. Glycoproteins form mixed disulphides with oxidoreductases during folding in living cells. Nature **402:**90-3.

380. **Loo, T. W., and D. M. Clarke.** 1995. P-glycoprotein. Associations between domains and between domains and molecular chaperones. J Biol Chem **270:**21839-44.

381. **Rajagopalan, S., Y. Xu, and M. B. Brenner.** 1994. Retention of unassembled components of integral membrane proteins by calnexin. Science **263:**387-90.

382. **Tector, M., and R. D. Salter.** 1995. Calnexin influences folding of human class I histocompatibility proteins but not their

assembly with beta 2-microglobulin. J Biol Chem **270:**19638-42.

383. **Zhang, Q., M. Tector, and R. D. Salter.** 1995. Calnexin recognizes carbohydrate and protein determinants of class I major histocompatibility complex molecules. J Biol Chem **270:**3944-8.

384. **Kearse, K. P., D. B. Williams, and A. Singer.** 1994. Persistence of glucose residues on core oligosaccharides prevents association of TCR alpha and TCR beta proteins with calnexin and results specifically in accelerated degradation of nascent TCR alpha proteins within the endoplasmic reticulum. Embo J **13:**3678-86.

385. **Wanamaker, C. P., and W. N. Green.** 2005. N-linked glycosylation is required for nicotinic receptor assembly but not for subunit associations with calnexin. J Biol Chem **280:**33800-10.

386. **Buchner, J., M. Schmidt, M. Fuchs, R. Jaenicke, R. Rudolph, F. X. Schmid, and T. Kiefhaber.** 1991. GroE facilitates refolding of citrate synthase by suppressing aggregation. Biochemistry **30:**1586-91.

387. **Jakob, U., H. Lilie, I. Meyer, and J. Buchner.** 1995. Transient interaction of Hsp90 with early unfolding intermediates of citrate synthase. Implications for heat shock in vivo. J Biol Chem **270:**7288-94.

388. **Hafizur, R. M., M. Yano, T. Gotoh, M. Mori, and K. Terada.** 2004. Modulation of chaperone activities of Hsp70 and Hsp70-2 by a mammalian DnaJ/Hsp40 homolog, DjA4. J Biochem **135:**193-200.

389. **Rizvi, S. M., L. Mancino, V. Thammavongsa, R. L. Cantley, and M. Raghavan.** 2004. A polypeptide binding conformation of calreticulin is induced by heat shock, calcium depletion, or by deletion of the C-terminal acidic region. Mol Cell **15:**913-23.

390. **Sandhu, N., K. Duus, C. S. Jorgensen, P. R. Hansen, S. W. Bruun, L. O. Pedersen, P. Hojrup, and G. Houen.** 2007. Peptide binding specificity of the chaperone calreticulin. Biochim Biophys Acta **1774:**701-13.

391. **Duus, K., P. R. Hansen, and G. Houen.** 2008. Interaction of calreticulin with amyloid beta peptide 1-42. Protein Pept Lett **15:**103-7.

392. **Stronge, V. S., Y. Saito, Y. Ihara, and D. B. Williams.** 2001. Relationship between calnexin and BiP in suppressing aggregation and promoting refolding of protein and glycoprotein substrates. J Biol Chem **276:**39779-87.

393. **Thammavongsa, V., L. Mancino, and M. Raghavan.** 2005. Polypeptide substrate recognition by calnexin requires specific conformations of the calnexin protein. J Biol Chem **280:**33497-505.

394. **Bessette, P. H., F. Aslund, J. Beckwith, and G. Georgiou.** 1999. Efficient folding of proteins with multiple disulfide bonds in the Escherichia coli cytoplasm. Proc Natl Acad Sci U S A **96:**13703-8.

395. **Bullock, W. O., J. M. Fernandez, and J. M. Short.** 1987. XL1-Blue: a high efficiency plasmid transforming *recA* *Escherichia coli* strain with betagalactosidase selection. BioTechniques **5:**376-378.

396. **Jung, H., S. Han, T. Kim, and C. Ban.** 2005. Crystallization and Preliminary X-ray Analysis of Native and Selenomethionyl Polymyxin Resistance Protein D from *E.coli*. Macromolecular Research **13:**549-552.

397. **Chen, C. W., and C. A. Thomas, Jr.** 1980. Recovery of DNA segments from agarose gels. Anal Biochem **101:**339-41.

398. **Marko, M. A., R. Chipperfield, and H. C. Birnboim.** 1982. A procedure for the large-scale isolation of highly purified plasmid DNA using alkaline extraction and binding to glass powder. Anal Biochem **121:**382-7.

399. **Boom, R., C. J. Sol, M. M. Salimans, C. L. Jansen, P. M. Wertheim-van Dillen, and J. van der Noordaa.** 1990. Rapid and simple method for purification of nucleic acids. J Clin Microbiol **28:**495-503.

400. **Sambrook, J., E. F. Fritsch, and T. Maniatis.** 1989. Molecular Cloning: a Laboratory Manual, 2 ed. Cold Spring Harbor Laboratory Press, Cold Spring Harbor, New York.

401. **Hanahan, D.** 1983. Studies on transformation of Escherichia coli with plasmids. J Mol Biol **166:**557-80.

402. **Fiedler, S., and R. Wirth.** 1988. Transformation of bacteria with plasmid DNA by electroporation. Anal Biochem **170:**38-44.

403. **Ho, S. N., H. D. Hunt, R. M. Horton, J. K. Pullen, and L. R. Pease.** 1989. Site-directed mutagenesis by overlap extension using the polymerase chain reaction. Gene **77:**51-9.

404. **Laemmli, U. K.** 1970. Cleavage of structural proteins during the assembly of the head of bacteriophage T4. Nature **227:**680-5.

405. **Jakob, U., T. Scheibel, S. Bose, J. Reinstein, and J. Buchner.** 1996. Assessment of the ATP binding properties of Hsp90. J Biol Chem **271:**10035-41.

406. **Bosl, B., V. Grimminger, and S. Walter.** 2005. Substrate binding to the molecular chaperone Hsp104 and its regulation by nucleotides. J Biol Chem **280:**38170-6.

407. **Schanstra, J. P., R. Rink, F. Pries, and D. B. Janssen.** 1993. Construction of an expression and site-directed mutagenesis system of haloalkane dehalogenase in Escherichia coli. Protein Expr Purif **4:**479-89.

408. **Kubo, Y., T. Tsunehiro, S. Nishikawa, M. Nakai, E. Ikeda, A. Toh-e, N. Morishima, T. Shibata, and T. Endo.** 1999. Two distinct mechanisms operate in the reactivation of heat-denatured proteins by the mitochondrial Hsp70/Mdj1p/Yge1p chaperone system. J Mol Biol **286:**447-64.

409. **Foyouzi-Youssefi, R., S. Arnaudeau, C. Borner, W. L. Kelley, J. Tschopp, D. P. Lew, N. Demaurex, and K. H. Krause.** 2000. Bcl-2 decreases the free Ca2+ concentration within the endoplasmic reticulum. Proc Natl Acad Sci U S A **97:**5723-8.

410. **Michalak, M., J. M. Robert Parker, and M. Opas.** 2002. Ca2+ signaling and calcium binding chaperones of the endoplasmic reticulum. Cell Calcium **32:**269-78.

411. **Bouvier, M., and W. F. Stafford.** 2000. Probing the three-dimensional structure of human calreticulin. Biochemistry **39:**14950-9.

412. **Ou, W. J., J. J. Bergeron, Y. Li, C. Y. Kang, and D. Y. Thomas.** 1995. Conformational changes induced in the endoplasmic reticulum luminal domain of calnexin by Mg-ATP and Ca2+. J Biol Chem **270:**18051-9.

413. **Guillen, E., and C. B. Hirschberg.** 1995. Transport of adenosine triphosphate into endoplasmic reticulum proteoliposomes. Biochemistry **34:**5472-6.

414. **Singh, J., and J. M. Thornton.** 1992. Atlas of protein side-chain interactions, vol. 1. Oxford University Press, Oxford.

415. **Freskgard, P. O., L. G. Martensson, P. Jonasson, B. H. Jonsson, and U. Carlsson.** 1994. Assignment of the contribution of the tryptophan residues to the circular dichroism spectrum of human carbonic anhydrase II. Biochemistry **33:**14281-8.

416. **Fourie, A. M., J. F. Sambrook, and M. J. Gething.** 1994. Common and divergent peptide binding specificities of hsp70 molecular chaperones. J Biol Chem **269:**30470-8.

417. **Gragerov, A., L. Zeng, X. Zhao, W. Burkholder, and M. E. Gottesman.** 1994. Specificity of DnaK-peptide binding. J Mol Biol **235:**848-54.

418. **Li, J., and B. Sha.** 2004. Peptide substrate identification for yeast Hsp40 Ydj1 by screening the phage display library. Biol Proced Online **6:**204-208.

419. **Li, J., and B. Sha.** 2005. Structure-based mutagenesis studies of the peptide substrate binding fragment of type I heat-shock protein 40. Biochem J **386:**453-60.

420. **Richarme, G., and M. Kohiyama.** 1993. Specificity of the Escherichia coli chaperone DnaK (70-kDa heat shock protein) for hydrophobic amino acids. J Biol Chem **268:**24074-7.

421. **Richarme, G., and M. Kohiyama.** 1994. Amino acid specificity of the Escherichia coli chaperone GroEL (heat shock protein 60). J Biol Chem **269:**7095-8.

422. **Rudiger, S., L. Germeroth, J. Schneider-Mergener, and B. Bukau.** 1997. Substrate specificity of the DnaK chaperone determined by screening cellulose-bound peptide libraries. Embo J **16:**1501-7.

423. **Kosen, P. A., T. E. Creighton, and E. R. Blout.** 1981. Circular dichroism spectroscopy of bovine pancreatic trypsin inhibitor and five altered conformational states. Relationship of conformation and the refolding pathway of the trypsin inhibitor. Biochemistry **20:**5744-54.

424. **Woody, R. W.** 1995. Circular dichroism. Methods Enzymol **246:**34-71.

425. **Hirst, J. D., and C. L. Brooks, 3rd.** 1994. Helicity, circular dichroism and molecular dynamics of proteins. J Mol Biol **243:**173-8.

426. **Woody, R. W.** 1994. Contributions of tryptophan side chains to the far-ultraviolet circular dichroism of proteins. Eur Biophys J **23:**253-62.

427. **Patil, A. R., C. J. Thomas, and A. Surolia.** 2000. Kinetics and the mechanism of interaction of the endoplasmic reticulum chaperone, calreticulin, with monoglucosylated (Glc1Man9GlcNAc2) substrate. J Biol Chem **275:**24348-24356.

428. **Arnaud, N., and J. Georges.** 1997. Fluorimetric determination of europium over a large dynamic range using its ternary complex with thenoyltrifluoroacetone and trioctylphosphine oxide in a micellar solution of Triton X-100. Analyst **122:**143-146.

429. **Urbanova, N., M. Kadar, K. Toth, B. Bogati, V. Andruch, and I. Bitter.** 2008. Fluorescent iminodiacetamide derivatives as potential ionophores for optical zinc ion-selective sensors. Anal Sci **24:**727-33.

430. **Okazaki, A., T. Ikura, K. Nikaido, and K. Kuwajima.** 1994. The chaperonin GroEL does not recognize apo-alpha-lactalbumin in the molten globule state. Nat Struct Biol **1:**439-46.

431. **Jiang, J., K. Prasad, E. M. Lafer, and R. Sousa.** 2005. Structural basis of interdomain communication in the Hsc70 chaperone. Mol Cell **20:**513-24.

432. **Carreno, B. M., K. L. Schreiber, D. J. McKean, I. Stroynowski, and T. H. Hansen.** 1995. Aglycosylated and phosphatidylinositol-anchored MHC class I molecules are associated with calnexin. Evidence implicating the class I-connecting peptide segment in calnexin association. J Immunol **154:**5173-80.

433. **Rajagopalan, S., and M. B. Brenner.** 1994. Calnexin retains unassembled major histocompatibility complex class I free heavy chains in the endoplasmic reticulum. J Exp Med **180:**407-12.

434. **Nagai, Y., and H. A. Popiel.** 2008. Conformational changes and aggregation of expanded polyglutamine proteins as therapeutic targets of the polyglutamine diseases: exposed beta-sheet hypothesis. Curr Pharm Des **14:**3267-79.

435. **Roychaudhuri, R., M. Yang, M. M. Hoshi, and D. B. Teplow.** 2009. Amyloid beta-protein assembly and Alzheimer disease. J Biol Chem **284:**4749-53.

436. **Kim, C., and S. J. Lee.** 2008. Controlling the mass action of alpha-synuclein in Parkinson's disease. J Neurochem **107:**303-16.

437. **Cyngiser, T. A.** 2008. Creutzfeldt-Jakob disease: a disease overview. Am J Electroneurodiagnostic Technol **48:**199-208.

438. **Rakhit, R., and A. Chakrabartty.** 2006. Structure, folding, and misfolding of Cu,Zn superoxide dismutase in amyotrophic lateral sclerosis. Biochim Biophys Acta **1762:**1025-37.

439. **Cheung, J. C., and C. M. Deber.** 2008. Misfolding of the cystic fibrosis transmembrane conductance regulator and disease. Biochemistry **47:**1465-73.

440. **Pirkl, F., E. Fischer, S. Modrow, and J. Buchner.** 2001. Localization of the chaperone domain of FKBP52. J Biol Chem **276:**37034-41.

441. **Lindner, R. A., A. Kapur, and J. A. Carver.** 1997. The interaction of the molecular chaperone, alpha-crystallin, with molten globule states of bovine alpha-lactalbumin. J Biol Chem **272:**27722-9.

442. **Wang, K., and B. I. Kurganov.** 2003. Kinetics of heat- and acidification-induced aggregation of firefly luciferase. Biophys Chem **106:**97-109.

443. **Conti, E., N. P. Franks, and P. Brick.** 1996. Crystal structure of firefly luciferase throws light on a superfamily of adenylate-forming enzymes. Structure **4:**287-98.

444. **Deluca, M.** 1976. Firefly luciferase. Adv Enzymol Relat Areas Mol Biol **44:**37-68.

445. **Branchini, B. R., R. A. Magyar, M. H. Murtiashaw, S. M. Anderson, L. C. Helgerson, and M. Zimmer.** 1999. Site-directed mutagenesis of firefly luciferase active site amino acids: a proposed model for bioluminescence color. Biochemistry **38:**13223-30.

446. **Wood, K. V.** 1995. The chemical mechanism and evolutionary development of beetle bioluminescence. Photochem and Photobiol **62:**662-673.

447. **Minami, M., M. Nakamura, Y. Emori, and Y. Minami.** 2001. Both the N- and C-terminal chaperone sites of Hsp90 participate in protein refolding. Eur J Biochem **268:**2520-4.

448. **Wang, K., and A. Spector.** 2001. ATP causes small heat shock proteins to release denatured protein. Eur J Biochem **268:**6335-45.

449. **Schneider, C., L. Sepp-Lorenzino, E. Nimmesgern, O. Ouerfelli, S. Danishefsky, N. Rosen, and F. U. Hartl.** 1996. Pharmacologic shifting of a balance between protein refolding and degradation mediated by Hsp90. Proc Natl Acad Sci U S A **93:**14536-41.

450. **Hermawan, A., and W. J. Chirico.** 1999. N-Ethylmaleimide-modified Hsp70 inhibits protein folding. Arch Biochem Biophys **369:**157-62.

451. **Goffin, L., and C. Georgopoulos.** 1998. Genetic and biochemical characterization of mutations affecting the carboxy-terminal domain of the Escherichia coli molecular chaperone DnaJ. Mol Microbiol **30:**329-40.

452. **Glover, J. R., and S. Lindquist.** 1998. Hsp104, Hsp70, and Hsp40: a novel chaperone system that rescues previously aggregated proteins. Cell **94:**73-82.

453. **Singer, M. A., and S. Lindquist.** 1998. Multiple effects of trehalose on protein folding in vitro and in vivo. Mol Cell **1:**639-48.

454. **Shao, F., M. W. Bader, U. Jakob, and J. C. Bardwell.** 2000. DsbG, a protein disulfide isomerase with chaperone activity. J Biol Chem **275:**13349-52.

455. **Artemova, N. V., A. S. Kasakov, Z. M. Bumagina, E. M. Lyutova, and B. Y. Gurvits.** 2008. Protein aggregates as depots for the release of biologically active compounds. Biochem Biophys Res Commun **377:**595-9.

456. **Akiyoshi, K., Y. Sasaki, and J. Sunamoto.** 1999. Molecular chaperone-like activity of hydrogel nanoparticles of hydrophobized pullulan: thermal stabilization with refolding of carbonic anhydrase B. Bioconjug Chem **10:**321-4.

457. **Hook, D. W., and J. J. Harding.** 1997. Molecular chaperones protect catalase against thermal stress. Eur J Biochem **247:**380-5.

458. **Kurganov, B. I., E. R. Rafikova, and E. N. Dobrov.** 2002. Kinetics of thermal aggregation of tobacco mosaic virus coat protein. Biochemistry (Mosc) **67:**525-33.

459. **Panyukov, Y., I. Yudin, V. Drachev, E. Dobrov, and B. Kurganov.** 2007. The study of amorphous aggregation of tobacco mosaic virus coat protein by dynamic light scattering. Biophys Chem **127:**9-18.

460. **Reddy, G. B., P. Y. Reddy, A. Vijayalakshmi, M. S. Kumar, P. Suryanarayana, and B. Sesikeran.** 2002. Effect of long-term dietary manipulation on the aggregation of rat lens crystallins: role of alpha-crystallin chaperone function. Mol Vis **8:**298-305.

461. **Roy, S. K., T. Hiyama, and H. Nakamoto.** 1999. Purification and characterization of the 16-kDa heat-shock-responsive protein from the thermophilic cyanobacterium Synechococcus vulcanus, which is an alpha-crystallin-related, small heat shock protein. Eur J Biochem **262:**406-16.

462. **Chamberlain, L. H., and R. D. Burgoyne.** 1997. The molecular chaperone function of the secretory vesicle cysteine string proteins. J Biol Chem **272:**31420-6.

463. **Mehrabi, M., S. Hosseinkhani, and S. Ghobadi.** 2008. Stabilization of firefly luciferase against thermal stress by osmolytes. Int J Biol Macromol **43:**187-91.

464. **Rudolf, R., P. J. Magalhaes, and T. Pozzan.** 2006. Direct in vivo monitoring of sarcoplasmic reticulum Ca2+ and cytosolic

cAMP dynamics in mouse skeletal muscle. J Cell Biol **173:**187-93.

465. **Adolfsen, R., and E. N. Moudrianakis.** 1978. Control of complex metal ion equilibria in biochemical reaction systems. Intrinsic and apparent stability constants of metal-adenine nucleotide complexes. J Biol Chem **253:**4378-9.

466. **Graf, E., and J. T. Penniston.** 1981. CaATP: the substrate, at low ATP concentrations, of Ca2+ ATPase from human erythrocyte membranes. J Biol Chem **256:**1587-92.

467. **Csermely, P., Y. Miyata, T. Schnaider, and I. Yahara.** 1995. Autophosphorylation of grp94 (endoplasmin). J Biol Chem **270:**6381-8.

468. **Rosser, M. F., and C. V. Nicchitta.** 2000. Ligand interactions in the adenosine nucleotide-binding domain of the Hsp90 chaperone, GRP94. I. Evidence for allosteric regulation of ligand binding. J Biol Chem **275:**22798-805.

469. **Csermely, P., and C. R. Kahn.** 1991. The 90-kDa heat shock protein (hsp-90) possesses an ATP binding site and autophosphorylating activity. J Biol Chem **266:**4943-50.

470. **Scheibel, T., S. Neuhofen, T. Weikl, C. Mayr, J. Reinstein, P. D. Vogel, and J. Buchner.** 1997. ATP-binding properties of human Hsp90. J Biol Chem **272:**18608-13.

471. **Soti, C., A. S. Sreedhart, and P. Csermely.** 2003. Apoptosis, necrosis and cellular senescence: chaperone occupancy as a potential switch. Aging Cell **2:**39-45.

472. **Zhang, K., and R. J. Kaufman.** 2006. The unfolded protein response: a stress signaling pathway critical for health and disease. Neurology **66:**S102-9.

473. **Tjoelker, L. W., C. E. Seyfried, R. L. Eddy, Jr., M. G. Byers, T. B. Shows, J. Calderon, R. B. Schreiber, and P. W. Gray.** 1994. Human, mouse, and rat calnexin cDNA cloning: identification of potential calcium binding motifs and gene localization to human chromosome 5. Biochemistry **33:**3229-36.

474. **Lentze, N., and F. Narberhaus.** 2004. Detection of oligomerisation and substrate recognition sites of small heat shock proteins by peptide arrays. Biochem Biophys Res Commun **325:**401-7.

475. **Davis, D. P., R. Khurana, S. Meredith, F. J. Stevens, and Y. Argon.** 1999. Mapping the major interaction between binding protein and Ig light chains to sites within the variable domain. J Immunol **163:**3842-50.

476. **Greene, L. E., R. Zinner, S. Naficy, and E. Eisenberg.** 1995. Effect of nucleotide on the binding of peptides to 70-kDa heat shock protein. J Biol Chem **270:**2967-73.

477. **Young, J. C., V. R. Agashe, K. Siegers, and F. U. Hartl.** 2004. Pathways of chaperone-mediated protein folding in the cytosol. Nat Rev Mol Cell Biol **5:**781-91.

478. **Pearl, L. H., and C. Prodromou.** 2006. Structure and mechanism of the hsp90 molecular chaperone machinery. Annu Rev Biochem **75:**271-94.

479. **Young, J. C., I. Moarefi, and F. U. Hartl.** 2001. Hsp90: a specialized but essential protein-folding tool. J Cell Biol **154:**267-73.

480. **Patil, A. R., C. J. Thomas, and A. Surolia.** 2000. Kinetics and the mechanism of interaction of the endoplasmic reticulum chaperone, calreticulin, with monoglucosylated (Glc1Man9GlcNAc2) substrate. J Biol Chem **275:**24348-56.

481. **Kuznetsov, G., L. B. Chen, and S. K. Nigam.** 1997. Multiple molecular chaperones complex with misfolded large oligomeric glycoproteins in the endoplasmic reticulum. J Biol Chem **272:**3057-63.

482. **Feng, W., M. M. Matzuk, K. Mountjoy, E. Bedows, R. W. Ruddon, and I. Boime.** 1995. The asparagine-linked oligosaccharides of the human chorionic gonadotropin beta subunit facilitate correct disulfide bond pairing. J Biol Chem **270:**11851-9.

483. **Hubbard, S. C., and P. W. Robbins.** 1979. Synthesis and processing of protein-linked oligosaccharides in vivo. J Biol Chem **254:**4568-76.

484. **Tatu, U., and A. Helenius.** 1997. Interactions between newly synthesized glycoproteins, calnexin and a network of

resident chaperones in the endoplasmic reticulum. J Cell Biol **136:**555-65.

485. **Rudiger, S., J. Schneider-Mergener, and B. Bukau.** 2001. Its substrate specificity characterizes the DnaJ co-chaperone as a scanning factor for the DnaK chaperone. Embo J **20:**1042-50.

486. **Knoblauch, N. T., S. Rudiger, H. J. Schonfeld, A. J. Driessen, J. Schneider-Mergener, and B. Bukau.** 1999. Substrate specificity of the SecB chaperone. J Biol Chem **274:**34219-25.

487. **dos Remedios, C. G., and P. D. Moens.** 1995. Fluorescence resonance energy transfer spectroscopy is a reliable "ruler" for measuring structural changes in proteins. Dispelling the problem of the unknown orientation factor. J Struct Biol **115:**175-85.

488. **Wu, P., and L. Brand.** 1994. Resonance energy transfer: methods and applications. Anal Biochem **218:**1-13.

489. **Clegg, R. M.** 1995. Fluorescence resonance energy transfer. Curr Opin Biotechnol **6:**103-10.

490. **Greeson, J. N., L. E. Organ, F. A. Pereira, and R. M. Raphael.** 2006. Assessment of prestin self-association using fluorescence resonance energy transfer. Brain Res **1091:**140-50.

491. **Tertoolen, L. G., C. Blanchetot, G. Jiang, J. Overvoorde, T. W. Gadella, Jr., T. Hunter, and J. den Hertog.** 2001. Dimerization of receptor protein-tyrosine phosphatase alpha in living cells. BMC Cell Biol **2:**8.

492. **Overton, M. C., and K. J. Blumer.** 2000. G-protein-coupled receptors function as oligomers in vivo. Curr Biol **10:**341-4.

493. **Tonaco, I. A., J. W. Borst, S. C. de Vries, G. C. Angenent, and R. G. Immink.** 2006. In vivo imaging of MADS-box transcription factor interactions. J Exp Bot **57:**33-42.

494. **Immink, R. G., T. W. Gadella, Jr., S. Ferrario, M. Busscher, and G. C. Angenent.** 2002. Analysis of MADS box protein-protein interactions in living plant cells. Proc Natl Acad Sci U S A **99:**2416-21.

495. **Yildiz, I., X. Gao, T. K. Harris, and F. M. Raymo.** 2007. Fluorescence resonance energy transfer in quantum dot-protein kinase assemblies. J Biomed Biotechnol **2007:**18081.

496. **Talaga, D. S., W. L. Lau, H. Roder, J. Tang, Y. Jia, W. F. DeGrado, and R. M. Hochstrasser.** 2000. Dynamics and folding of single two-stranded coiled-coil peptides studied by fluorescent energy transfer confocal microscopy. Proc Natl Acad Sci U S A **97:**13021-6.

497. **Deniz, A. A., T. A. Laurence, G. S. Beligere, M. Dahan, A. B. Martin, D. S. Chemla, P. E. Dawson, P. G. Schultz, and S. Weiss.** 2000. Single-molecule protein folding: diffusion fluorescence resonance energy transfer studies of the denaturation of chymotrypsin inhibitor 2. Proc Natl Acad Sci U S A **97:**5179-84.

498. **Michalet, X., S. Weiss, and M. Jager.** 2006. Single-molecule fluorescence studies of protein folding and conformational dynamics. Chem Rev **106:**1785-813.

499. **Tapley, T. L., J. L. Korner, M. T. Barge, J. Hupfeld, J. A. Schauerte, A. Gafni, U. Jakob, and J. C. Bardwell.** 2009. Structural plasticity of an acid-activated chaperone allows promiscuous substrate binding. Proc Natl Acad Sci U S A **106:**5557-62.

500. **Rye, H. S.** 2001. Application of fluorescence resonance energy transfer to the GroEL-GroES chaperonin reaction. Methods **24:**278-88.

501. **Jackson, M. R., M. F. Cohen-Doyle, P. A. Peterson, and D. B. Williams.** 1994. Regulation of MHC class I transport by the molecular chaperone, calnexin (p88, IP90). Science **263:**384-7.

502. **Christodoulou, S., A. E. Lockyer, J. M. Foster, J. D. Hoheisel, and D. B. Roberts.** 1997. Nucleotide sequence of a Drosophila melanogaster cDNA encoding a calnexin homologue. Gene **191:**143-8.

503. **Parker, C. G., L. I. Fessler, R. E. Nelson, and J. H. Fessler.** 1995. Drosophila UDP-glucose:glycoprotein glucosyltransferase: sequence and characterization of an enzyme that distinguishes between denatured and native proteins. Embo J **14:**1294-303.

504. **Smith, M. J.** 1992. Nucleotide sequence of a Drosophila melanogaster gene encoding a calreticulin homologue. DNA Seq **3:**247-50.